Electronic Supplementary Material (ESI) for Physical Chemistry Chemical Physics.


Supporting Information for

# Effects of orbital angles on the modeling of conjugated systems with curvature

Yanbo Han,[†] Mengyang Li,[‡] and Xiang Zhao[*,†]

†*Institute of Molecular Science and Applied Chemistry, School of Chemistry, Xi'an Jiaotong University, Xi'an 710049, China*

‡*School of Physics, Xidian University, Xi'an 710071, China*

E-mail: xzhao@mail.xjtu.edu.cn

# Contents

# 1 Pearson correlation coefficients between reference energy with models

Table 1: Pearson correlation coefficients between different charge state $C_{20-70}$ isomer relative energy and prediction by CSI model without NAPP.

| $2n$ | $C_{2n}$* | $C_{2n}^{2-}$ | $C_{2n}^{4-}$ | $C_{2n}^{6-}$ | $C_{2n}^{2+}$ | $C_{2n}^{4+}$ | $C_{2n}^{6+}$ |
|---|---|---|---|---|---|---|---|
| 30 | 0.97 | 1.00 | 0.97 | 1.00 | 0.89 | 0.99 | 0.99 |
| 32 | 0.98 | 0.88 | 0.94 | 0.64 | 0.17 | -0.45 | -0.65 |
| 34 | 0.96 | 0.75 | 0.97 | 0.73 | -0.26 | -0.97 | -0.97 |
| 36 | 0.97 | 0.85 | 0.90 | 0.83 | 0.18 | -0.40 | -0.94 |
| 38 | 0.97 | 0.97 | 0.96 | 0.86 | -0.04 | -0.18 | -0.35 |
| 40 | 0.98 | 0.98 | 0.93 | 0.80 | 0.14 | -0.06 | -0.09 |
| 42 | 0.96 | 0.93 | 0.93 | 0.91 | -0.04 | -0.11 | 0.24 |
| 44 | 0.96 | 0.90 | 0.94 | 0.92 | -0.52 | -0.70 | -0.65 |
| 46 | 0.96 | 0.90 | 0.94 | 0.92 | -0.55 | -0.81 | -0.79 |
| 48 | 0.95 | 0.89 | 0.94 | 0.93 | -0.40 | -0.80 | -0.86 |
| 50 | 0.97 | 0.89 | 0.94 | 0.92 | -0.40 | -0.79 | -0.91 |
| 52 | 0.96 | 0.90 | 0.94 | 0.92 | -0.05 | -0.66 | -0.89 |
| 54 | 0.96 | 0.89 | 0.94 | 0.94 | -0.22 | -0.47 | -0.75 |
| 56 | 0.96 | 0.90 | 0.93 | 0.93 | -0.17 | -0.57 | -0.62 |
| 58 | 0.95 | 0.89 | 0.94 | 0.94 | -0.27 | -0.60 | -0.62 |
| 60 | 0.95 | 0.90 | 0.94 | 0.94 | -0.32 | -0.67 | -0.72 |
| 62 | 0.95 | 0.89 | 0.93 | 0.93 | -0.26 | -0.65 | -0.75 |
| 64 | 0.95 | 0.89 | 0.94 | 0.94 | -0.25 | -0.66 | -0.78 |
| 66 | 0.94 | 0.88 | 0.94 | 0.94 | -0.29 | -0.64 | -0.78 |
| 68 | 0.94 | 0.89 | 0.94 | 0.94 | -0.23 | -0.64 | -0.78 |
| 70 | 0.94 | 0.89 | 0.94 | 0.94 | -0.25 | -0.65 | -0.78 |

* Pearson correlation coefficients between 0.2NAPP terms and energies.

Table 2: Pearson correlation coefficients between different charge state $C_{20-70}$ isomer relative energy and prediction by CSI model with NAPP.[1]

| $2n$ | $C_{2n}$* | $C_{2n}^{2-}$ | $C_{2n}^{4-}$ | $C_{2n}^{6-}$ | $C_{2n}^{2+}$ | $C_{2n}^{4+}$ | $C_{2n}^{6+}$ |
|---|---|---|---|---|---|---|---|
| 30 | 0.97 | 0.99 | 0.98 | 0.98 | 1.00 | 0.98 | 0.99 |
| 32 | 0.98 | 0.99 | 0.99 | 0.82 | 0.89 | 0.78 | 0.37 |
| 34 | 0.96 | 0.96 | 0.92 | 0.91 | 0.93 | 0.61 | 0.63 |
| 36 | 0.97 | 0.97 | 0.97 | 0.96 | 0.95 | 0.88 | 0.81 |
| 38 | 0.97 | 0.97 | 0.97 | 0.95 | 0.97 | 0.95 | 0.92 |
| 40 | 0.98 | 0.98 | 0.98 | 0.96 | 0.96 | 0.92 | 0.84 |
| 42 | 0.96 | 0.97 | 0.96 | 0.95 | 0.94 | 0.92 | 0.86 |
| 44 | 0.96 | 0.97 | 0.96 | 0.94 | 0.95 | 0.93 | 0.90 |
| 46 | 0.96 | 0.96 | 0.96 | 0.94 | 0.95 | 0.89 | 0.84 |
| 48 | 0.95 | 0.95 | 0.95 | 0.93 | 0.94 | 0.89 | 0.82 |
| 50 | 0.97 | 0.97 | 0.96 | 0.95 | 0.96 | 0.93 | 0.88 |
| 52 | 0.96 | 0.96 | 0.95 | 0.94 | 0.95 | 0.92 | 0.87 |
| 54 | 0.96 | 0.96 | 0.95 | 0.94 | 0.94 | 0.91 | 0.87 |
| 56 | 0.96 | 0.96 | 0.95 | 0.95 | 0.95 | 0.91 | 0.88 |
| 58 | 0.95 | 0.95 | 0.95 | 0.94 | 0.94 | 0.91 | 0.86 |
| 60 | 0.95 | 0.95 | 0.95 | 0.94 | 0.95 | 0.92 | 0.88 |
| 62 | 0.95 | 0.95 | 0.94 | 0.94 | 0.94 | 0.92 | 0.88 |
| 64 | 0.95 | 0.95 | 0.94 | 0.93 | 0.94 | 0.92 | 0.89 |
| 66 | 0.94 | 0.94 | 0.94 | 0.93 | 0.94 | 0.92 | 0.89 |
| 68 | 0.94 | 0.94 | 0.93 | 0.93 | 0.93 | 0.91 | 0.89 |
| 70 | 0.94 | 0.94 | 0.93 | 0.92 | 0.93 | 0.91 | 0.88 |

* CSI is not available for neutral fullerenes, so here are coefficients between 0.2NAPP terms and energies as in Table 1.

Table 3: Pearson correlation coefficients between different charge state $C_{20-70}$ isomer energy and prediction by XCSI model with angles but without distances.

| $2n$ | $C_{2n}$ | $C_{2n}^{2-}$ | $C_{2n}^{4-}$ | $C_{2n}^{6-}$ | $C_{2n}^{2+}$ | $C_{2n}^{4+}$ | $C_{2n}^{6+}$ |
|---|---|---|---|---|---|---|---|
| 30 | 0.96 | 0.99 | 0.95 | 1.00 | 0.86 | 0.44 | 0.96 |
| 32 | 0.96 | 0.89 | 0.58 | 0.51 | 0.51 | 0.78 | 0.10 |
| 34 | 0.96 | 0.93 | 0.51 | 0.98 | 0.93 | 0.66 | 0.97 |
| 36 | 0.94 | 0.93 | 0.87 | 0.85 | 0.91 | 0.88 | 0.83 |
| 38 | 0.91 | 0.92 | 0.84 | 0.91 | 0.97 | 0.95 | 0.93 |
| 40 | 0.94 | 0.95 | 0.86 | 0.91 | 0.92 | 0.95 | 0.92 |
| 42 | 0.91 | 0.91 | 0.86 | 0.88 | 0.90 | 0.90 | 0.91 |
| 44 | 0.94 | 0.91 | 0.88 | 0.91 | 0.91 | 0.91 | 0.87 |
| 46 | 0.95 | 0.94 | 0.86 | 0.92 | 0.93 | 0.89 | 0.88 |
| 48 | 0.95 | 0.94 | 0.90 | 0.93 | 0.92 | 0.90 | 0.86 |
| 50 | 0.96 | 0.95 | 0.90 | 0.93 | 0.95 | 0.94 | 0.90 |
| 52 | 0.95 | 0.94 | 0.89 | 0.93 | 0.95 | 0.94 | 0.91 |
| 54 | 0.96 | 0.95 | 0.90 | 0.93 | 0.95 | 0.94 | 0.93 |
| 56 | 0.96 | 0.95 | 0.91 | 0.94 | 0.95 | 0.95 | 0.93 |
| 58 | 0.95 | 0.95 | 0.91 | 0.93 | 0.95 | 0.94 | 0.93 |
| 60 | 0.96 | 0.95 | 0.92 | 0.94 | 0.95 | 0.95 | 0.93 |
| 62 | 0.96 | 0.95 | 0.92 | 0.94 | 0.95 | 0.95 | 0.93 |
| 64 | 0.96 | 0.95 | 0.92 | 0.94 | 0.96 | 0.95 | 0.93 |
| 66 | 0.96 | 0.95 | 0.92 | 0.94 | 0.96 | 0.95 | 0.93 |
| 68 | 0.96 | 0.95 | 0.93 | 0.94 | 0.96 | 0.95 | 0.94 |
| 70 | 0.96 | 0.95 | 0.93 | 0.94 | 0.96 | 0.95 | 0.94 |

Table 4: Pearson correlation coefficients between different charge state $C_{20-70}$ isomer energy and prediction by XCSI model with angles and distances.

| $2n$ | $C_{2n}$ | $C_{2n}^{2-}$ | $C_{2n}^{4-}$ | $C_{2n}^{6-}$ | $C_{2n}^{2+}$ | $C_{2n}^{4+}$ | $C_{2n}^{6+}$ |
|---|---|---|---|---|---|---|---|
| 30 | 0.99 | 0.98 | 1.00 | 1.00 | 0.93 | 0.85 | 0.99 |
| 32 | 0.88 | 0.96 | 0.89 | 0.47 | 0.53 | 0.56 | 0.31 |
| 34 | 0.96 | 0.99 | 0.81 | 0.95 | 0.91 | 0.49 | 0.98 |
| 36 | 0.96 | 0.97 | 0.95 | 0.97 | 0.92 | 0.85 | 0.80 |
| 38 | 0.95 | 0.96 | 0.93 | 0.99 | 0.98 | 0.96 | 0.91 |
| 40 | 0.95 | 0.98 | 0.96 | 0.97 | 0.94 | 0.96 | 0.94 |
| 42 | 0.94 | 0.96 | 0.95 | 0.97 | 0.92 | 0.92 | 0.92 |
| 44 | 0.96 | 0.96 | 0.96 | 0.97 | 0.93 | 0.94 | 0.90 |
| 46 | 0.96 | 0.97 | 0.95 | 0.97 | 0.92 | 0.89 | 0.89 |
| 48 | 0.96 | 0.97 | 0.97 | 0.98 | 0.92 | 0.90 | 0.86 |
| 50 | 0.97 | 0.98 | 0.97 | 0.98 | 0.96 | 0.94 | 0.91 |
| 52 | 0.97 | 0.98 | 0.96 | 0.98 | 0.96 | 0.95 | 0.92 |
| 54 | 0.97 | 0.98 | 0.97 | 0.98 | 0.96 | 0.95 | 0.94 |
| 56 | 0.97 | 0.98 | 0.97 | 0.98 | 0.96 | 0.96 | 0.95 |
| 58 | 0.97 | 0.98 | 0.97 | 0.98 | 0.96 | 0.95 | 0.95 |
| 60 | 0.98 | 0.98 | 0.97 | 0.98 | 0.96 | 0.96 | 0.95 |
| 62 | 0.97 | 0.98 | 0.97 | 0.98 | 0.96 | 0.96 | 0.95 |
| 64 | 0.98 | 0.98 | 0.97 | 0.98 | 0.97 | 0.96 | 0.95 |
| 66 | 0.98 | 0.98 | 0.97 | 0.98 | 0.97 | 0.96 | 0.95 |
| 68 | 0.98 | 0.98 | 0.98 | 0.98 | 0.97 | 0.96 | 0.95 |
| 70 | 0.98 | 0.98 | 0.98 | 0.98 | 0.97 | 0.96 | 0.95 |

Table 5: Pearson correlation coefficients between different charge state $C_{20-70}$ isomer energy and prediction by XCSI model with angles and distances, without using adjacent matrix mask.

| $2n$ | $C_{2n}$ | $C_{2n}^{2-}$ | $C_{2n}^{4-}$ | $C_{2n}^{6-}$ | $C_{2n}^{2+}$ | $C_{2n}^{4+}$ | $C_{2n}^{6+}$ |
|---|---|---|---|---|---|---|---|
| 30 | 0.99 | 0.98 | 1.00 | 1.00 | 0.94 | 0.84 | 0.99 |
| 32 | 0.87 | 0.96 | 0.90 | 0.51 | 0.52 | 0.55 | 0.29 |
| 34 | 0.95 | 0.99 | 0.82 | 0.96 | 0.90 | 0.46 | 0.98 |
| 36 | 0.96 | 0.98 | 0.95 | 0.97 | 0.91 | 0.85 | 0.79 |
| 38 | 0.95 | 0.96 | 0.94 | 0.99 | 0.98 | 0.95 | 0.90 |
| 40 | 0.95 | 0.98 | 0.96 | 0.98 | 0.94 | 0.96 | 0.93 |
| 42 | 0.93 | 0.96 | 0.95 | 0.97 | 0.91 | 0.91 | 0.91 |
| 44 | 0.96 | 0.97 | 0.96 | 0.97 | 0.92 | 0.93 | 0.90 |
| 46 | 0.96 | 0.97 | 0.96 | 0.98 | 0.92 | 0.89 | 0.89 |
| 48 | 0.96 | 0.97 | 0.97 | 0.98 | 0.92 | 0.89 | 0.86 |
| 50 | 0.97 | 0.98 | 0.97 | 0.98 | 0.96 | 0.94 | 0.91 |
| 52 | 0.97 | 0.98 | 0.97 | 0.98 | 0.96 | 0.95 | 0.91 |
| 54 | 0.97 | 0.98 | 0.97 | 0.98 | 0.96 | 0.95 | 0.93 |
| 56 | 0.97 | 0.98 | 0.97 | 0.98 | 0.96 | 0.95 | 0.94 |
| 58 | 0.97 | 0.98 | 0.97 | 0.98 | 0.96 | 0.95 | 0.94 |
| 60 | 0.97 | 0.98 | 0.98 | 0.98 | 0.96 | 0.95 | 0.95 |
| 62 | 0.97 | 0.98 | 0.98 | 0.98 | 0.96 | 0.95 | 0.94 |
| 64 | 0.97 | 0.98 | 0.98 | 0.98 | 0.96 | 0.95 | 0.95 |
| 66 | 0.98 | 0.98 | 0.98 | 0.98 | 0.96 | 0.96 | 0.94 |
| 68 | 0.98 | 0.98 | 0.98 | 0.98 | 0.97 | 0.96 | 0.95 |
| 70 | 0.98 | 0.98 | 0.98 | 0.98 | 0.97 | 0.96 | 0.95 |

Table 6: Pearson correlation coefficients between different charge state $C_{20-70}$ isomer energy and prediction by XCSI model with distances but without angles.

| $2n$ | $C_{2n}$ | $C_{2n}^{2-}$ | $C_{2n}^{4-}$ | $C_{2n}^{6-}$ | $C_{2n}^{2+}$ | $C_{2n}^{4+}$ | $C_{2n}^{6+}$ |
|---|---|---|---|---|---|---|---|
| 30 | 0.99 | 0.98 | 1.00 | 0.98 | 0.87 | 0.34 | -0.99 |
| 32 | 0.87 | 0.84 | 0.83 | 0.05 | 0.39 | 0.14 | -0.35 |
| 34 | 0.93 | 0.91 | 0.55 | 0.90 | 0.83 | 0.17 | 0.47 |
| 36 | 0.88 | 0.88 | 0.92 | 0.92 | 0.78 | 0.51 | 0.22 |
| 38 | 0.89 | 0.92 | 0.90 | 0.95 | 0.94 | 0.91 | 0.81 |
| 40 | 0.89 | 0.96 | 0.88 | 0.96 | 0.85 | 0.88 | 0.82 |
| 42 | 0.86 | 0.94 | 0.89 | 0.94 | 0.79 | 0.78 | 0.69 |
| 44 | 0.91 | 0.95 | 0.92 | 0.94 | 0.84 | 0.82 | 0.65 |
| 46 | 0.90 | 0.95 | 0.87 | 0.95 | 0.77 | 0.69 | 0.61 |
| 48 | 0.90 | 0.96 | 0.92 | 0.95 | 0.80 | 0.74 | 0.66 |
| 50 | 0.93 | 0.95 | 0.92 | 0.95 | 0.90 | 0.84 | 0.72 |
| 52 | 0.90 | 0.96 | 0.90 | 0.96 | 0.86 | 0.85 | 0.79 |
| 54 | 0.89 | 0.96 | 0.91 | 0.95 | 0.86 | 0.85 | 0.84 |
| 56 | 0.90 | 0.96 | 0.93 | 0.96 | 0.85 | 0.84 | 0.85 |
| 58 | 0.90 | 0.96 | 0.91 | 0.96 | 0.83 | 0.83 | 0.84 |
| 60 | 0.91 | 0.97 | 0.93 | 0.96 | 0.85 | 0.82 | 0.82 |
| 62 | 0.91 | 0.97 | 0.93 | 0.96 | 0.84 | 0.82 | 0.81 |
| 64 | 0.91 | 0.97 | 0.92 | 0.96 | 0.85 | 0.81 | 0.81 |
| 66 | 0.91 | 0.97 | 0.93 | 0.96 | 0.85 | 0.82 | 0.80 |
| 68 | 0.91 | 0.97 | 0.93 | 0.97 | 0.85 | 0.83 | 0.82 |
| 70 | 0.91 | 0.97 | 0.92 | 0.97 | 0.85 | 0.83 | 0.82 |

Table 7: Pearson correlation coefficients between different charge state $C_{20-70}$ isomer energy and prediction by XCSI model with distances but without angles, without using adjacent matrix mask.

| $2n$ | $C_{2n}$ | $C_{2n}^{2-}$ | $C_{2n}^{4-}$ | $C_{2n}^{6-}$ | $C_{2n}^{2+}$ | $C_{2n}^{4+}$ | $C_{2n}^{6+}$ |
|---|---|---|---|---|---|---|---|
| 30 | 0.99 | 0.98 | 0.86 | 0.98 | 0.89 | 0.37 | -0.89 |
| 32 | 0.86 | 0.84 | 0.84 | 0.10 | 0.38 | 0.09 | -0.35 |
| 34 | 0.92 | 0.93 | 0.59 | 0.91 | 0.82 | 0.12 | 0.44 |
| 36 | 0.87 | 0.89 | 0.93 | 0.93 | 0.76 | 0.50 | 0.19 |
| 38 | 0.88 | 0.93 | 0.91 | 0.96 | 0.94 | 0.91 | 0.81 |
| 40 | 0.89 | 0.96 | 0.89 | 0.96 | 0.85 | 0.88 | 0.80 |
| 42 | 0.85 | 0.94 | 0.90 | 0.94 | 0.77 | 0.77 | 0.68 |
| 44 | 0.90 | 0.95 | 0.93 | 0.95 | 0.83 | 0.81 | 0.64 |
| 46 | 0.89 | 0.95 | 0.89 | 0.95 | 0.76 | 0.68 | 0.59 |
| 48 | 0.90 | 0.96 | 0.93 | 0.96 | 0.78 | 0.72 | 0.65 |
| 50 | 0.92 | 0.95 | 0.93 | 0.96 | 0.90 | 0.83 | 0.70 |
| 52 | 0.90 | 0.96 | 0.91 | 0.96 | 0.85 | 0.84 | 0.78 |
| 54 | 0.89 | 0.96 | 0.92 | 0.96 | 0.84 | 0.84 | 0.83 |
| 56 | 0.89 | 0.96 | 0.94 | 0.96 | 0.84 | 0.83 | 0.84 |
| 58 | 0.89 | 0.97 | 0.92 | 0.96 | 0.82 | 0.81 | 0.83 |
| 60 | 0.91 | 0.97 | 0.93 | 0.97 | 0.84 | 0.81 | 0.81 |
| 62 | 0.90 | 0.97 | 0.93 | 0.96 | 0.83 | 0.80 | 0.79 |
| 64 | 0.90 | 0.97 | 0.93 | 0.96 | 0.83 | 0.80 | 0.79 |
| 66 | 0.90 | 0.97 | 0.93 | 0.97 | 0.84 | 0.81 | 0.78 |
| 68 | 0.90 | 0.97 | 0.94 | 0.97 | 0.84 | 0.81 | 0.80 |
| 70 | 0.90 | 0.97 | 0.93 | 0.97 | 0.84 | 0.82 | 0.81 |

Table 8: Pearson correlation coefficients between different charge state $C_{20-70}$ isomer energy and prediction by XCSI model with angles using POAV2,[2] without using adjacent matrix mask.

| $2n$ | $C_{2n}$ | $C_{2n}^{2-}$ | $C_{2n}^{4-}$ | $C_{2n}^{6-}$ | $C_{2n}^{2+}$ | $C_{2n}^{4+}$ | $C_{2n}^{6+}$ |
|---|---|---|---|---|---|---|---|
| 30 | 0.98 | 0.99 | 1.00 | 1.00 | 0.93 | 0.88 | 0.98 |
| 32 | 0.90 | 0.97 | 0.91 | 0.62 | 0.57 | 0.67 | 0.40 |
| 34 | 0.94 | 0.98 | 0.82 | 0.97 | 0.91 | 0.43 | 0.96 |
| 36 | 0.96 | 0.97 | 0.96 | 0.97 | 0.91 | 0.86 | 0.78 |
| 38 | 0.94 | 0.97 | 0.95 | 0.99 | 0.97 | 0.95 | 0.90 |
| 40 | 0.95 | 0.98 | 0.96 | 0.98 | 0.93 | 0.95 | 0.92 |
| 42 | 0.94 | 0.97 | 0.96 | 0.97 | 0.90 | 0.90 | 0.89 |
| 44 | 0.96 | 0.98 | 0.97 | 0.97 | 0.93 | 0.93 | 0.90 |
| 46 | 0.96 | 0.98 | 0.96 | 0.98 | 0.92 | 0.88 | 0.88 |
| 48 | 0.96 | 0.98 | 0.98 | 0.98 | 0.92 | 0.89 | 0.86 |
| 50 | 0.98 | 0.99 | 0.97 | 0.98 | 0.96 | 0.94 | 0.92 |
| 52 | 0.97 | 0.98 | 0.97 | 0.98 | 0.96 | 0.95 | 0.92 |
| 54 | 0.97 | 0.98 | 0.98 | 0.98 | 0.95 | 0.95 | 0.94 |
| 56 | 0.97 | 0.99 | 0.98 | 0.98 | 0.96 | 0.95 | 0.95 |
| 58 | 0.97 | 0.99 | 0.98 | 0.98 | 0.96 | 0.95 | 0.95 |
| 60 | 0.98 | 0.99 | 0.98 | 0.98 | 0.96 | 0.95 | 0.95 |
| 62 | 0.98 | 0.99 | 0.98 | 0.98 | 0.96 | 0.95 | 0.95 |
| 64 | 0.98 | 0.99 | 0.98 | 0.98 | 0.96 | 0.96 | 0.95 |
| 66 | 0.98 | 0.99 | 0.98 | 0.98 | 0.97 | 0.96 | 0.95 |
| 68 | 0.98 | 0.99 | 0.98 | 0.98 | 0.97 | 0.96 | 0.95 |
| 70 | 0.98 | 0.99 | 0.98 | 0.98 | 0.97 | 0.96 | 0.96 |

Table 9: Pearson correlation coefficients between different charge state $C_{20-70}$ isomer energy and prediction by SpookyNet pretrained model[3] on QM7-X.

| $2n$ | $C_{2n}$ | $C_{2n}^{2-}$ | $C_{2n}^{4-}$ | $C_{2n}^{6-}$ | $C_{2n}^{2+}$ | $C_{2n}^{4+}$ | $C_{2n}^{6+}$ |
|---|---|---|---|---|---|---|---|
| 30 | 0.95 | 0.96 | 0.99 | -0.98 | 0.98 | 0.95 | 0.99 |
| 32 | 0.99 | 1.00 | 0.89 | 0.83 | 0.94 | 0.92 | 0.60 |
| 34 | 0.98 | 0.96 | 0.90 | 0.42 | 0.98 | 0.94 | 0.92 |
| 36 | 0.99 | 0.98 | 0.95 | 0.89 | 0.98 | 1.00 | 0.98 |
| 38 | 0.99 | 0.97 | 0.93 | 0.93 | 0.99 | 1.00 | 0.98 |
| 40 | 0.98 | 0.97 | 0.97 | 0.92 | 0.99 | 0.99 | 0.98 |
| 42 | 0.98 | 0.96 | 0.97 | 0.94 | 0.99 | 0.99 | 0.99 |
| 44 | 0.98 | 0.98 | 0.97 | 0.96 | 0.98 | 0.98 | 0.98 |
| 46 | 0.98 | 0.98 | 0.97 | 0.96 | 0.98 | 0.97 | 0.97 |
| 48 | 0.99 | 0.98 | 0.98 | 0.97 | 0.99 | 0.98 | 0.96 |
| 50 | 0.99 | 0.98 | 0.98 | 0.98 | 0.99 | 0.99 | 0.98 |
| 52 | 0.99 | 0.98 | 0.98 | 0.97 | 0.99 | 0.99 | 0.98 |
| 54 | 0.99 | 0.98 | 0.98 | 0.98 | 0.99 | 0.99 | 0.99 |
| 56 | 0.99 | 0.98 | 0.99 | 0.98 | 0.99 | 0.99 | 0.99 |
| 58 | 0.99 | 0.99 | 0.99 | 0.98 | 0.99 | 0.99 | 0.99 |
| 60 | 0.99 | 0.99 | 0.99 | 0.98 | 0.99 | 0.99 | 0.99 |
| 62 | 0.99 | 0.99 | 0.99 | 0.98 | 0.99 | 0.99 | 0.99 |
| 64 | 0.99 | 0.99 | 0.99 | 0.98 | 0.99 | 0.99 | 0.99 |
| 66 | 0.99 | 0.99 | 0.99 | 0.99 | 0.99 | 0.99 | 0.99 |
| 68 | 0.99 | 0.99 | 0.99 | 0.99 | 0.99 | 0.99 | 0.99 |
| 70 | 0.99 | 0.99 | 0.99 | 0.99 | 0.99 | 0.99 | 0.99 |

Table 10: Pearson correlation coefficients between different charge state $C_{20-70}$ isomer energy and prediction by SchNet pretrained model[4,5] on QM9.

| $2n$ | $C_{2n}$ |
|---|---|
| 30 | 0.98 |
| 32 | 0.94 |
| 34 | 0.02 |
| 36 | 0.66 |
| 38 | 0.71 |
| 40 | 0.56 |
| 42 | 0.80 |
| 44 | 0.63 |
| 46 | 0.77 |
| 48 | 0.49 |
| 50 | 0.40 |
| 52 | 0.42 |
| 54 | 0.31 |
| 56 | 0.06 |
| 58 | -0.26 |
| 60 | -0.46 |
| 62 | -0.61 |
| 64 | -0.70 |
| 66 | -0.77 |
| 68 | -0.81 |
| 70 | -0.83 |

# 2 Correlation between xTB energies and prediction by CSI model without NAPP

Predictions by CSI model without NAPP are calculated by

$$E_{\mathrm{CSI}}^{\mathrm{nonapp}} \equiv X_i^q \equiv \begin{cases} \sum_{k=n-q/2+1}^{n} \chi_{k,i}^q & \text{if } q > 0 \\ \sum_{k=n+1}^{n-q/2} \chi_{k,i}^q & \text{if } q < 0 \end{cases} \tag{1}$$

.

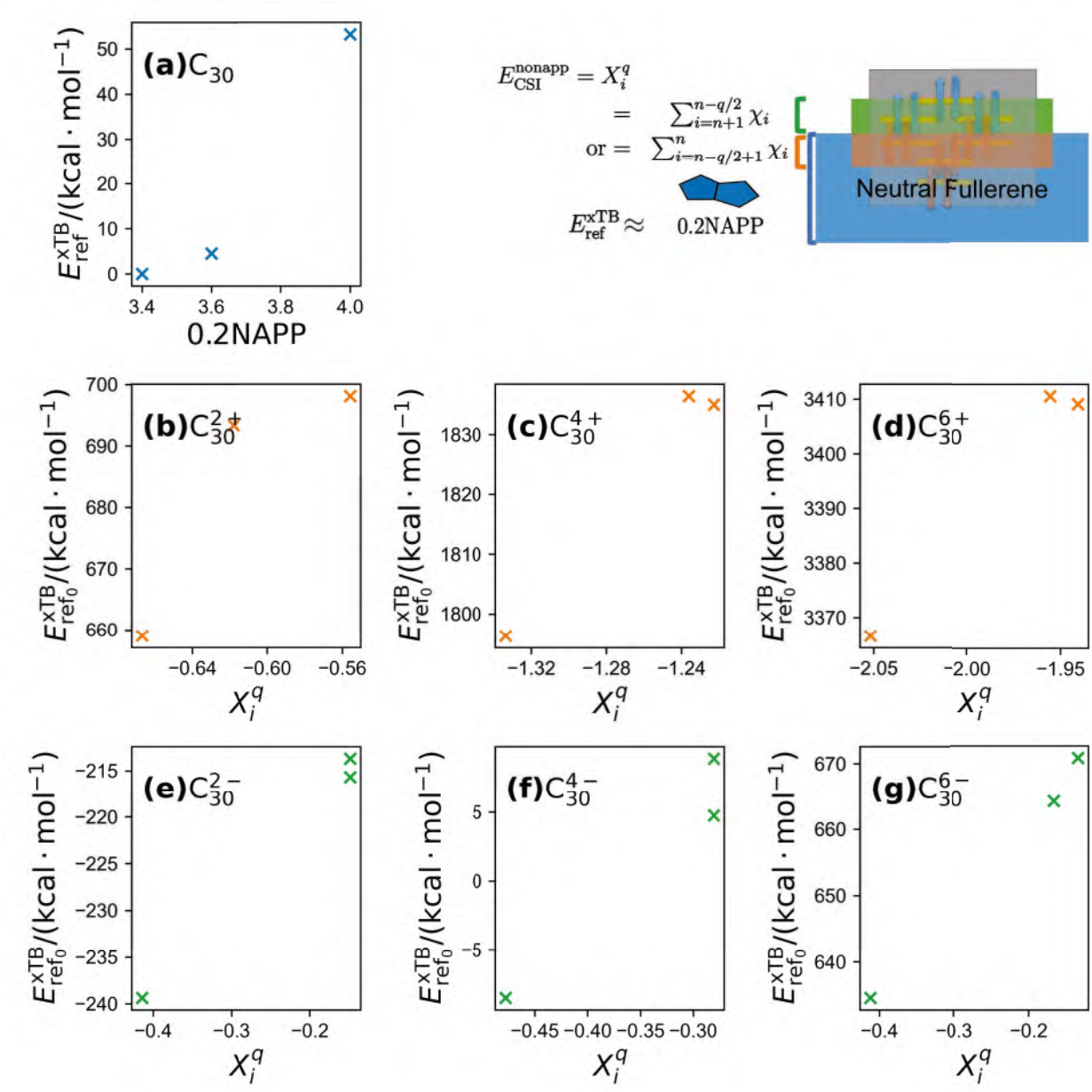


Figure 1: **(a)** Correlation between xTB energies of $C_{30}$ isomers relative to the most stable one and 0.2NAPP. **(b - g)** Correlation between xTB energies relative to the electrically neutral isomers and values of CSI model without NAPP of $C_{30}$ isomers with charge 2+, 4+, 6+, 2-, 4-, 6-, respectively.

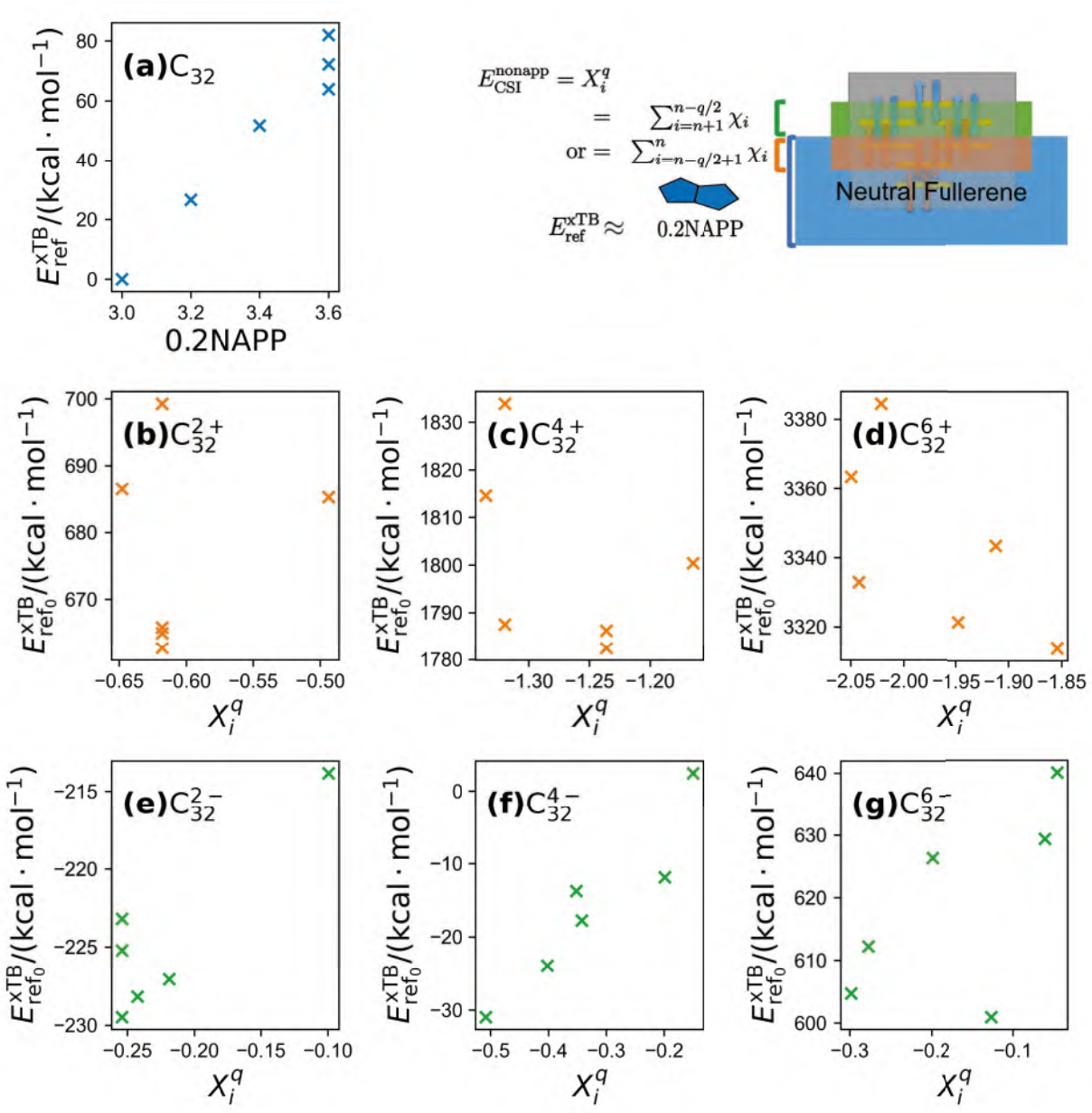


Figure 2: **(a)** Correlation between xTB energies of $C_{32}$ isomers relative to the most stable one and 0.2NAPP. **(b - g)** Correlation between xTB energies relative to the electrically neutral isomers and values of CSI model without NAPP of $C_{32}$ isomers with charge 2+, 4+, 6+, 2-, 4-, 6-, respectively.

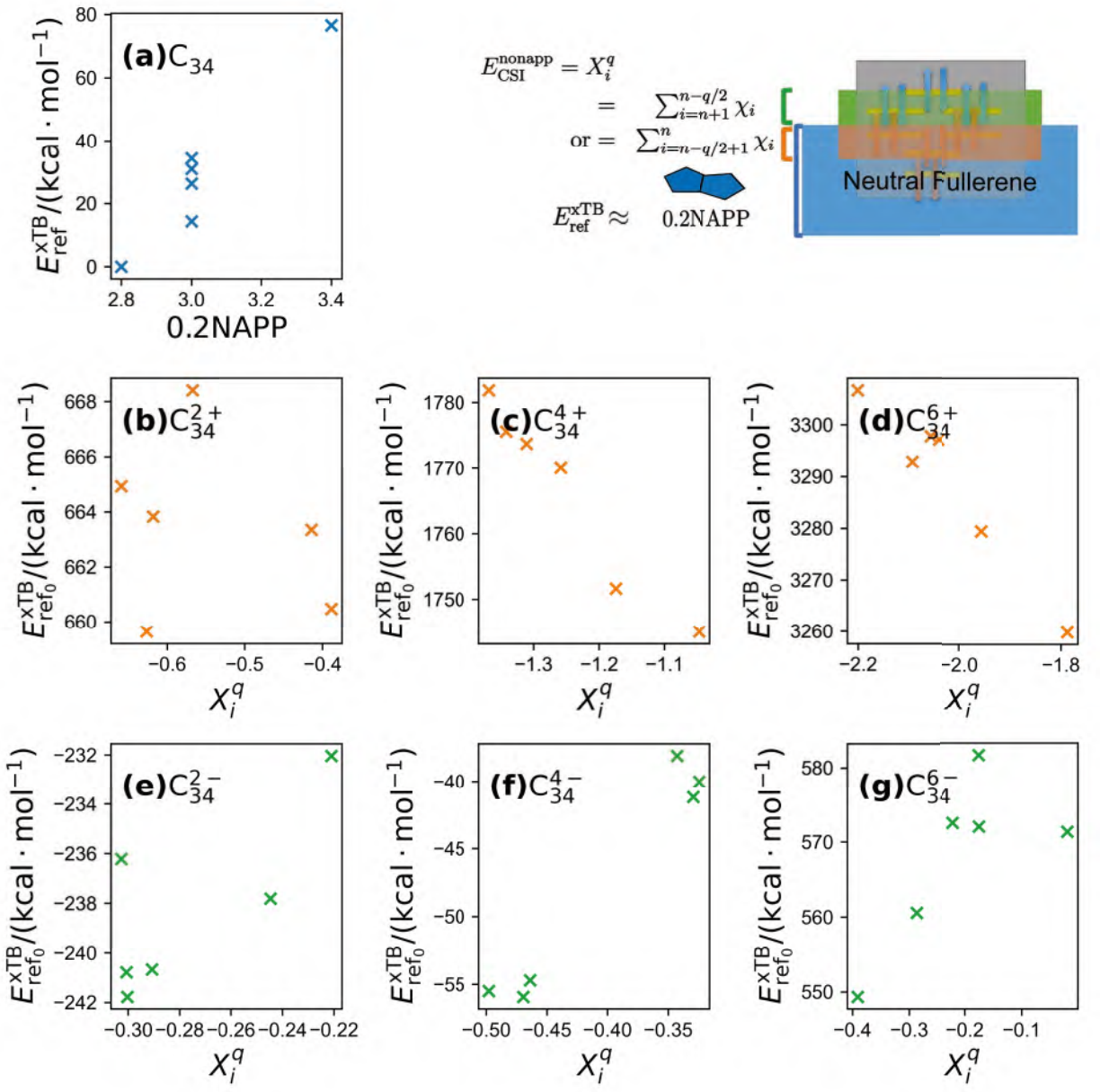


Figure 3: **(a)** Correlation between xTB energies of $C_{34}$ isomers relative to the most stable one and 0.2NAPP. **(b - g)** Correlation between xTB energies relative to the electrically neutral isomers and values of CSI model without NAPP of $C_{34}$ isomers with charge 2+, 4+, 6+, 2-, 4-, 6-, respectively.

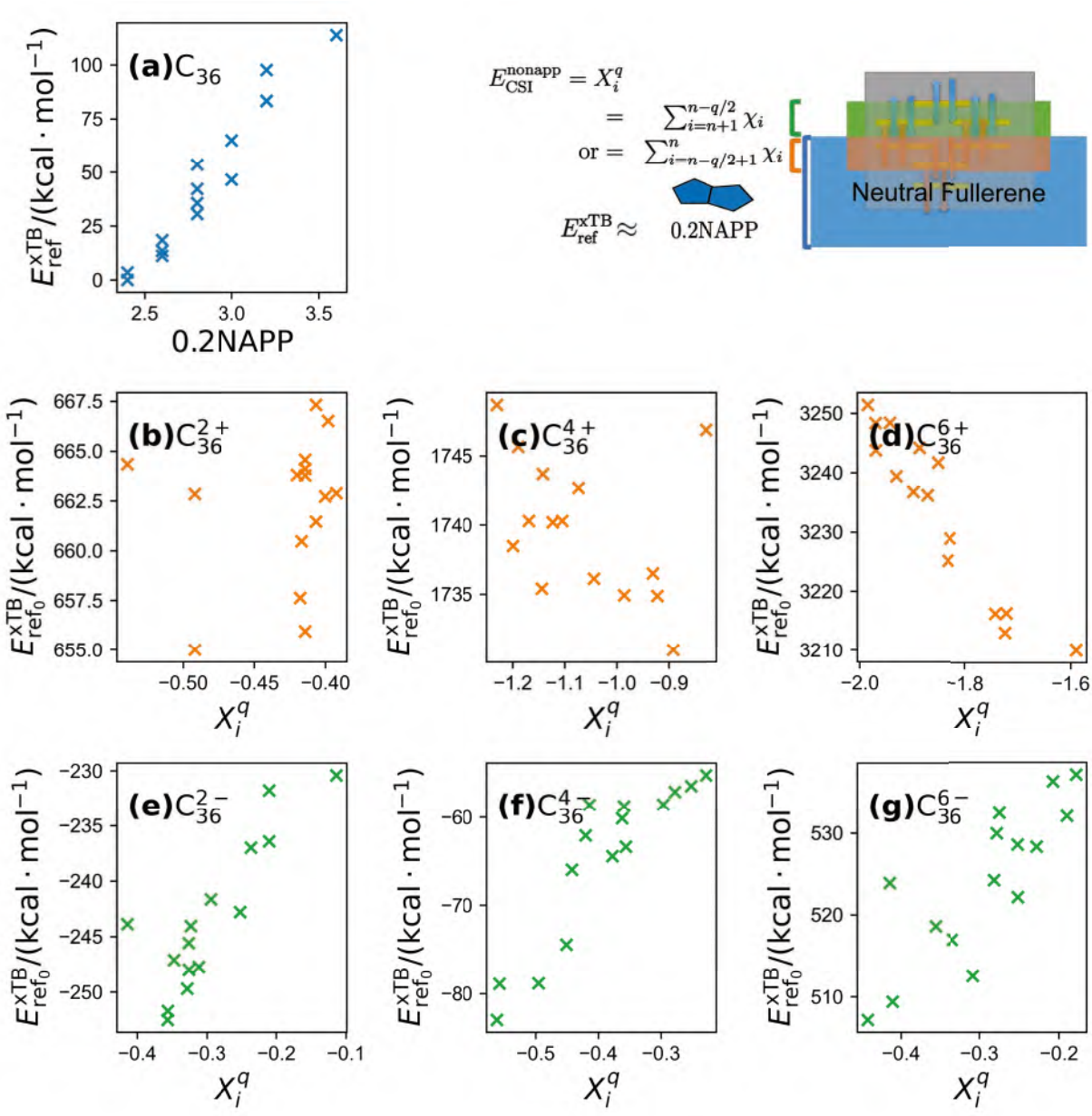


Figure 4: **(a)** Correlation between xTB energies of $C_{36}$ isomers relative to the most stable one and 0.2NAPP. **(b - g)** Correlation between xTB energies relative to the electrically neutral isomers and values of CSI model without NAPP of $C_{36}$ isomers with charge 2+, 4+, 6+, 2-, 4-, 6-, respectively.

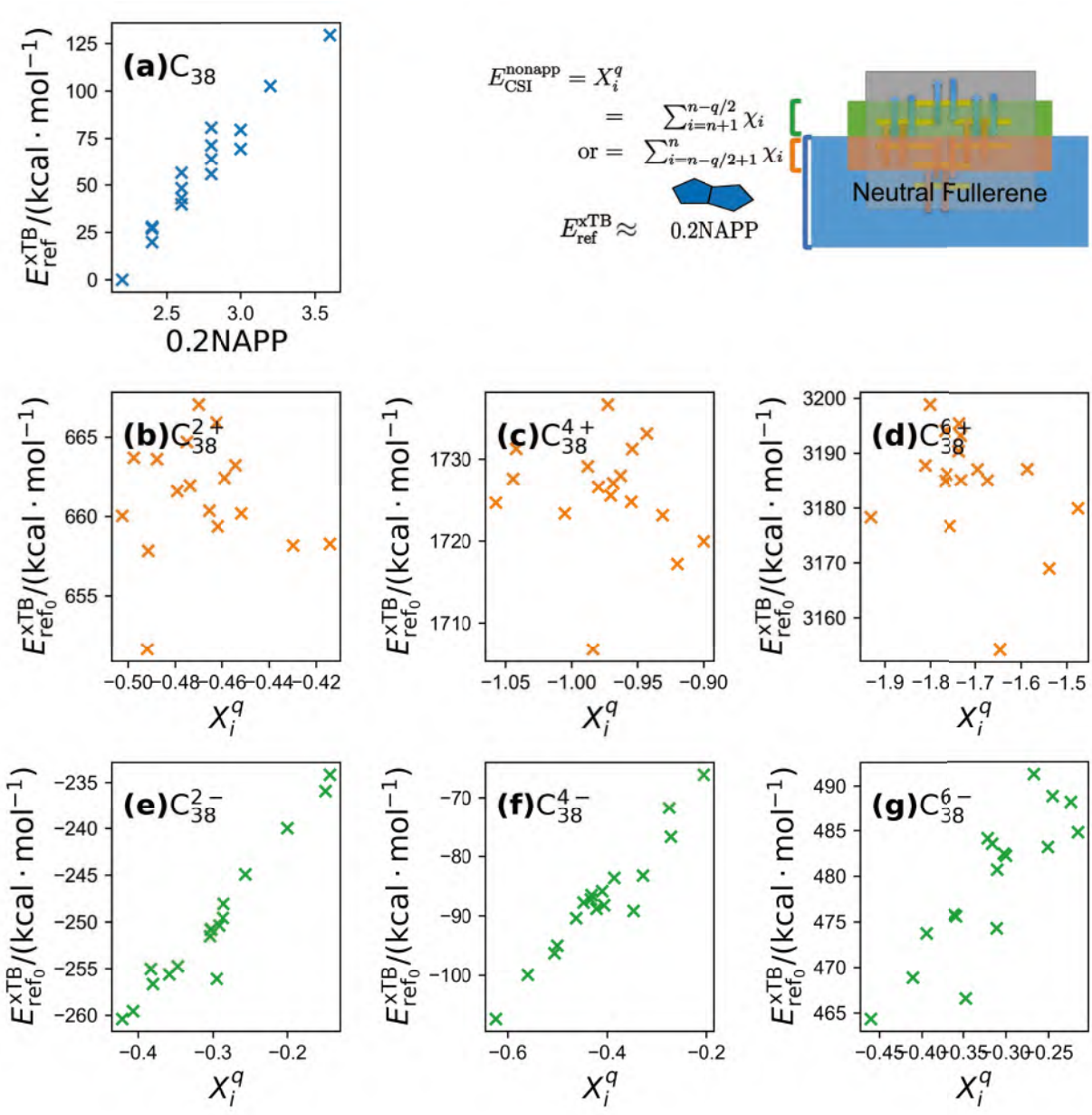


Figure 5: **(a)** Correlation between xTB energies of $C_{38}$ isomers relative to the most stable one and 0.2NAPP. **(b - g)** Correlation between xTB energies relative to the electrically neutral isomers and values of CSI model without NAPP of $C_{38}$ isomers with charge 2+, 4+, 6+, 2-, 4-, 6-, respectively.

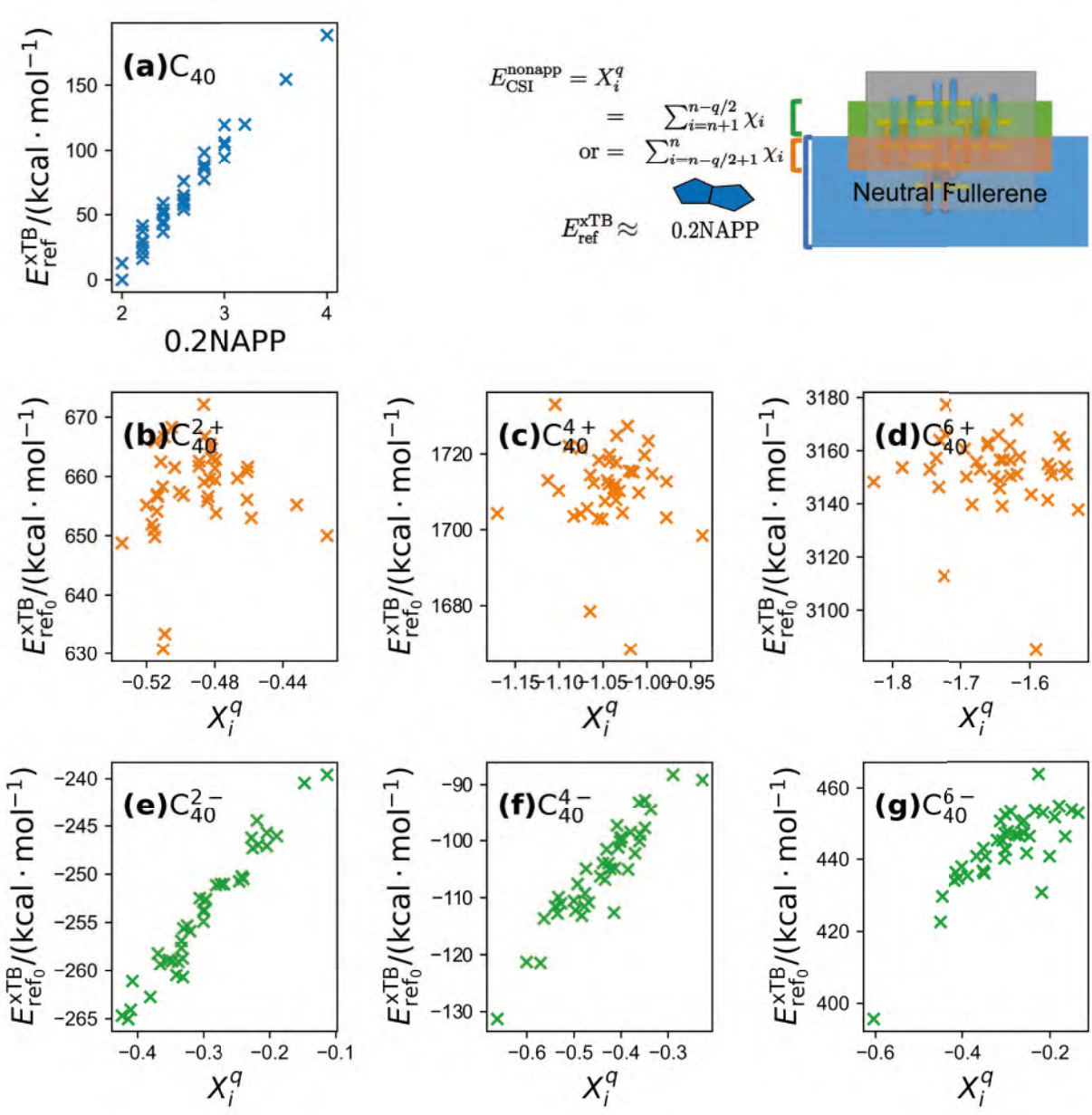


Figure 6: **(a)** Correlation between xTB energies of $C_{40}$ isomers relative to the most stable one and 0.2NAPP. **(b - g)** Correlation between xTB energies relative to the electrically neutral isomers and values of CSI model without NAPP of $C_{40}$ isomers with charge 2+, 4+, 6+, 2-, 4-, 6-, respectively.

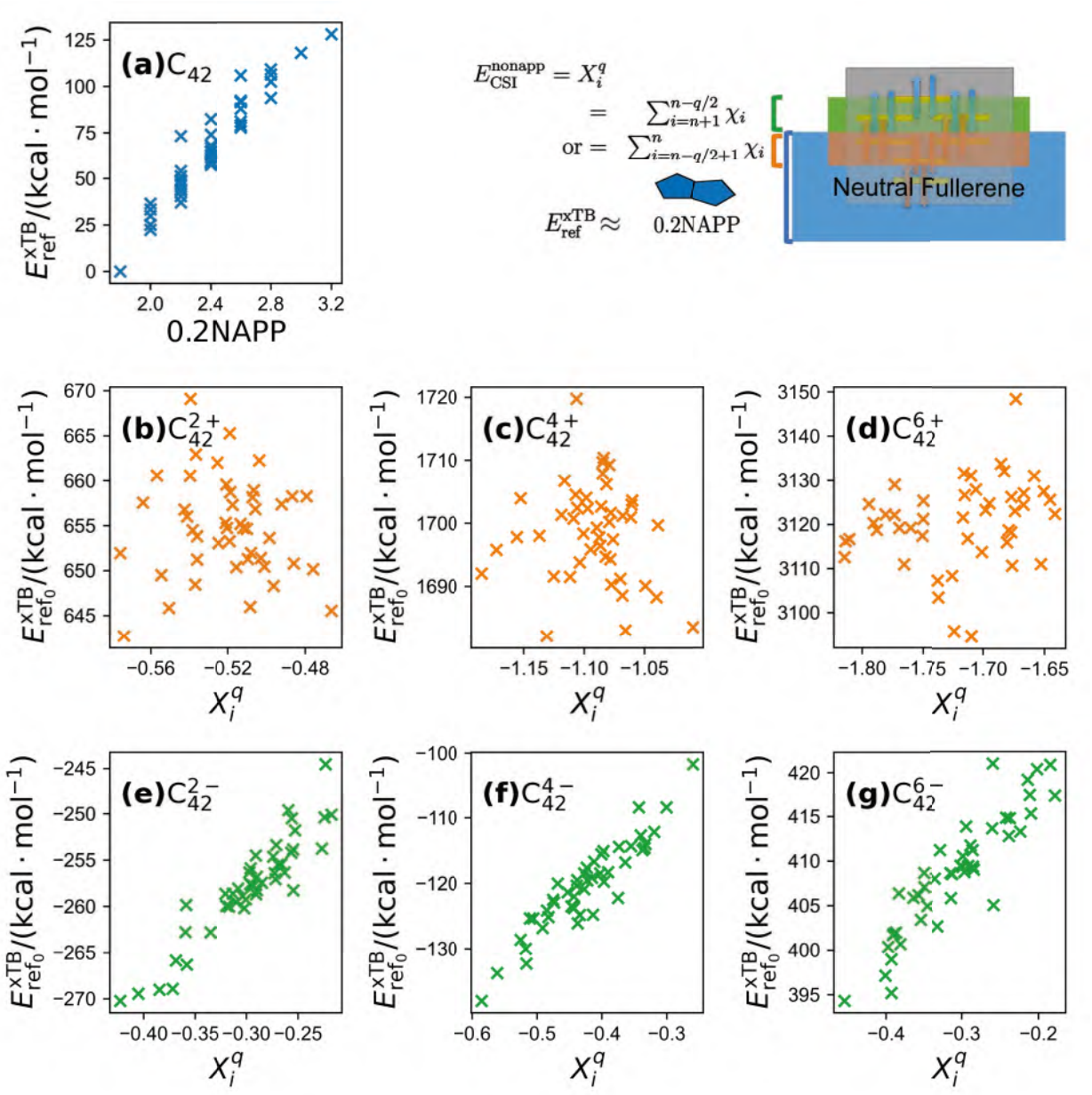


Figure 7: **(a)** Correlation between xTB energies of $C_{42}$ isomers relative to the most stable one and 0.2NAPP. **(b - g)** Correlation between xTB energies relative to the electrically neutral isomers and values of CSI model without NAPP of $C_{42}$ isomers with charge 2+, 4+, 6+, 2-, 4-, 6-, respectively.

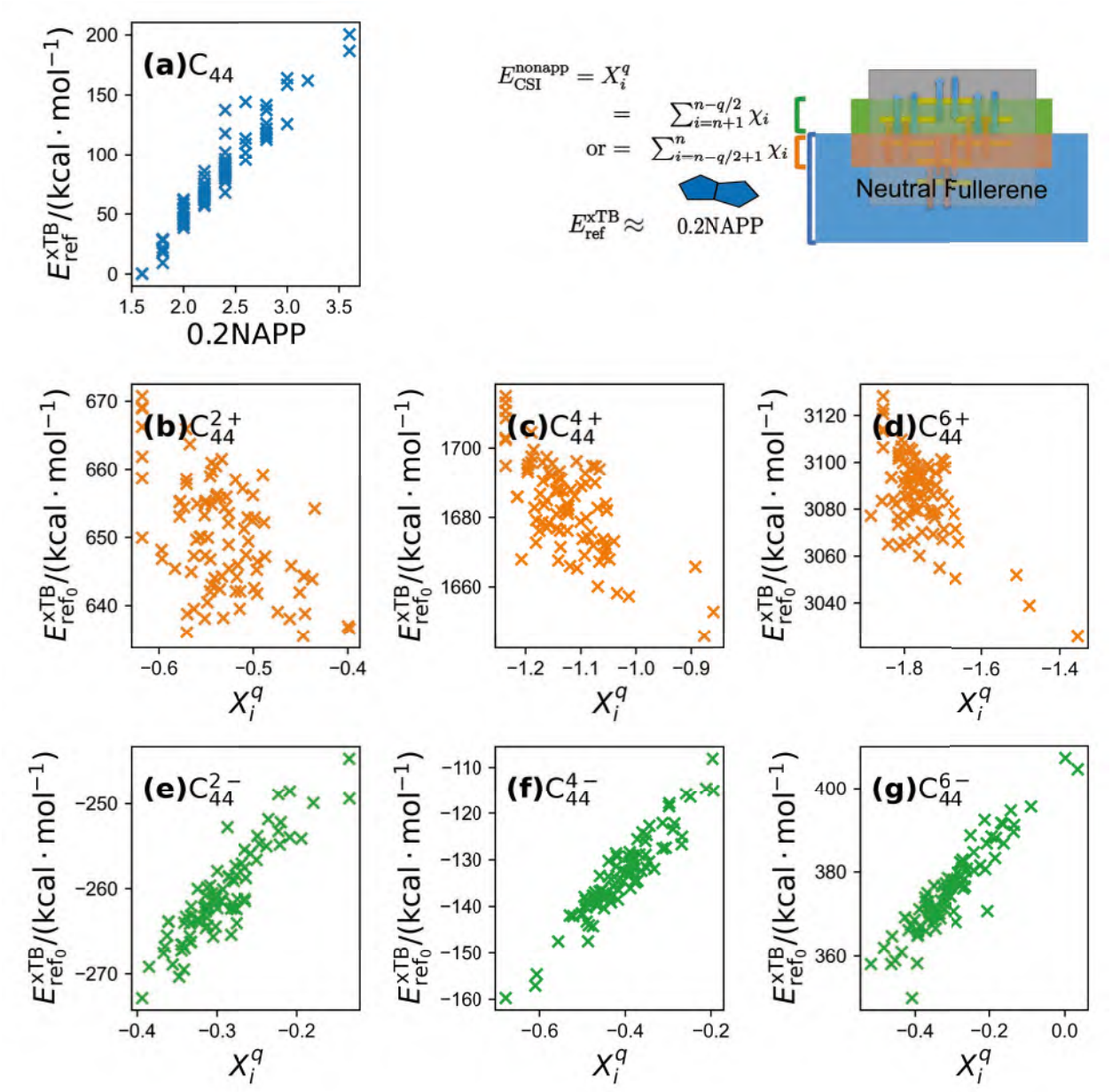


Figure 8: **(a)** Correlation between xTB energies of $C_{44}$ isomers relative to the most stable one and 0.2NAPP. **(b - g)** Correlation between xTB energies relative to the electrically neutral isomers and values of CSI model without NAPP of $C_{44}$ isomers with charge 2+, 4+, 6+, 2-, 4-, 6-, respectively.

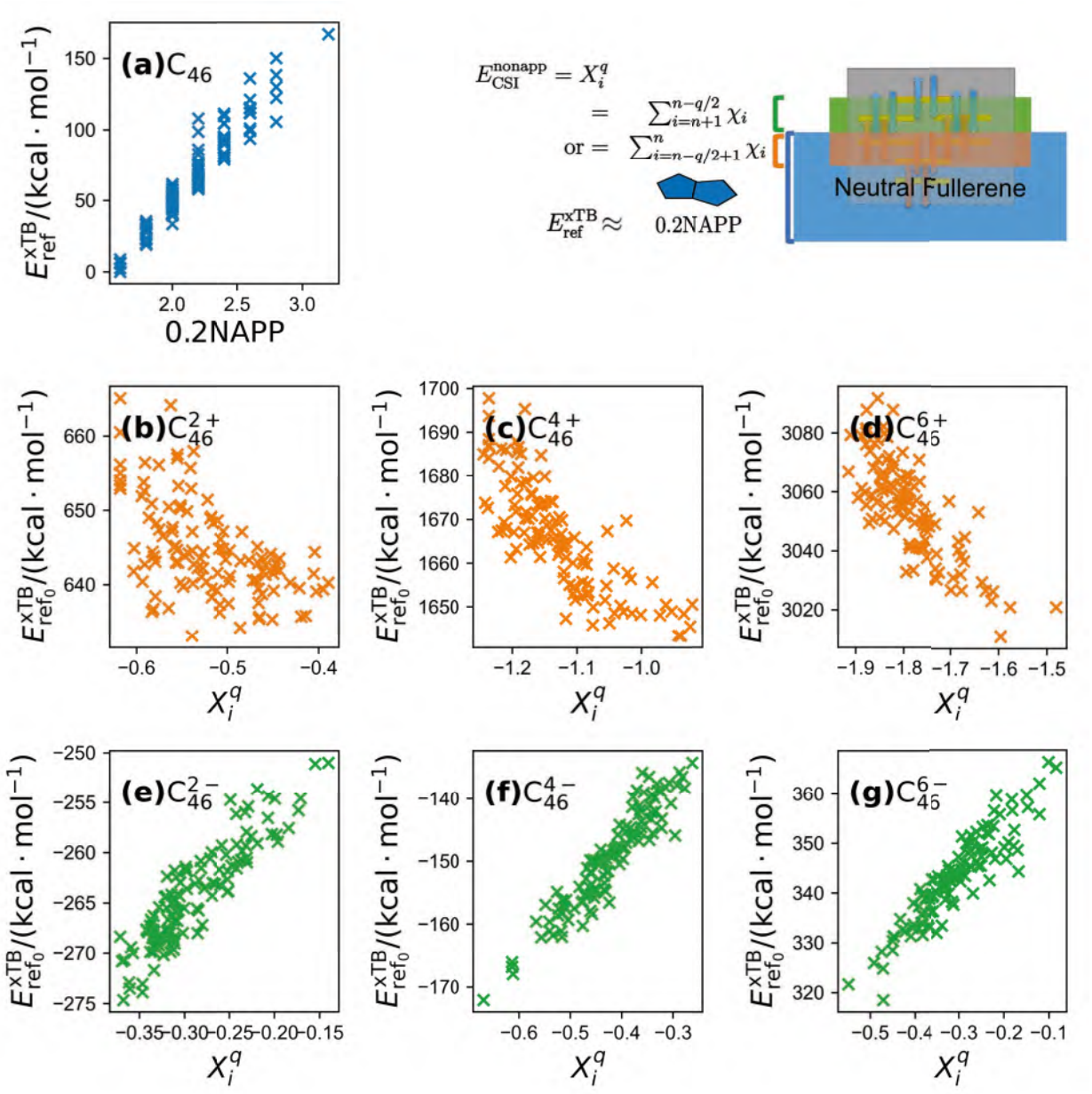


Figure 9: **(a)** Correlation between xTB energies of $C_{46}$ isomers relative to the most stable one and 0.2NAPP. **(b - g)** Correlation between xTB energies relative to the electrically neutral isomers and values of CSI model without NAPP of $C_{46}$ isomers with charge 2+, 4+, 6+, 2-, 4-, 6-, respectively.

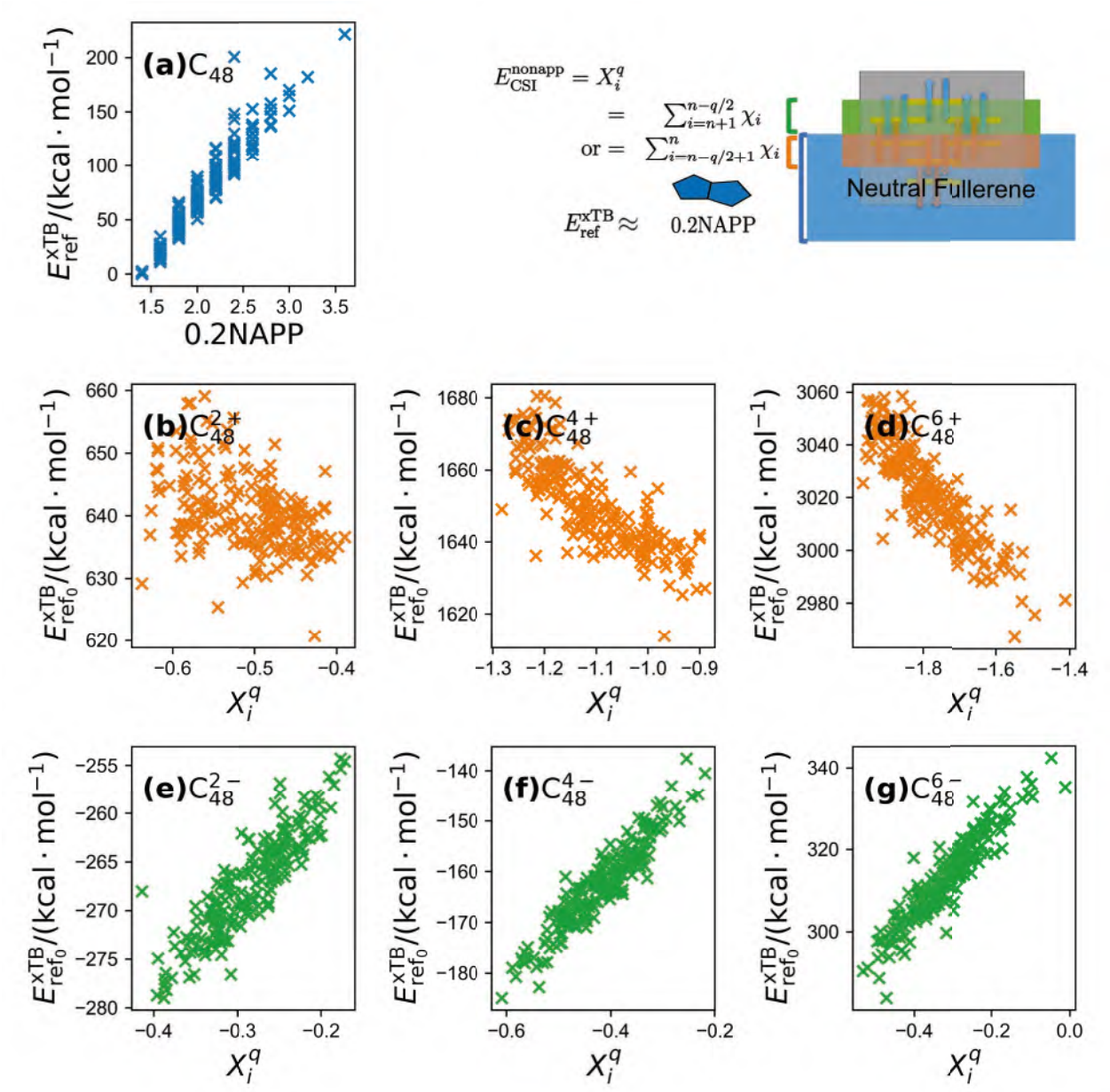


Figure 10: **(a)** Correlation between xTB energies of $C_{48}$ isomers relative to the most stable one and 0.2NAPP. **(b - g)** Correlation between xTB energies relative to the electrically neutral isomers and values of CSI model without NAPP of $C_{48}$ isomers with charge 2+, 4+, 6+, 2-, 4-, 6-, respectively.

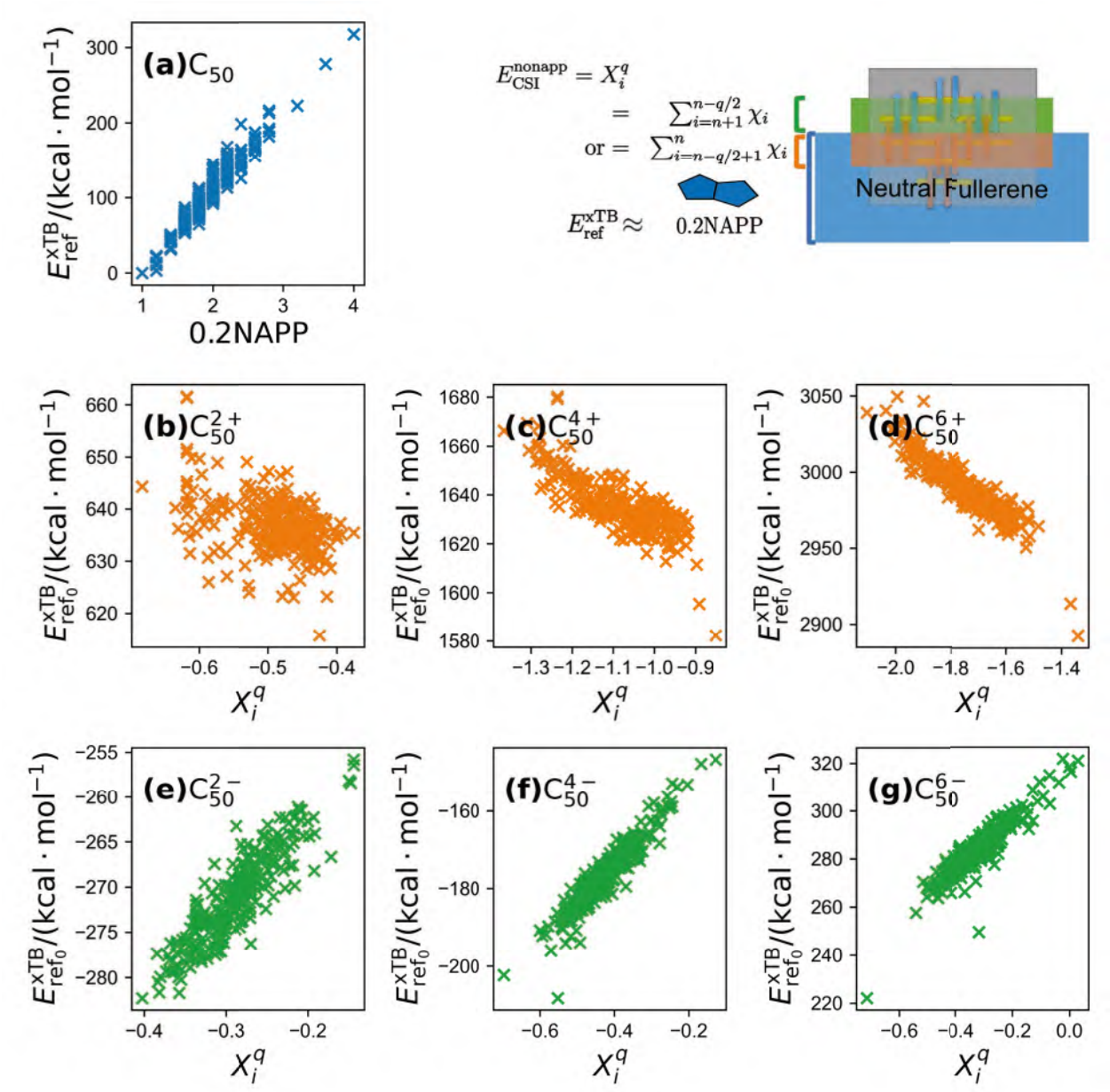


Figure 11: **(a)** Correlation between xTB energies of $C_{50}$ isomers relative to the most stable one and 0.2NAPP. **(b - g)** Correlation between xTB energies relative to the electrically neutral isomers and values of CSI model without NAPP of $C_{50}$ isomers with charge 2+, 4+, 6+, 2-, 4-, 6-, respectively.

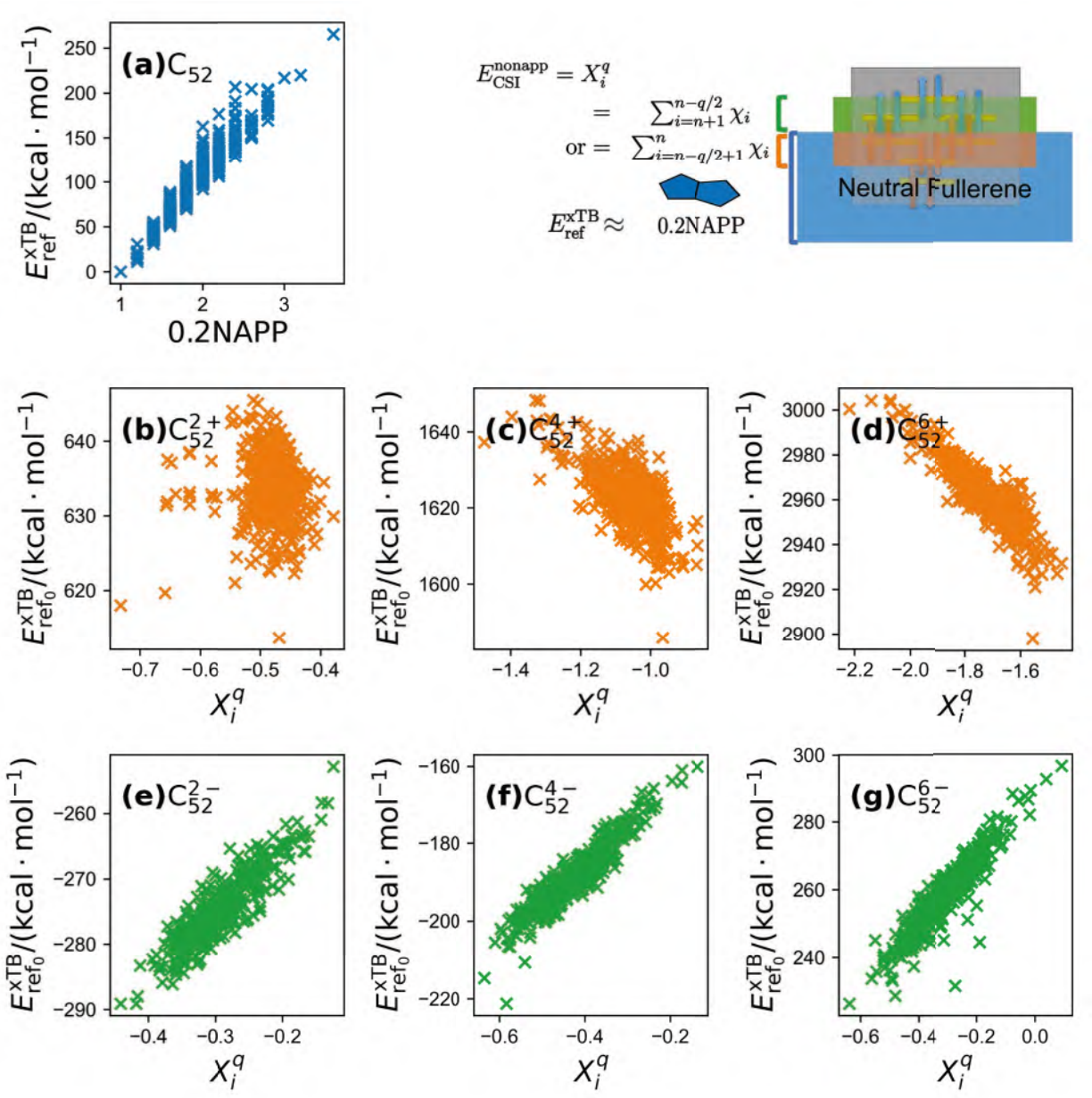


Figure 12: **(a)** Correlation between xTB energies of $C_{52}$ isomers relative to the most stable one and 0.2NAPP. **(b - g)** Correlation between xTB energies relative to the electrically neutral isomers and values of CSI model without NAPP of $C_{52}$ isomers with charge 2+, 4+, 6+, 2-, 4-, 6-, respectively.

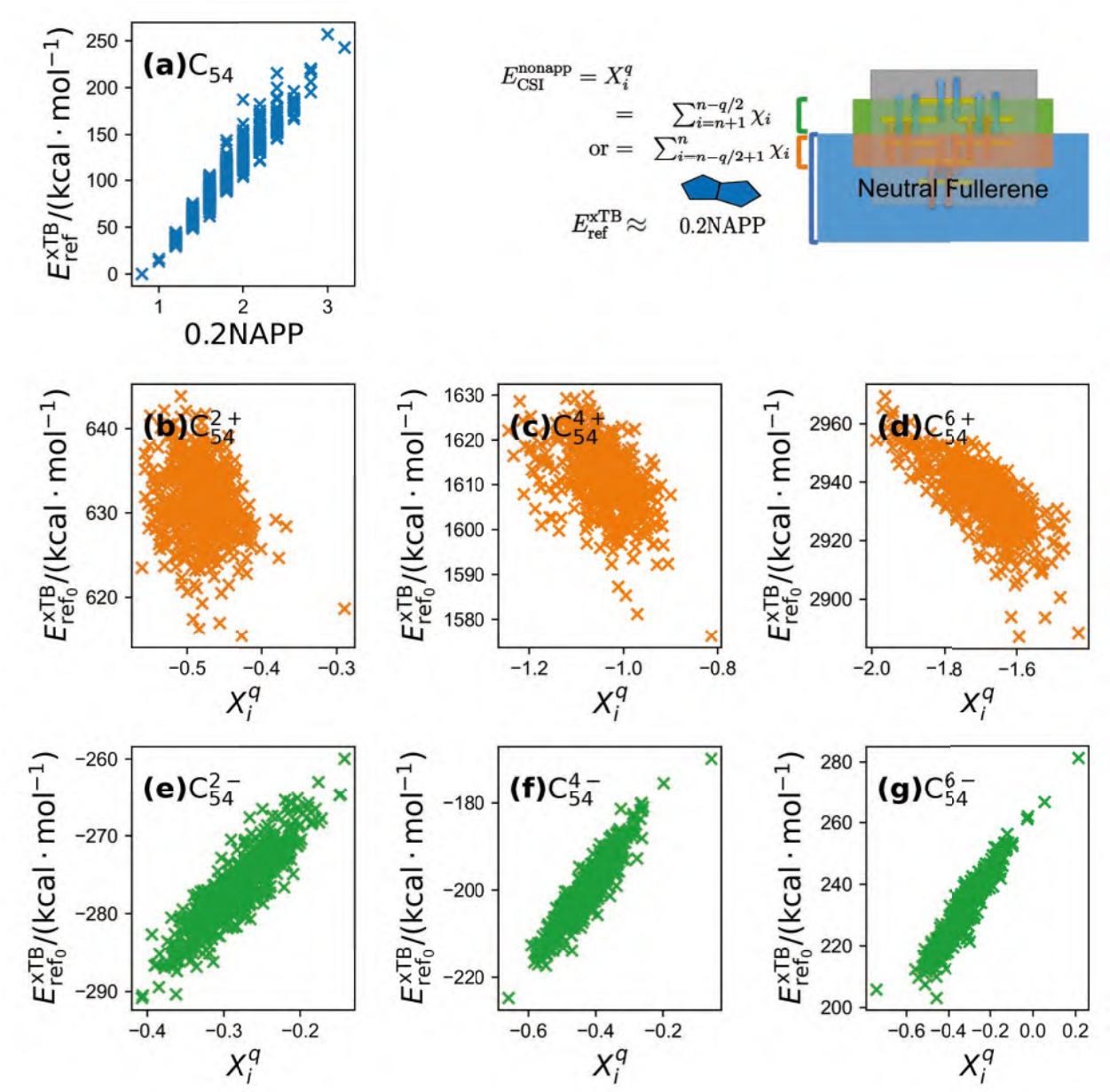


Figure 13: **(a)** Correlation between xTB energies of $C_{54}$ isomers relative to the most stable one and 0.2NAPP. **(b - g)** Correlation between xTB energies relative to the electrically neutral isomers and values of CSI model without NAPP of $C_{54}$ isomers with charge 2+, 4+, 6+, 2-, 4-, 6-, respectively.

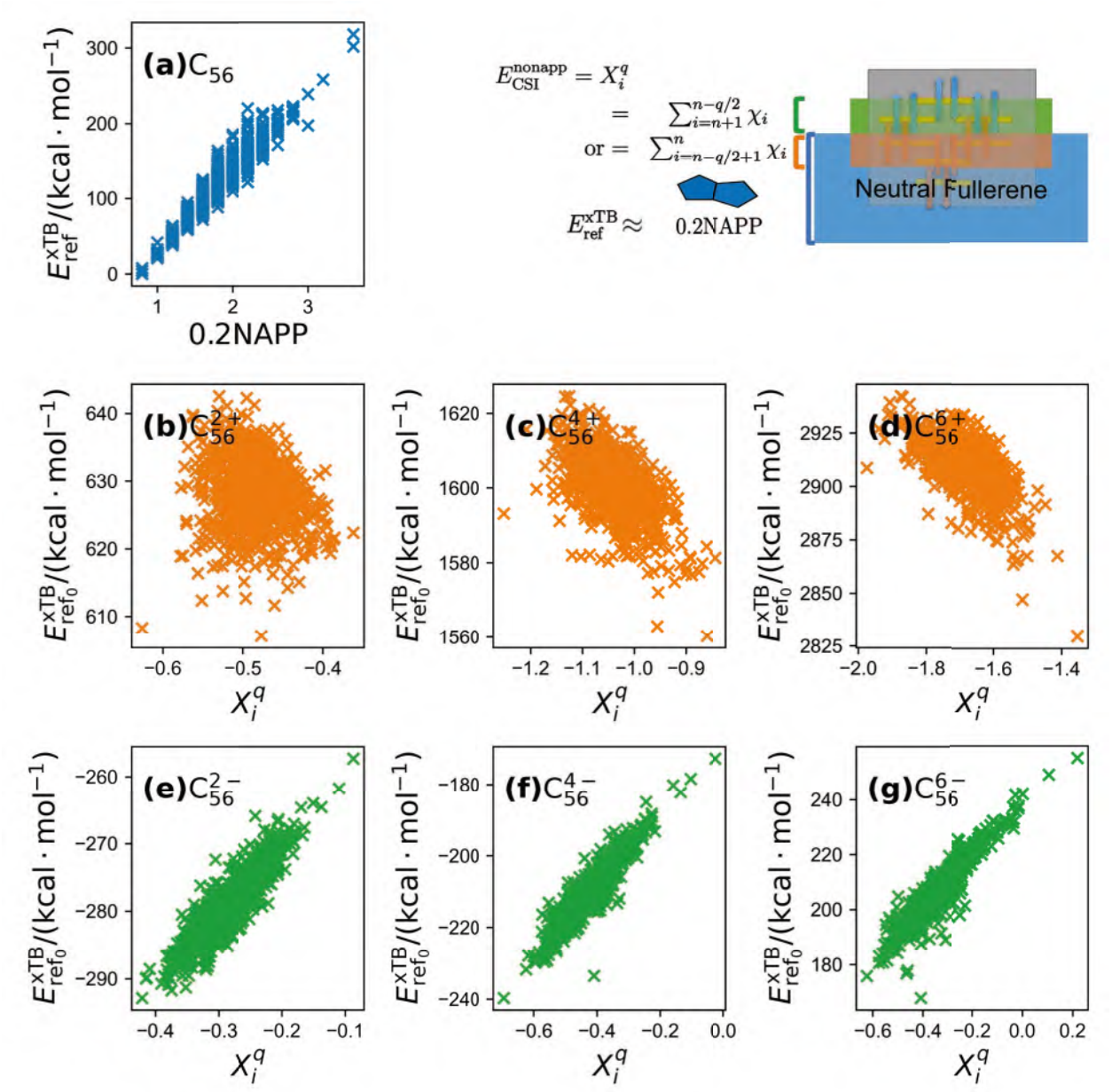


Figure 14: **(a)** Correlation between xTB energies of $C_{56}$ isomers relative to the most stable one and 0.2NAPP. **(b - g)** Correlation between xTB energies relative to the electrically neutral isomers and values of CSI model without NAPP of $C_{56}$ isomers with charge 2+, 4+, 6+, 2-, 4-, 6-, respectively.

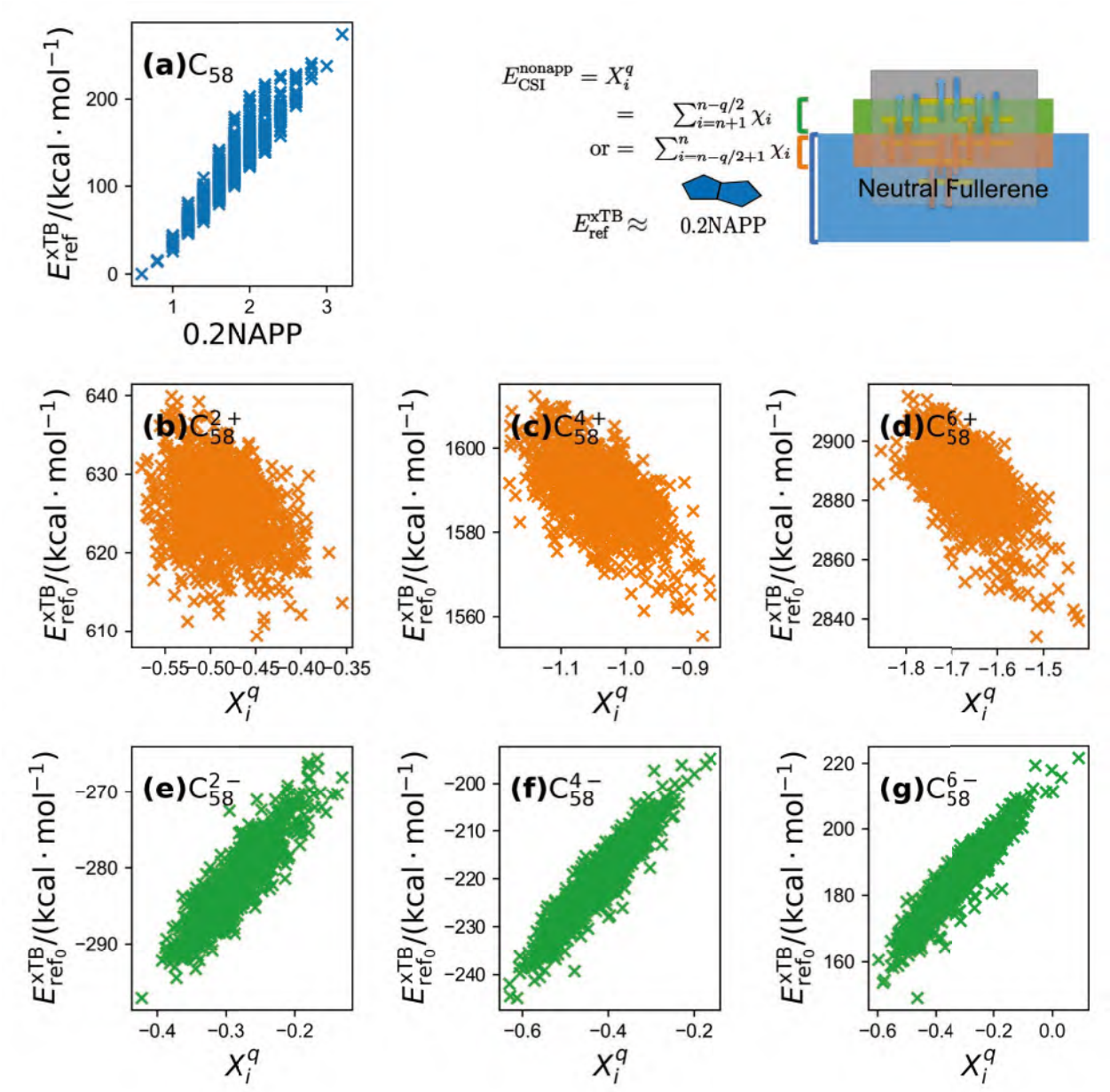


Figure 15: **(a)** Correlation between xTB energies of $C_{58}$ isomers relative to the most stable one and 0.2NAPP. **(b - g)** Correlation between xTB energies relative to the electrically neutral isomers and values of CSI model without NAPP of $C_{58}$ isomers with charge 2+, 4+, 6+, 2-, 4-, 6-, respectively.

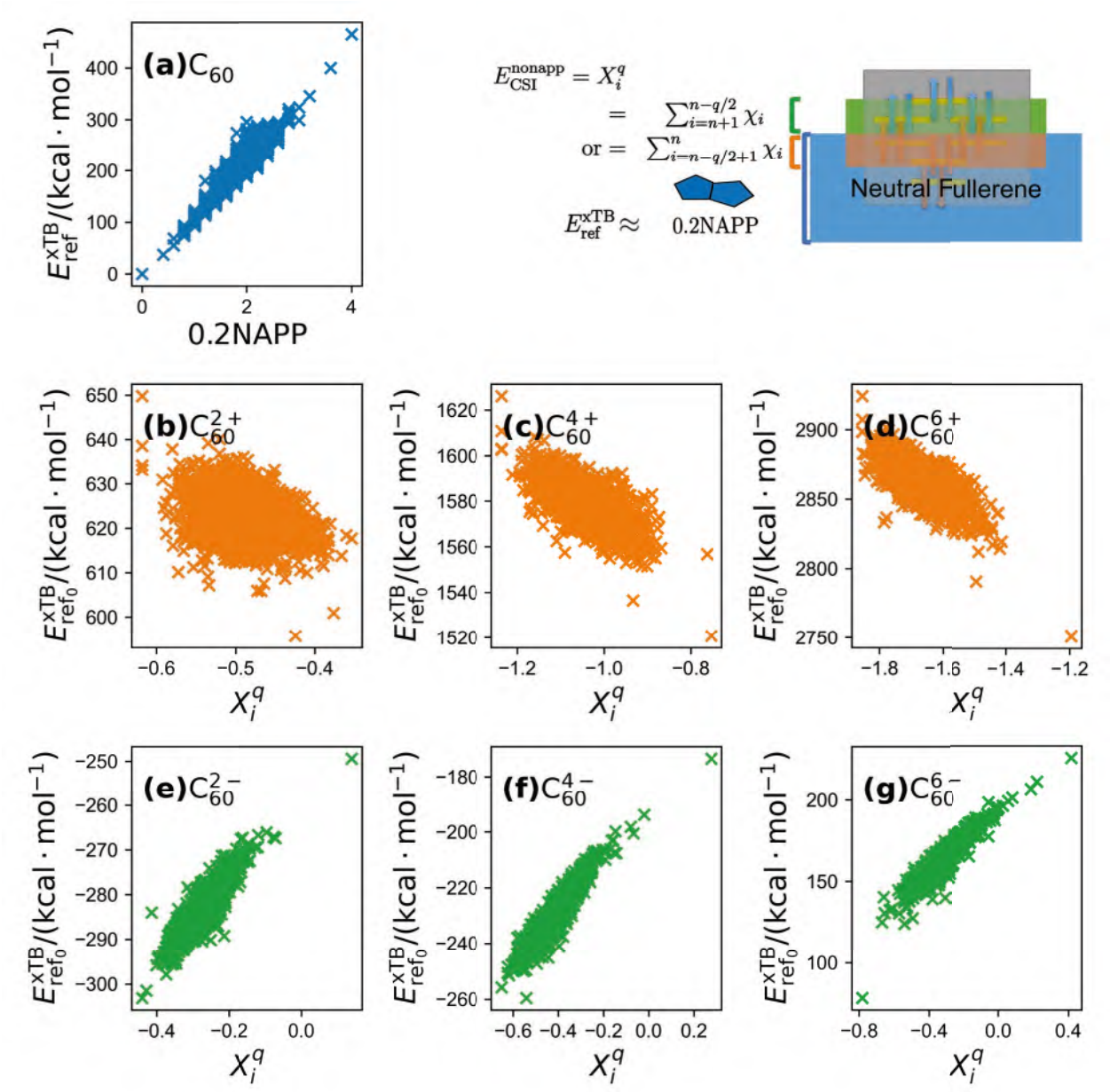


Figure 16: **(a)** Correlation between xTB energies of $C_{60}$ isomers relative to the most stable one and 0.2NAPP. **(b - g)** Correlation between xTB energies relative to the electrically neutral isomers and values of CSI model without NAPP of $C_{60}$ isomers with charge 2+, 4+, 6+, 2-, 4-, 6-, respectively.

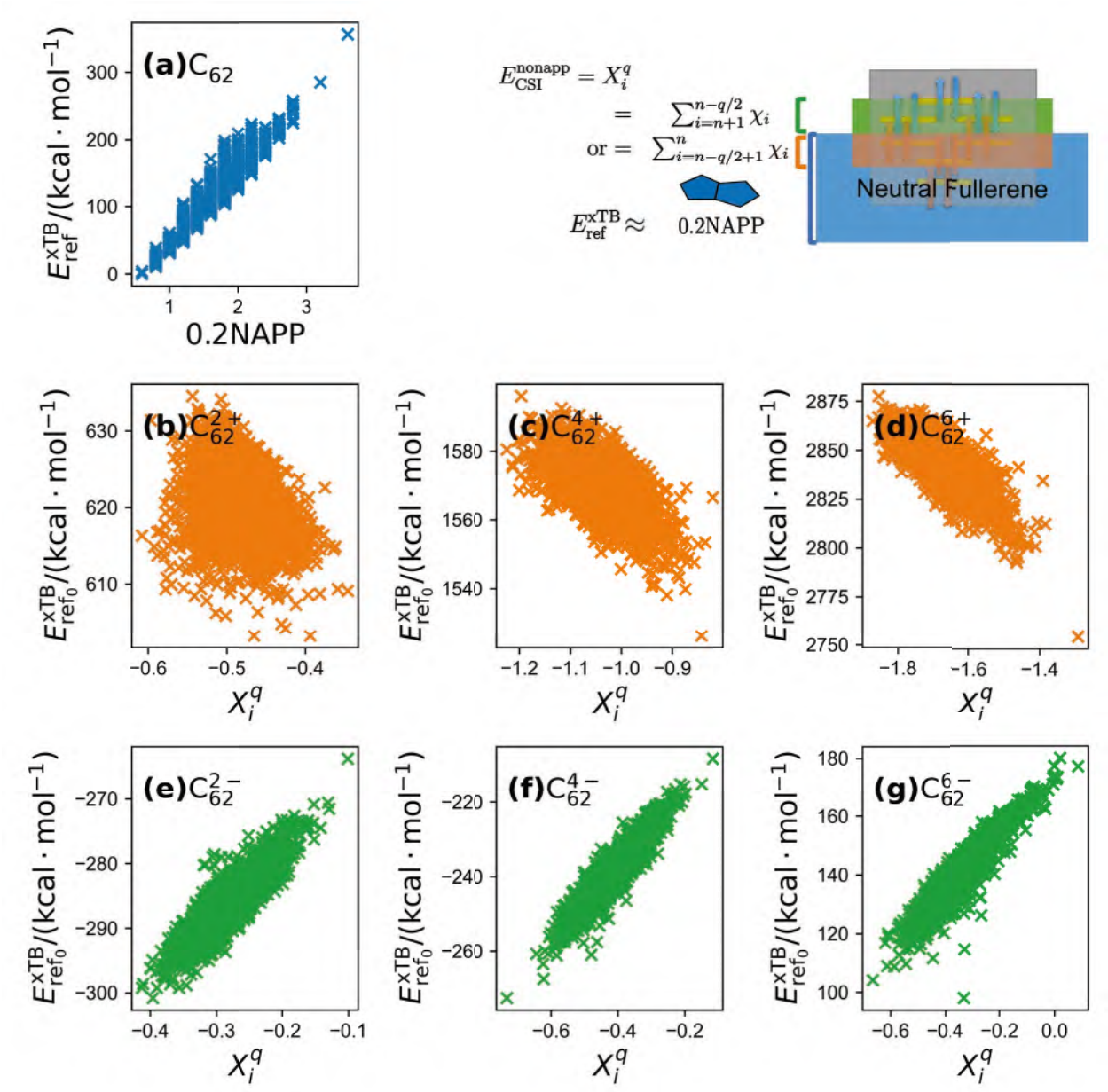


Figure 17: **(a)** Correlation between xTB energies of $C_{62}$ isomers relative to the most stable one and 0.2NAPP. **(b - g)** Correlation between xTB energies relative to the electrically neutral isomers and values of CSI model without NAPP of $C_{62}$ isomers with charge 2+, 4+, 6+, 2-, 4-, 6-, respectively.

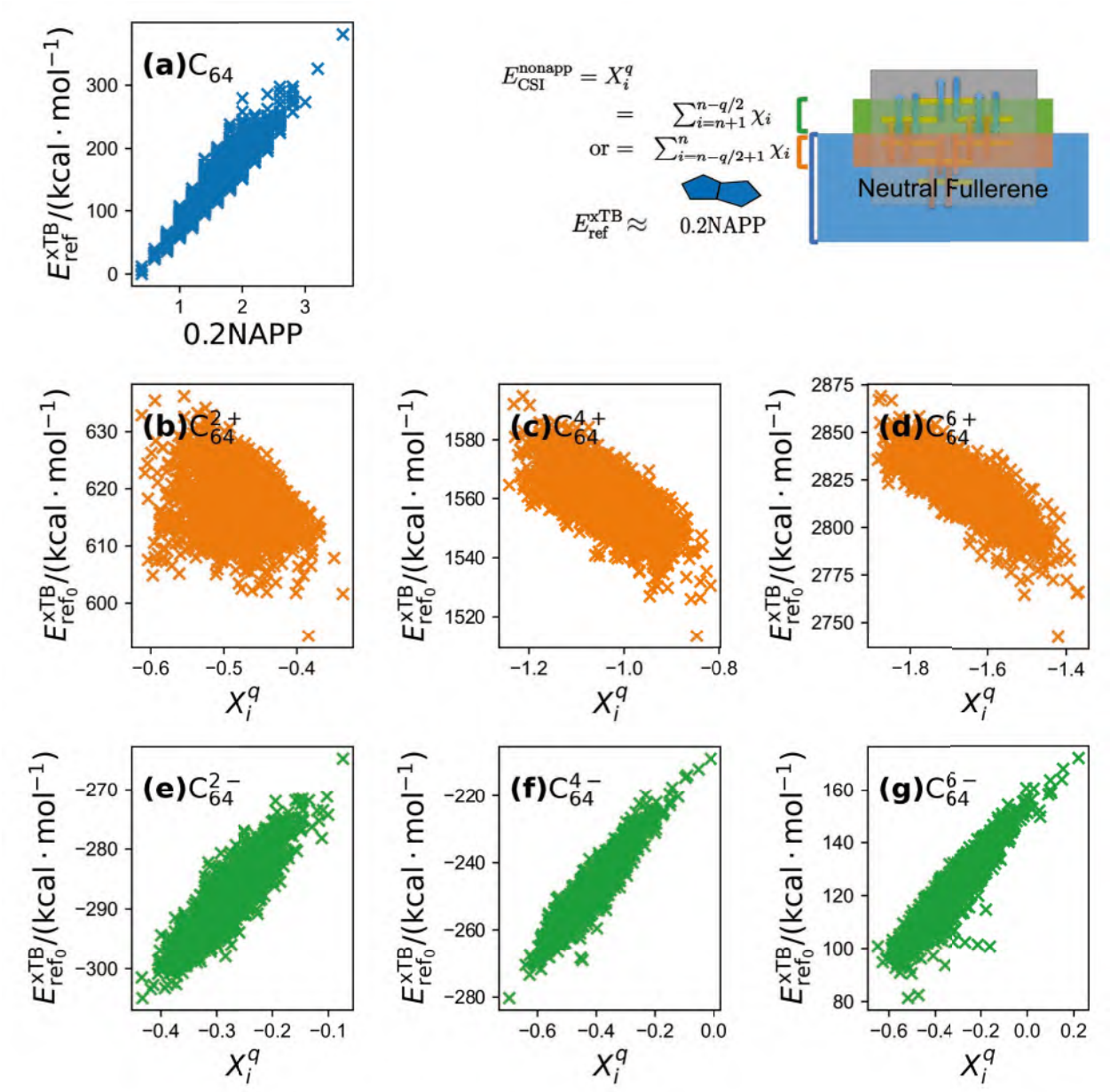


Figure 18: **(a)** Correlation between xTB energies of $C_{64}$ isomers relative to the most stable one and 0.2NAPP. **(b - g)** Correlation between xTB energies relative to the electrically neutral isomers and values of CSI model without NAPP of $C_{64}$ isomers with charge 2+, 4+, 6+, 2-, 4-, 6-, respectively.

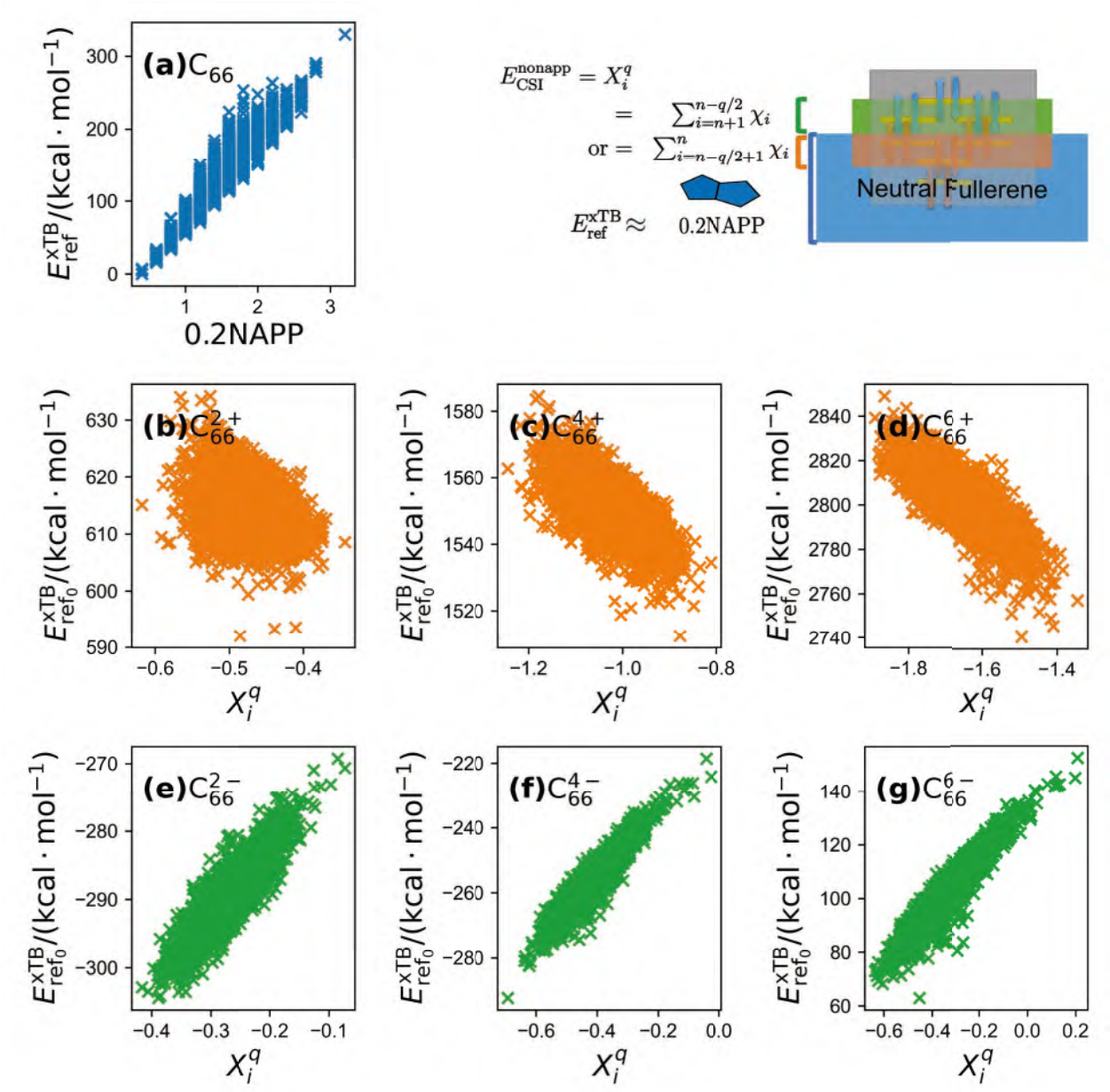


Figure 19: **(a)** Correlation between xTB energies of $C_{66}$ isomers relative to the most stable one and 0.2NAPP. **(b - g)** Correlation between xTB energies relative to the electrically neutral isomers and values of CSI model without NAPP of $C_{66}$ isomers with charge 2+, 4+, 6+, 2-, 4-, 6-, respectively.

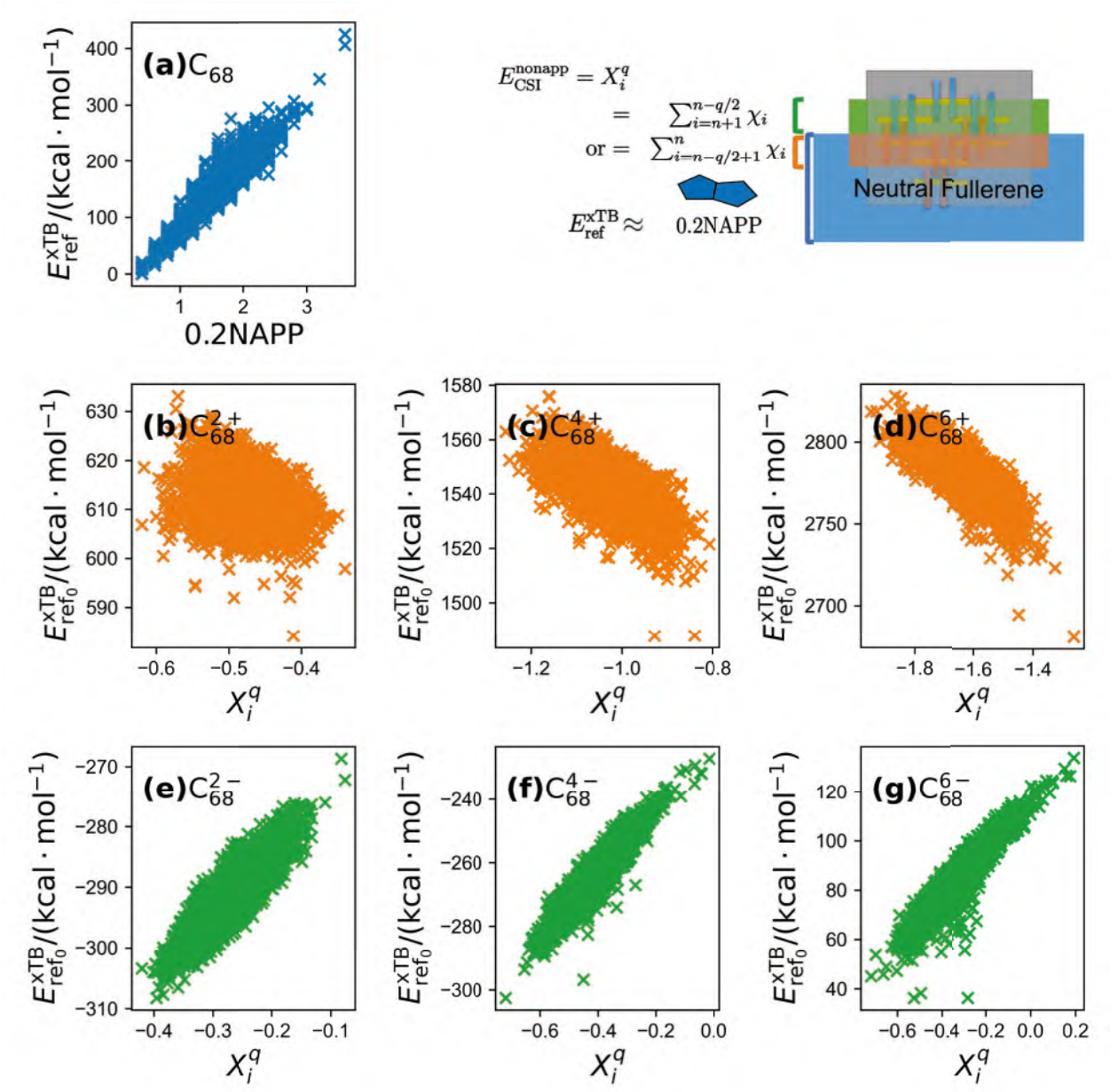


Figure 20: **(a)** Correlation between xTB energies of $C_{68}$ isomers relative to the most stable one and 0.2NAPP. **(b - g)** Correlation between xTB energies relative to the electrically neutral isomers and values of CSI model without NAPP of $C_{68}$ isomers with charge 2+, 4+, 6+, 2-, 4-, 6-, respectively.

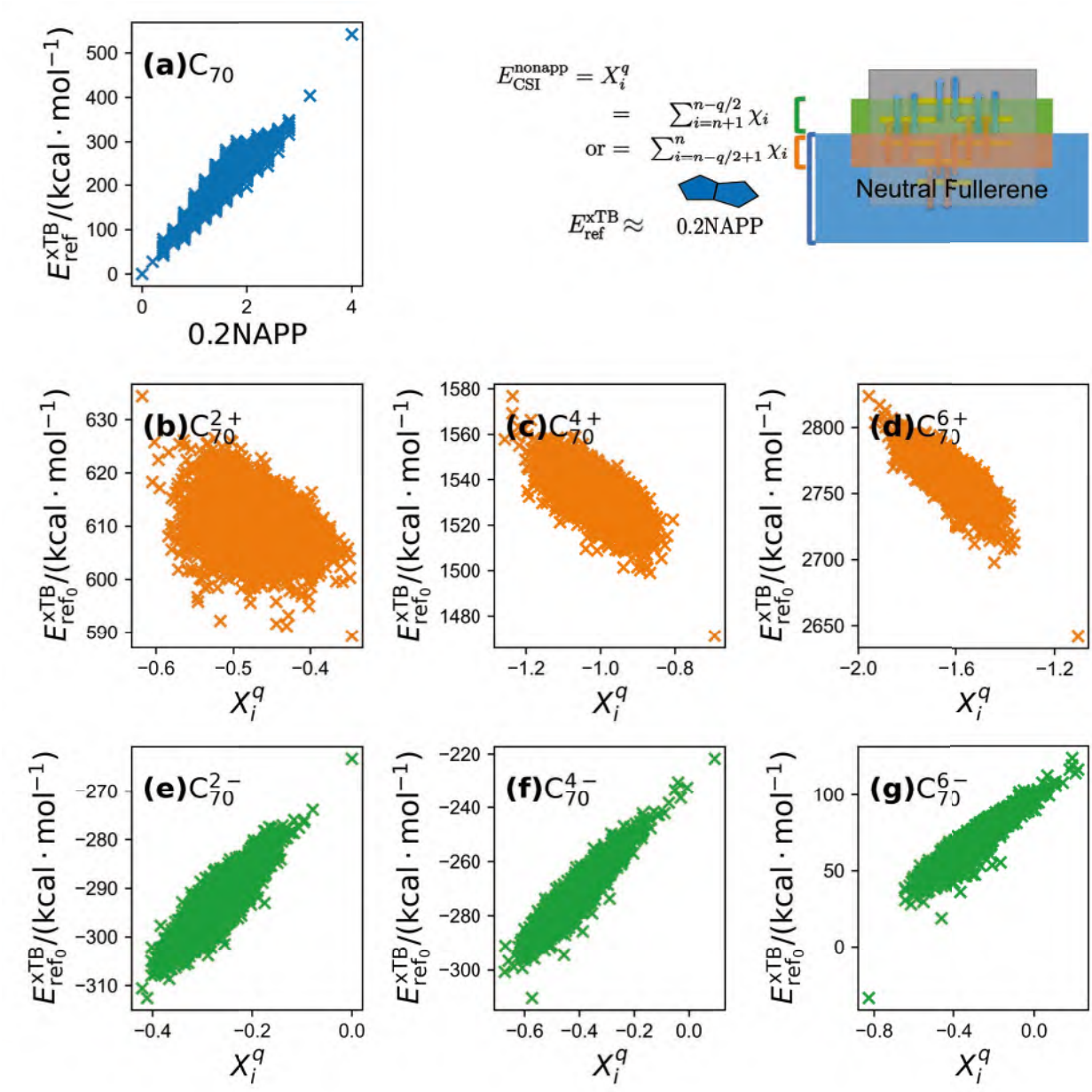


Figure 21: **(a)** Correlation between xTB energies of $C_{70}$ isomers relative to the most stable one and 0.2NAPP. **(b - g)** Correlation between xTB energies relative to the electrically neutral isomers and values of CSI model without NAPP of $C_{70}$ isomers with charge 2+, 4+, 6+, 2-, 4-, 6-, respectively.

# 3 Correlation between xTB energies and prediction by CSI model with NAPP

This section is a reproducing of RefWang et al.[1]. Predictions by CSI model with NAPP are calculated by

$$E_{\mathrm{CSI}}^{\mathrm{nonapp}} \equiv X_i^q + 0.2\mathrm{NAPP} \tag{2}$$

, where

$$X_i^q \equiv \begin{cases} \sum_{k=n-q/2+1}^{n} \chi_{k,i}^q & \text{if } q > 0 \\ \sum_{k=n+1}^{n-q/2} \chi_{k,i}^q & \text{if } q < 0 \end{cases} \tag{3}$$

.

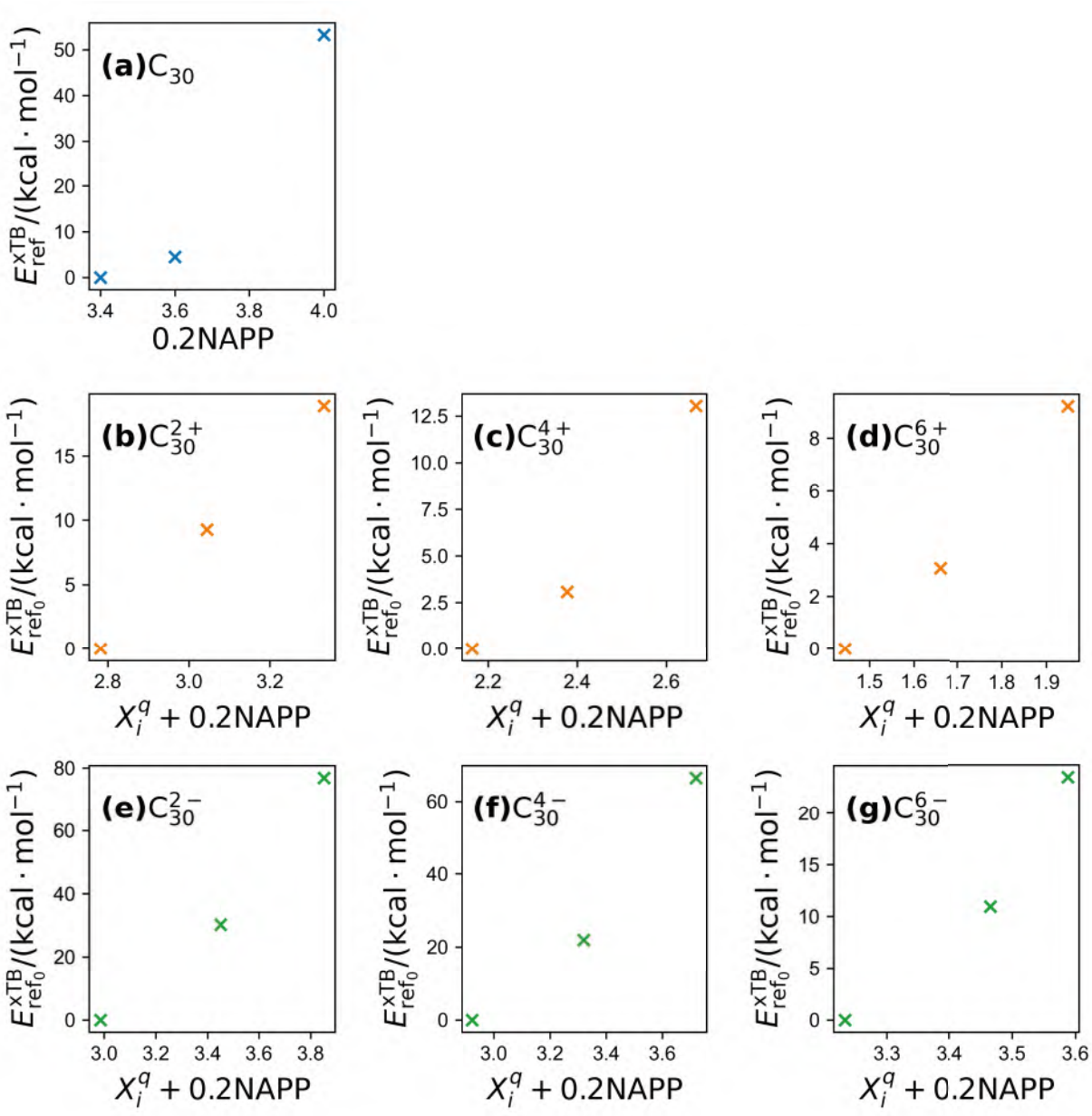


Figure 22: **(a)** Correlation between xTB energies of $C_{30}$ isomers relative to the most stable one and 0.2NAPP. **(b - g)** Correlation between xTB energies relative to the electrically neutral isomers and values of CSI model with NAPP term of $C_{30}$ isomers with charge 2+, 4+, 6+, 2-, 4-, 6-, respectively.

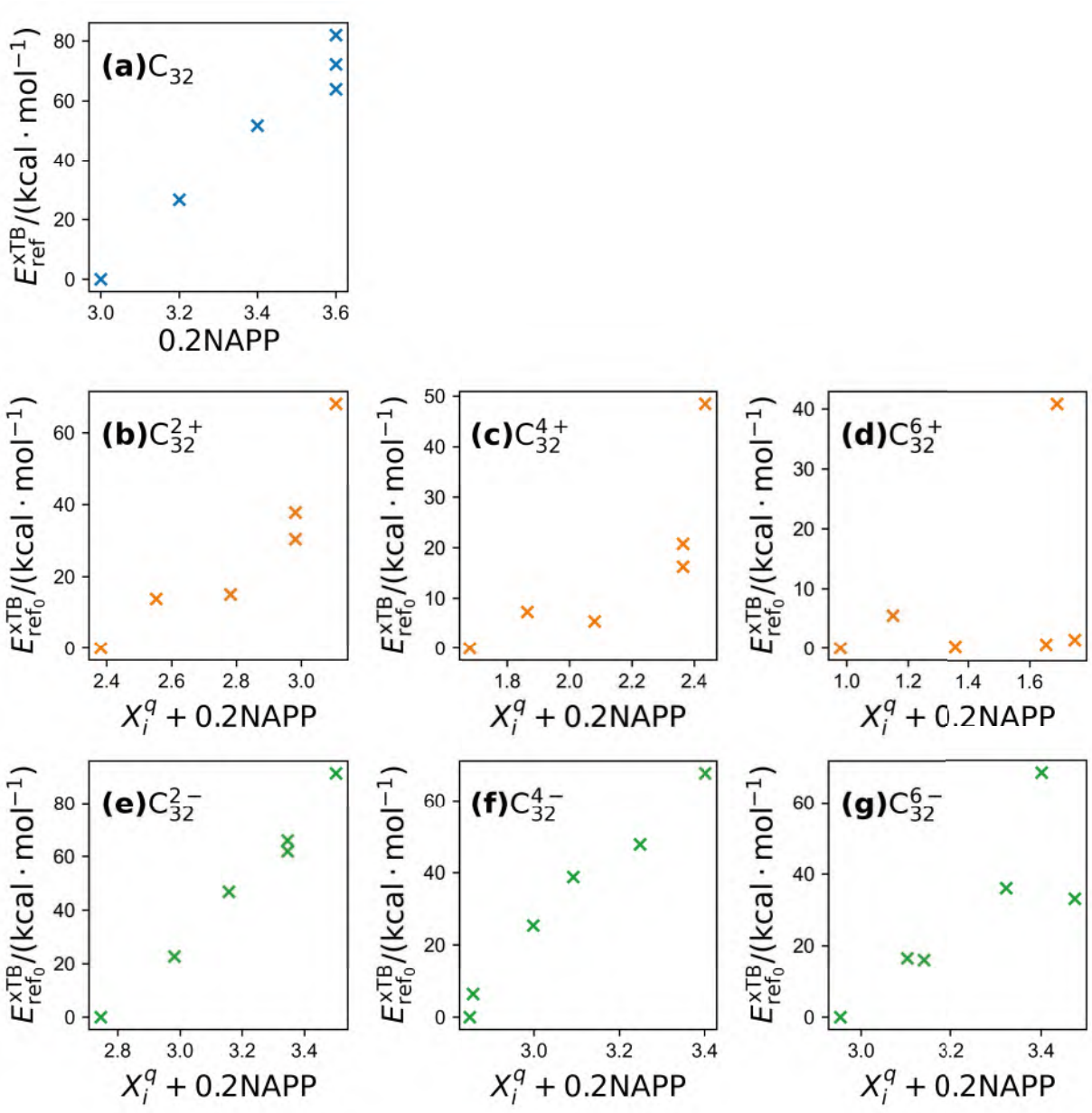


Figure 23: **(a)** Correlation between xTB energies of $C_{32}$ isomers relative to the most stable one and 0.2NAPP. **(b - g)** Correlation between xTB energies relative to the electrically neutral isomers and values of CSI model with NAPP term of $C_{32}$ isomers with charge 2+, 4+, 6+, 2-, 4-, 6-, respectively.

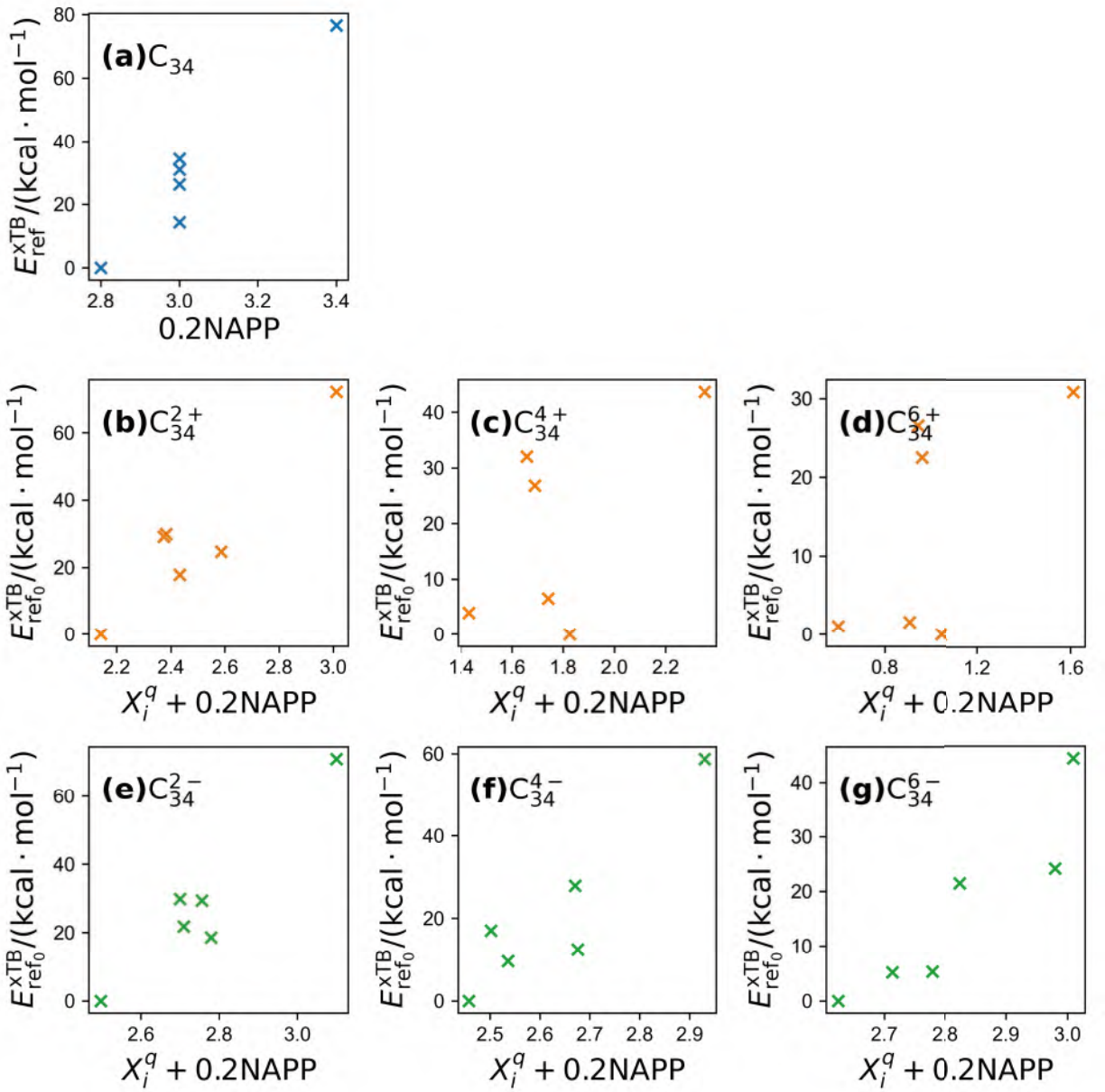


Figure 24: **(a)** Correlation between xTB energies of $C_{34}$ isomers relative to the most stable one and 0.2NAPP. **(b - g)** Correlation between xTB energies relative to the electrically neutral isomers and values of CSI model with NAPP term of $C_{34}$ isomers with charge 2+, 4+, 6+, 2-, 4-, 6-, respectively.

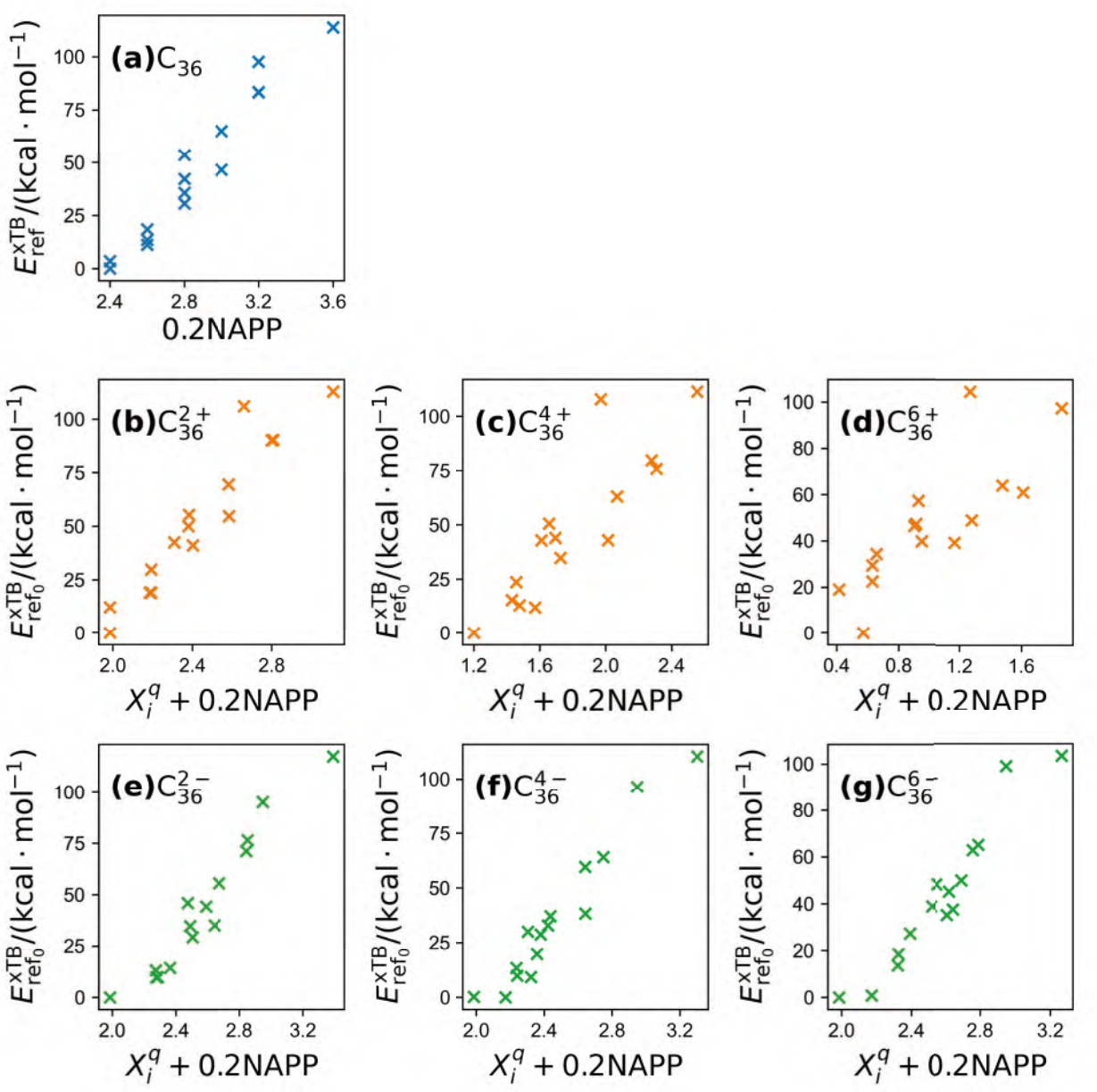


Figure 25: **(a)** Correlation between xTB energies of $C_{36}$ isomers relative to the most stable one and 0.2NAPP. **(b - g)** Correlation between xTB energies relative to the electrically neutral isomers and values of CSI model with NAPP term of $C_{36}$ isomers with charge 2+, 4+, 6+, 2-, 4-, 6-, respectively.

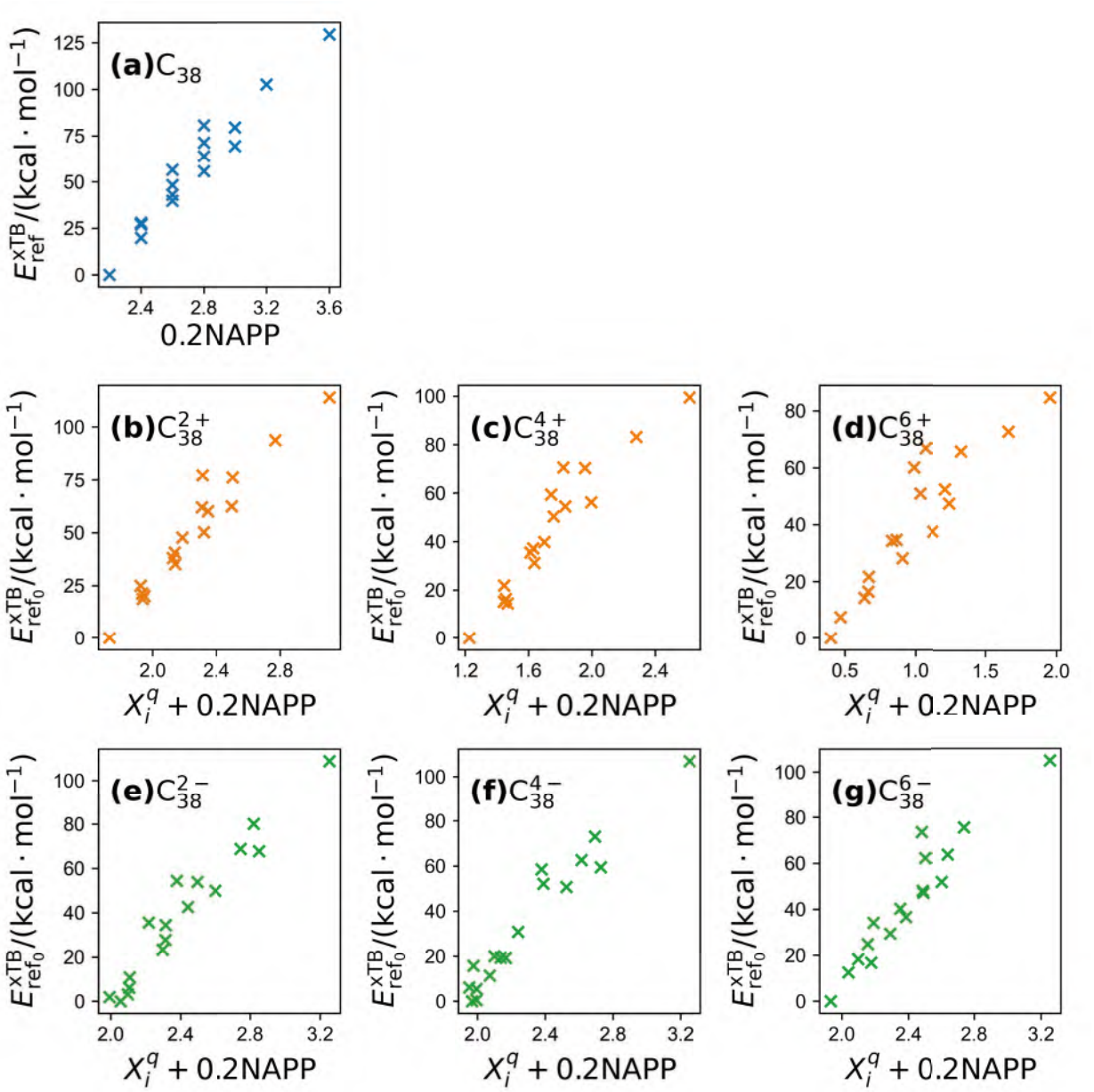


Figure 26: **(a)** Correlation between xTB energies of $C_{38}$ isomers relative to the most stable one and 0.2NAPP. **(b - g)** Correlation between xTB energies relative to the electrically neutral isomers and values of CSI model with NAPP term of $C_{38}$ isomers with charge 2+, 4+, 6+, 2-, 4-, 6-, respectively.

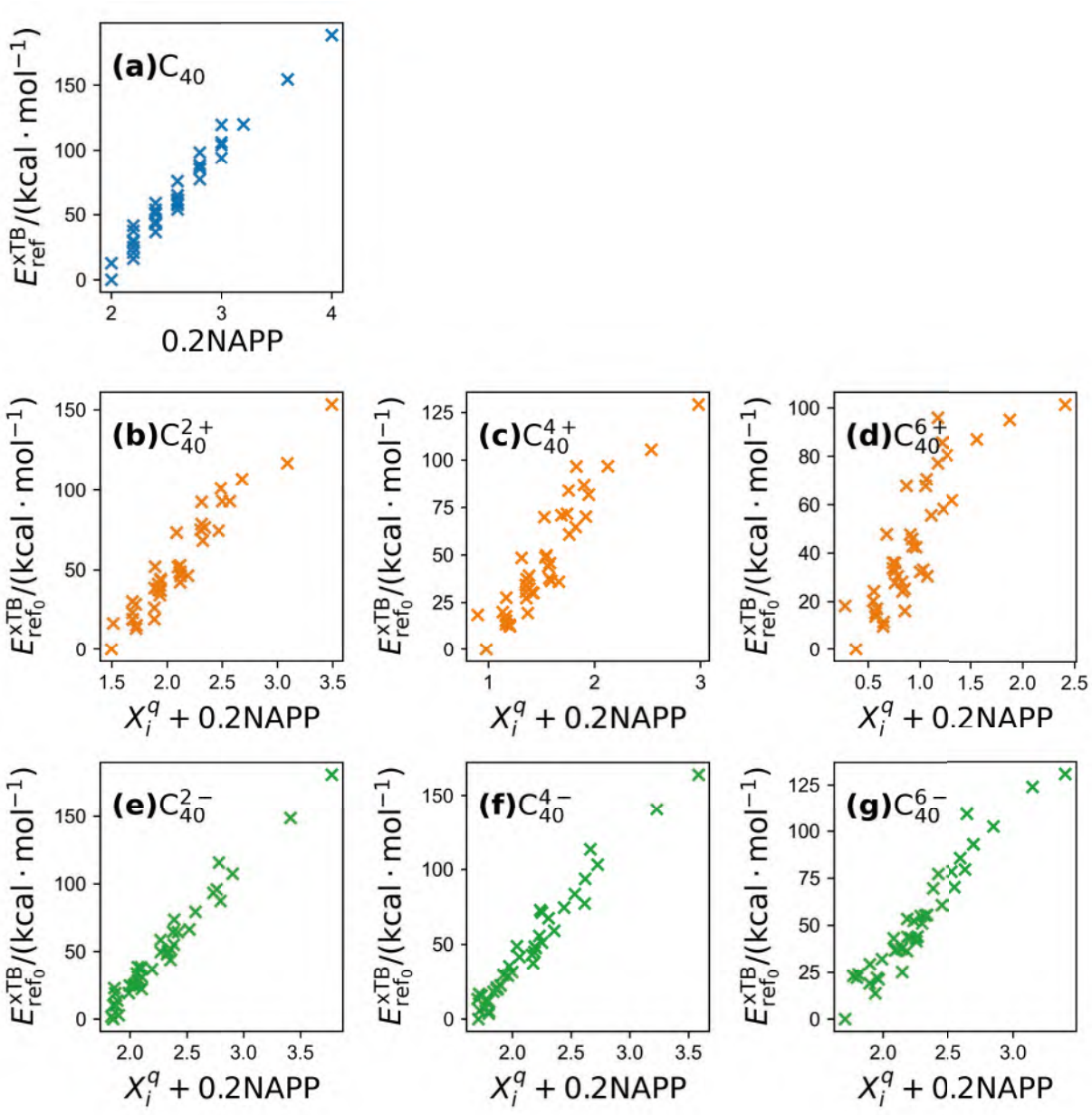


Figure 27: **(a)** Correlation between xTB energies of $C_{40}$ isomers relative to the most stable one and 0.2NAPP. **(b - g)** Correlation between xTB energies relative to the electrically neutral isomers and values of CSI model with NAPP term of $C_{40}$ isomers with charge 2+, 4+, 6+, 2-, 4-, 6-, respectively.

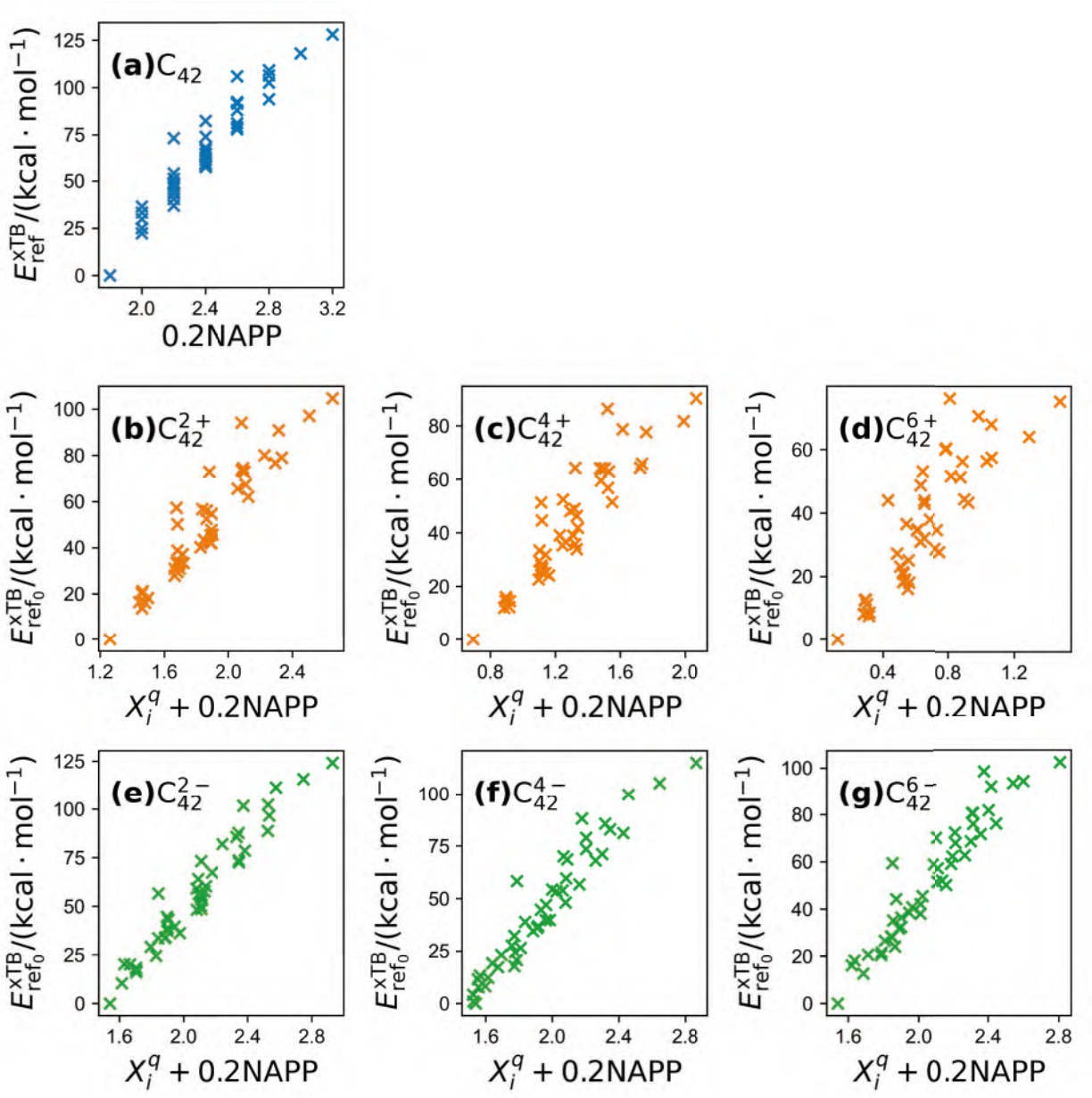


Figure 28: **(a)** Correlation between xTB energies of $C_{42}$ isomers relative to the most stable one and 0.2NAPP. **(b - g)** Correlation between xTB energies relative to the electrically neutral isomers and values of CSI model with NAPP term of $C_{42}$ isomers with charge 2+, 4+, 6+, 2-, 4-, 6-, respectively.

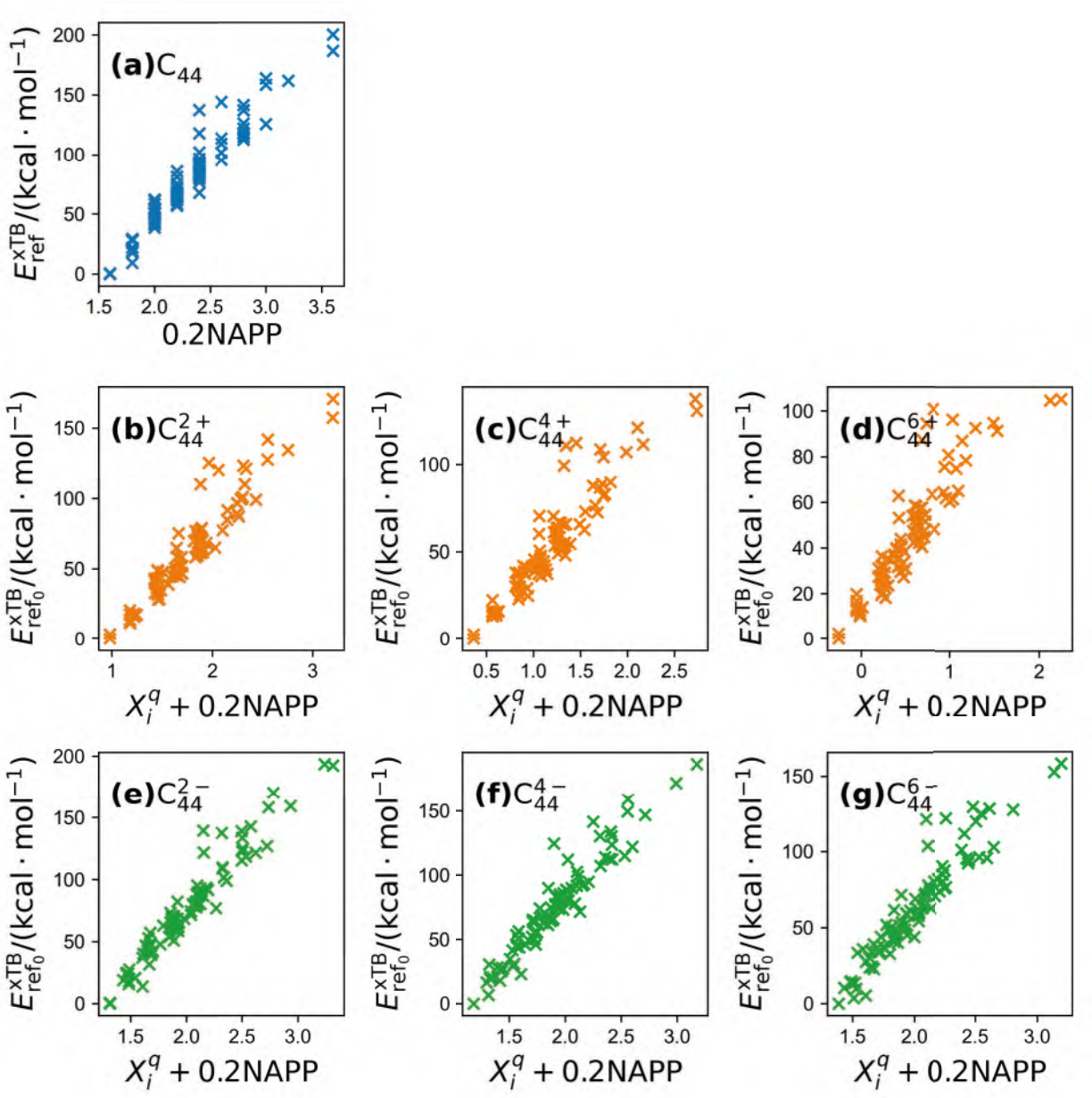


Figure 29: **(a)** Correlation between xTB energies of $C_{44}$ isomers relative to the most stable one and 0.2NAPP. **(b - g)** Correlation between xTB energies relative to the electrically neutral isomers and values of CSI model with NAPP term of $C_{44}$ isomers with charge 2+, 4+, 6+, 2-, 4-, 6-, respectively.

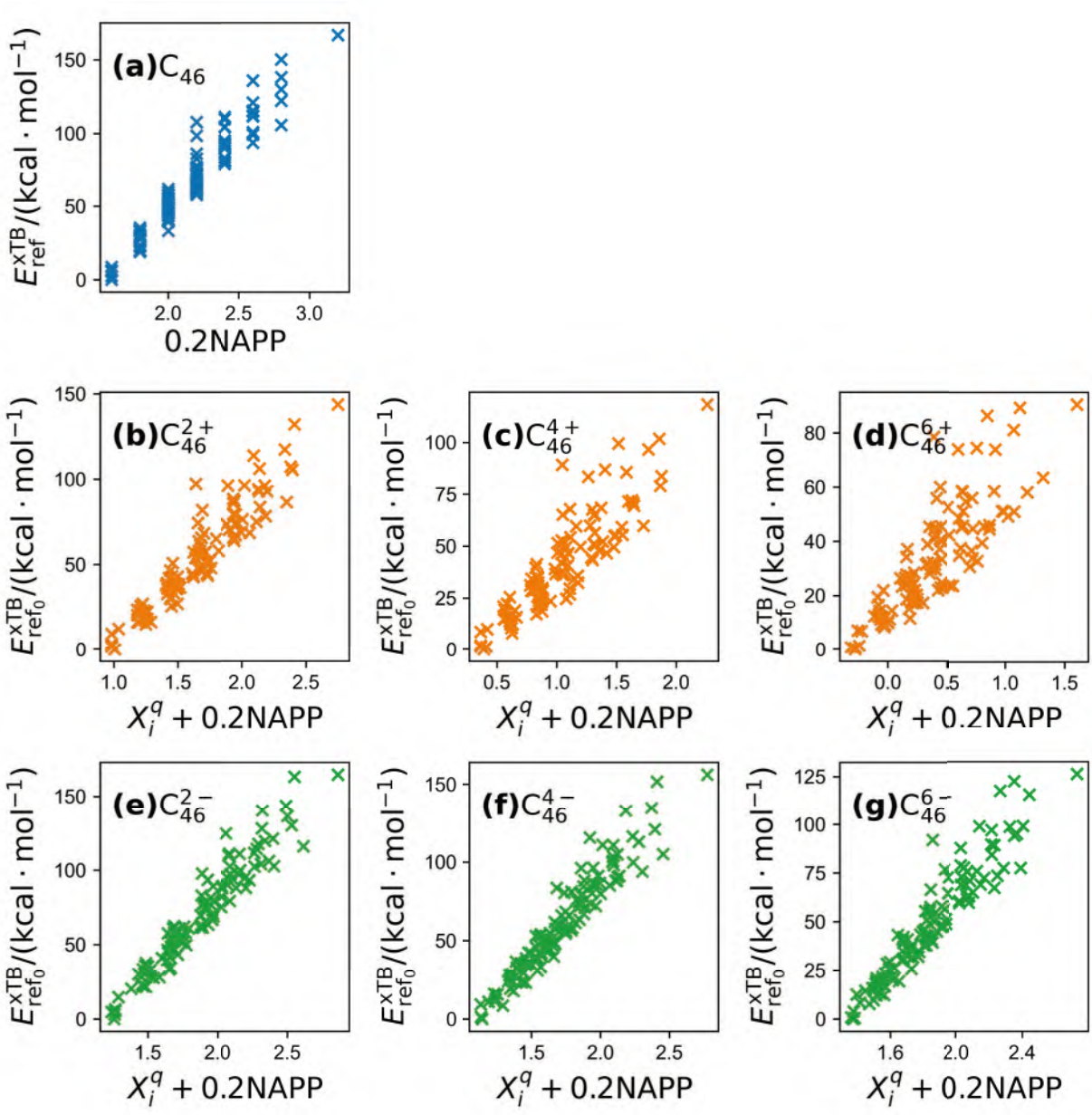


Figure 30: **(a)** Correlation between xTB energies of $C_{46}$ isomers relative to the most stable one and 0.2NAPP. **(b - g)** Correlation between xTB energies relative to the electrically neutral isomers and values of CSI model with NAPP term of $C_{46}$ isomers with charge 2+, 4+, 6+, 2-, 4-, 6-, respectively.

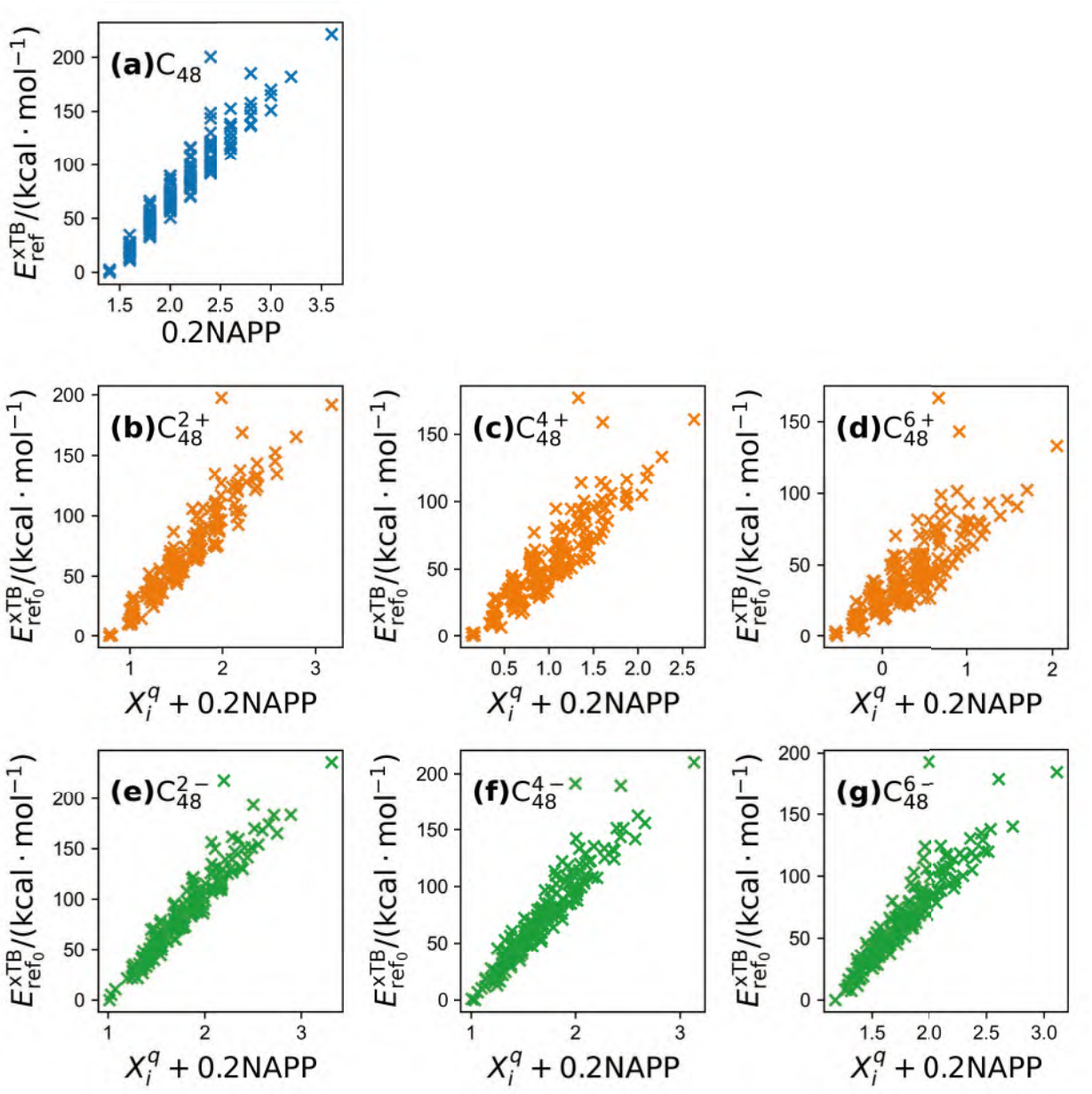


Figure 31: **(a)** Correlation between xTB energies of $C_{48}$ isomers relative to the most stable one and 0.2NAPP. **(b - g)** Correlation between xTB energies relative to the electrically neutral isomers and values of CSI model with NAPP term of $C_{48}$ isomers with charge 2+, 4+, 6+, 2-, 4-, 6-, respectively.

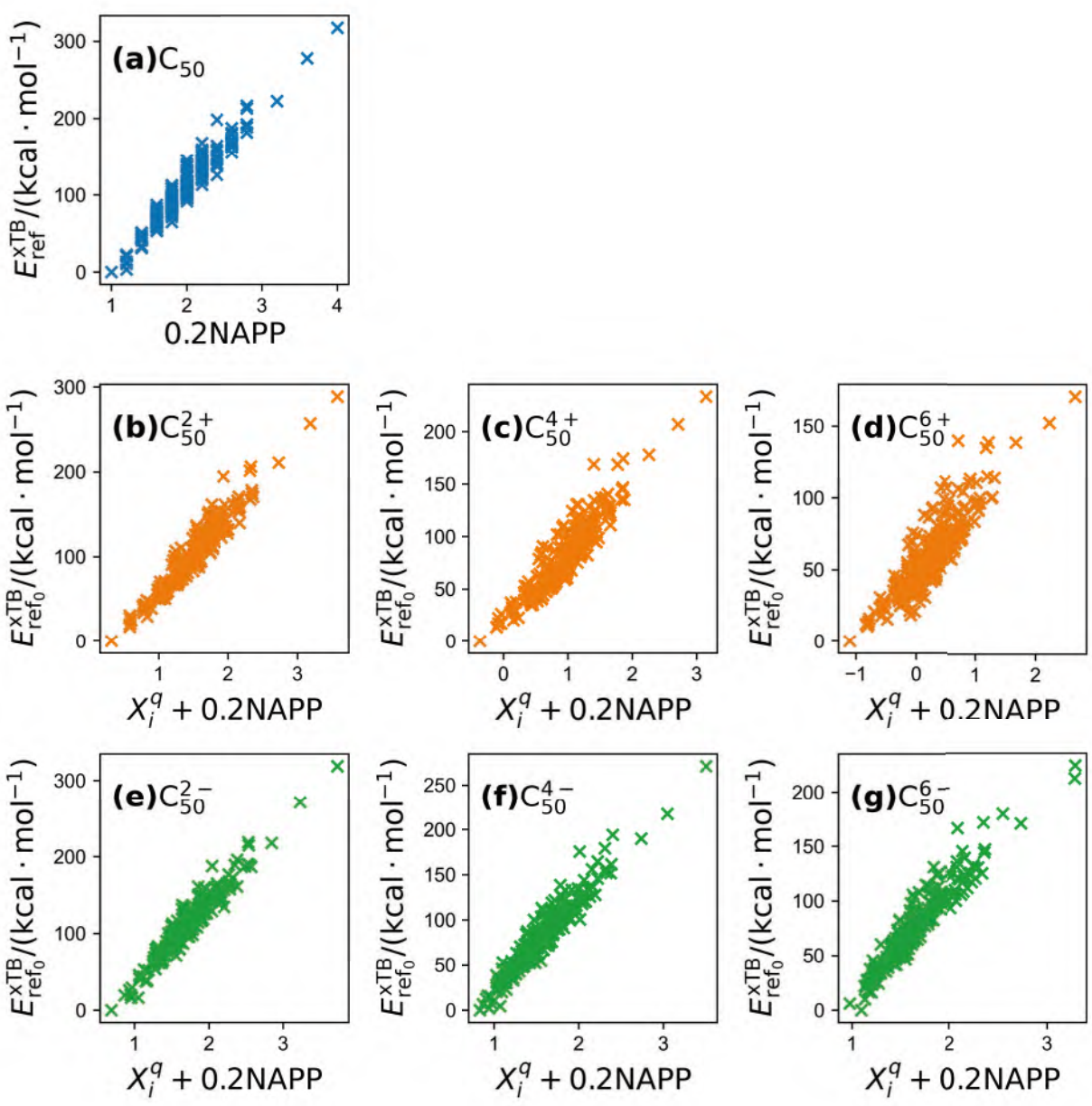


Figure 32: **(a)** Correlation between xTB energies of $C_{50}$ isomers relative to the most stable one and 0.2NAPP. **(b - g)** Correlation between xTB energies relative to the electrically neutral isomers and values of CSI model with NAPP term of $C_{50}$ isomers with charge 2+, 4+, 6+, 2-, 4-, 6-, respectively.

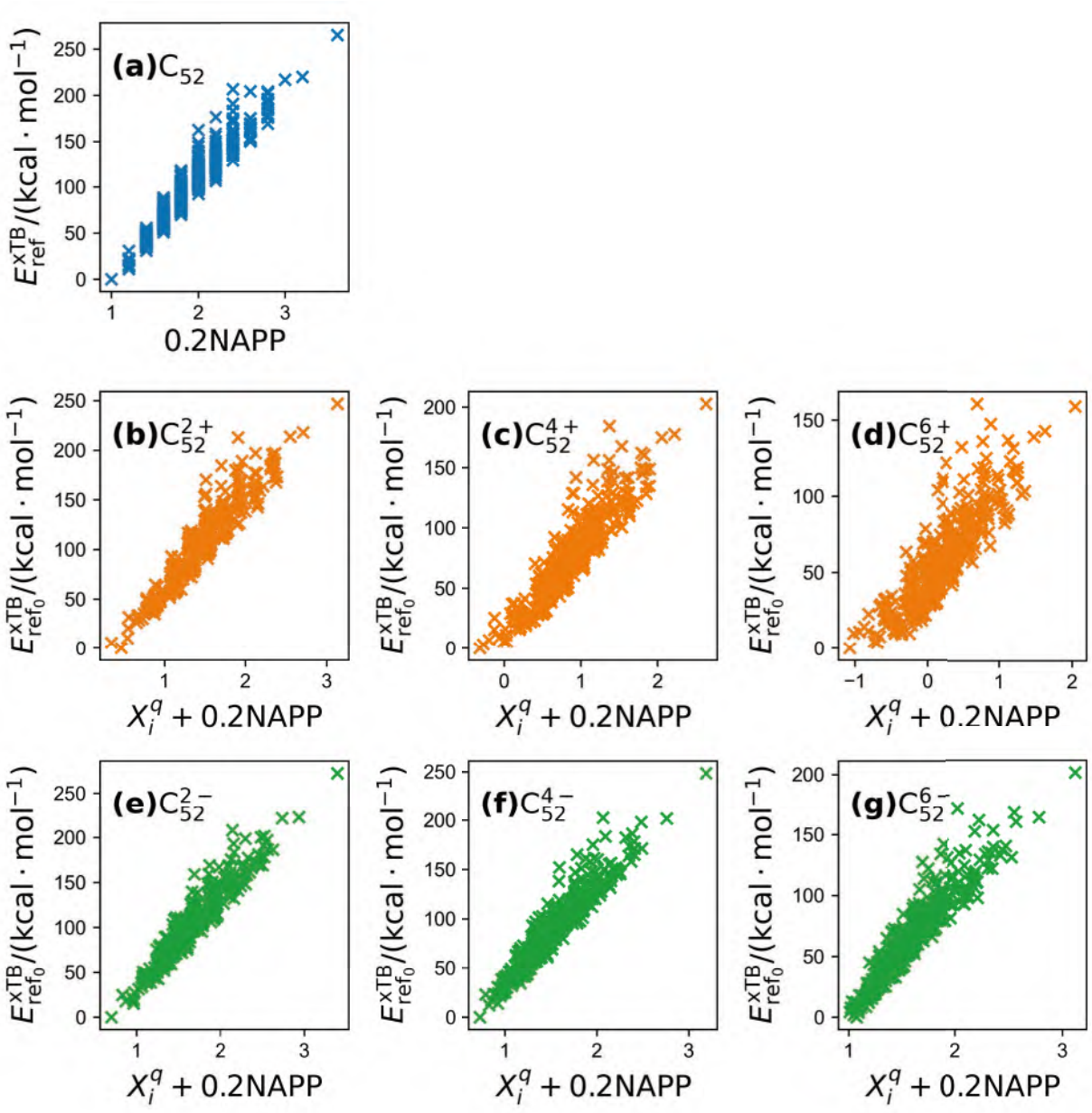


Figure 33: **(a)** Correlation between xTB energies of $C_{52}$ isomers relative to the most stable one and 0.2NAPP. **(b - g)** Correlation between xTB energies relative to the electrically neutral isomers and values of CSI model with NAPP term of $C_{52}$ isomers with charge 2+, 4+, 6+, 2-, 4-, 6-, respectively.

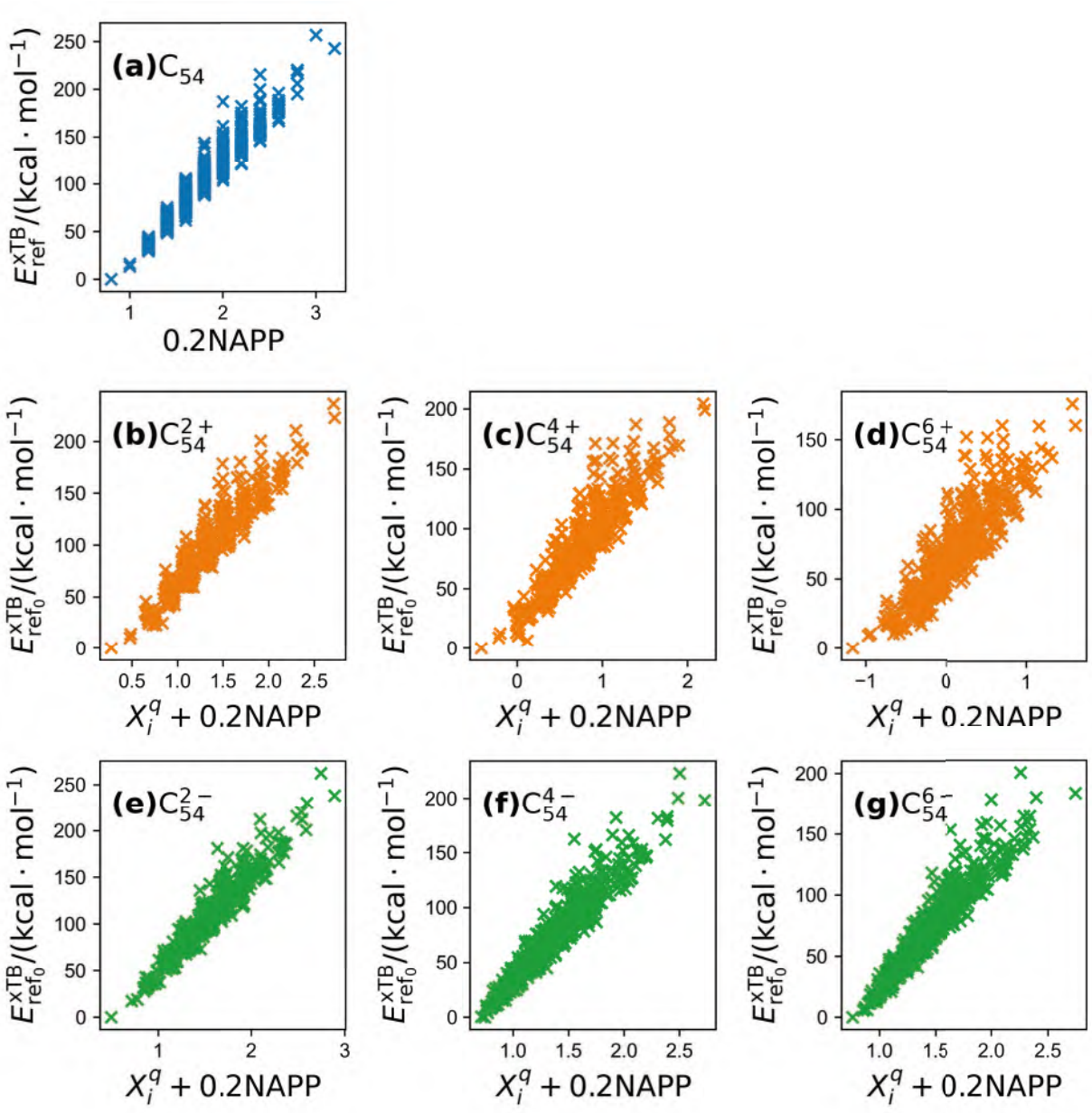


Figure 34: **(a)** Correlation between xTB energies of $C_{54}$ isomers relative to the most stable one and 0.2NAPP. **(b - g)** Correlation between xTB energies relative to the electrically neutral isomers and values of CSI model with NAPP term of $C_{54}$ isomers with charge 2+, 4+, 6+, 2-, 4-, 6-, respectively.

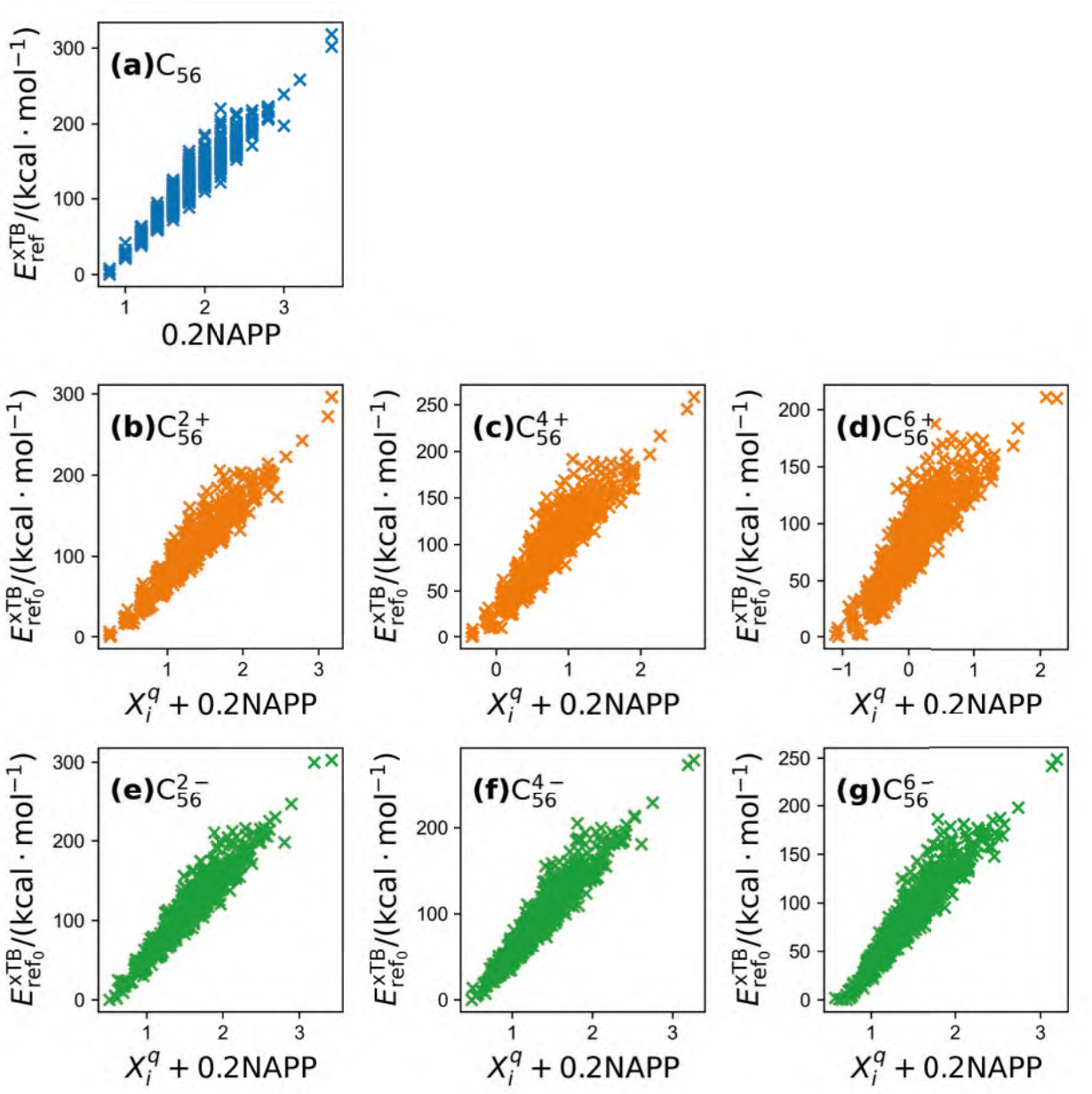


Figure 35: **(a)** Correlation between xTB energies of $C_{56}$ isomers relative to the most stable one and 0.2NAPP. **(b - g)** Correlation between xTB energies relative to the electrically neutral isomers and values of CSI model with NAPP term of $C_{56}$ isomers with charge 2+, 4+, 6+, 2-, 4-, 6-, respectively.

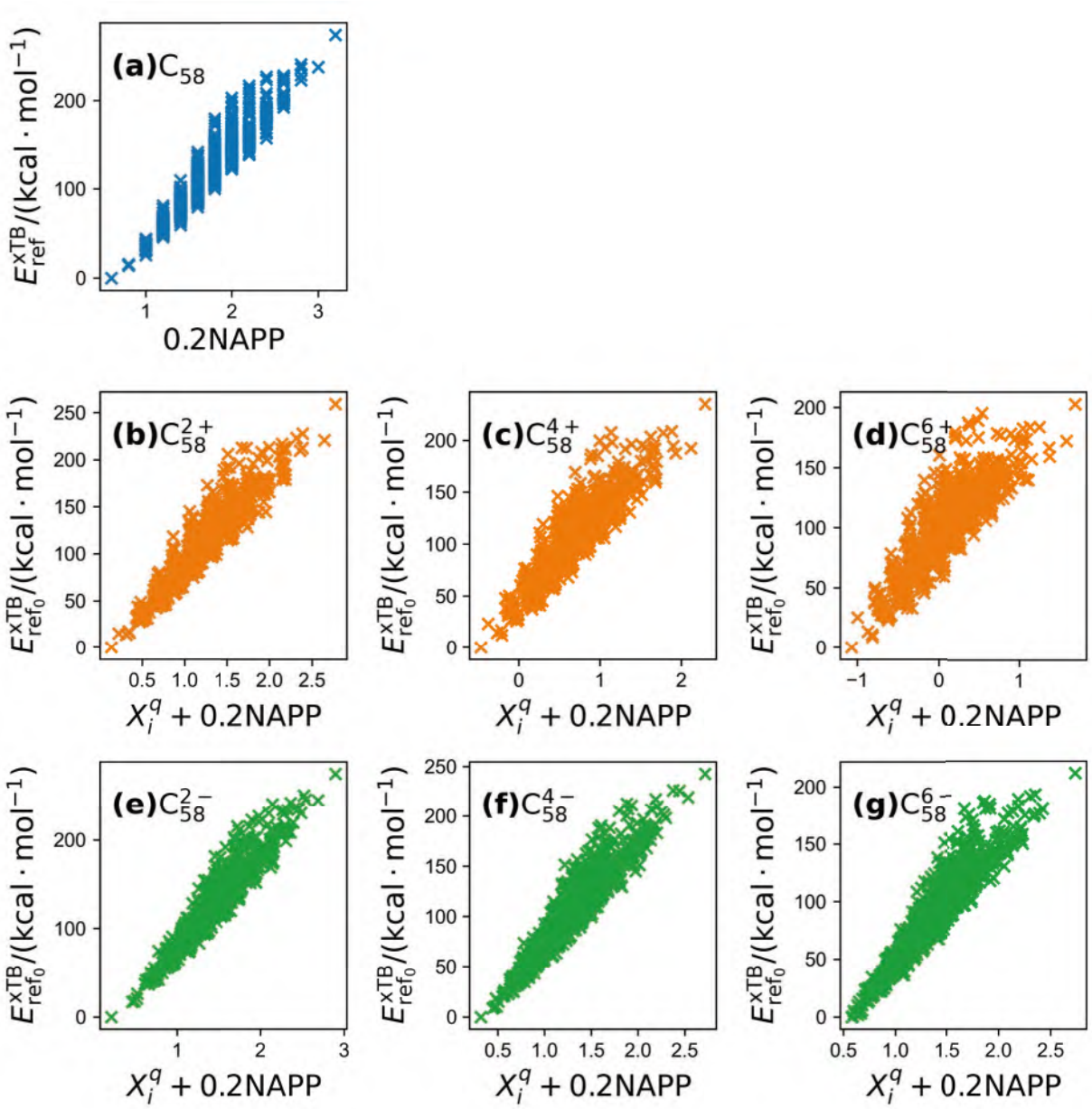


Figure 36: **(a)** Correlation between xTB energies of $C_{58}$ isomers relative to the most stable one and 0.2NAPP. **(b - g)** Correlation between xTB energies relative to the electrically neutral isomers and values of CSI model with NAPP term of $C_{58}$ isomers with charge 2+, 4+, 6+, 2-, 4-, 6-, respectively.

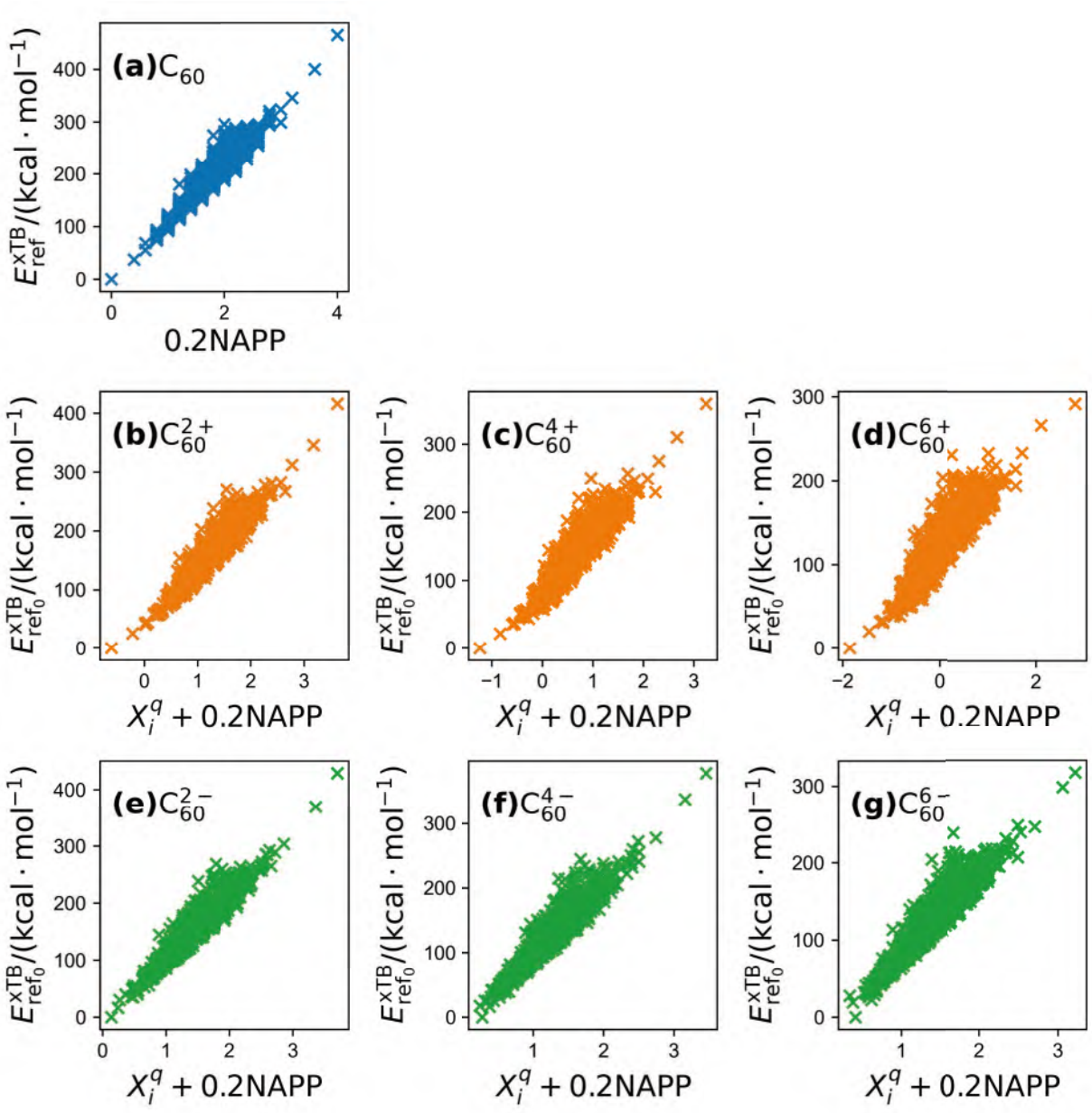


Figure 37: **(a)** Correlation between xTB energies of $C_{60}$ isomers relative to the most stable one and 0.2NAPP. **(b - g)** Correlation between xTB energies relative to the electrically neutral isomers and values of CSI model with NAPP term of $C_{60}$ isomers with charge 2+, 4+, 6+, 2-, 4-, 6-, respectively.

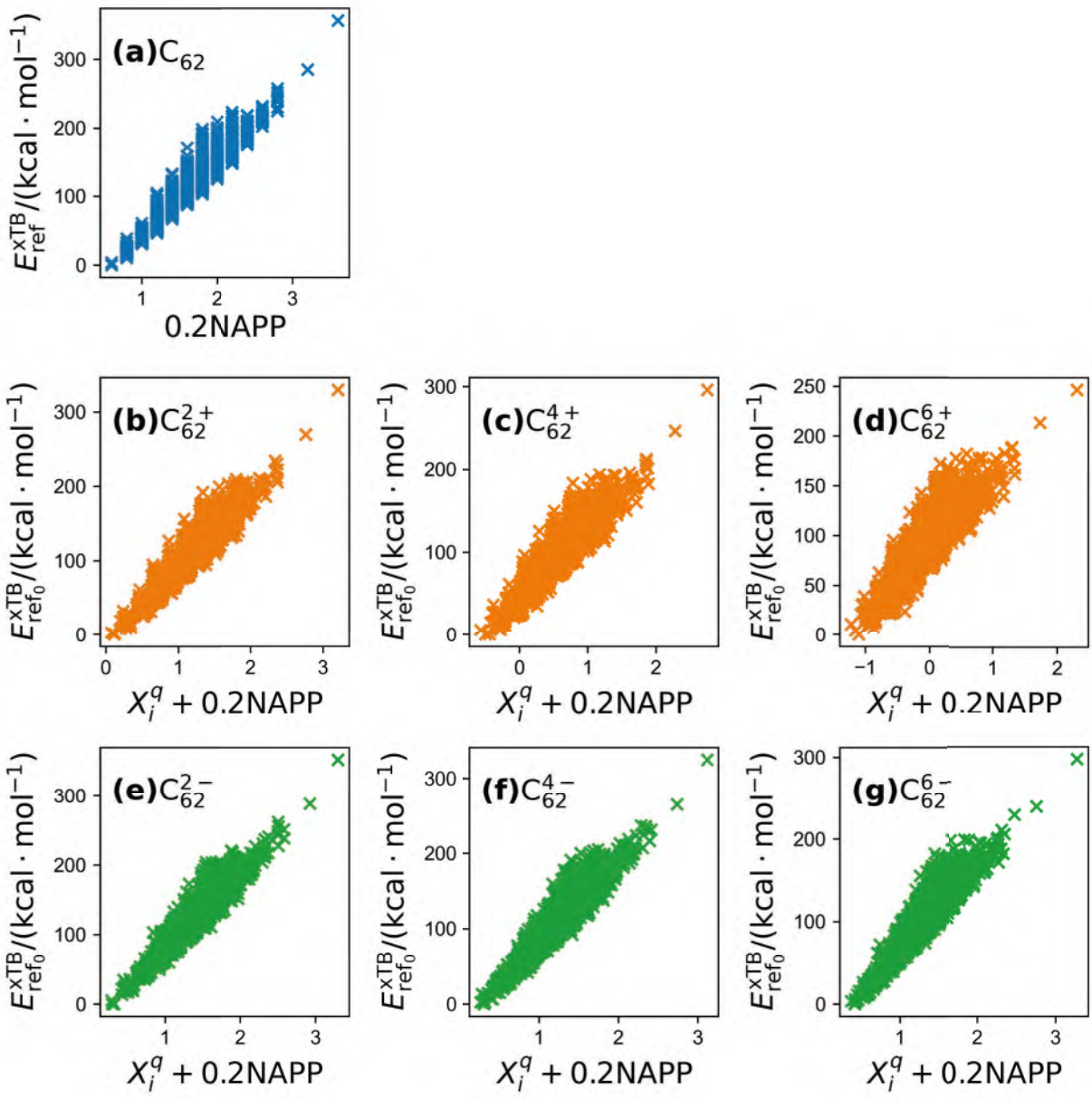


Figure 38: **(a)** Correlation between xTB energies of $C_{62}$ isomers relative to the most stable one and 0.2NAPP. **(b - g)** Correlation between xTB energies relative to the electrically neutral isomers and values of CSI model with NAPP term of $C_{62}$ isomers with charge 2+, 4+, 6+, 2-, 4-, 6-, respectively.

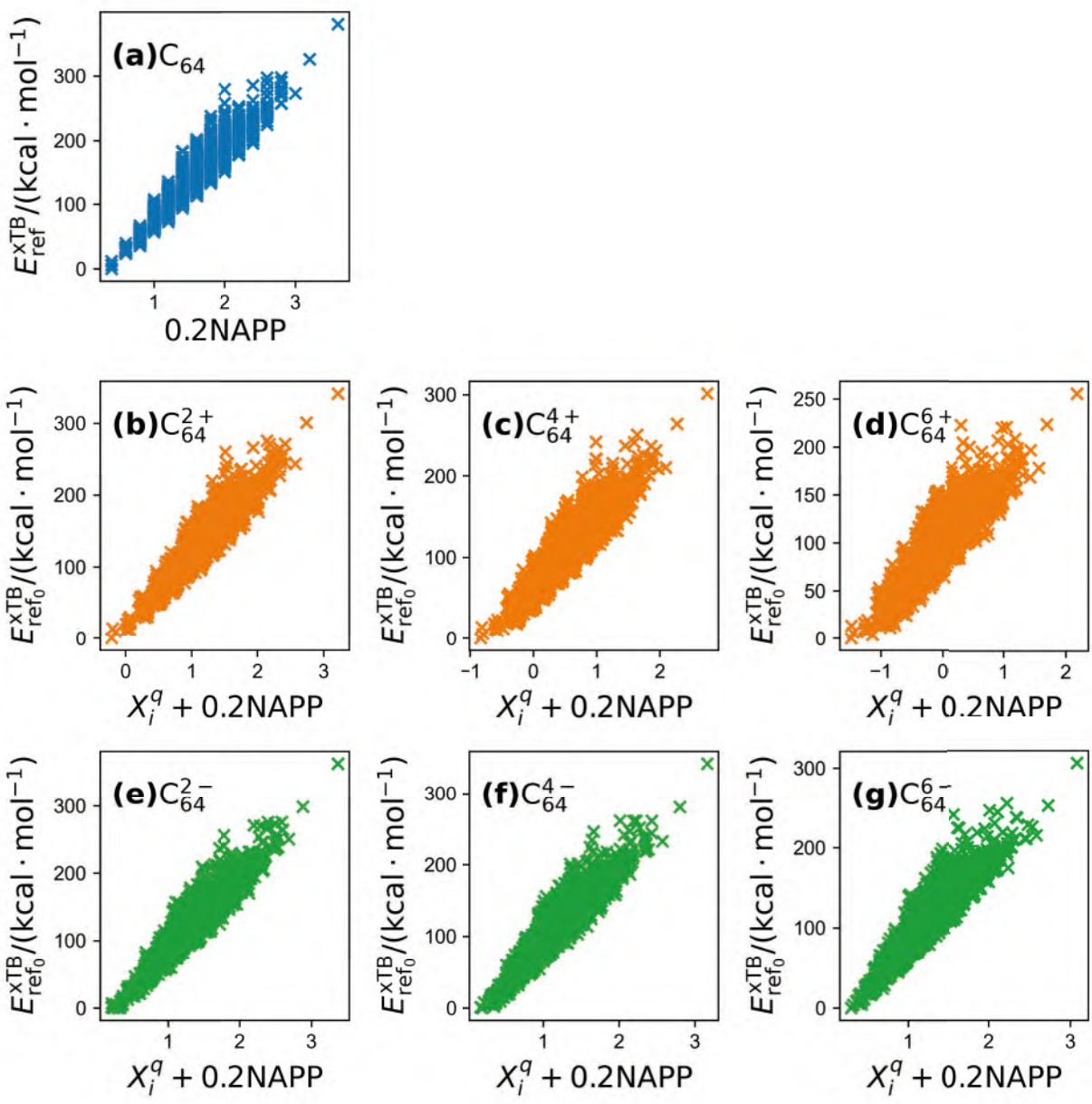


Figure 39: **(a)** Correlation between xTB energies of $C_{64}$ isomers relative to the most stable one and 0.2NAPP. **(b - g)** Correlation between xTB energies relative to the electrically neutral isomers and values of CSI model with NAPP term of $C_{64}$ isomers with charge 2+, 4+, 6+, 2-, 4-, 6-, respectively.

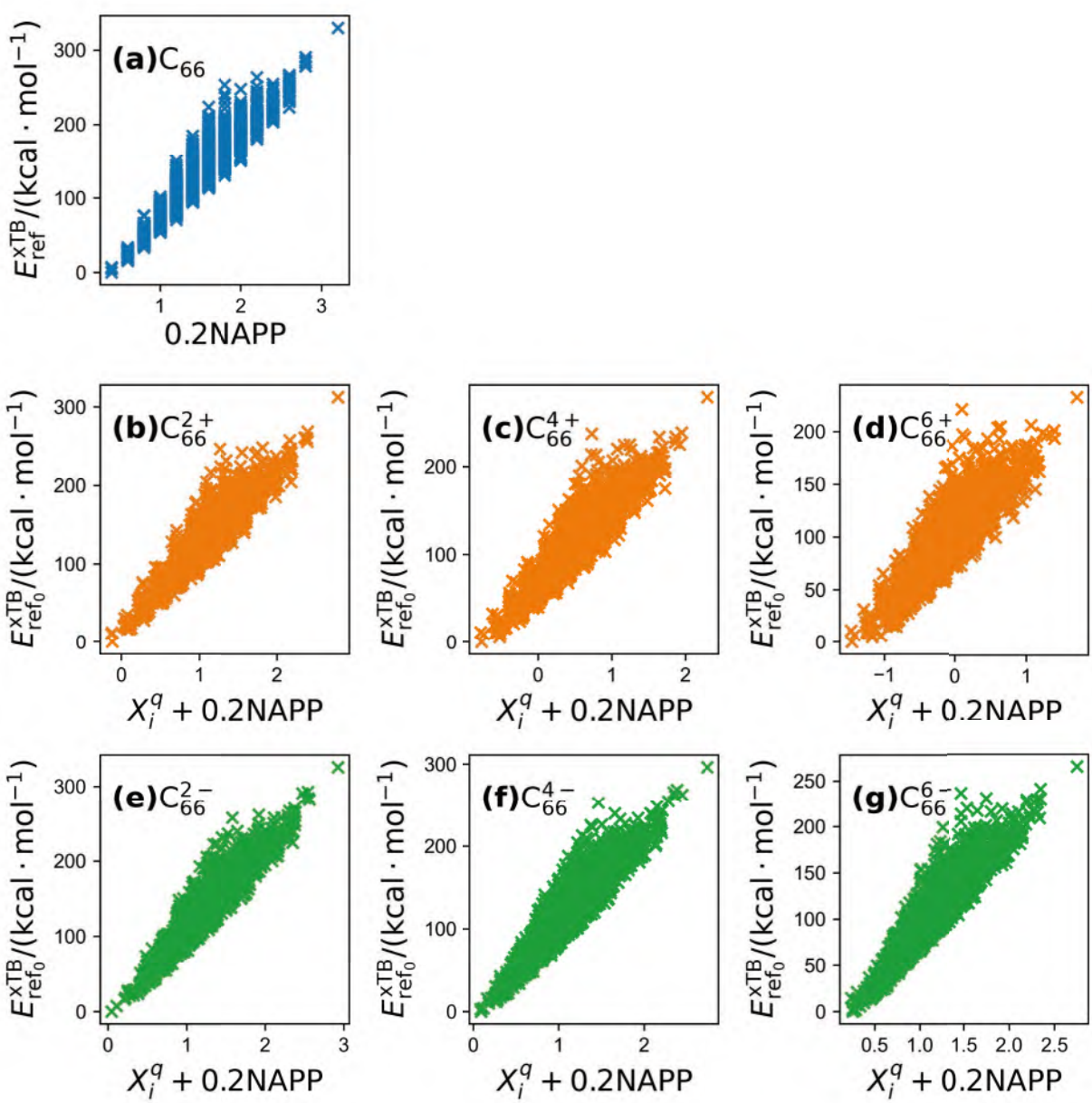


Figure 40: **(a)** Correlation between xTB energies of $C_{66}$ isomers relative to the most stable one and 0.2NAPP. **(b - g)** Correlation between xTB energies relative to the electrically neutral isomers and values of CSI model with NAPP term of $C_{66}$ isomers with charge 2+, 4+, 6+, 2-, 4-, 6-, respectively.

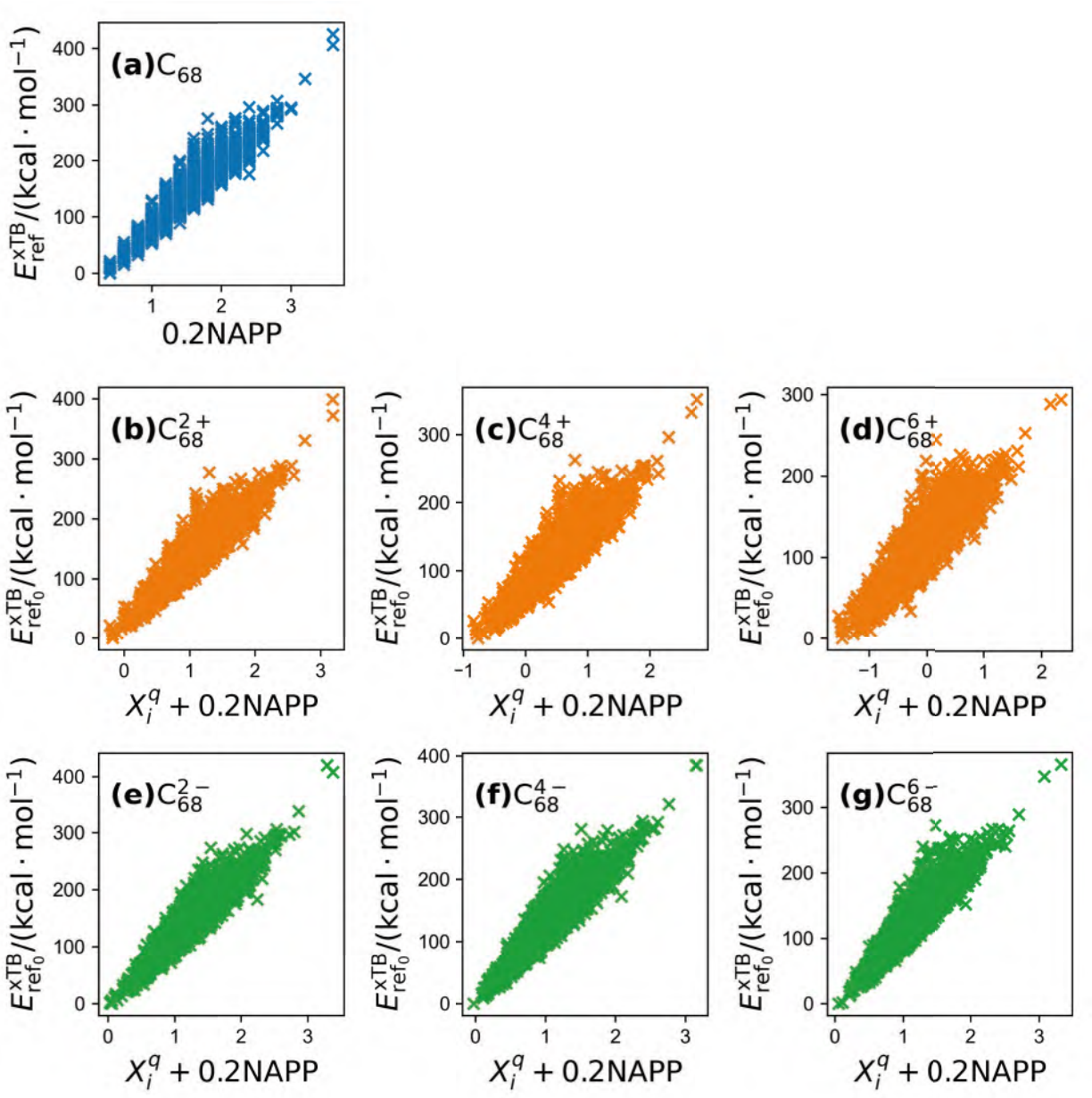


Figure 41: **(a)** Correlation between xTB energies of $C_{68}$ isomers relative to the most stable one and 0.2NAPP. **(b - g)** Correlation between xTB energies relative to the electrically neutral isomers and values of CSI model with NAPP term of $C_{68}$ isomers with charge 2+, 4+, 6+, 2-, 4-, 6-, respectively.

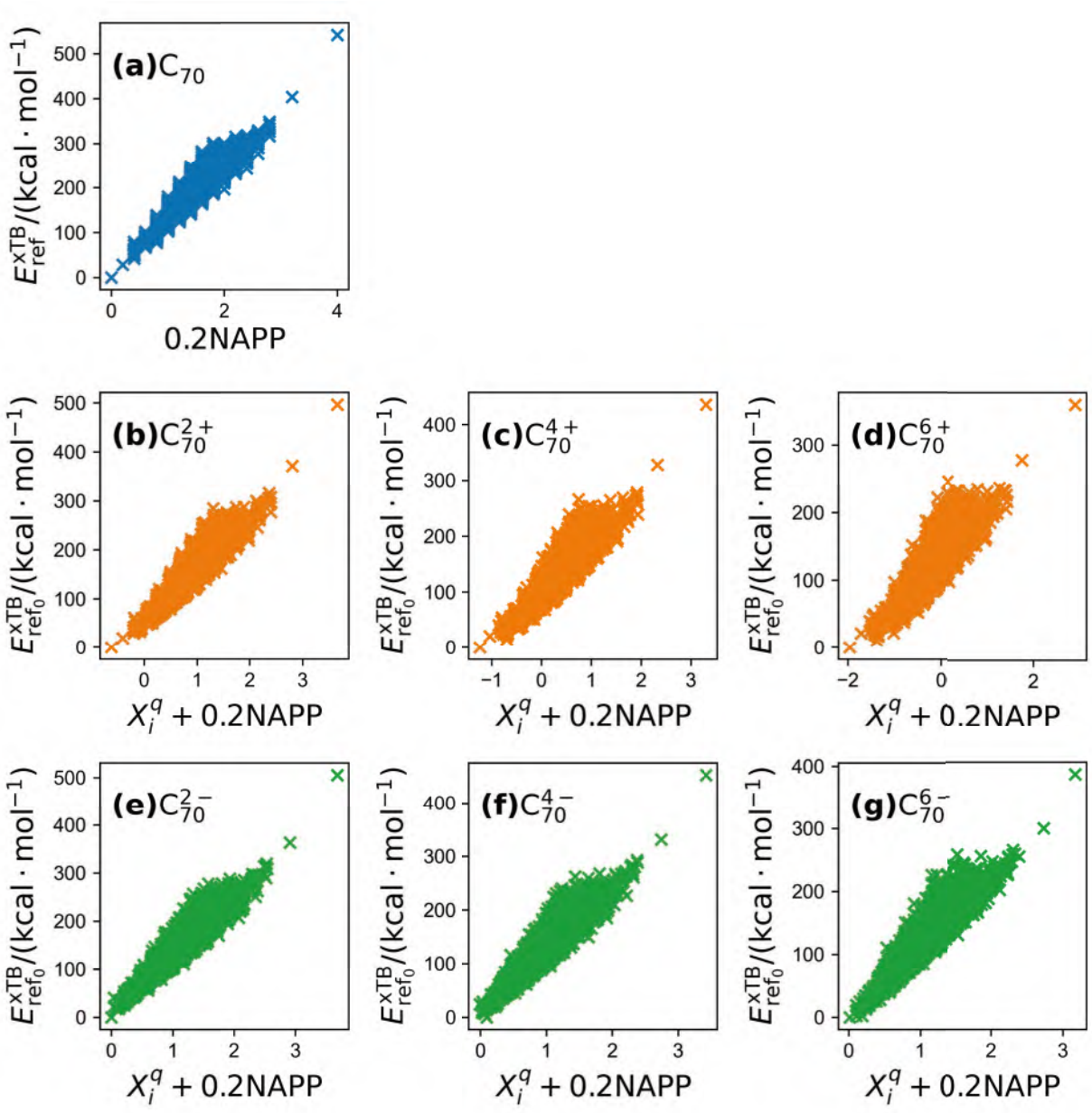


Figure 42: **(a)** Correlation between xTB energies of $C_{70}$ isomers relative to the most stable one and 0.2NAPP. **(b - g)** Correlation between xTB energies relative to the electrically neutral isomers and values of CSI model with NAPP term of $C_{70}$ isomers with charge 2+, 4+, 6+, 2-, 4-, 6-, respectively.

# 4 Correlation between xTB energies and prediction by XCSI model with angles but without distances

Predictions by XCSI model with angles but without distances are calculated by

$$E_{\mathrm{XCSI}}^{\mathrm{angle,nodis}} \equiv \sum_{k=i}^{n} \chi_{k,i}^{q}(\theta) \tag{4}$$

where $\chi_{k,i}^{q}$ is eigenvalues of extended adjacency matrix, whose elements are

$$h_{ij}^{k} = \begin{cases} \cos\theta_{ij}\beta' & i,j\text{are neighbors} \\ 0 & \text{others} \end{cases} \tag{5}$$

.

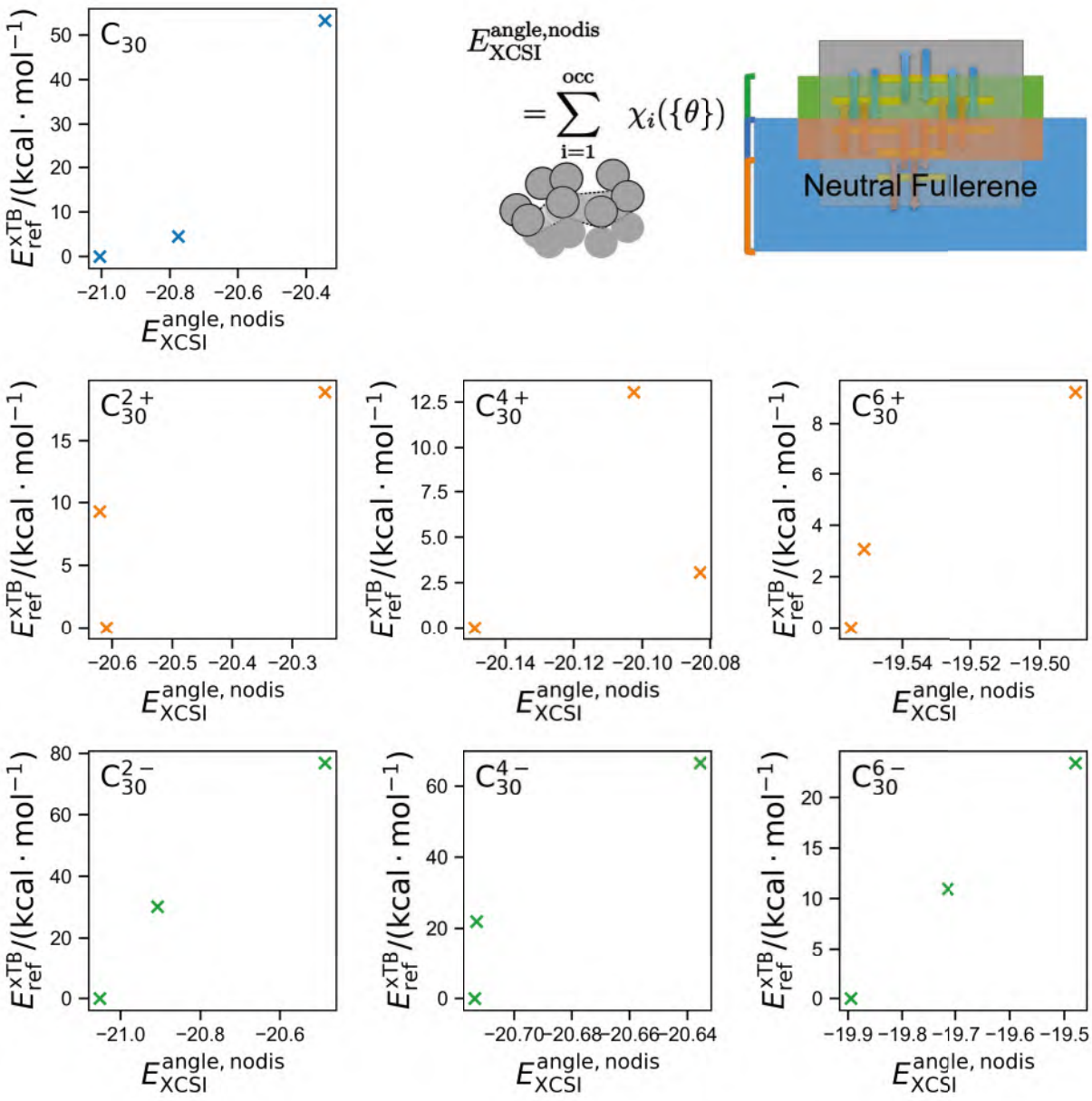


Figure 43: Correlation between xTB energies of $C_{30}$ isomers relative to the most stable one and prediction by XCSI model with angles but without distances of $C_{30}$ isomers without and with charge 2+, 4+, 6+, 2-, 4-, 6-, respectively.

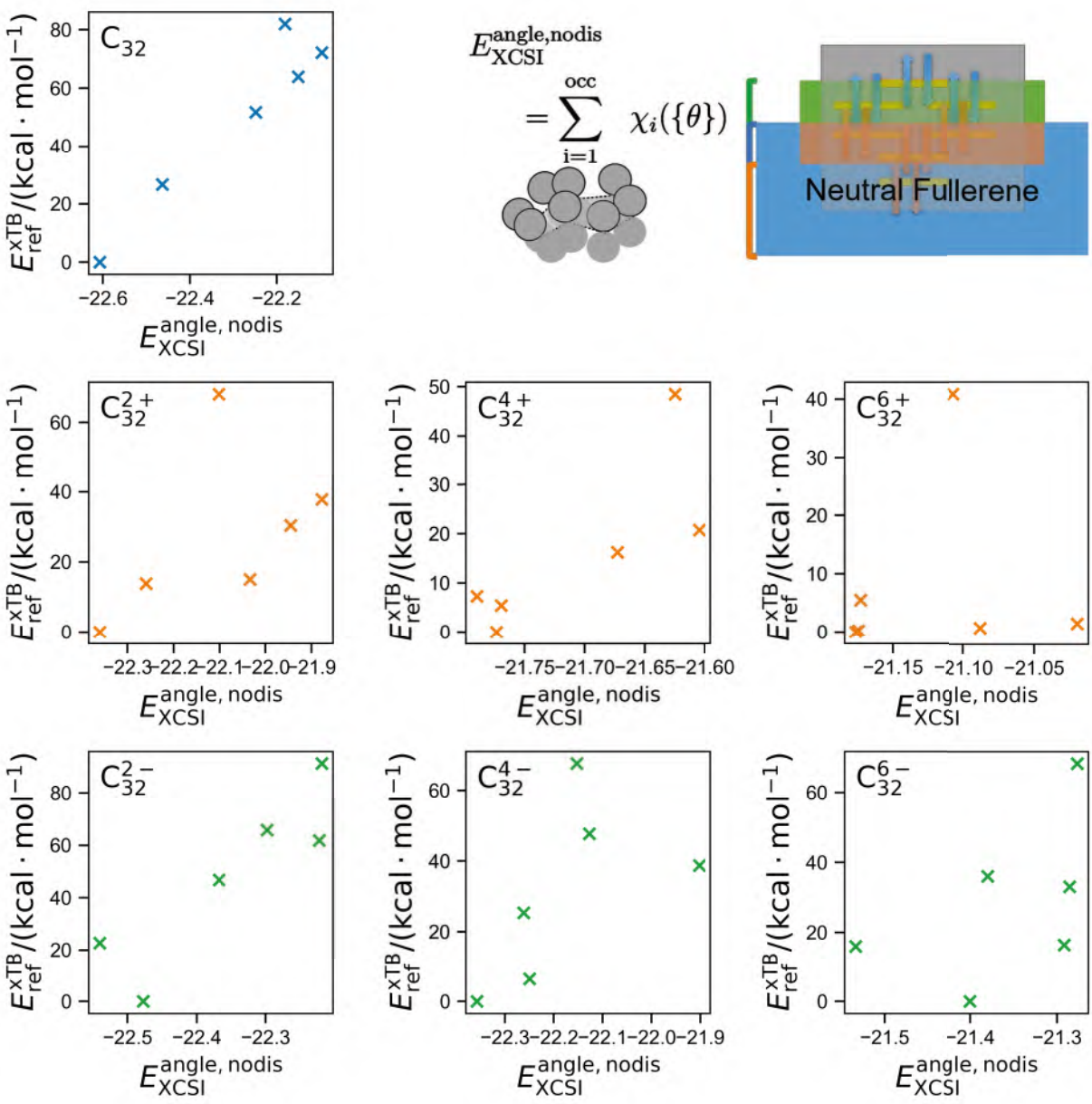


Figure 44: Correlation between xTB energies of $C_{32}$ isomers relative to the most stable one and prediction by XCSI model with angles but without distances of $C_{32}$ isomers without and with charge 2+, 4+, 6+, 2-, 4-, 6-, respectively.

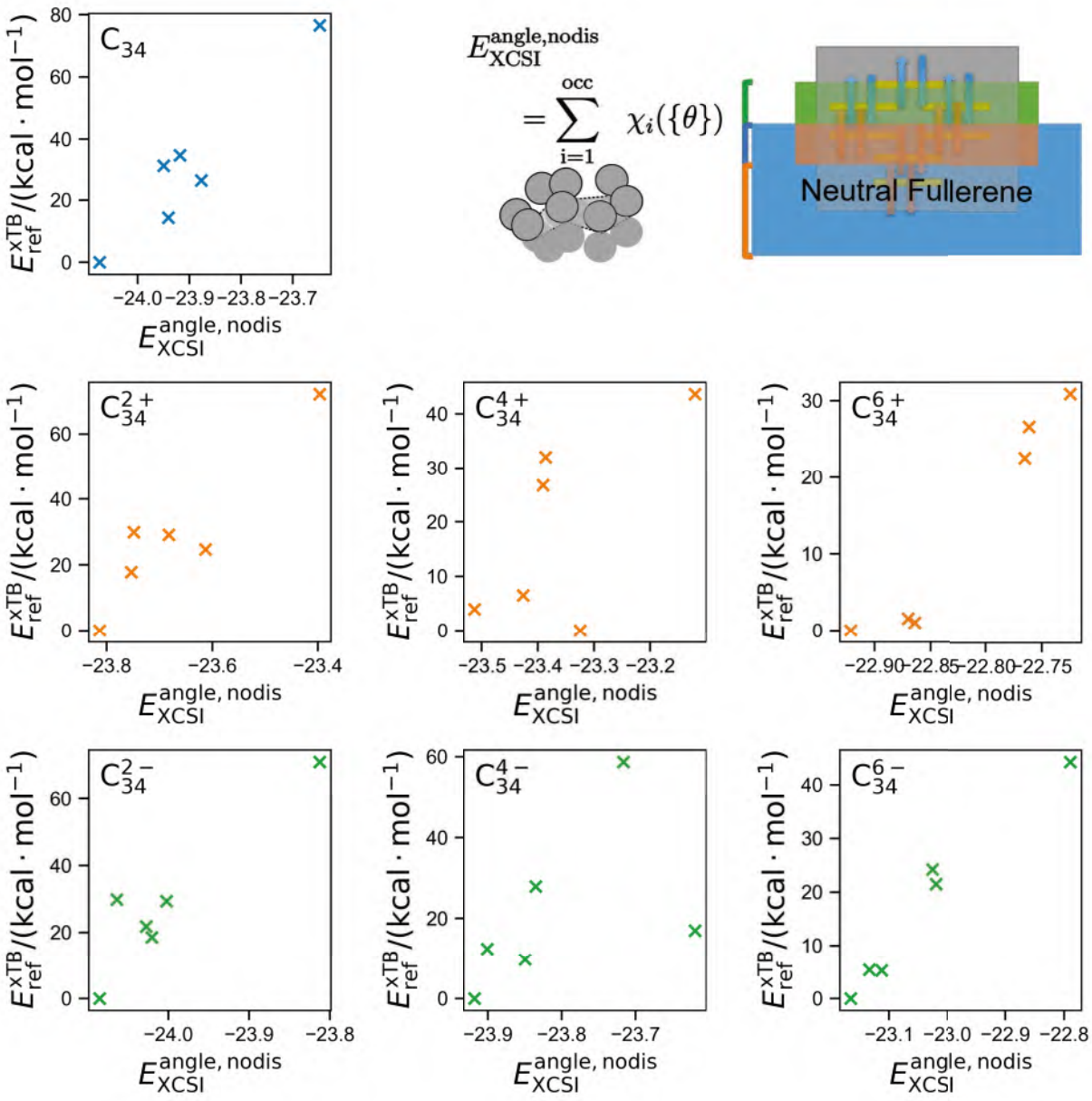


Figure 45: Correlation between xTB energies of $C_{34}$ isomers relative to the most stable one and prediction by XCSI model with angles but without distances of $C_{34}$ isomers without and with charge 2+, 4+, 6+, 2-, 4-, 6-, respectively.

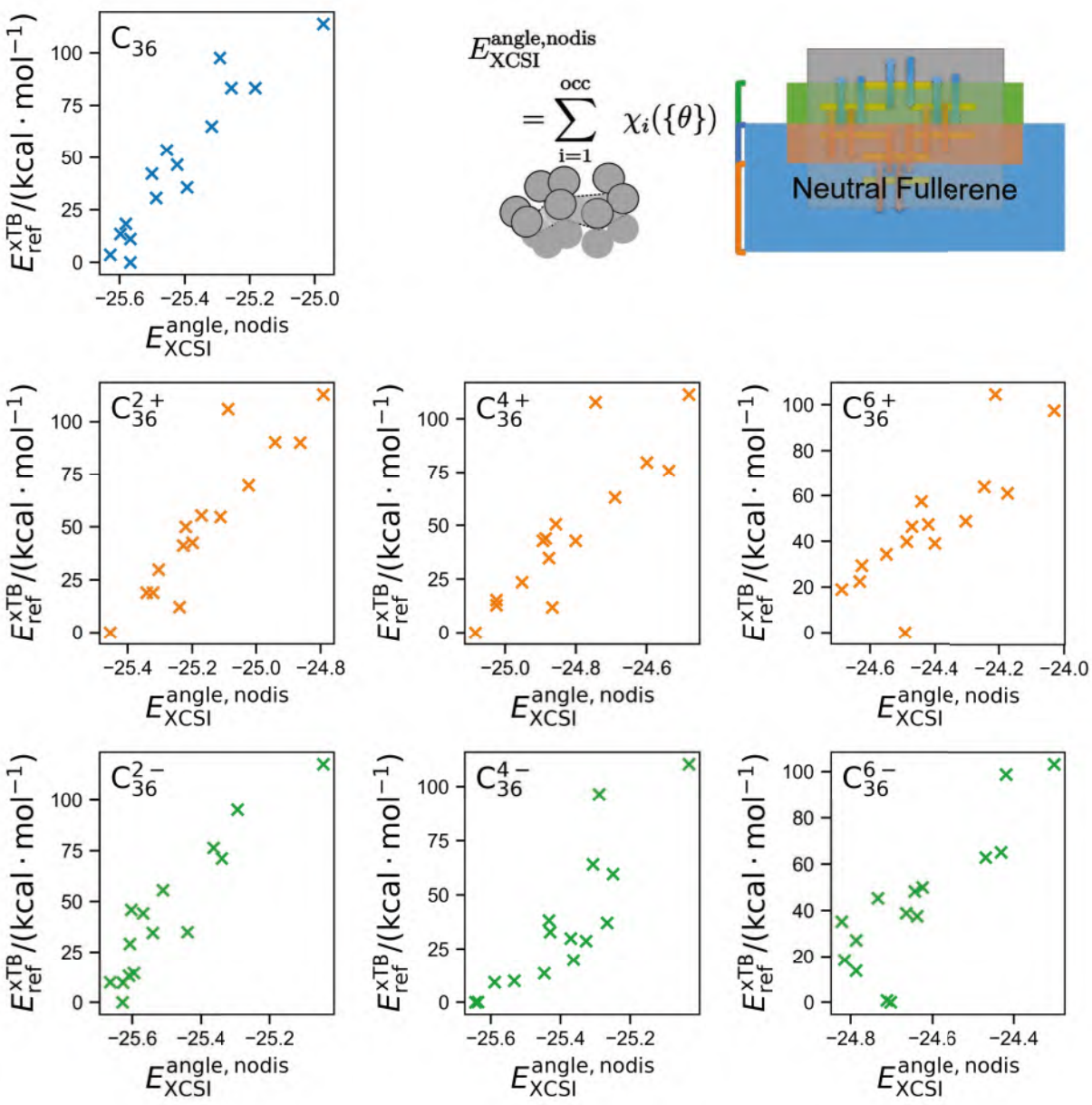


Figure 46: Correlation between xTB energies of $C_{36}$ isomers relative to the most stable one and prediction by XCSI model with angles but without distances of $C_{36}$ isomers without and with charge 2+, 4+, 6+, 2-, 4-, 6-, respectively.

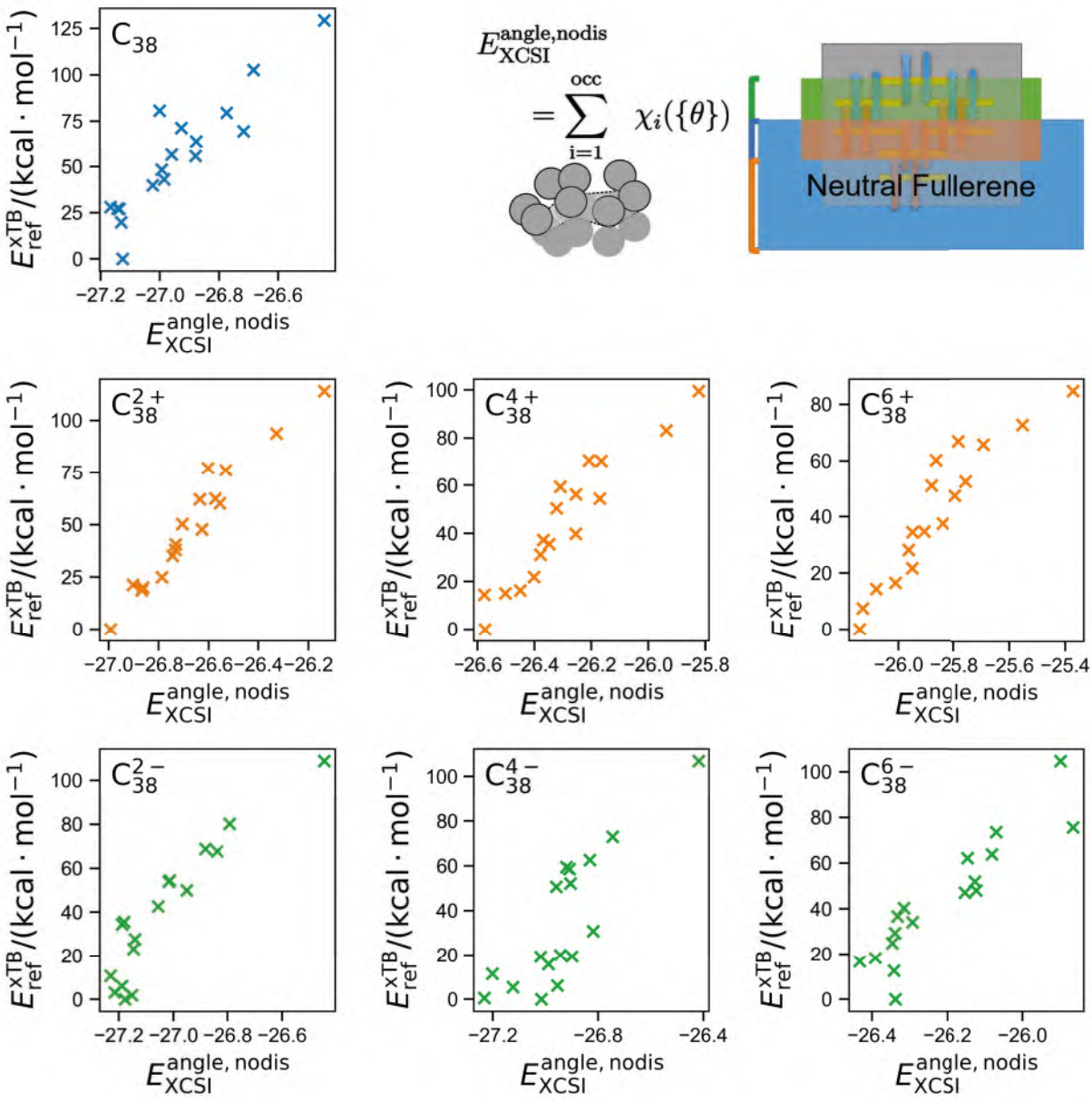


Figure 47: Correlation between xTB energies of $C_{38}$ isomers relative to the most stable one and prediction by XCSI model with angles but without distances of $C_{38}$ isomers without and with charge 2+, 4+, 6+, 2-, 4-, 6-, respectively.

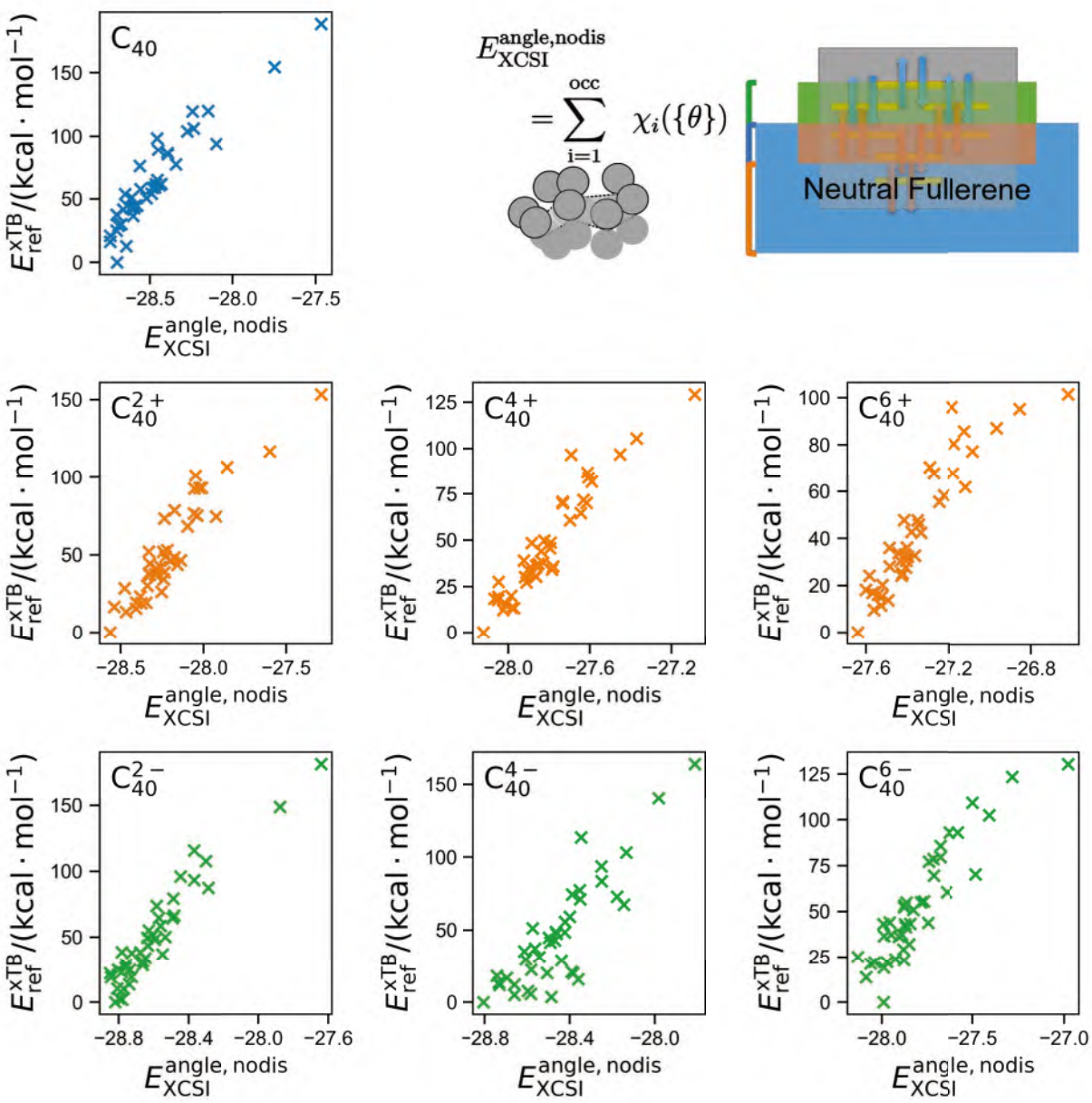


Figure 48: Correlation between xTB energies of $C_{40}$ isomers relative to the most stable one and prediction by XCSI model with angles but without distances of $C_{40}$ isomers without and with charge 2+, 4+, 6+, 2-, 4-, 6-, respectively.

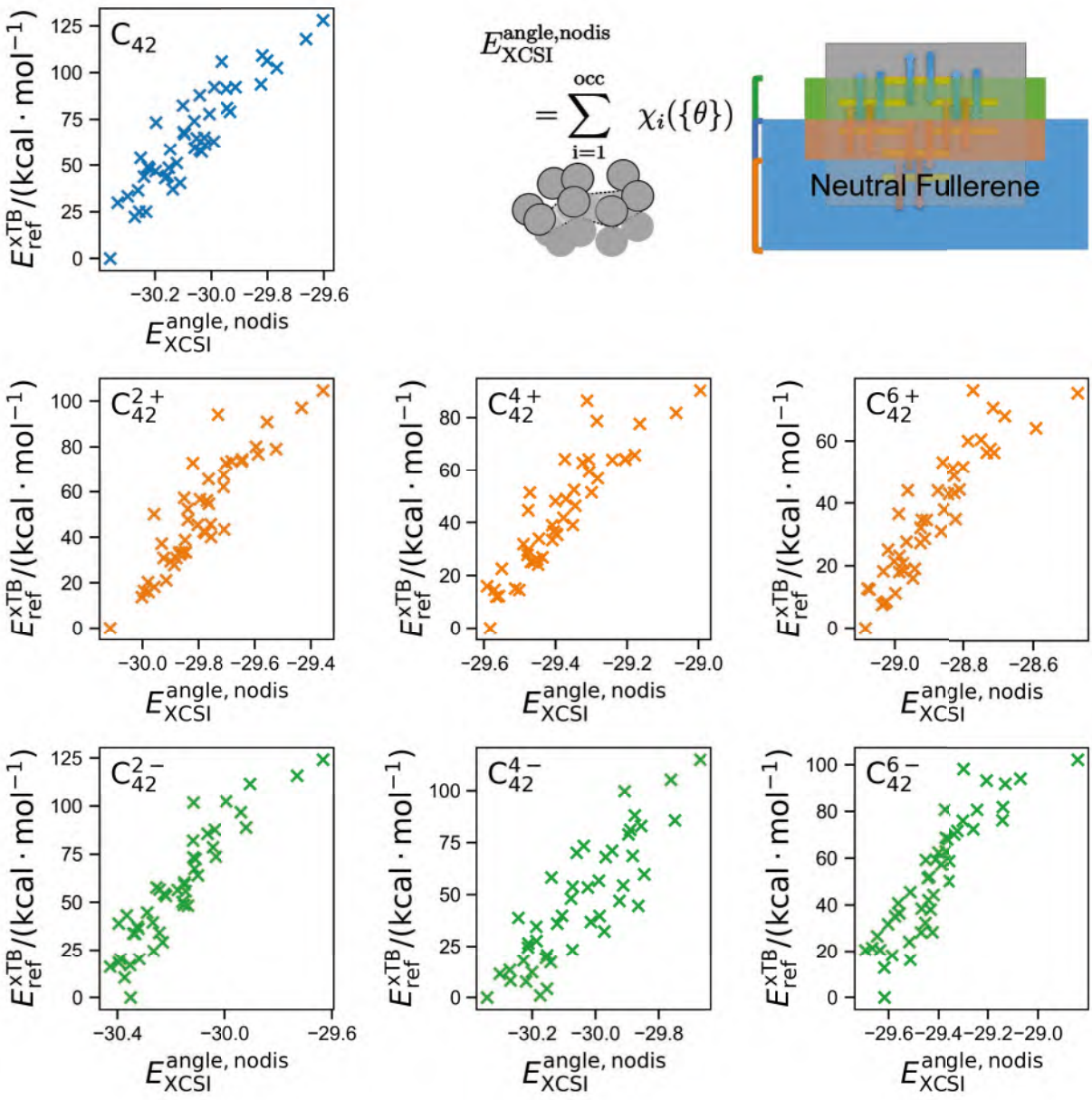


Figure 49: Correlation between xTB energies of $C_{42}$ isomers relative to the most stable one and prediction by XCSI model with angles but without distances of $C_{42}$ isomers without and with charge 2+, 4+, 6+, 2-, 4-, 6-, respectively.

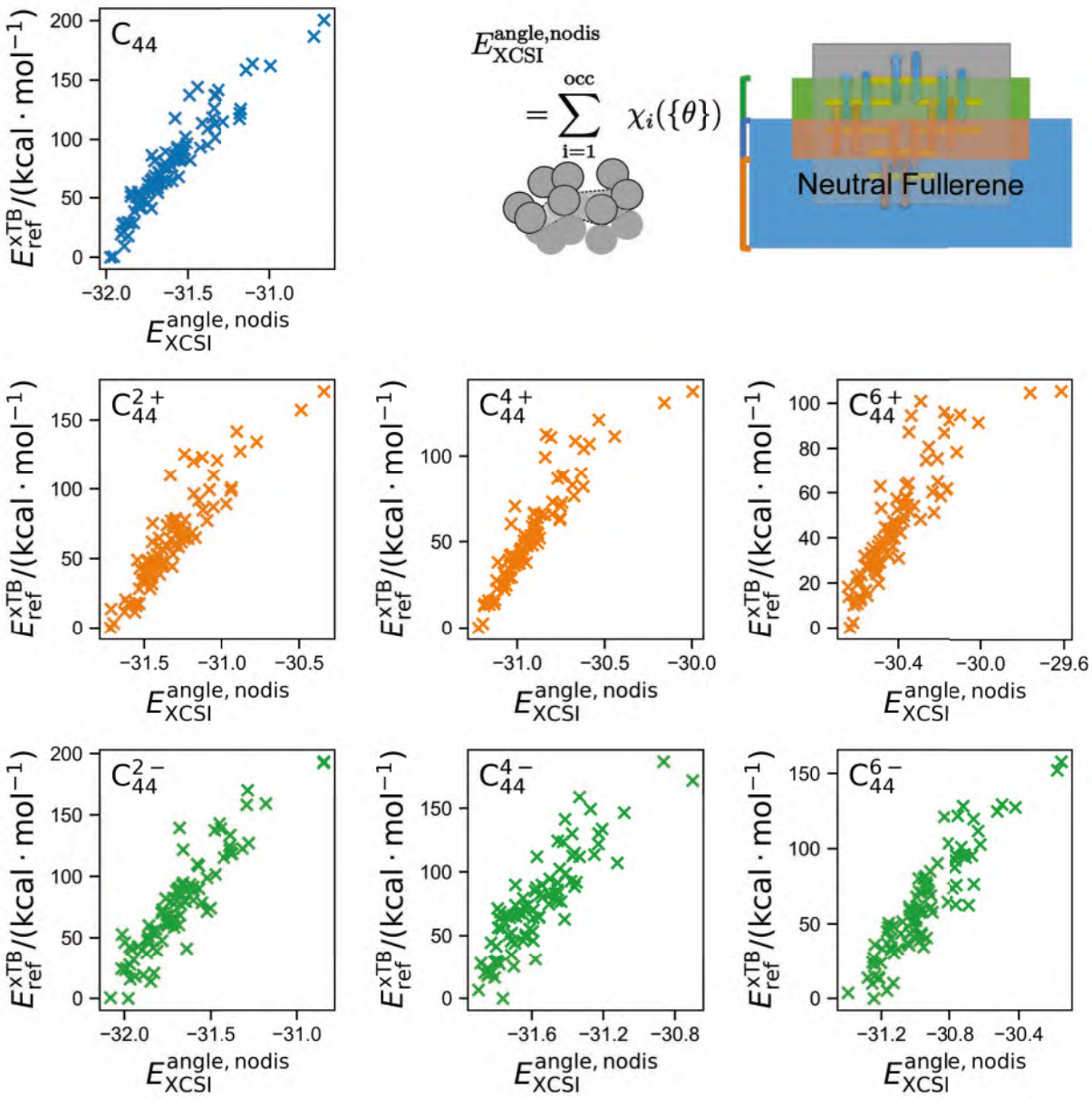


Figure 50: Correlation between xTB energies of $C_{44}$ isomers relative to the most stable one and prediction by XCSI model with angles but without distances of $C_{44}$ isomers without and with charge 2+, 4+, 6+, 2-, 4-, 6-, respectively.

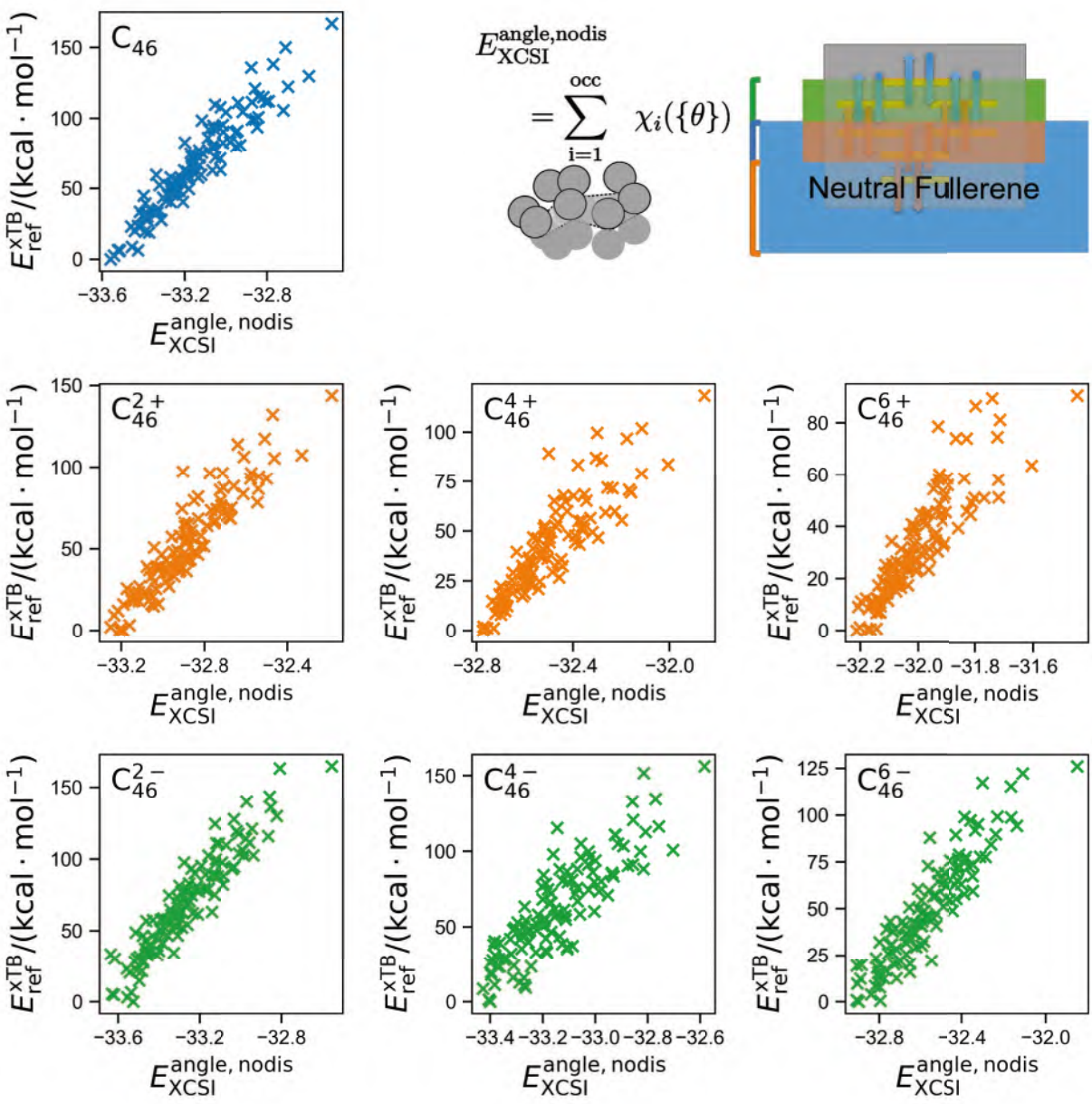


Figure 51: Correlation between xTB energies of $C_{46}$ isomers relative to the most stable one and prediction by XCSI model with angles but without distances of $C_{46}$ isomers without and with charge 2+, 4+, 6+, 2-, 4-, 6-, respectively.

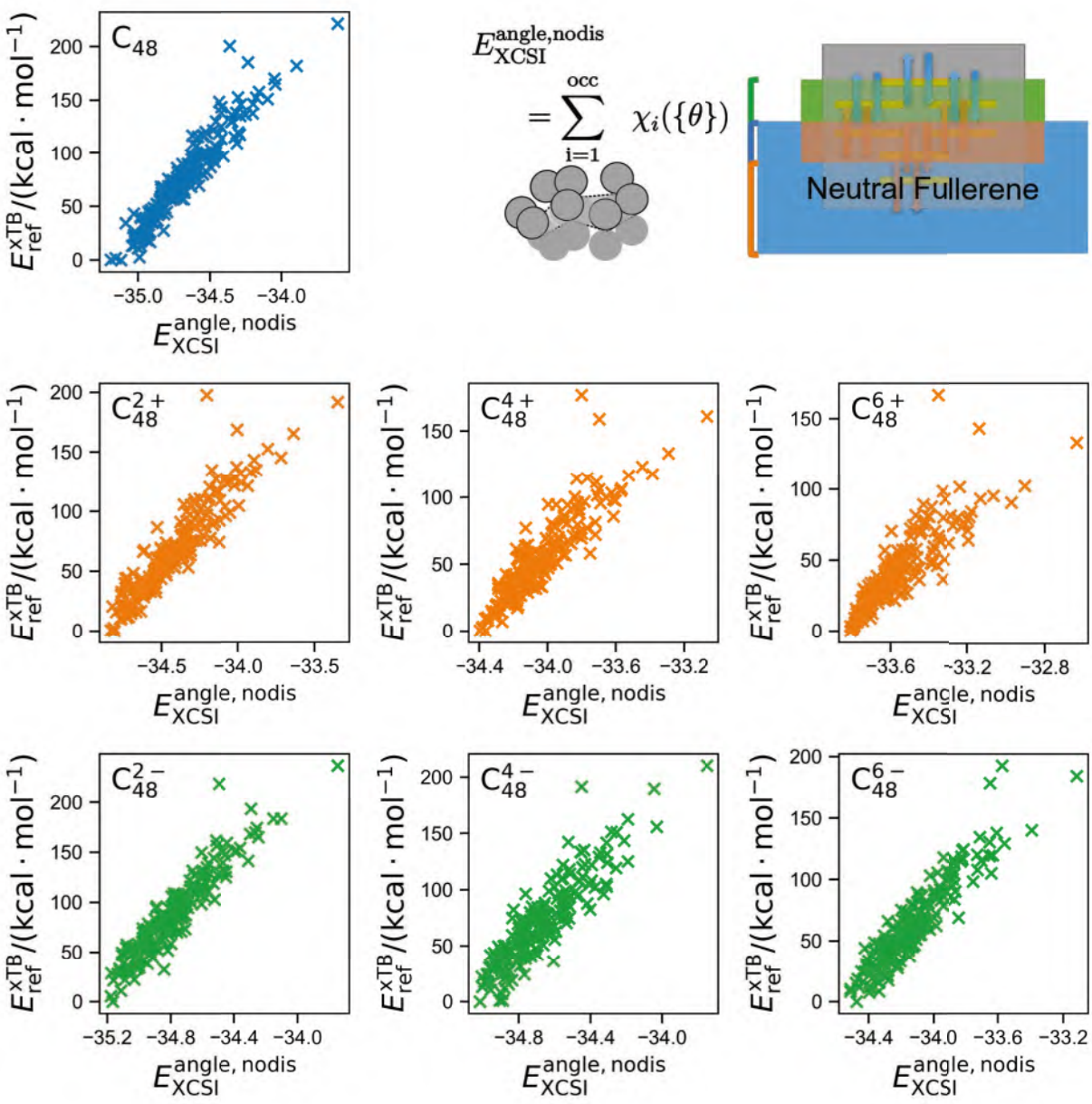


Figure 52: Correlation between xTB energies of $C_{48}$ isomers relative to the most stable one and prediction by XCSI model with angles but without distances of $C_{48}$ isomers without and with charge 2+, 4+, 6+, 2-, 4-, 6-, respectively.

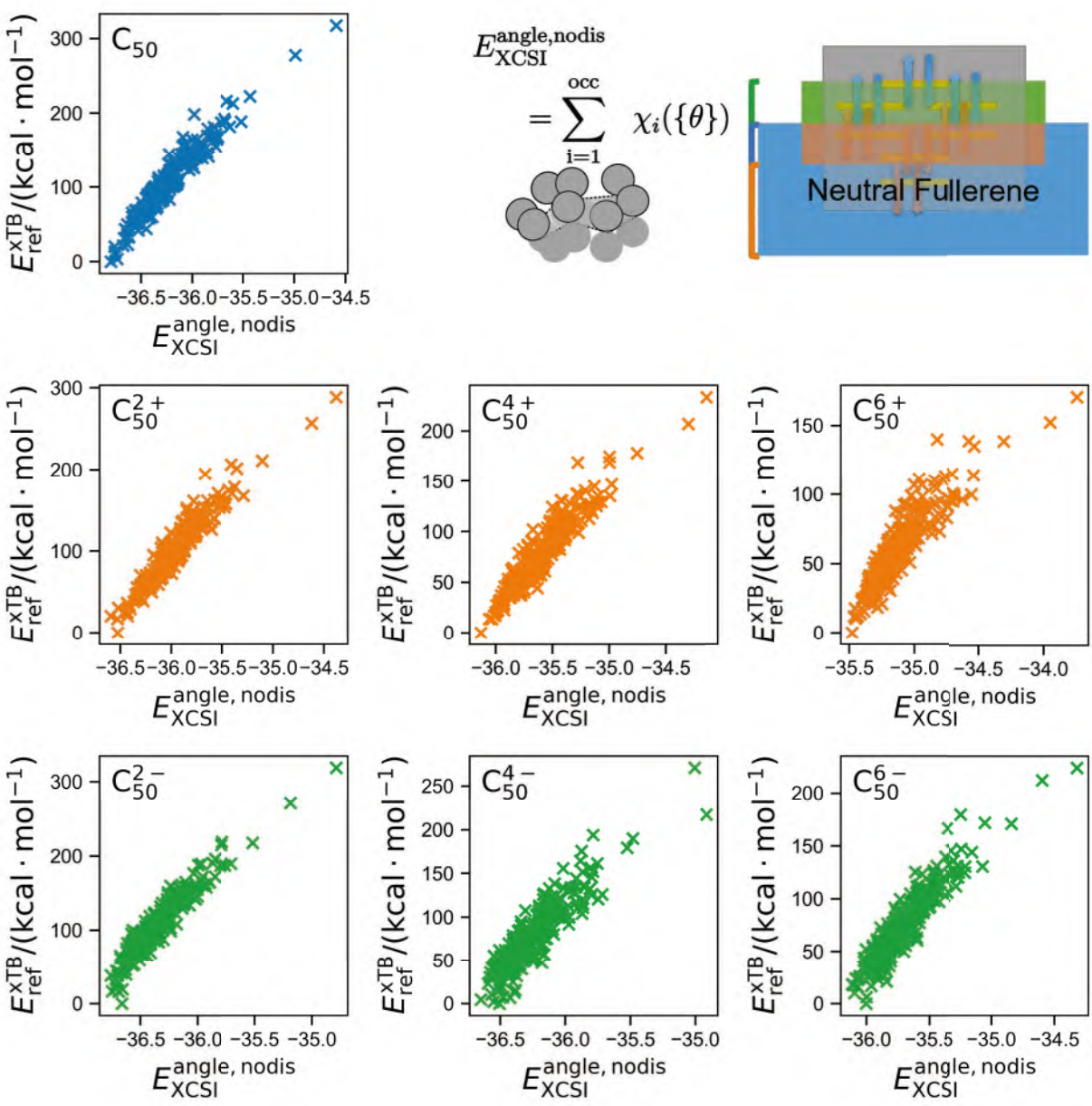


Figure 53: Correlation between xTB energies of $C_{50}$ isomers relative to the most stable one and prediction by XCSI model with angles but without distances of $C_{50}$ isomers without and with charge 2+, 4+, 6+, 2-, 4-, 6-, respectively.

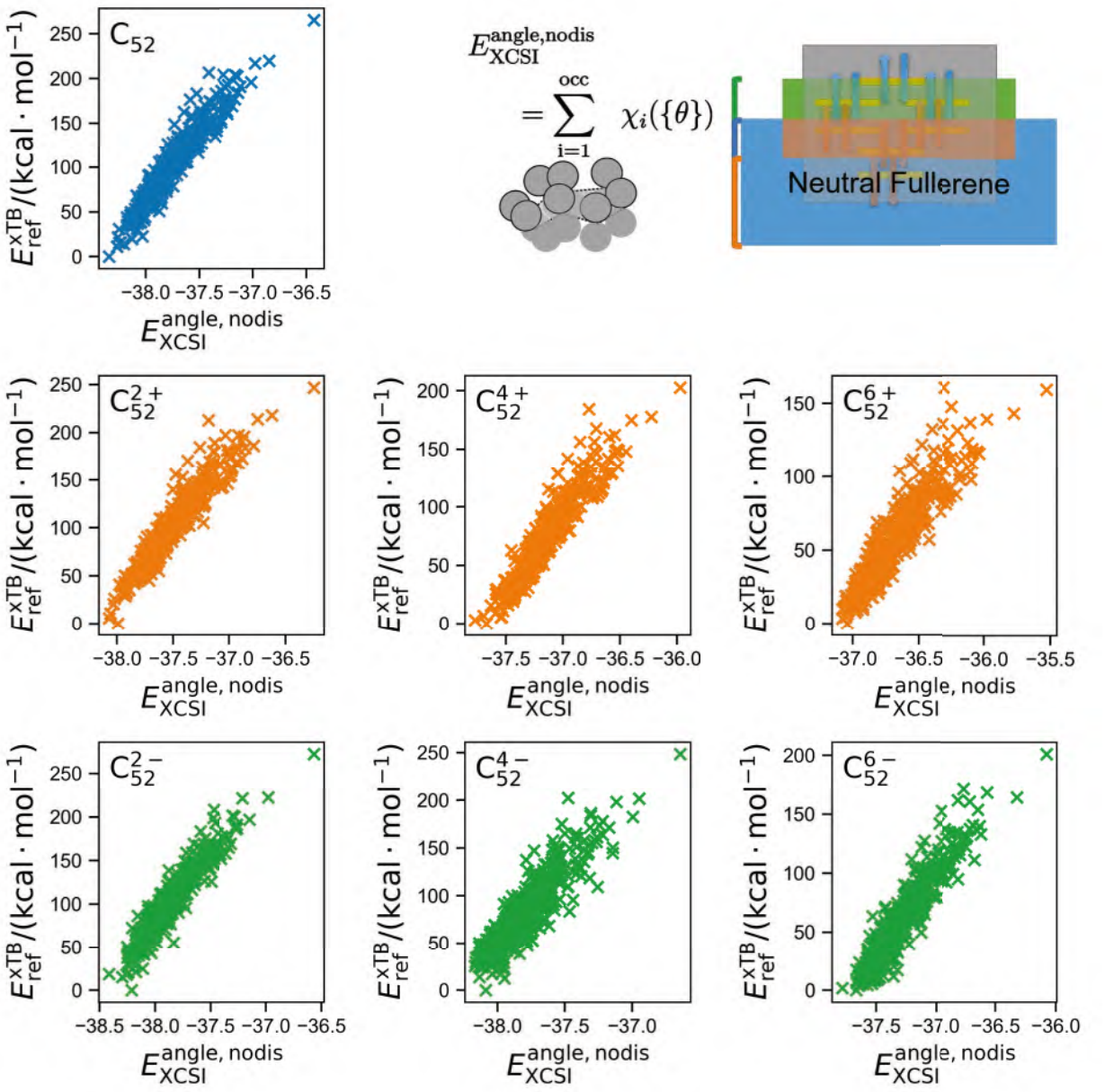


Figure 54: Correlation between xTB energies of $C_{52}$ isomers relative to the most stable one and prediction by XCSI model with angles but without distances of $C_{52}$ isomers without and with charge 2+, 4+, 6+, 2-, 4-, 6-, respectively.

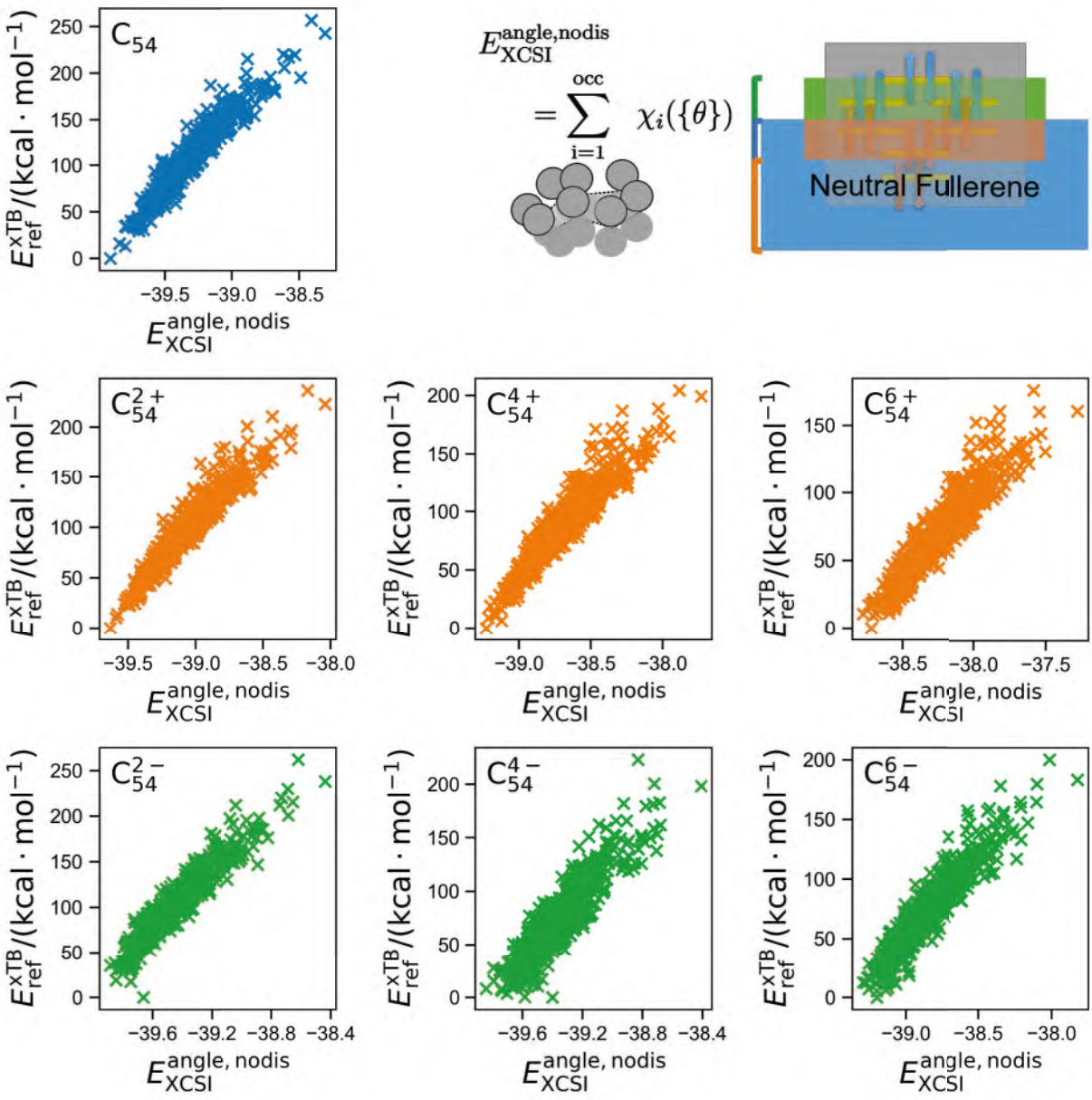


Figure 55: Correlation between xTB energies of $C_{54}$ isomers relative to the most stable one and prediction by XCSI model with angles but without distances of $C_{54}$ isomers without and with charge 2+, 4+, 6+, 2-, 4-, 6-, respectively.

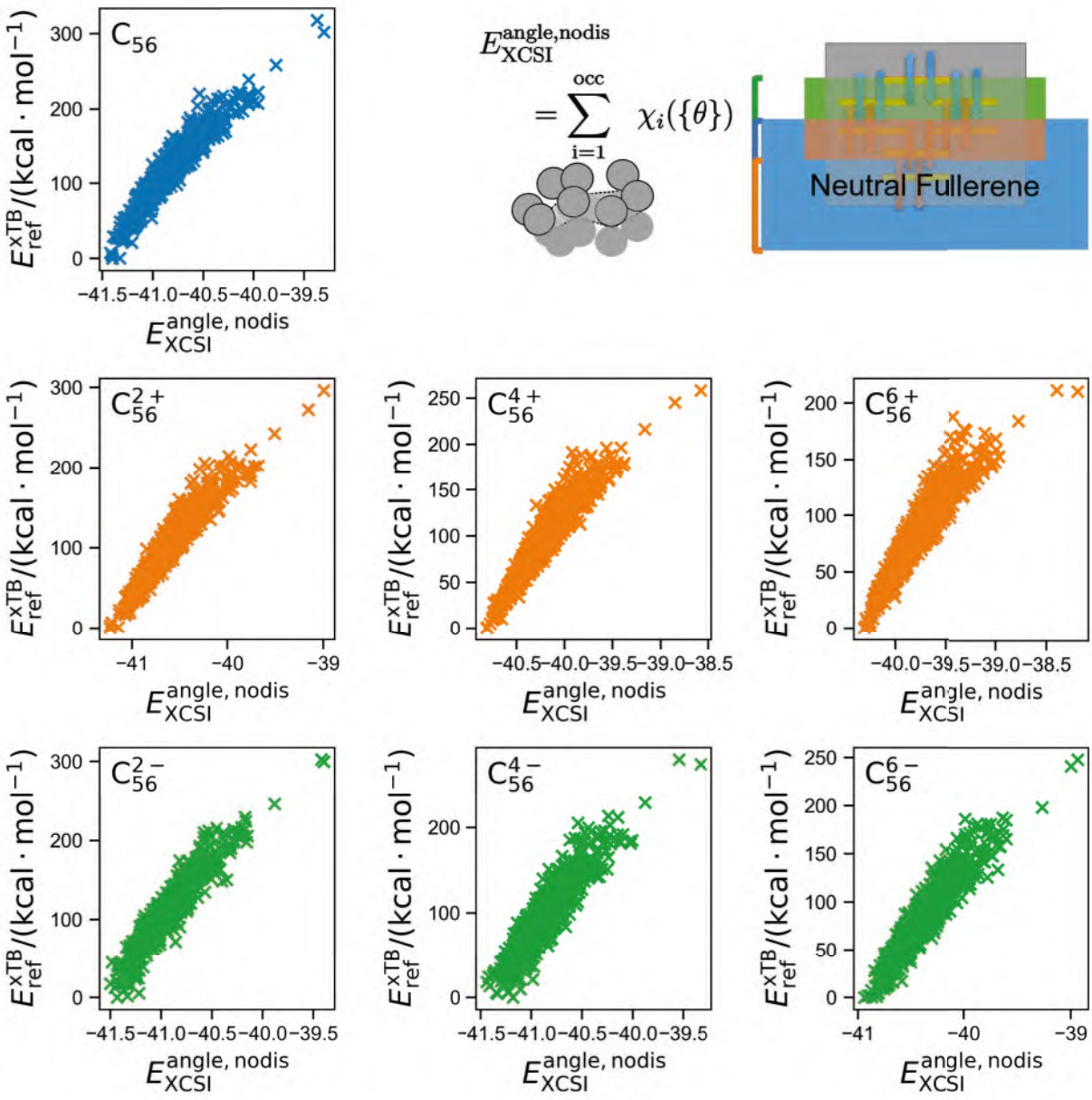


Figure 56: Correlation between xTB energies of $C_{56}$ isomers relative to the most stable one and prediction by XCSI model with angles but without distances of $C_{56}$ isomers without and with charge 2+, 4+, 6+, 2-, 4-, 6-, respectively.

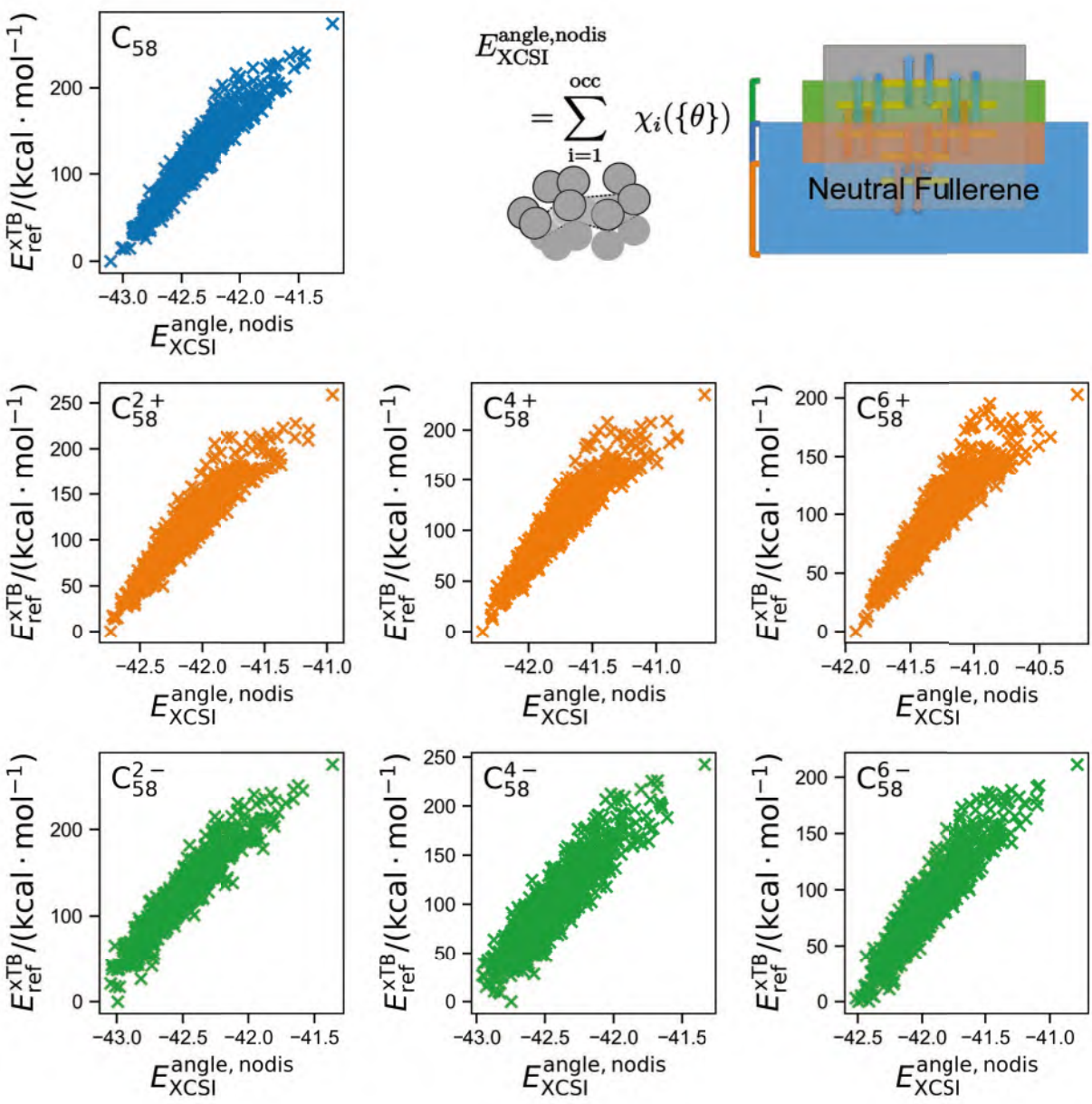


Figure 57: Correlation between xTB energies of $C_{58}$ isomers relative to the most stable one and prediction by XCSI model with angles but without distances of $C_{58}$ isomers without and with charge 2+, 4+, 6+, 2-, 4-, 6-, respectively.

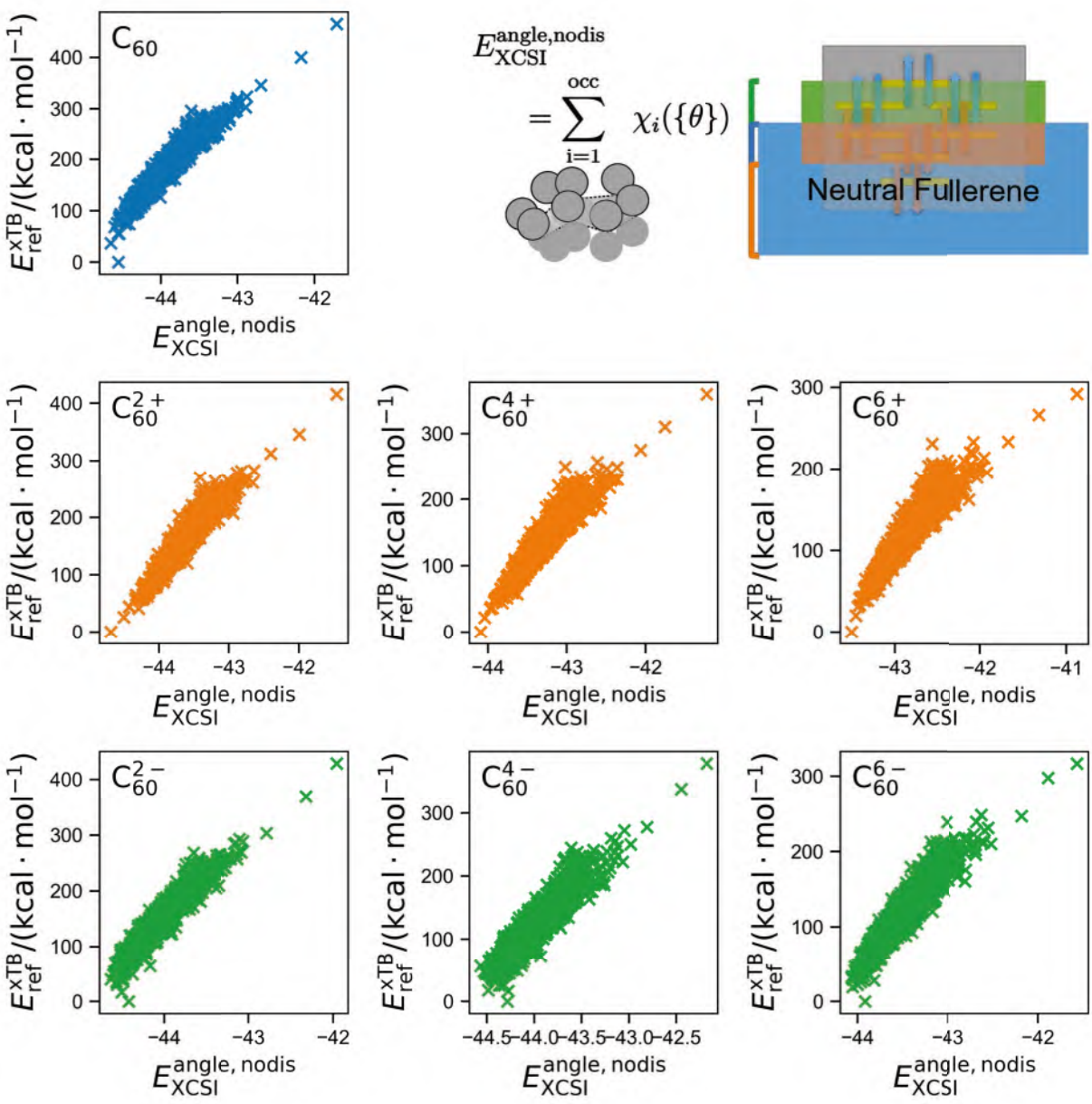


Figure 58: Correlation between xTB energies of $C_{60}$ isomers relative to the most stable one and prediction by XCSI model with angles but without distances of $C_{60}$ isomers without and with charge 2+, 4+, 6+, 2-, 4-, 6-, respectively.

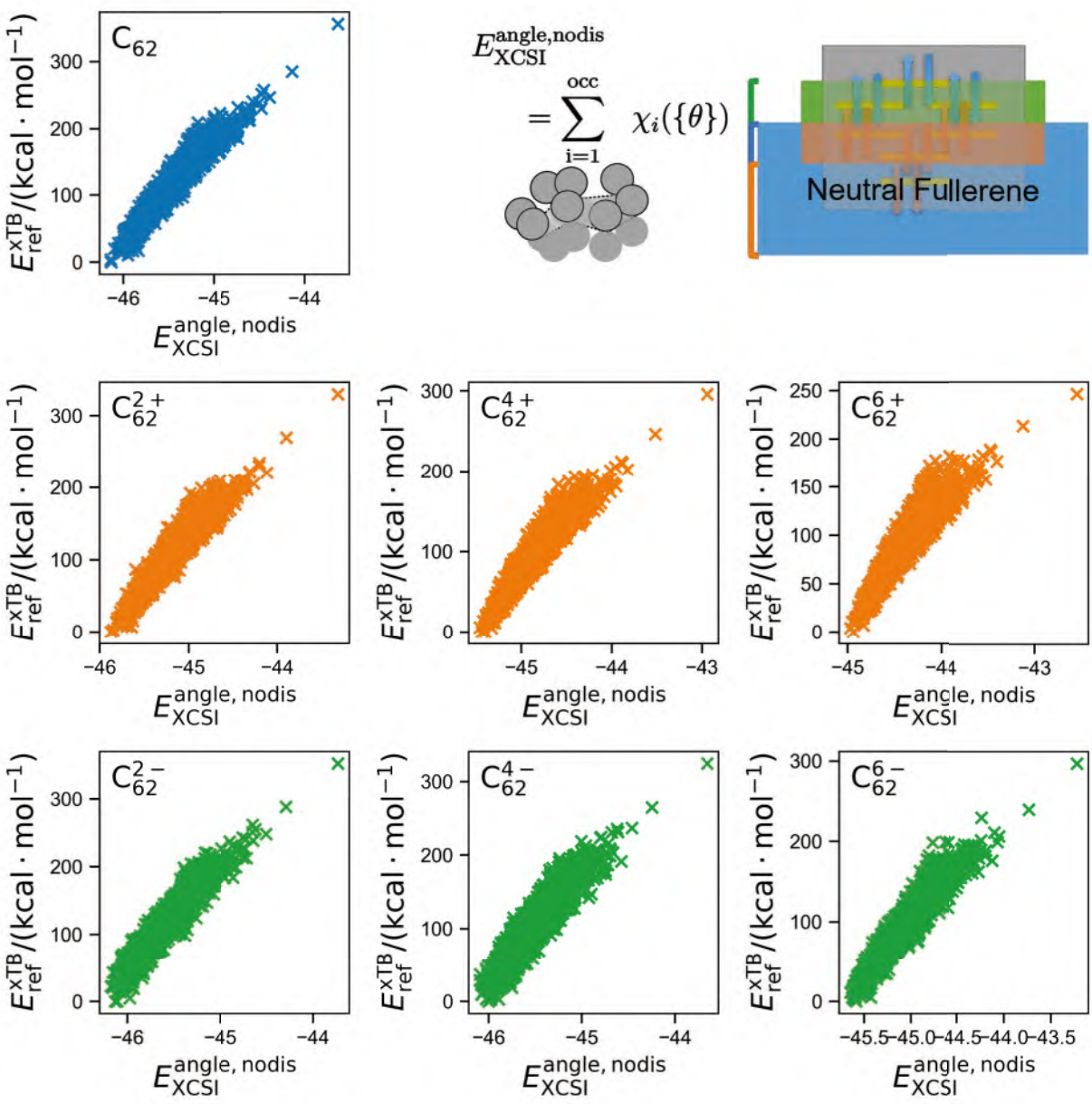


Figure 59: Correlation between xTB energies of $C_{62}$ isomers relative to the most stable one and prediction by XCSI model with angles but without distances of $C_{62}$ isomers without and with charge 2+, 4+, 6+, 2-, 4-, 6-, respectively.

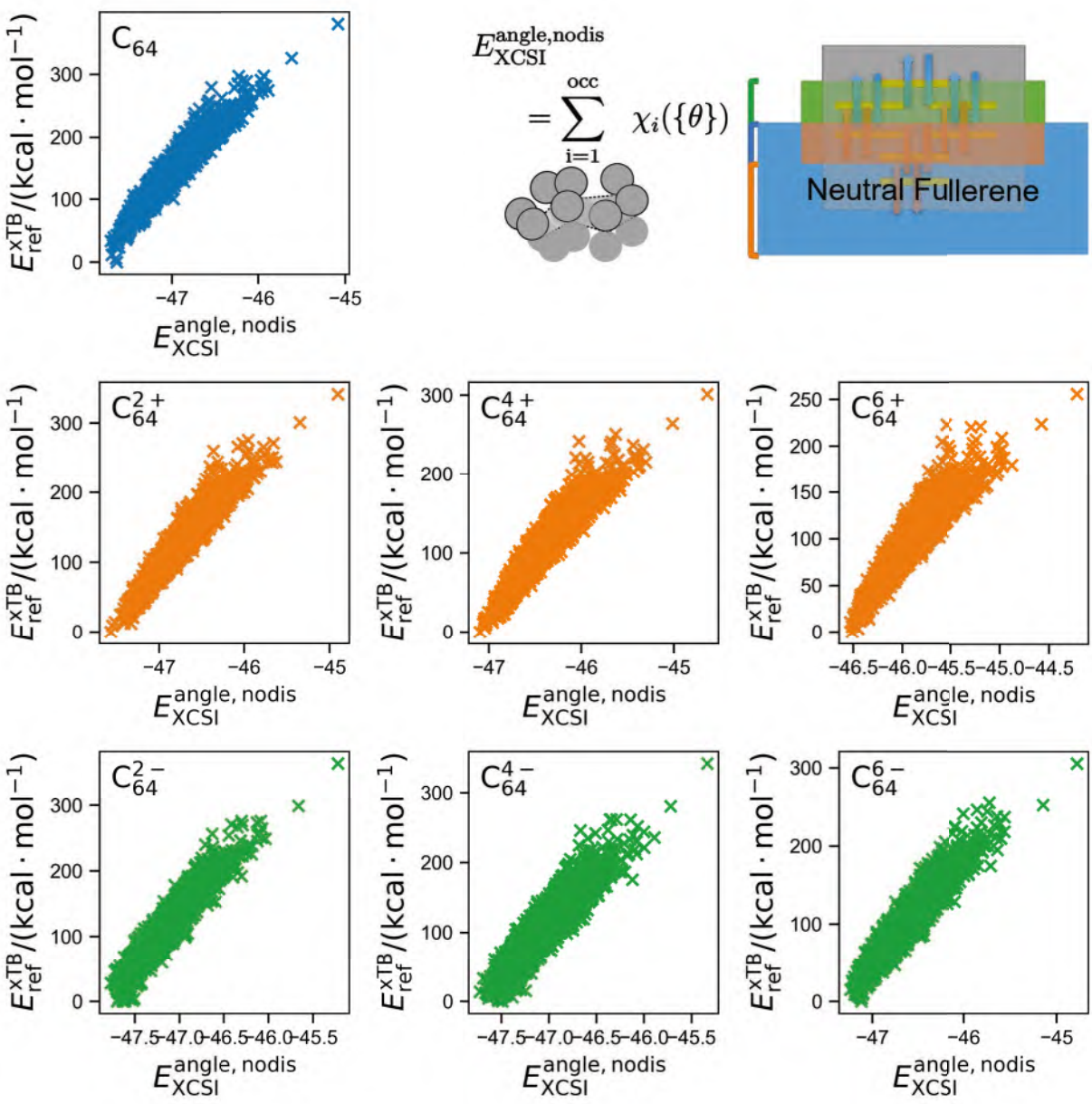


Figure 60: Correlation between xTB energies of $C_{64}$ isomers relative to the most stable one and prediction by XCSI model with angles but without distances of $C_{64}$ isomers without and with charge 2+, 4+, 6+, 2-, 4-, 6-, respectively.

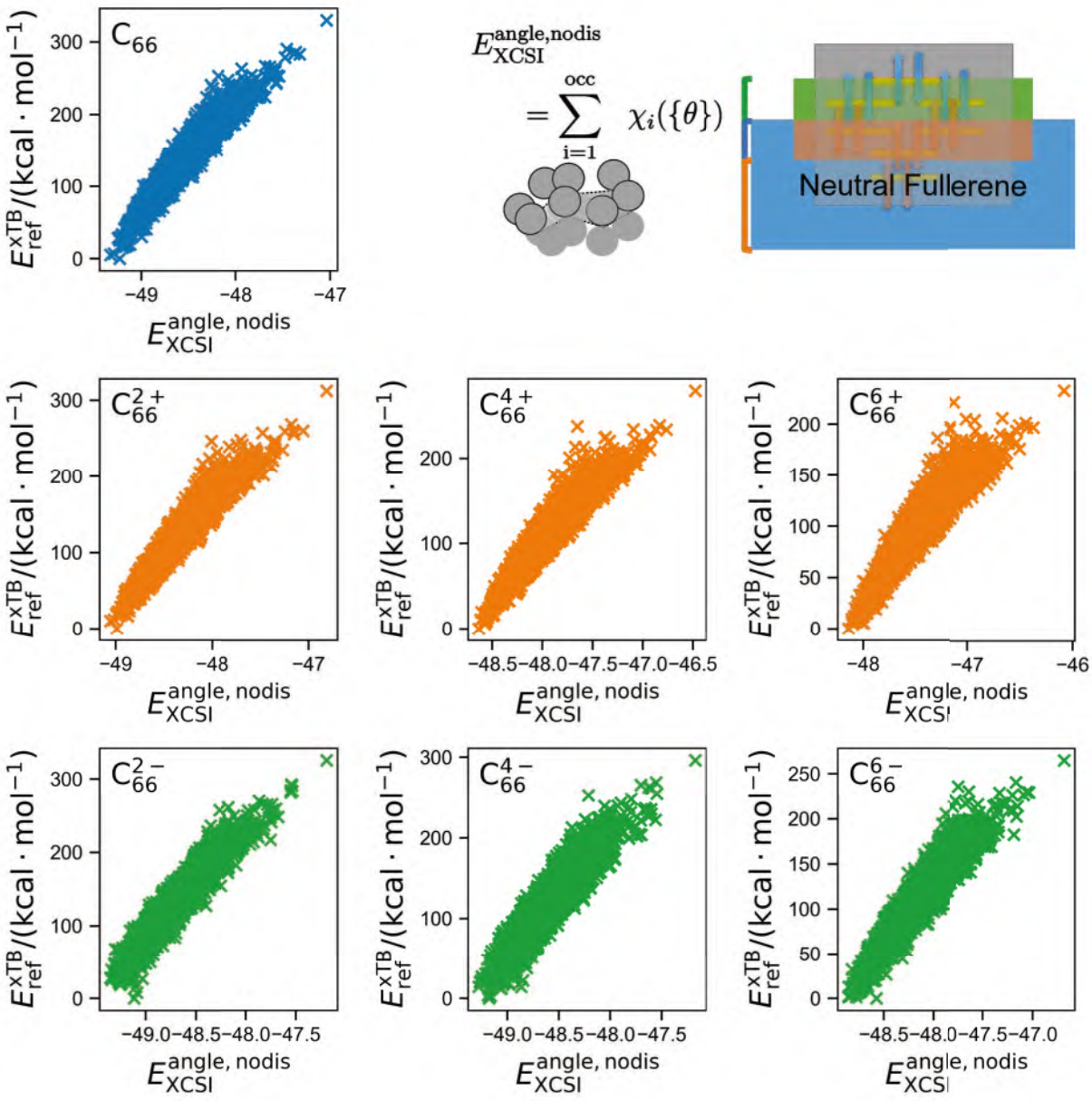


Figure 61: Correlation between xTB energies of $C_{66}$ isomers relative to the most stable one and prediction by XCSI model with angles but without distances of $C_{66}$ isomers without and with charge 2+, 4+, 6+, 2-, 4-, 6-, respectively.

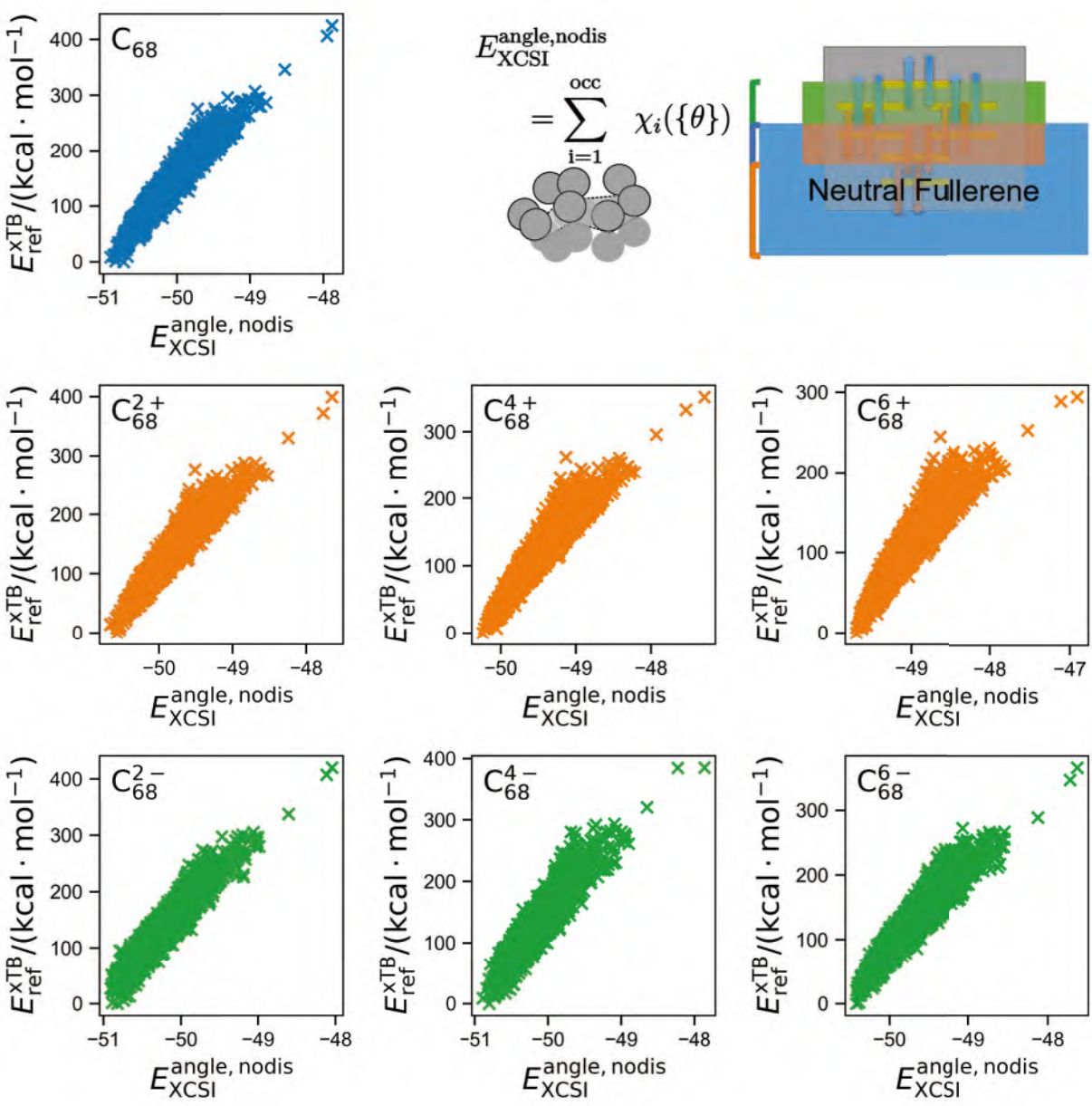


Figure 62: Correlation between xTB energies of $C_{68}$ isomers relative to the most stable one and prediction by XCSI model with angles but without distances of $C_{68}$ isomers without and with charge 2+, 4+, 6+, 2-, 4-, 6-, respectively.

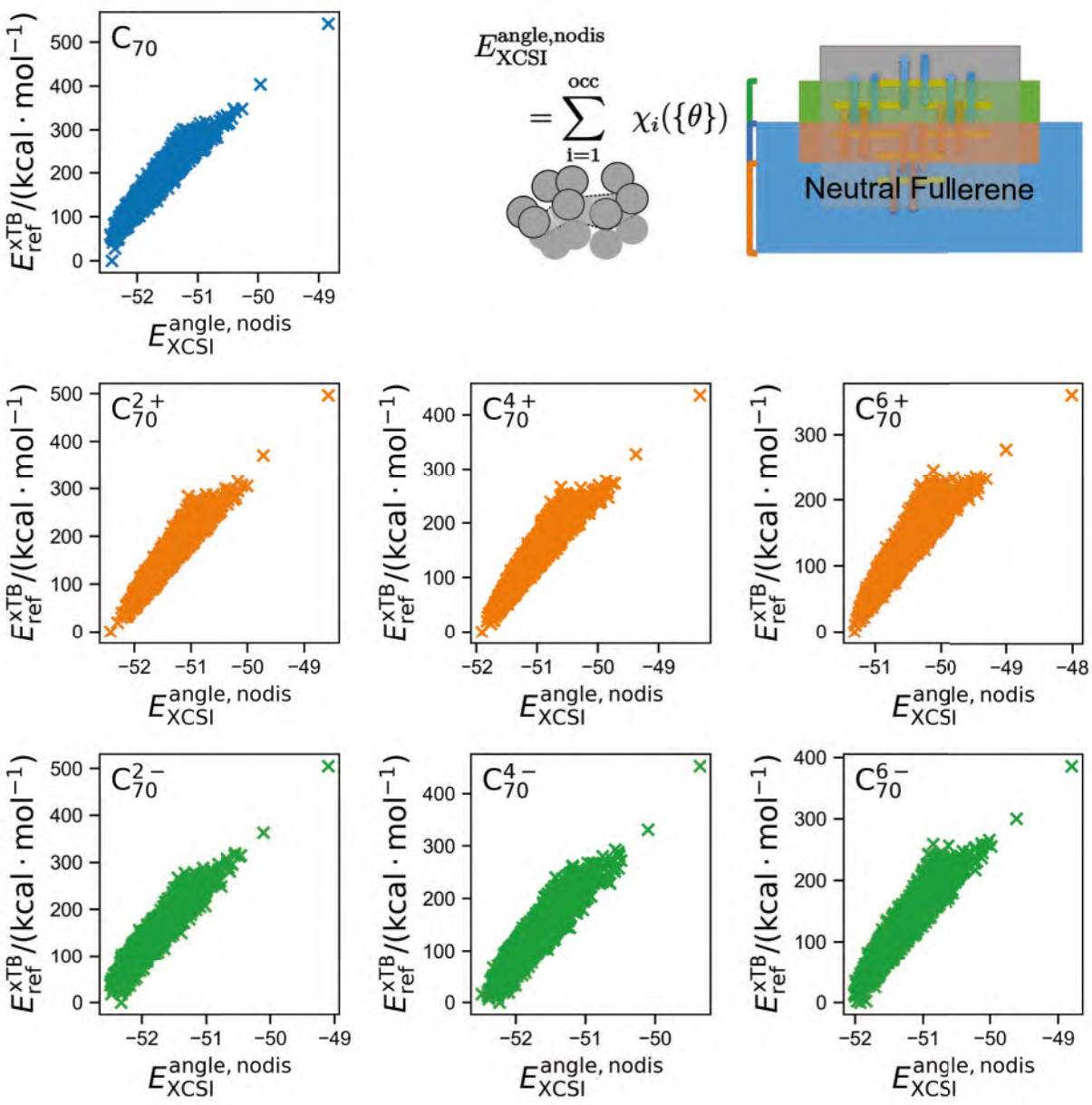


Figure 63: Correlation between xTB energies of $C_{70}$ isomers relative to the most stable one and prediction by XCSI model with angles but without distances of $C_{70}$ isomers without and with charge 2+, 4+, 6+, 2-, 4-, 6-, respectively.

# 5 Correlation between xTB energies and prediction by XCSI model with angles and distances

Predictions by XCSI model with angles and distances are calculated by

$$E_{\mathrm{XCSI}}^{\mathrm{angle,nodis}} \equiv \sum_{k=i}^{n} \chi_{k,i}^{q}(\{\theta, d\}) \tag{6}$$

where $\chi_{k,i}^{q}$ is eigenvalues of extended adjacency matrix, whose elements are

$$h_{ij}^{k} = \begin{cases} \cos\theta_{ij} \exp\left(-d_{ij}^{2}\right) \beta' & i, j \text{are neighbors} \\ 0 & \text{others} \end{cases} \tag{7}$$

.

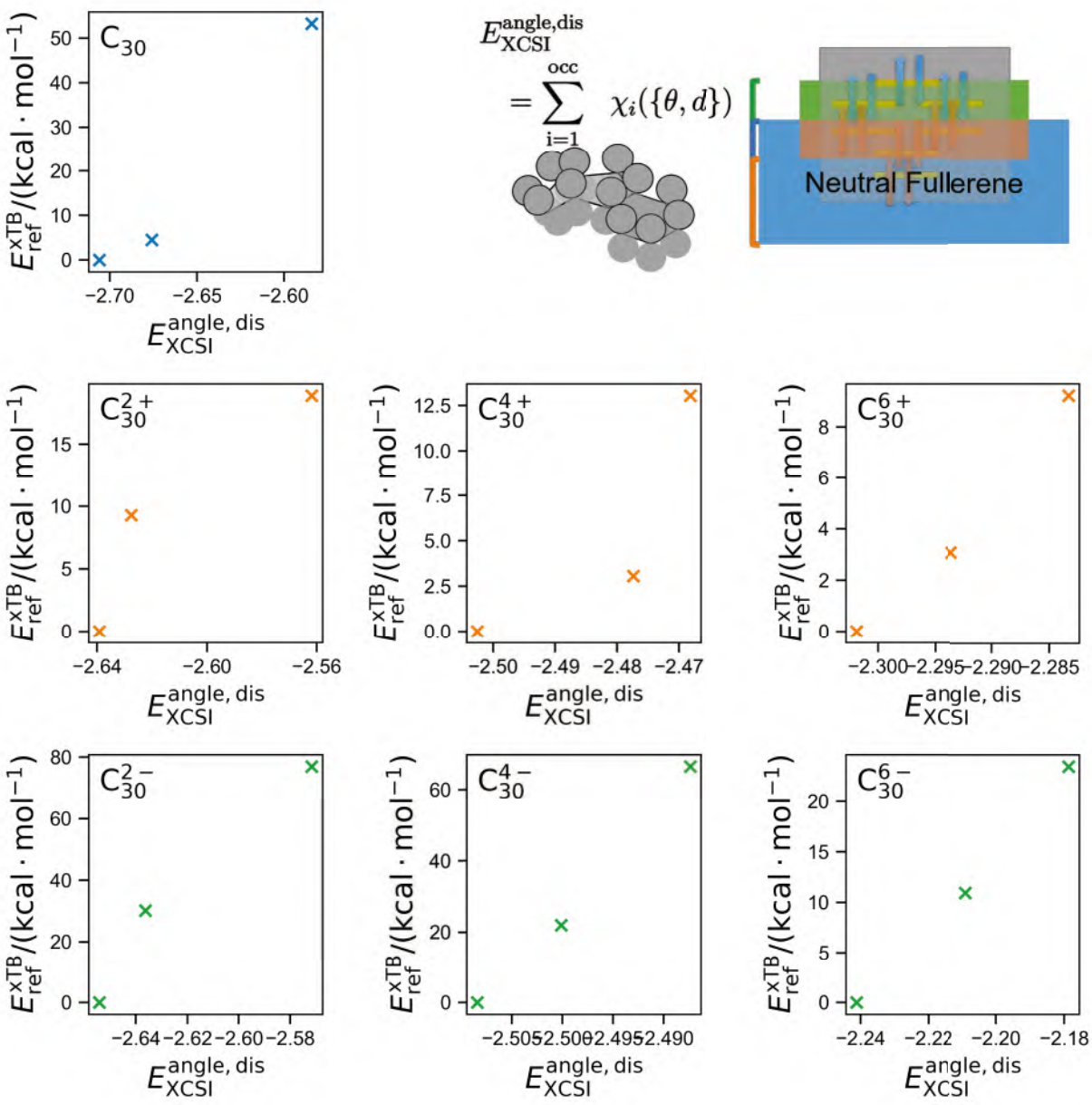


Figure 64: Correlation between xTB energies of $C_{30}$ isomers relative to the most stable one and prediction by XCSI model with angles and distances of $C_{30}$ isomers without and with charge 2+, 4+, 6+, 2-, 4-, 6-, respectively.

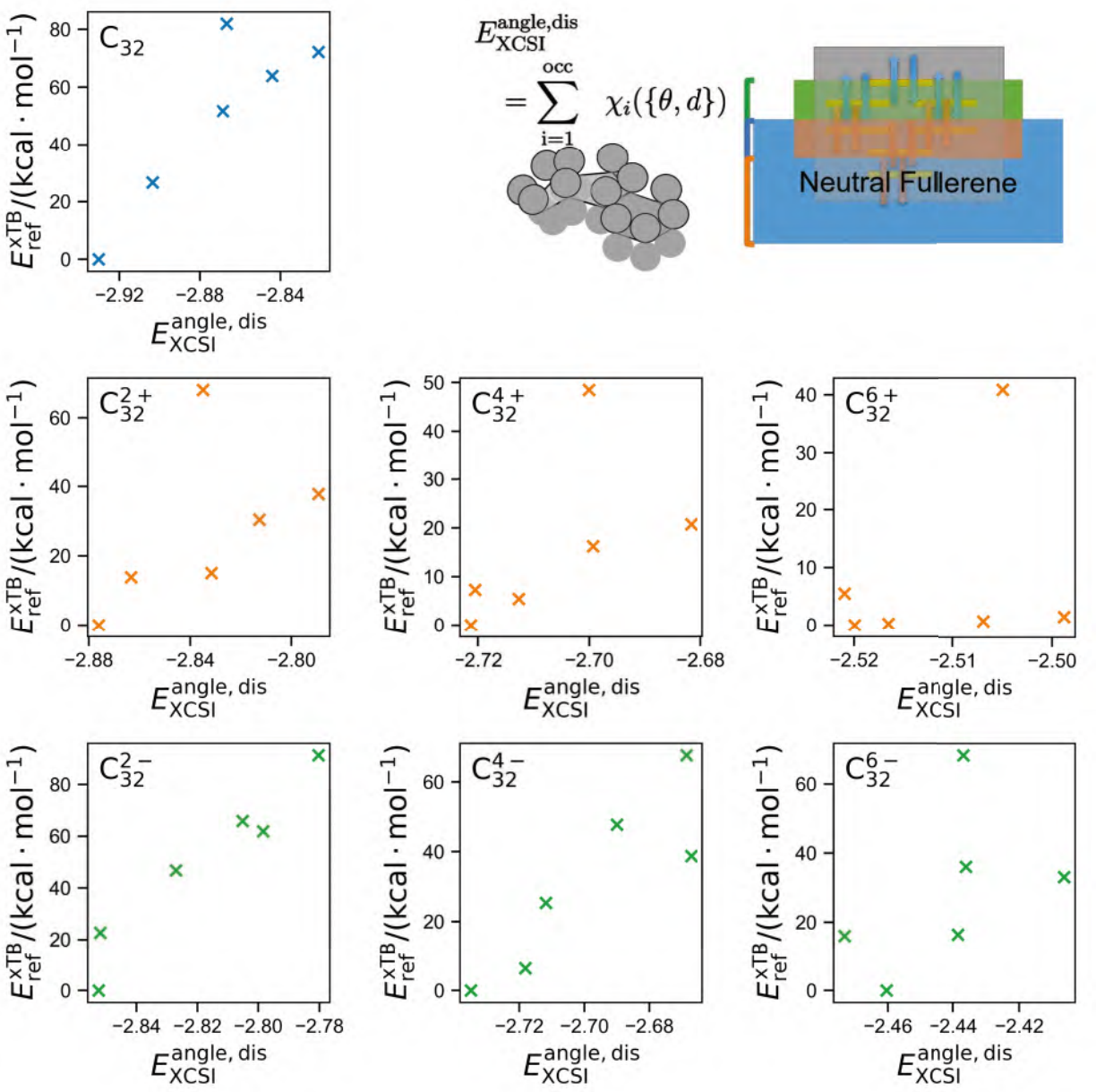


Figure 65: Correlation between xTB energies of $C_{32}$ isomers relative to the most stable one and prediction by XCSI model with angles and distances of $C_{32}$ isomers without and with charge 2+, 4+, 6+, 2-, 4-, 6-, respectively.

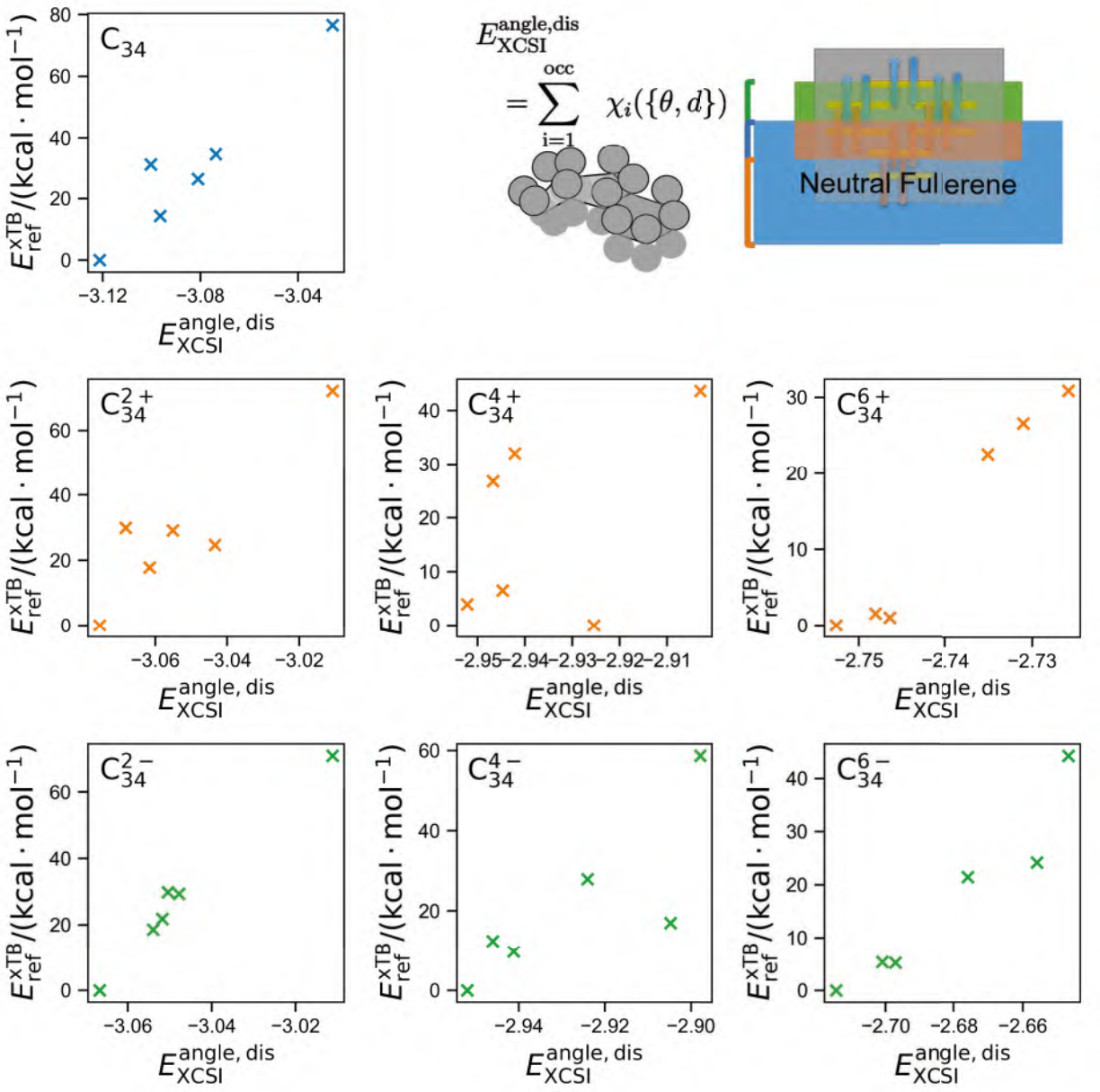


Figure 66: Correlation between xTB energies of $C_{34}$ isomers relative to the most stable one and prediction by XCSI model with angles and distances of $C_{34}$ isomers without and with charge 2+, 4+, 6+, 2-, 4-, 6-, respectively.

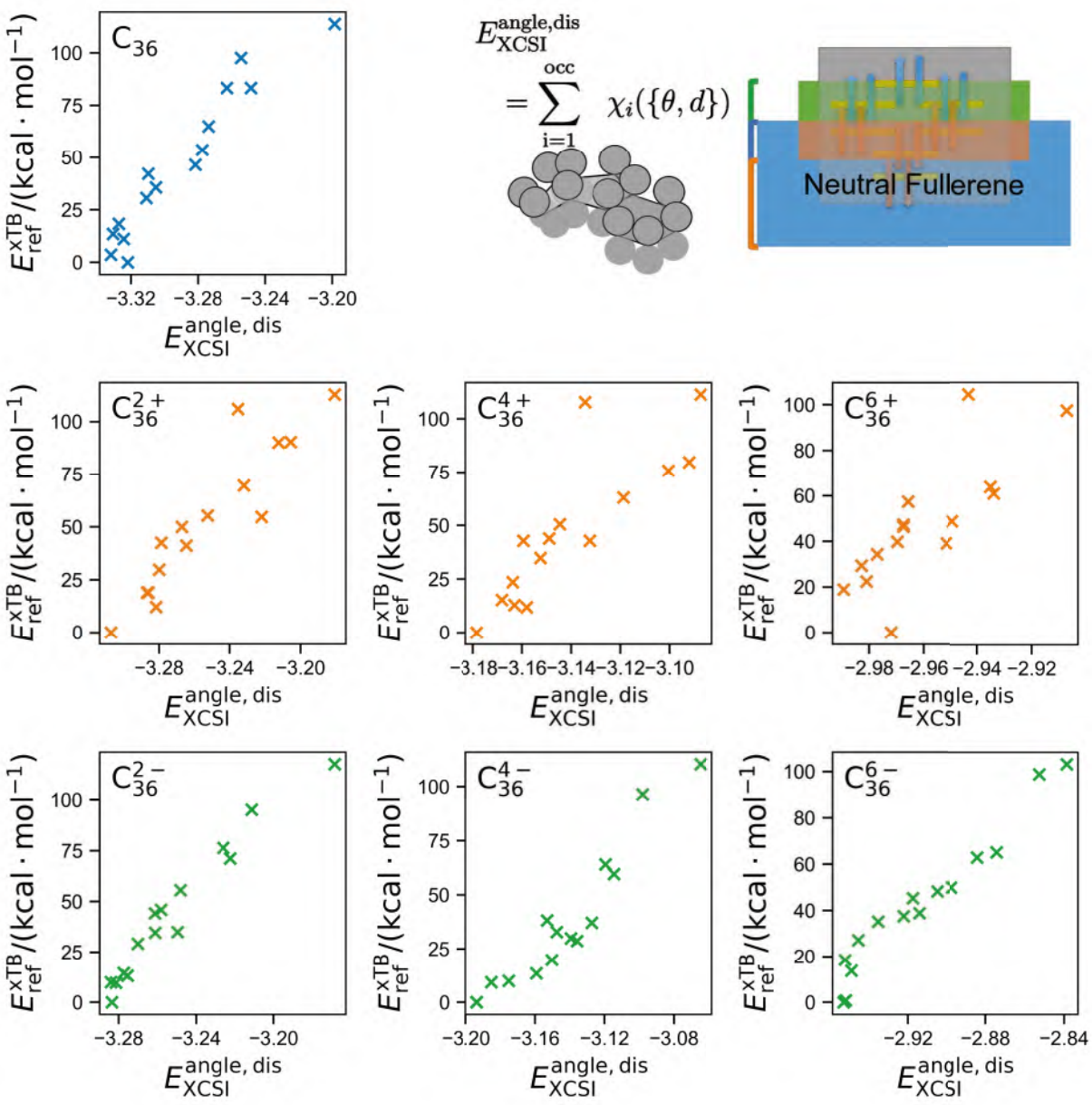


Figure 67: Correlation between xTB energies of $C_{36}$ isomers relative to the most stable one and prediction by XCSI model with angles and distances of $C_{36}$ isomers without and with charge 2+, 4+, 6+, 2-, 4-, 6-, respectively.

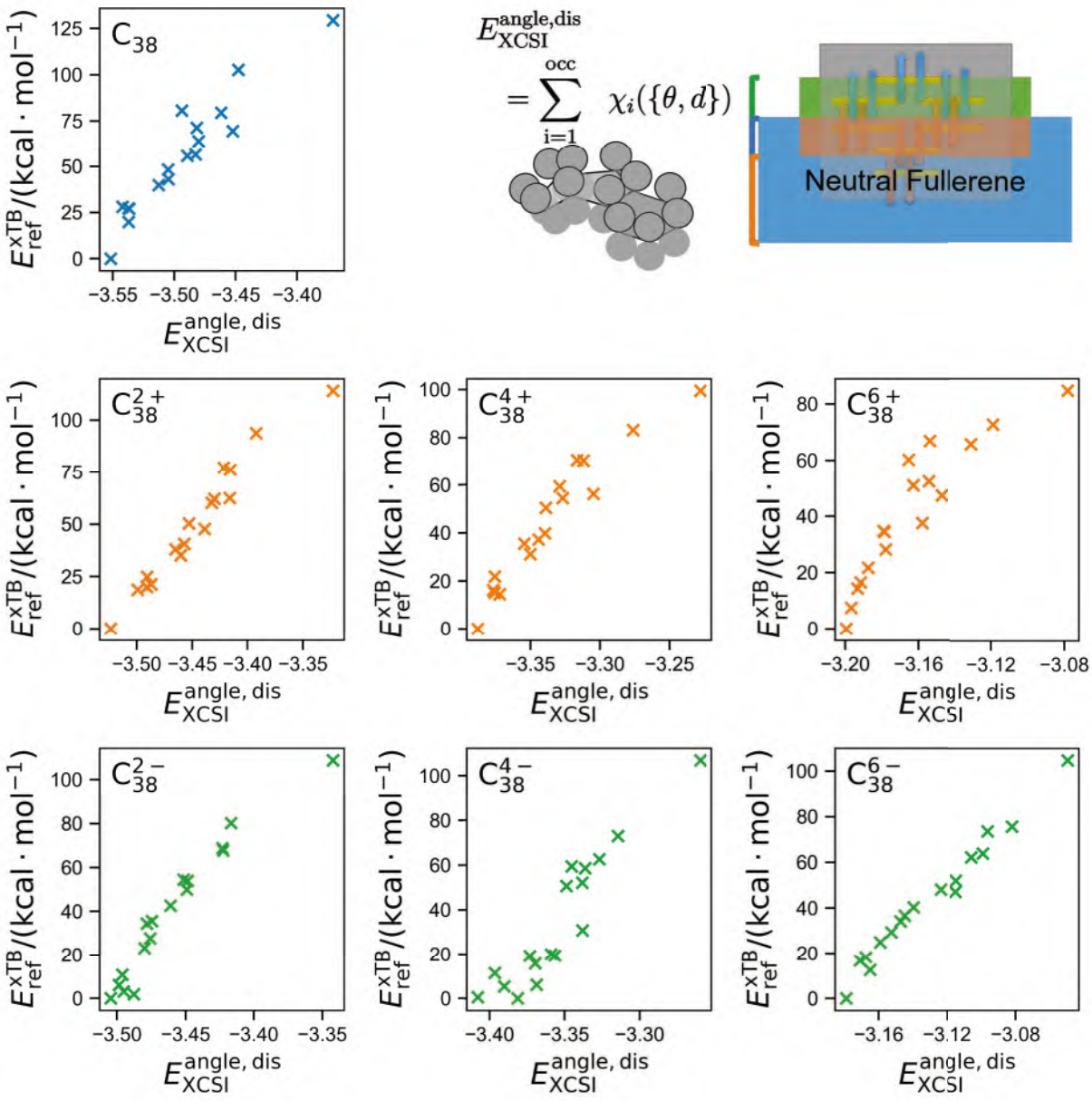


Figure 68: Correlation between xTB energies of $C_{38}$ isomers relative to the most stable one and prediction by XCSI model with angles and distances of $C_{38}$ isomers without and with charge 2+, 4+, 6+, 2-, 4-, 6-, respectively.

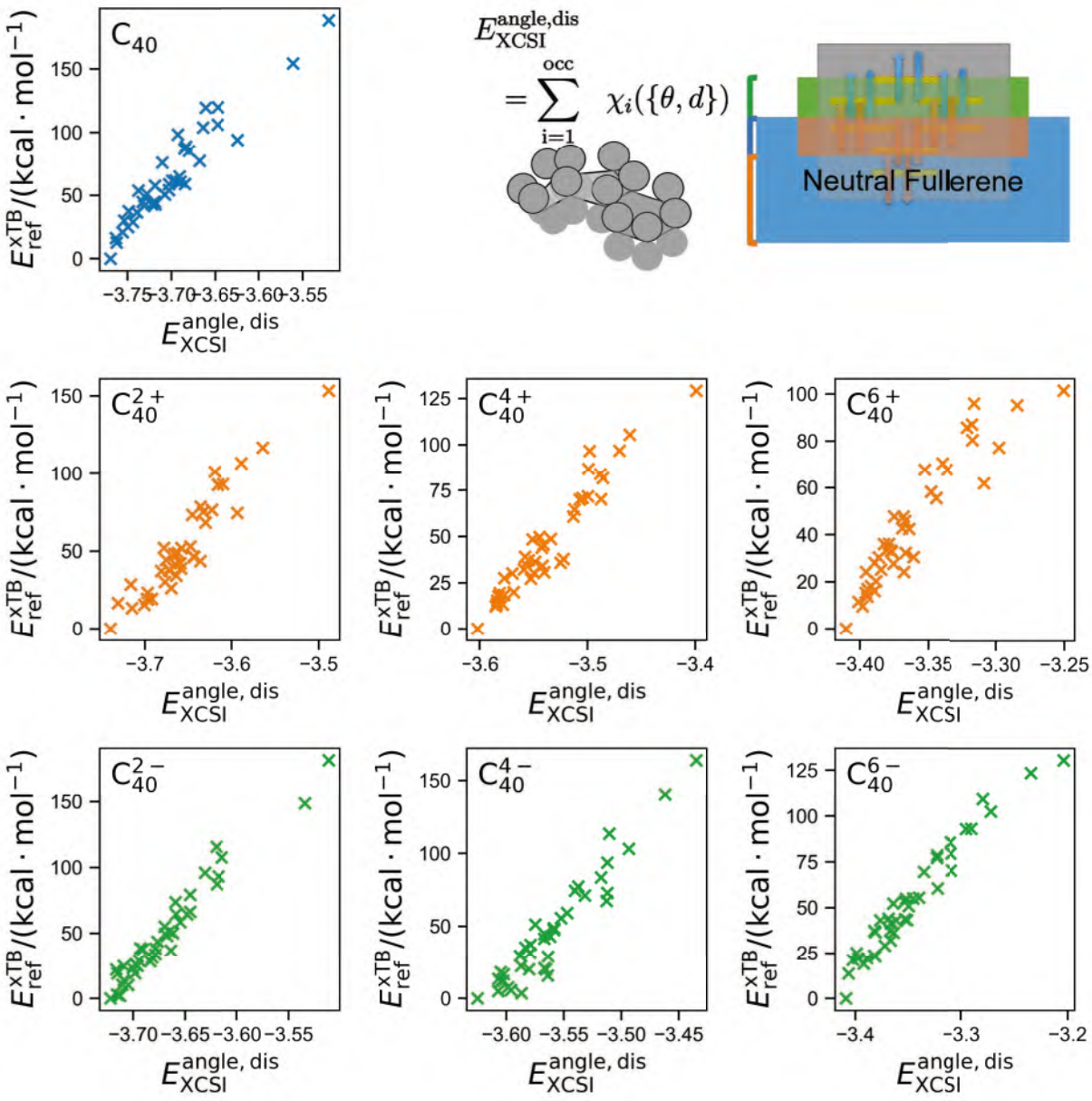


Figure 69: Correlation between xTB energies of $C_{40}$ isomers relative to the most stable one and prediction by XCSI model with angles and distances of $C_{40}$ isomers without and with charge 2+, 4+, 6+, 2-, 4-, 6-, respectively.

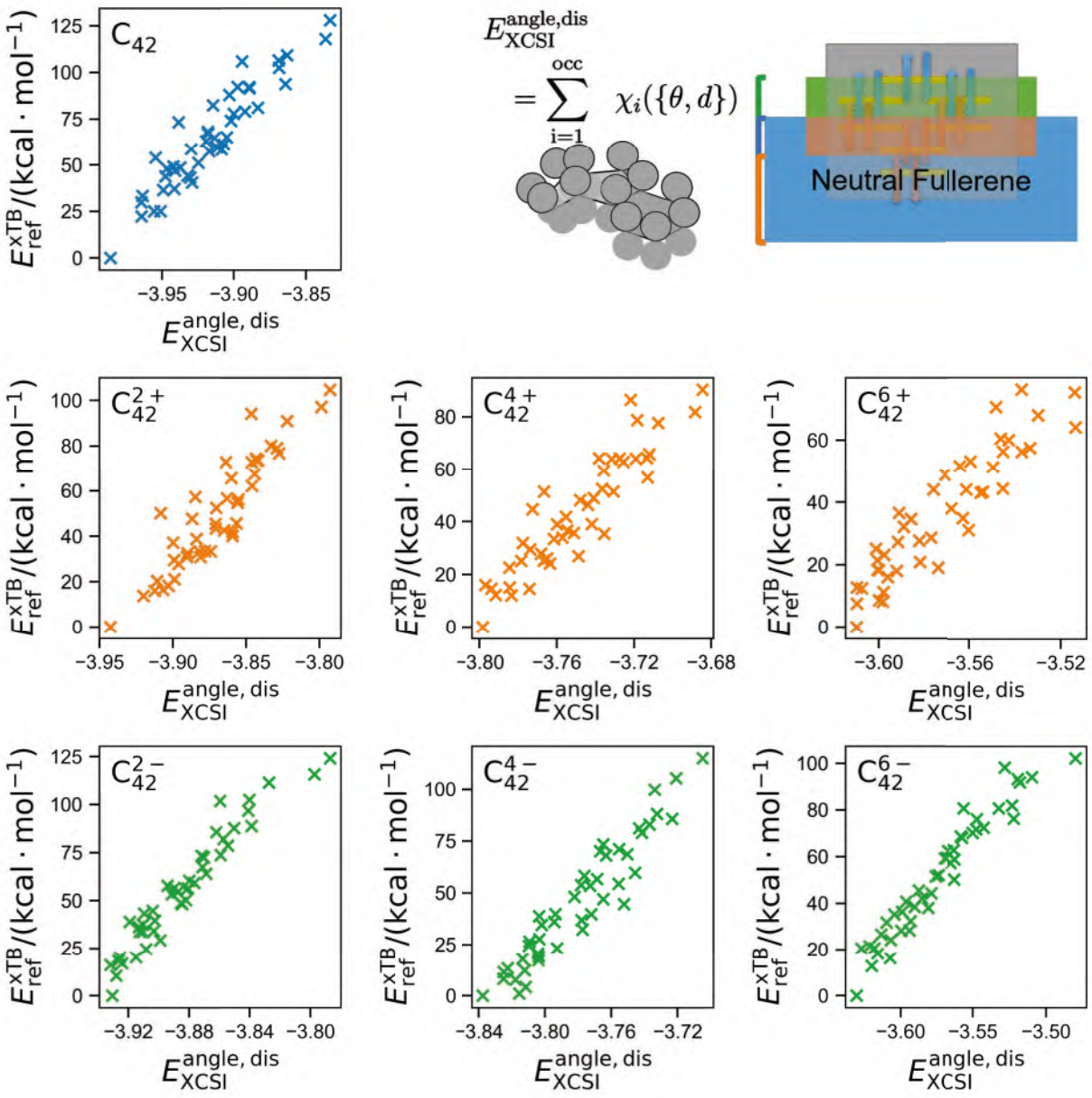


Figure 70: Correlation between xTB energies of $C_{42}$ isomers relative to the most stable one and prediction by XCSI model with angles and distances of $C_{42}$ isomers without and with charge 2+, 4+, 6+, 2-, 4-, 6-, respectively.

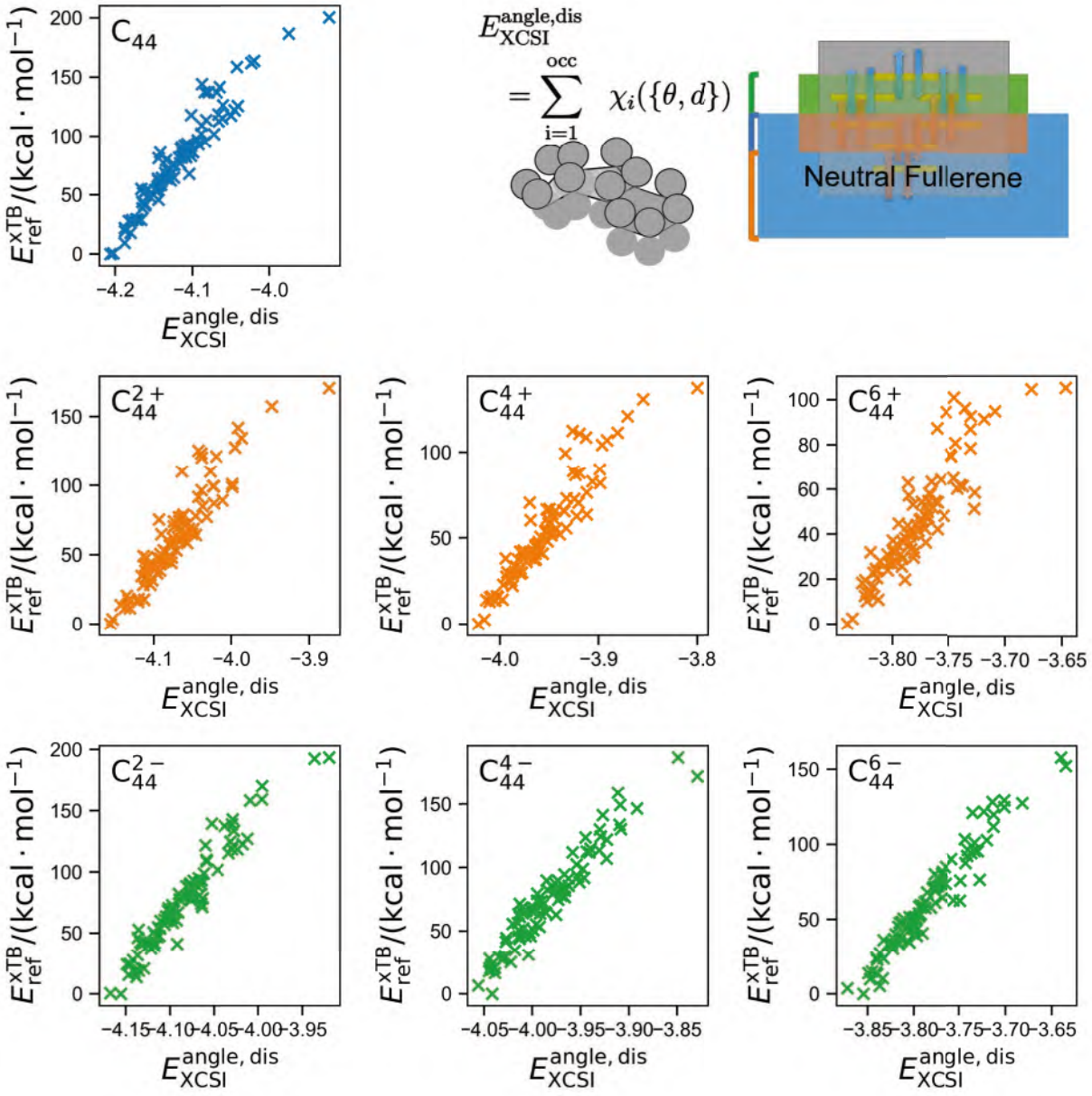


Figure 71: Correlation between xTB energies of $C_{44}$ isomers relative to the most stable one and prediction by XCSI model with angles and distances of $C_{44}$ isomers without and with charge 2+, 4+, 6+, 2-, 4-, 6-, respectively.

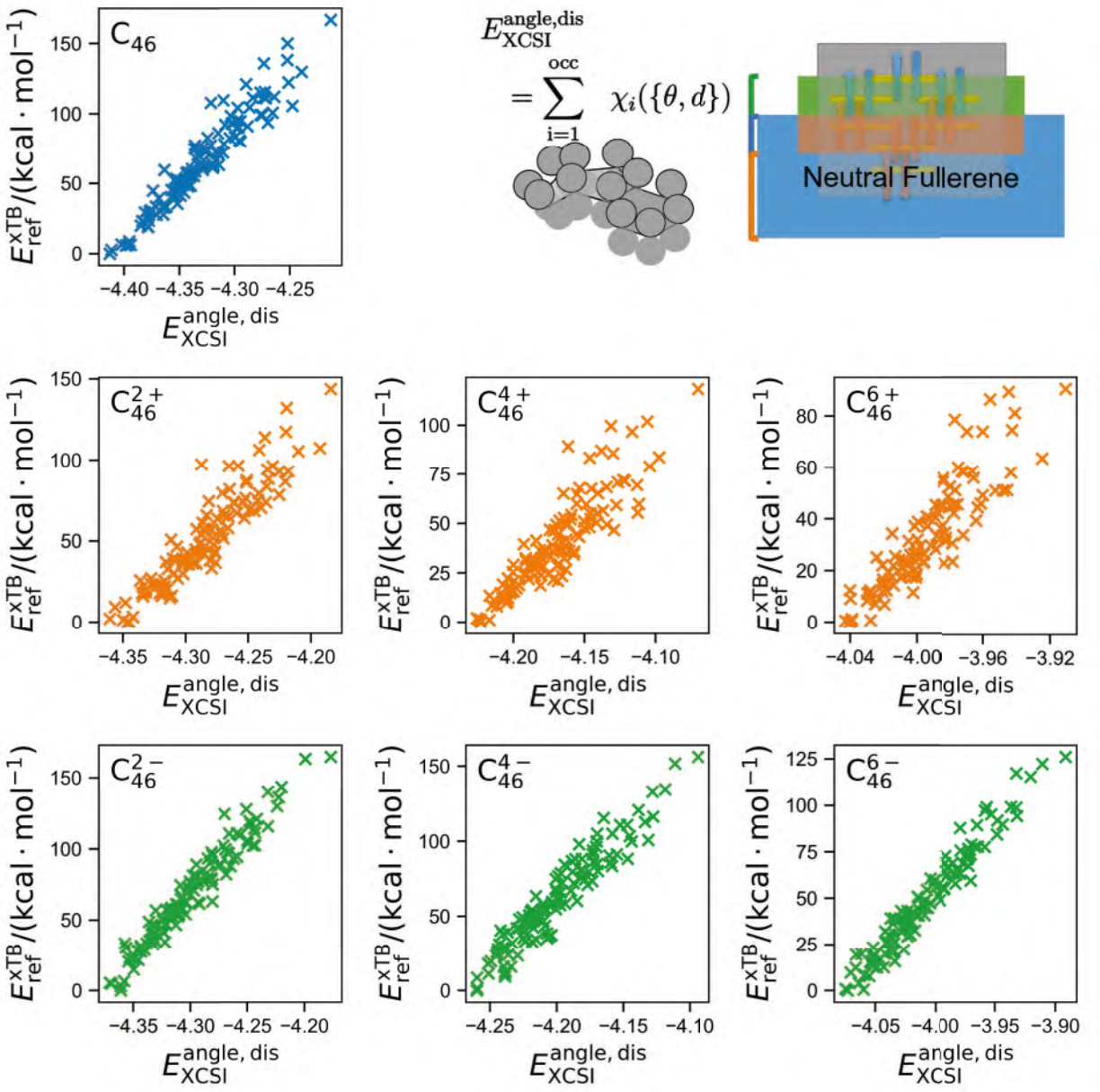


Figure 72: Correlation between xTB energies of $C_{46}$ isomers relative to the most stable one and prediction by XCSI model with angles and distances of $C_{46}$ isomers without and with charge 2+, 4+, 6+, 2-, 4-, 6-, respectively.

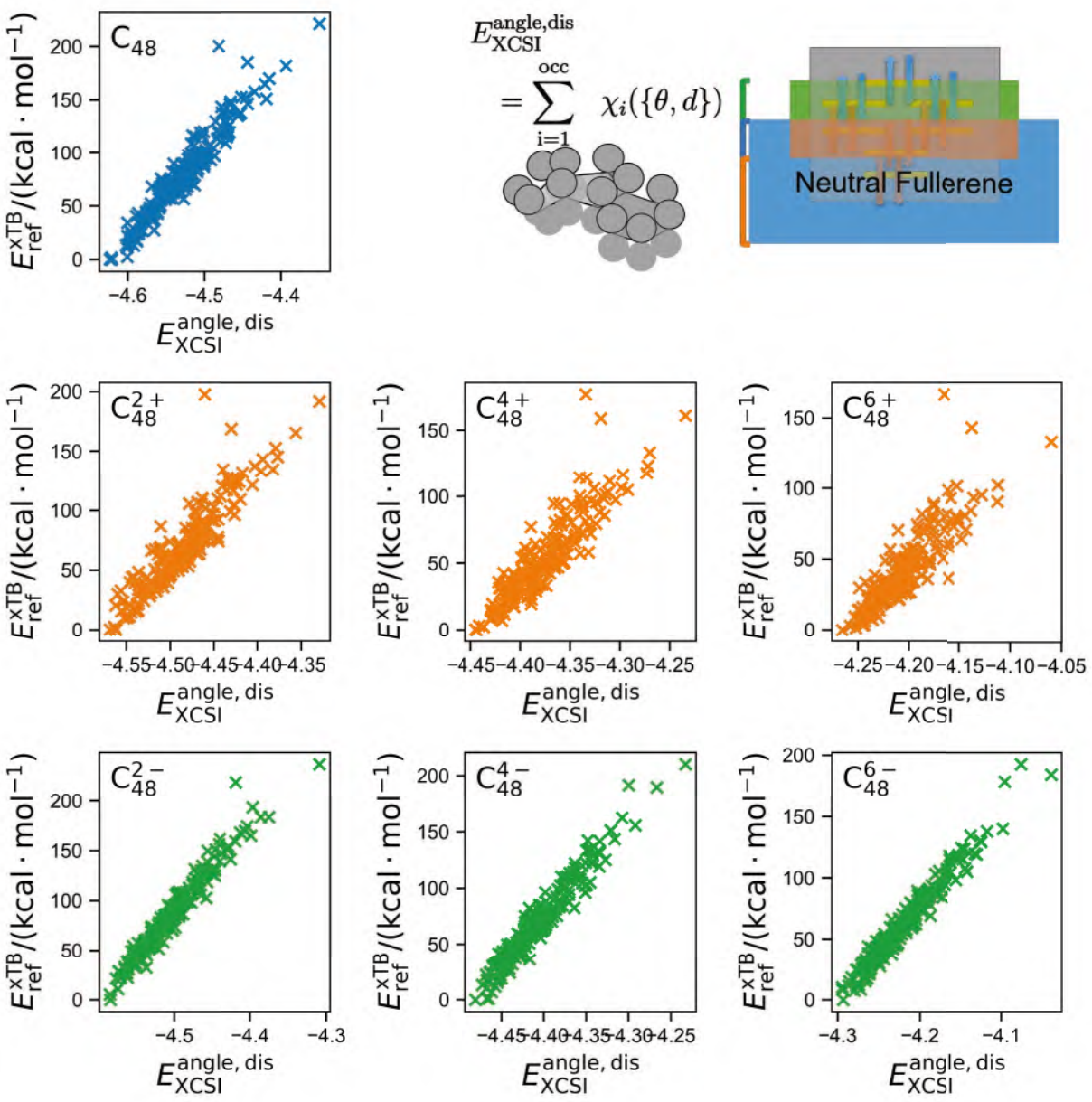


Figure 73: Correlation between xTB energies of $C_{48}$ isomers relative to the most stable one and prediction by XCSI model with angles and distances of $C_{48}$ isomers without and with charge 2+, 4+, 6+, 2-, 4-, 6-, respectively.

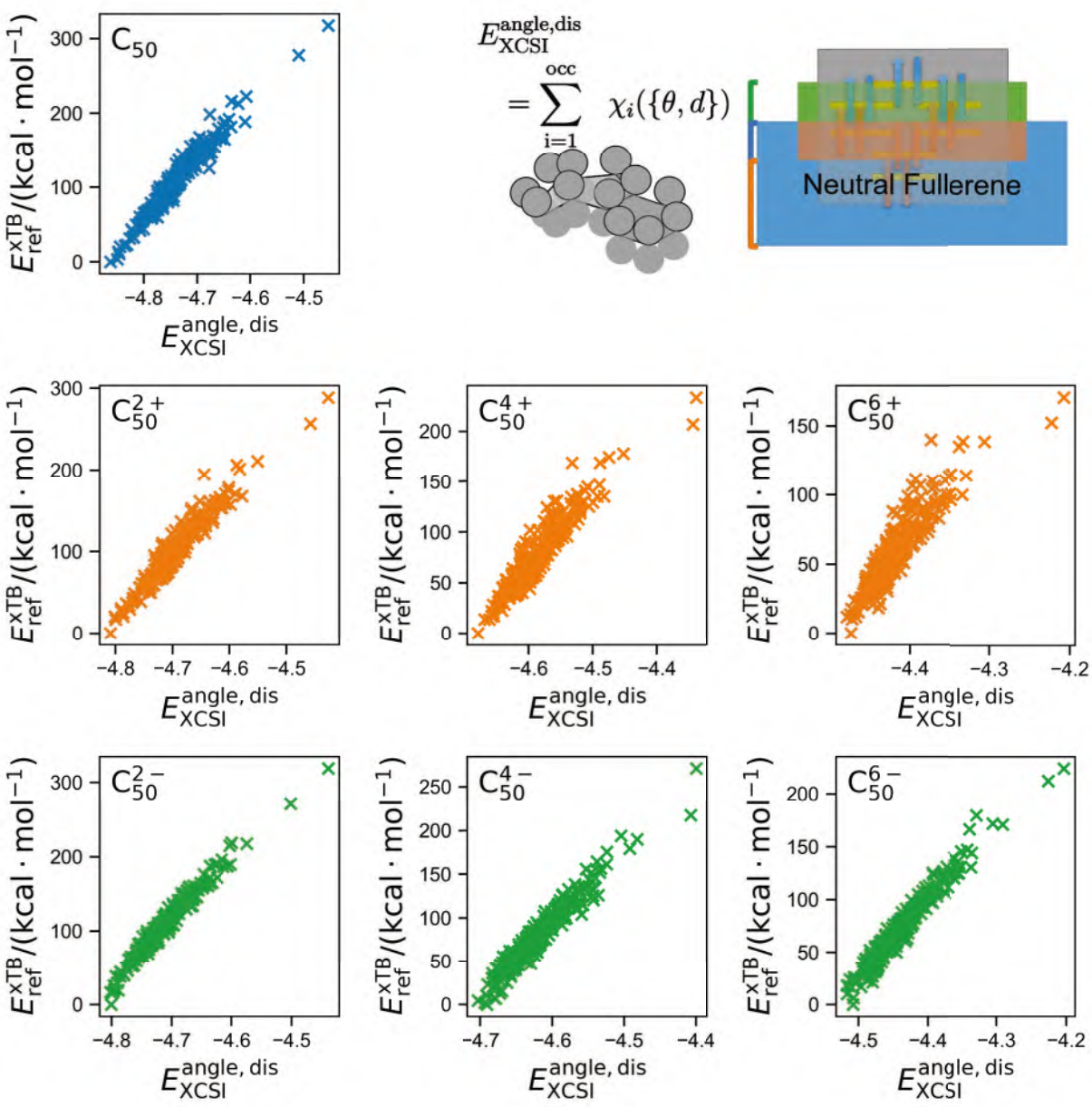


Figure 74: Correlation between xTB energies of $C_{50}$ isomers relative to the most stable one and prediction by XCSI model with angles and distances of $C_{50}$ isomers without and with charge 2+, 4+, 6+, 2-, 4-, 6-, respectively.

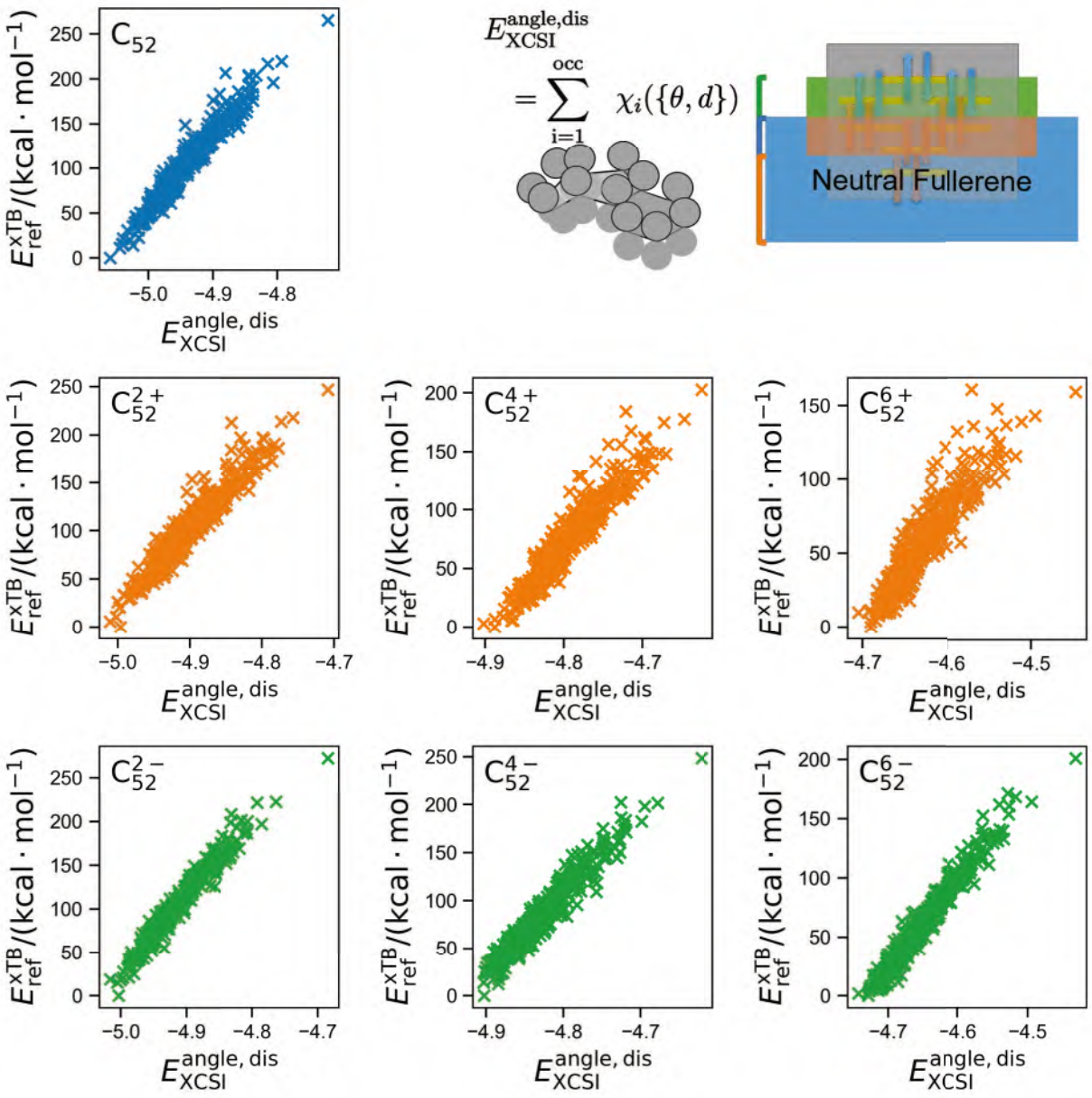


Figure 75: Correlation between xTB energies of $C_{52}$ isomers relative to the most stable one and prediction by XCSI model with angles and distances of $C_{52}$ isomers without and with charge 2+, 4+, 6+, 2-, 4-, 6-, respectively.

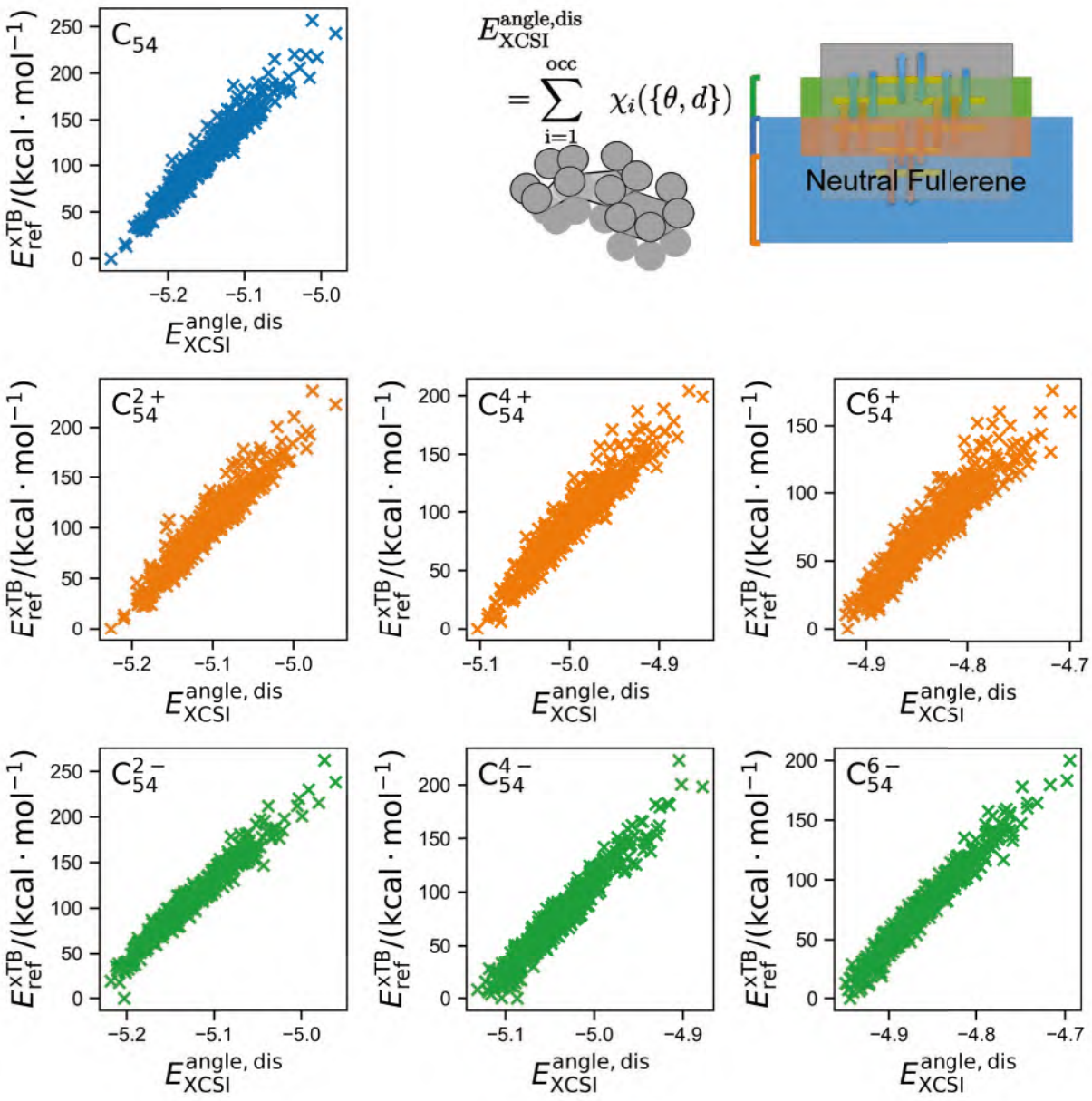


Figure 76: Correlation between xTB energies of $C_{54}$ isomers relative to the most stable one and prediction by XCSI model with angles and distances of $C_{54}$ isomers without and with charge 2+, 4+, 6+, 2-, 4-, 6-, respectively.

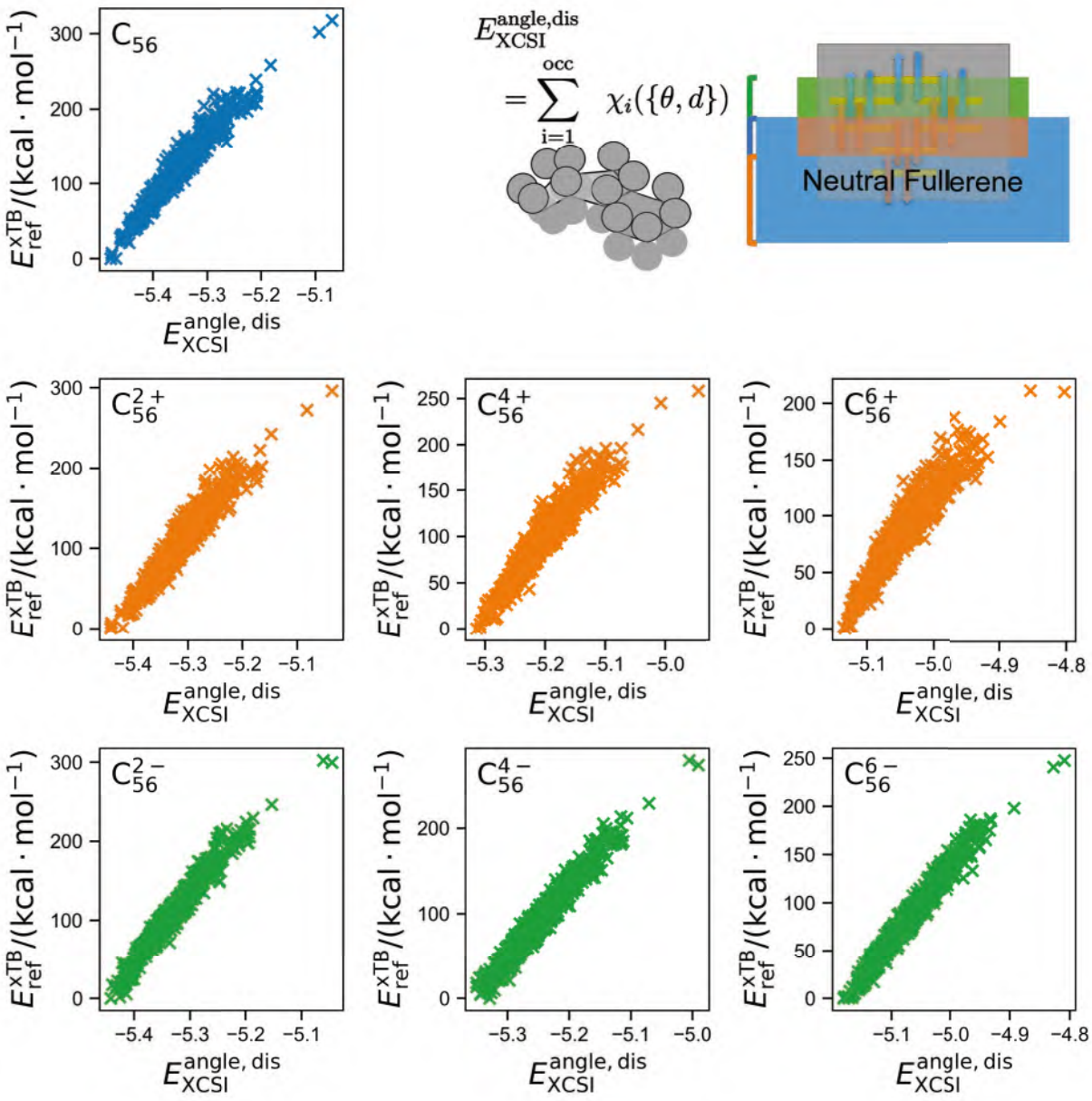


Figure 77: Correlation between xTB energies of $C_{56}$ isomers relative to the most stable one and prediction by XCSI model with angles and distances of $C_{56}$ isomers without and with charge 2+, 4+, 6+, 2-, 4-, 6-, respectively.

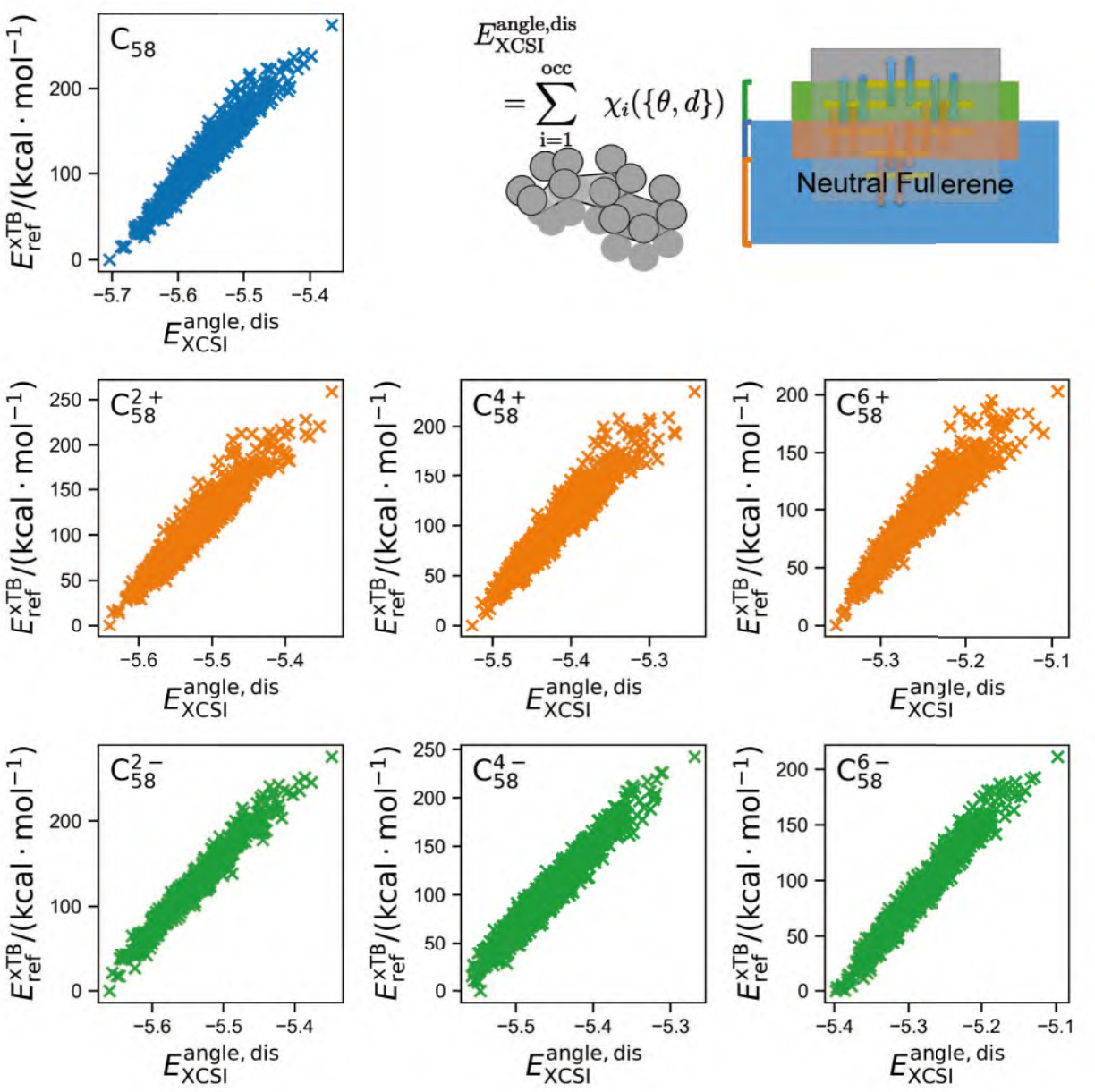


Figure 78: Correlation between xTB energies of $C_{58}$ isomers relative to the most stable one and prediction by XCSI model with angles and distances of $C_{58}$ isomers without and with charge 2+, 4+, 6+, 2-, 4-, 6-, respectively.

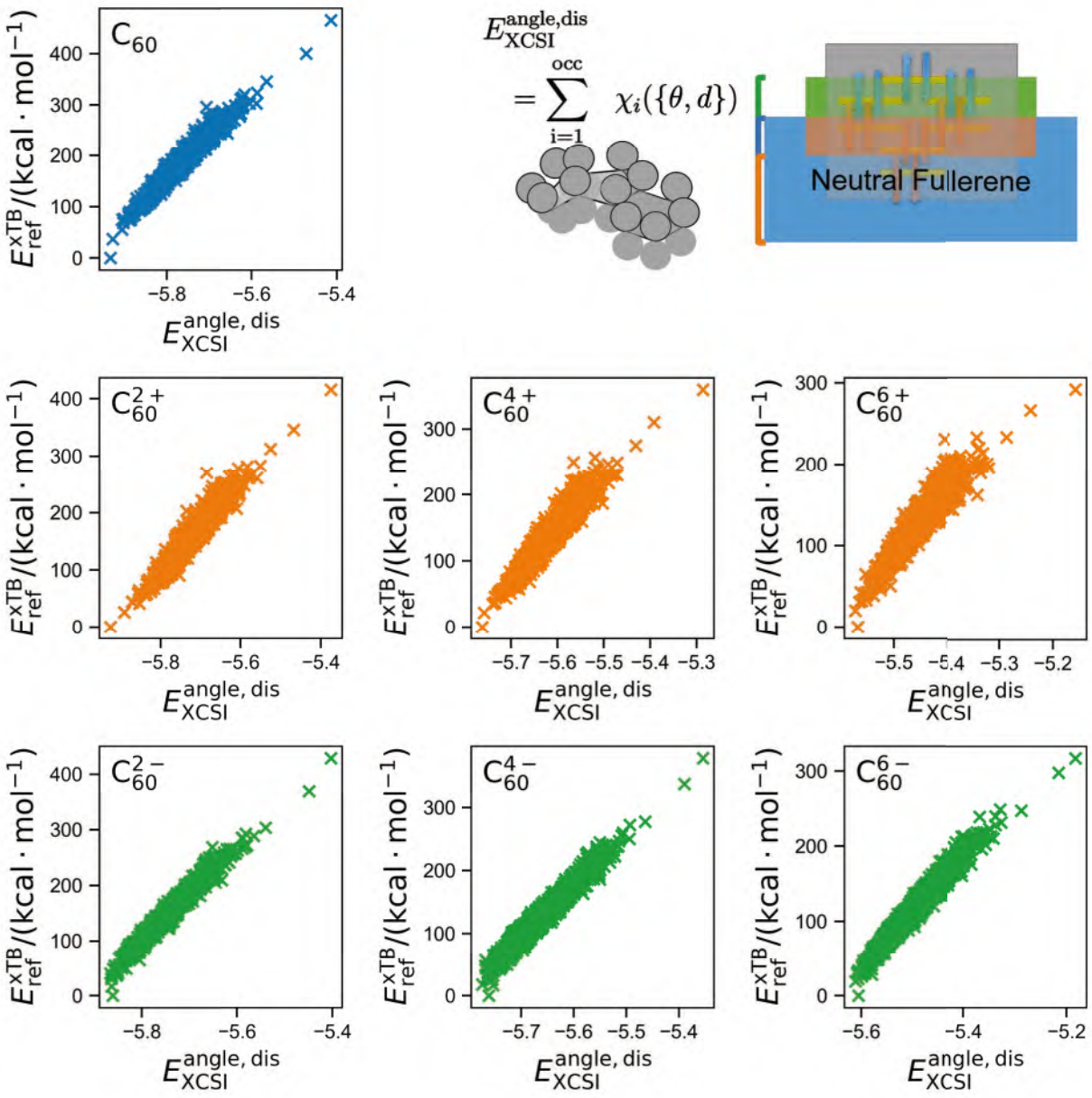


Figure 79: Correlation between xTB energies of $C_{60}$ isomers relative to the most stable one and prediction by XCSI model with angles and distances of $C_{60}$ isomers without and with charge 2+, 4+, 6+, 2-, 4-, 6-, respectively.

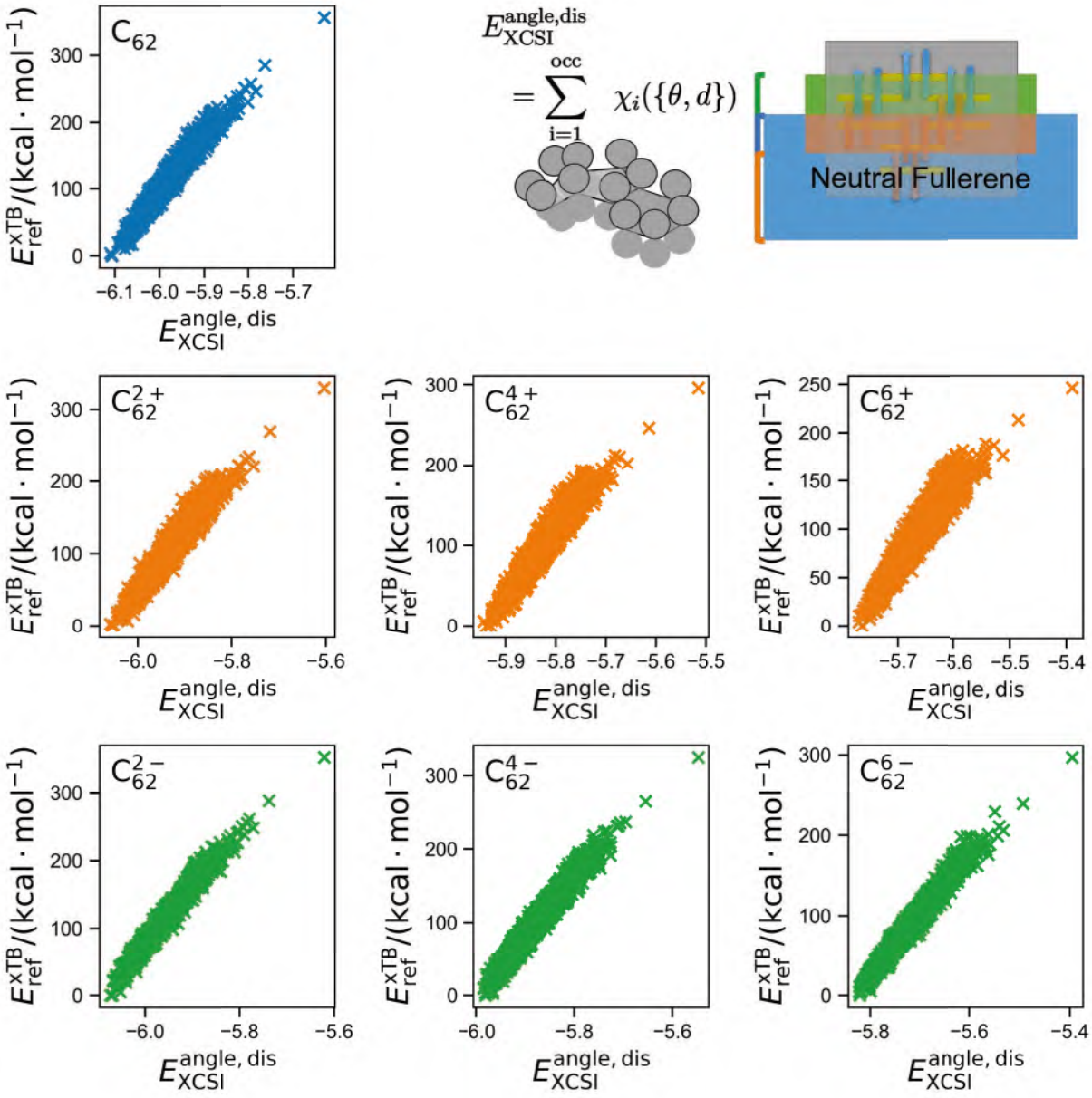


Figure 80: Correlation between xTB energies of $C_{62}$ isomers relative to the most stable one and prediction by XCSI model with angles and distances of $C_{62}$ isomers without and with charge 2+, 4+, 6+, 2-, 4-, 6-, respectively.

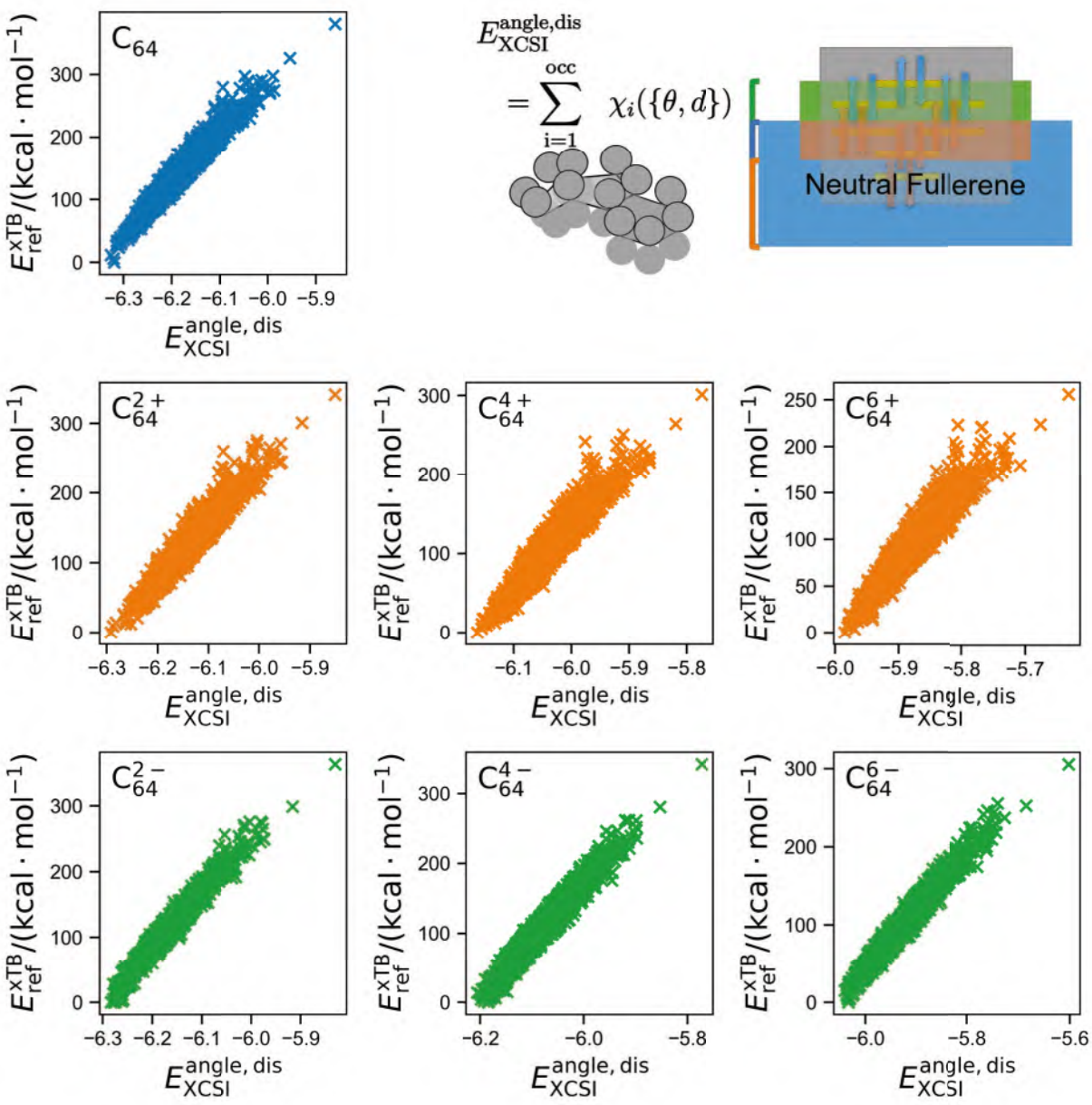


Figure 81: Correlation between xTB energies of $C_{64}$ isomers relative to the most stable one and prediction by XCSI model with angles and distances of $C_{64}$ isomers without and with charge 2+, 4+, 6+, 2-, 4-, 6-, respectively.

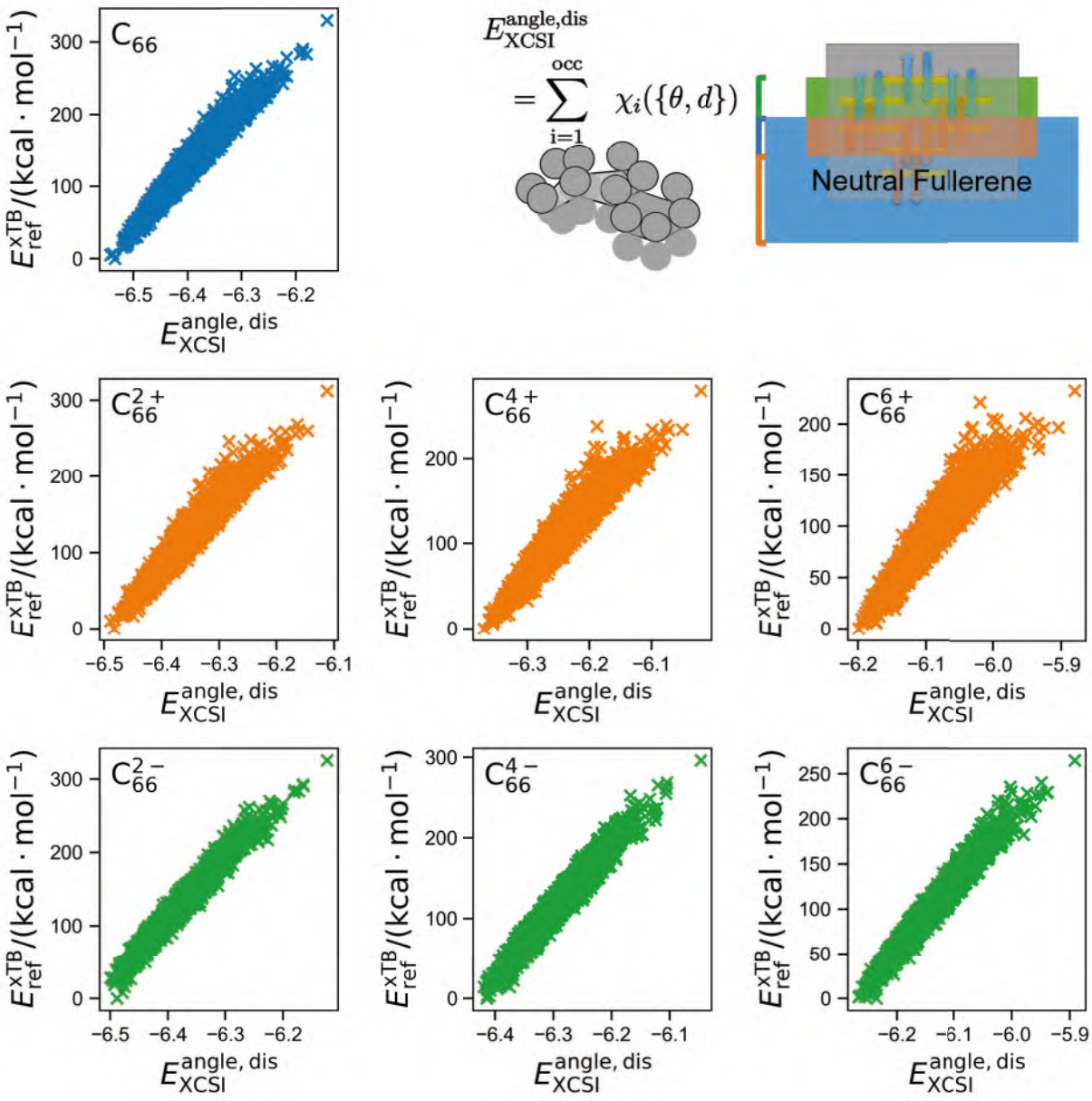


Figure 82: Correlation between xTB energies of $C_{66}$ isomers relative to the most stable one and prediction by XCSI model with angles and distances of $C_{66}$ isomers without and with charge 2+, 4+, 6+, 2-, 4-, 6-, respectively.

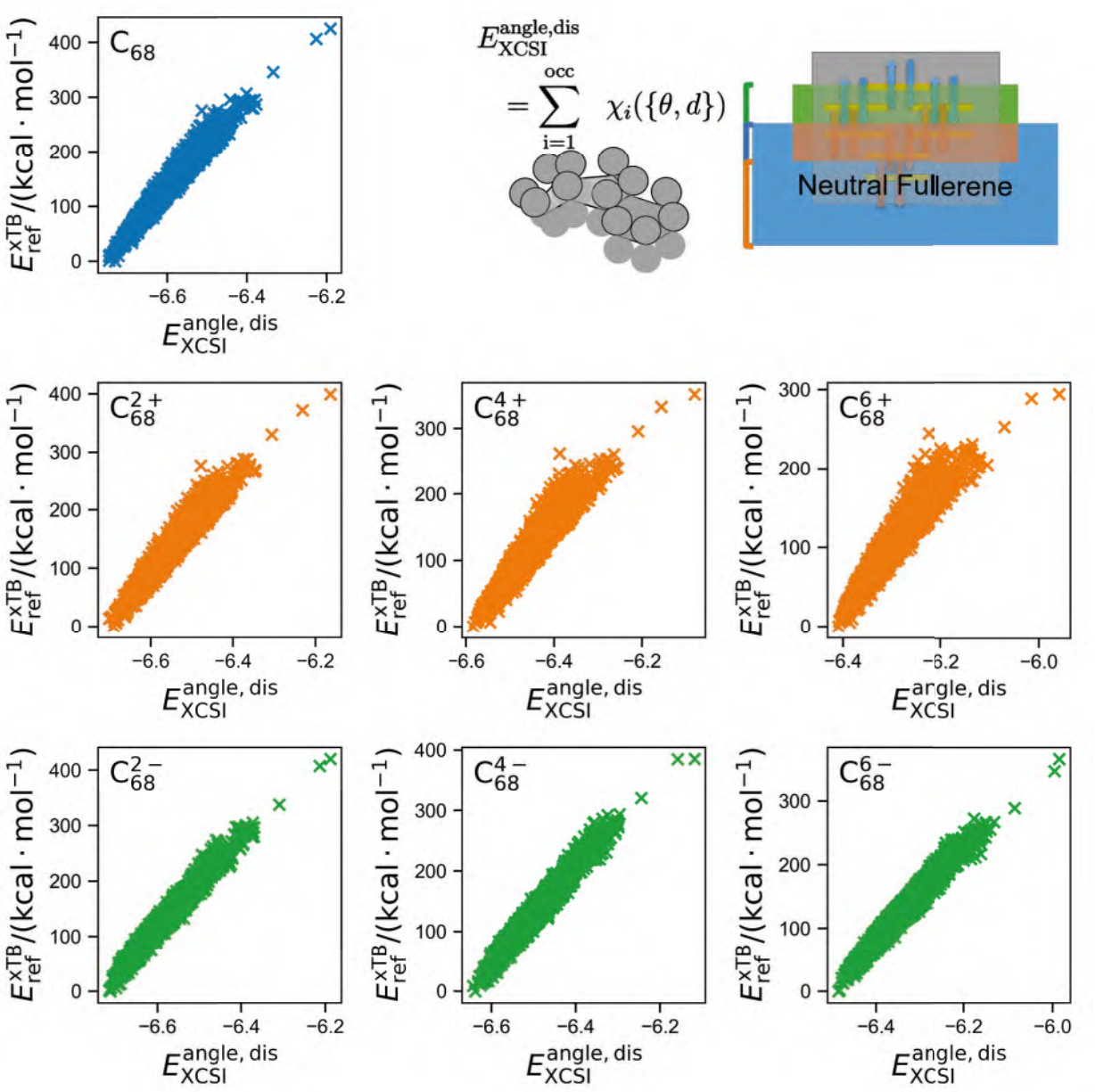


Figure 83: Correlation between xTB energies of $C_{68}$ isomers relative to the most stable one and prediction by XCSI model with angles and distances of $C_{68}$ isomers without and with charge 2+, 4+, 6+, 2-, 4-, 6-, respectively.

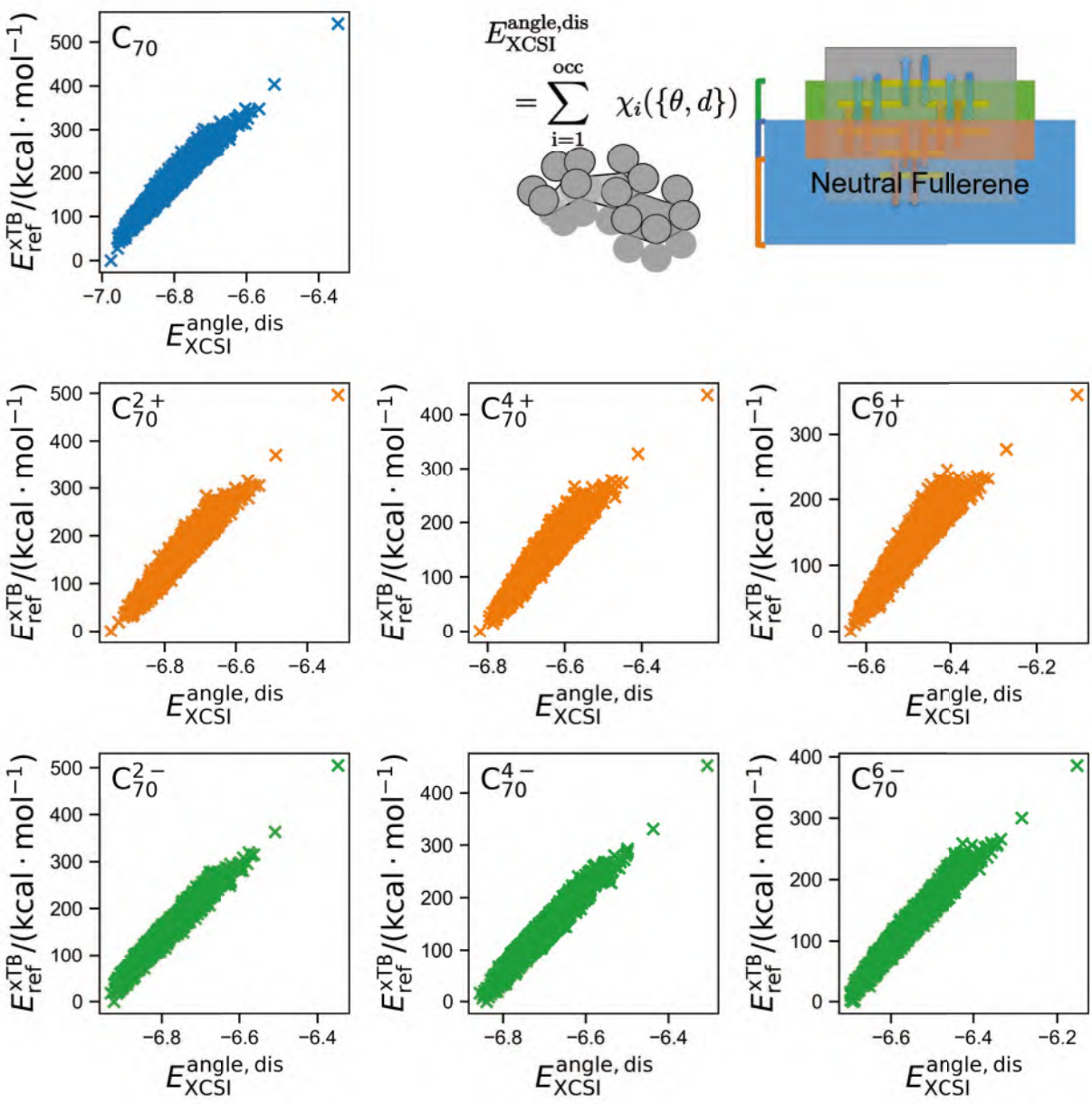


Figure 84: Correlation between xTB energies of $C_{70}$ isomers relative to the most stable one and prediction by XCSI model with angles and distances of $C_{70}$ isomers without and with charge 2+, 4+, 6+, 2-, 4-, 6-, respectively.

# 6 Correlation between xTB energies and prediction by XCSI model with angles and distances, without using adjacent matrix mask

Predictions by XCSI model with angles and distances, without using adjacent matrix mask, are calculated by

$$E_{\mathrm{XCSI}}^{\mathrm{angle,nodis}} \equiv \sum_{k=i}^{n} \chi_{k,i}^{q}(\{\theta, d\}) \tag{8}$$

where $\chi_{k,i}^{q}$ is eigenvalues of extended adjacency matrix, whose elements are

$$h_{ij}^{k} = \begin{cases} \cos\theta_{ij} \exp\left(-d_{ij}^{2}\right) \beta' & i \neq j \\ 0 & i = j \end{cases} \tag{9}$$

.

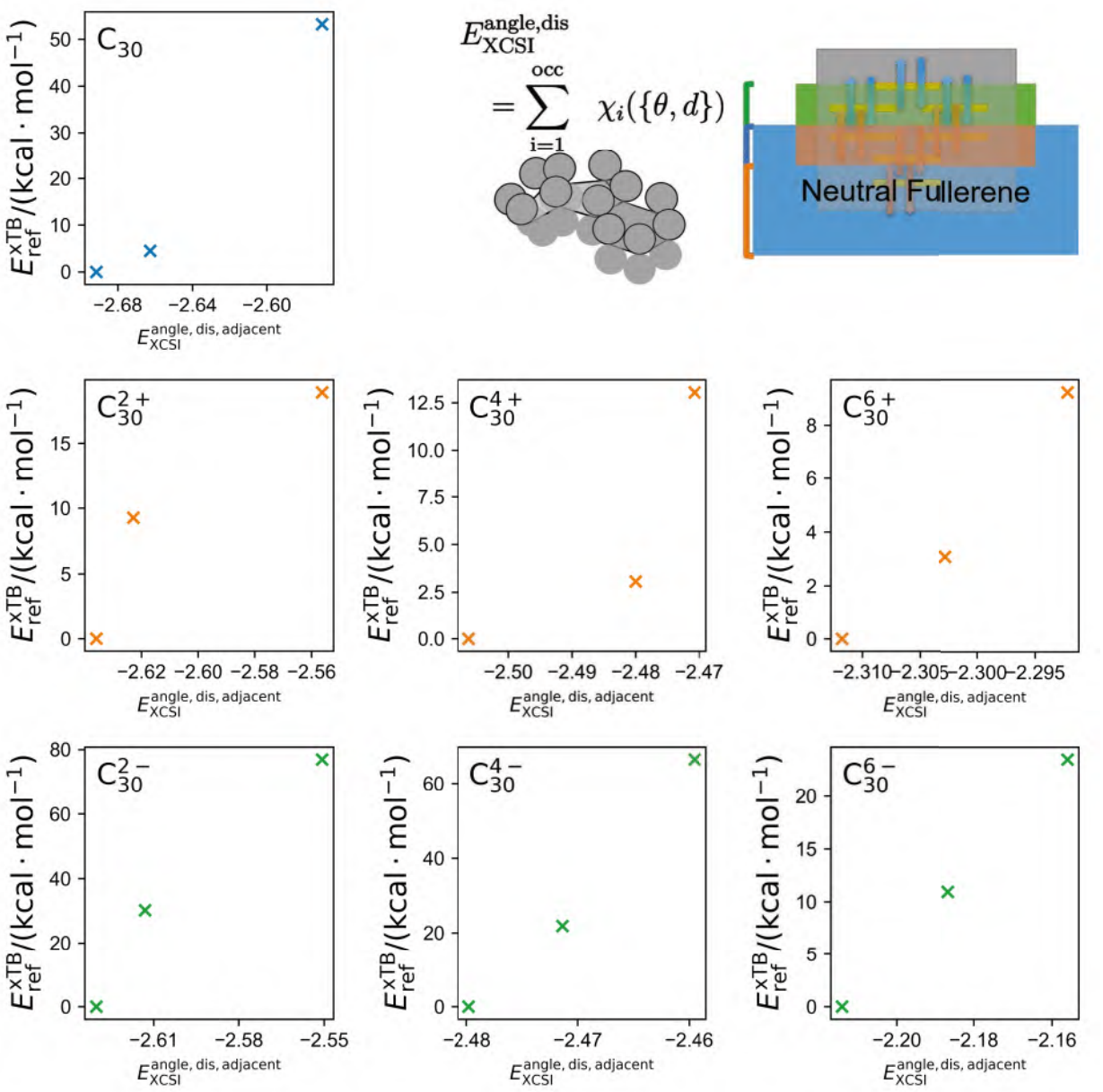


Figure 85: Correlation between xTB energies of $C_{30}$ isomers relative to the most stable one and prediction by XCSI model with angles and distances, without using adjacent matrix mask of $C_{30}$ isomers without and with charge 2+, 4+, 6+, 2-, 4-, 6-, respectively.

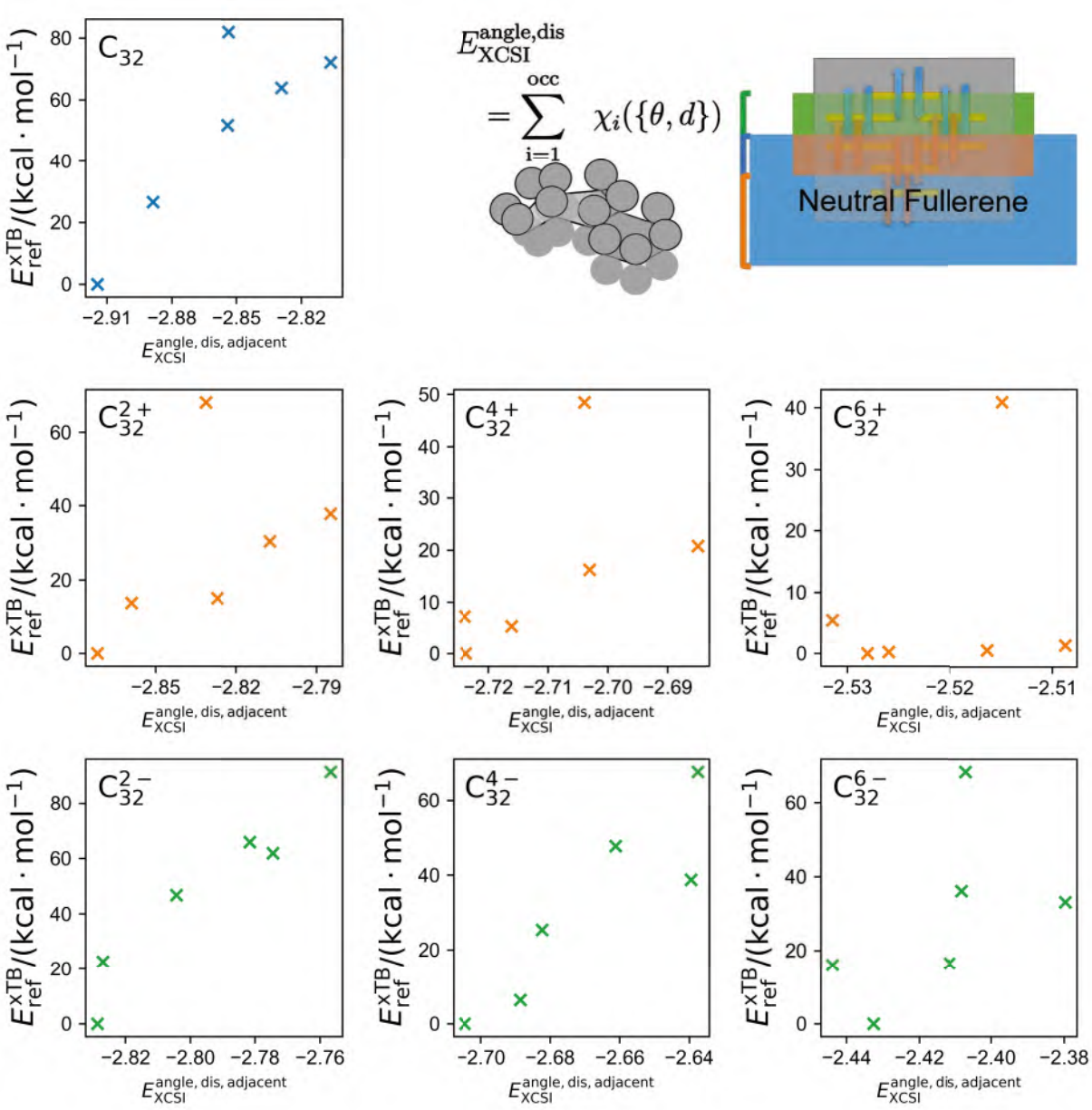


Figure 86: Correlation between xTB energies of $C_{32}$ isomers relative to the most stable one and prediction by XCSI model with angles and distances, without using adjacent matrix mask of $C_{32}$ isomers without and with charge 2+, 4+, 6+, 2-, 4-, 6-, respectively.

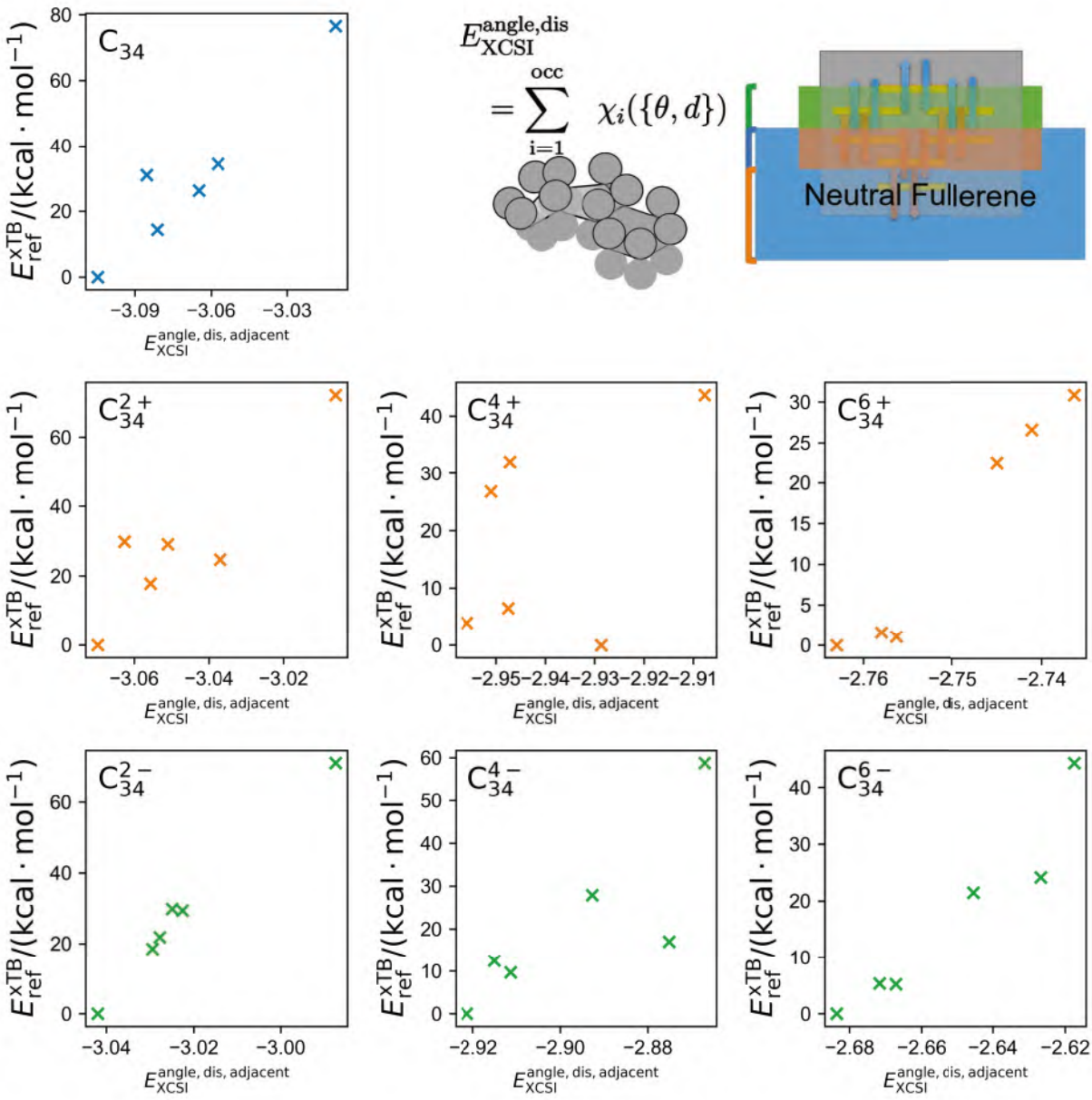


Figure 87: Correlation between xTB energies of $C_{34}$ isomers relative to the most stable one and prediction by XCSI model with angles and distances, without using adjacent matrix mask of $C_{34}$ isomers without and with charge 2+, 4+, 6+, 2-, 4-, 6-, respectively.

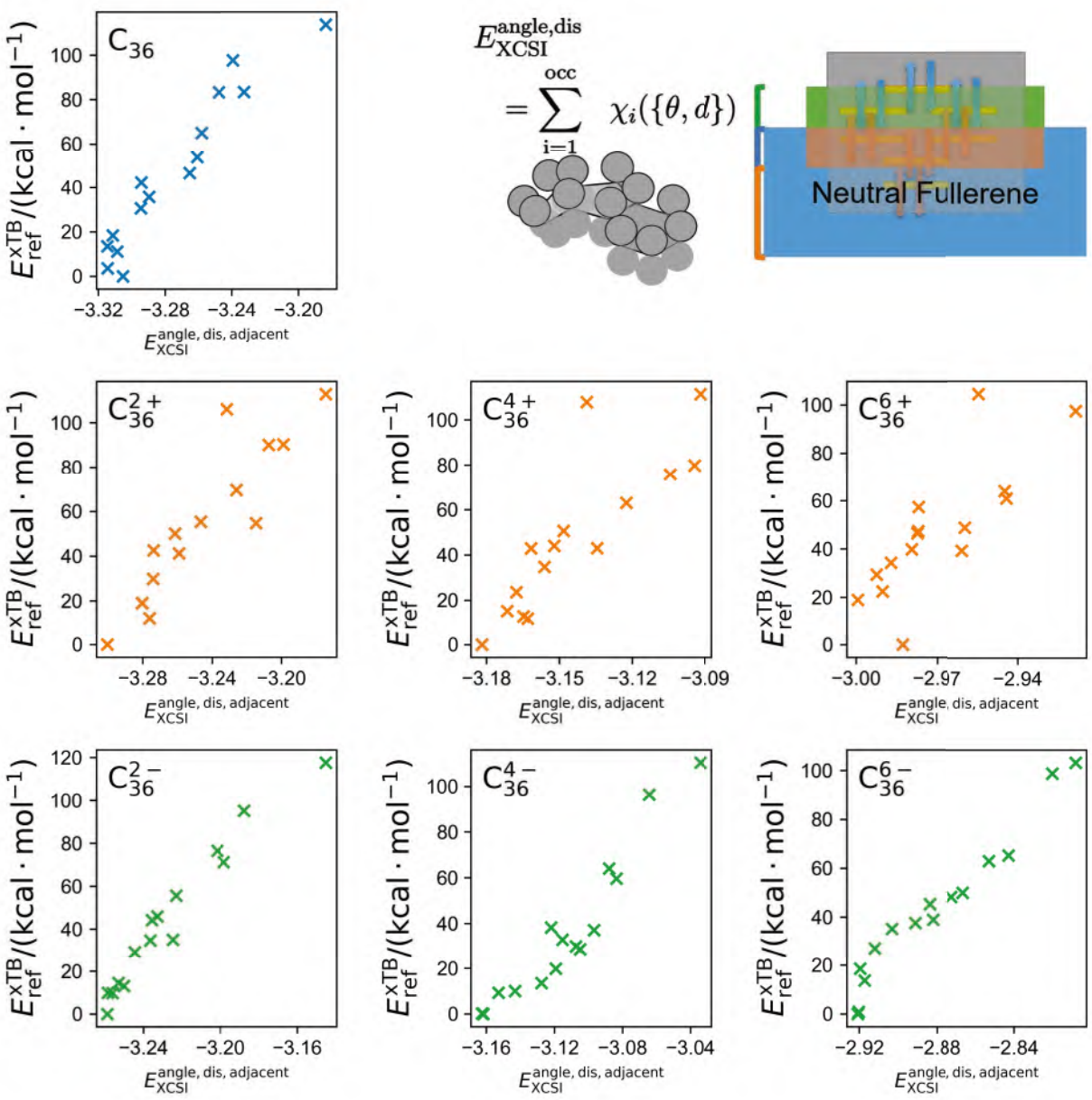


Figure 88: Correlation between xTB energies of $C_{36}$ isomers relative to the most stable one and prediction by XCSI model with angles and distances, without using adjacent matrix mask of $C_{36}$ isomers without and with charge 2+, 4+, 6+, 2-, 4-, 6-, respectively.

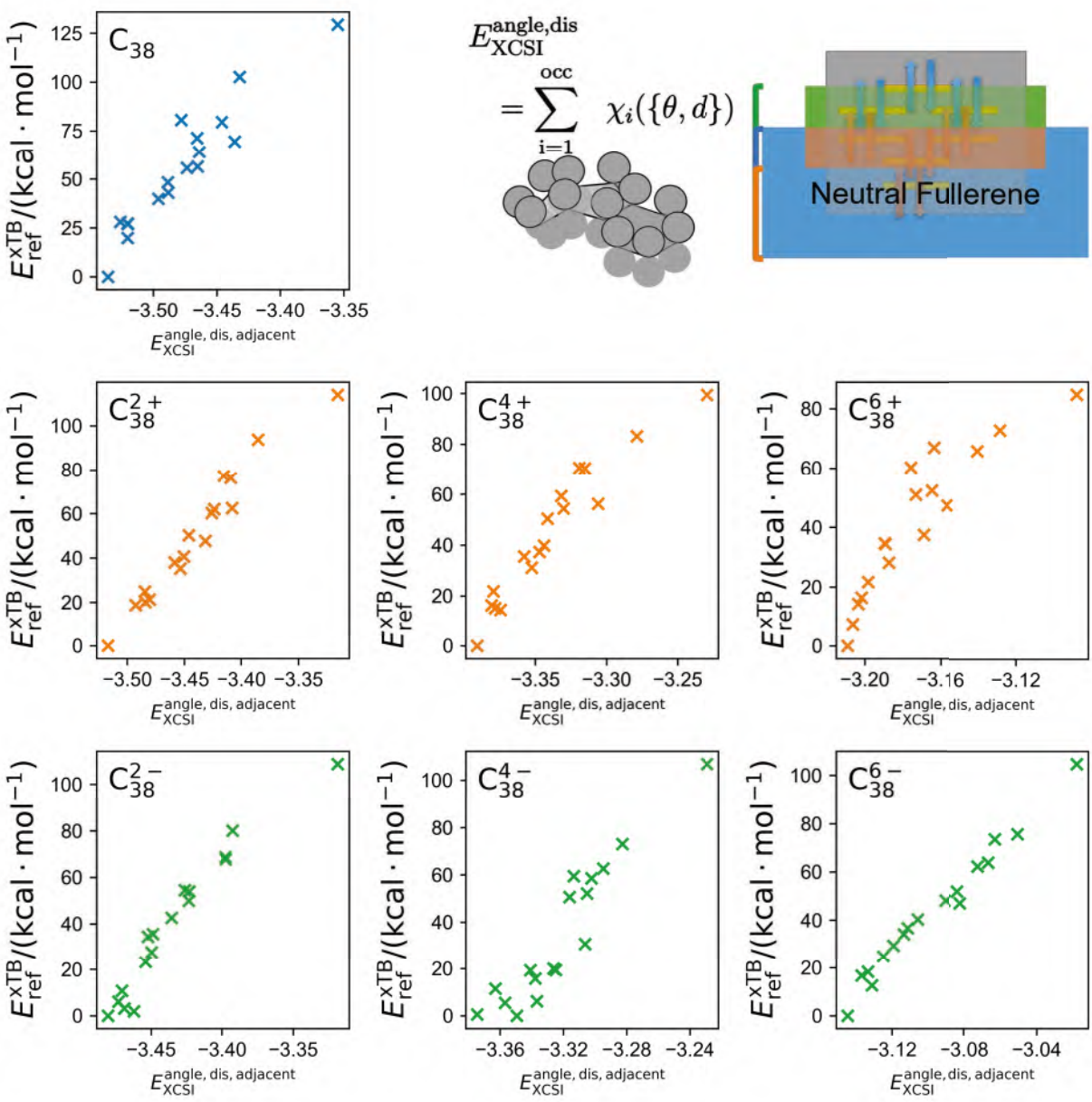


Figure 89: Correlation between xTB energies of $C_{38}$ isomers relative to the most stable one and prediction by XCSI model with angles and distances, without using adjacent matrix mask of $C_{38}$ isomers without and with charge 2+, 4+, 6+, 2-, 4-, 6-, respectively.

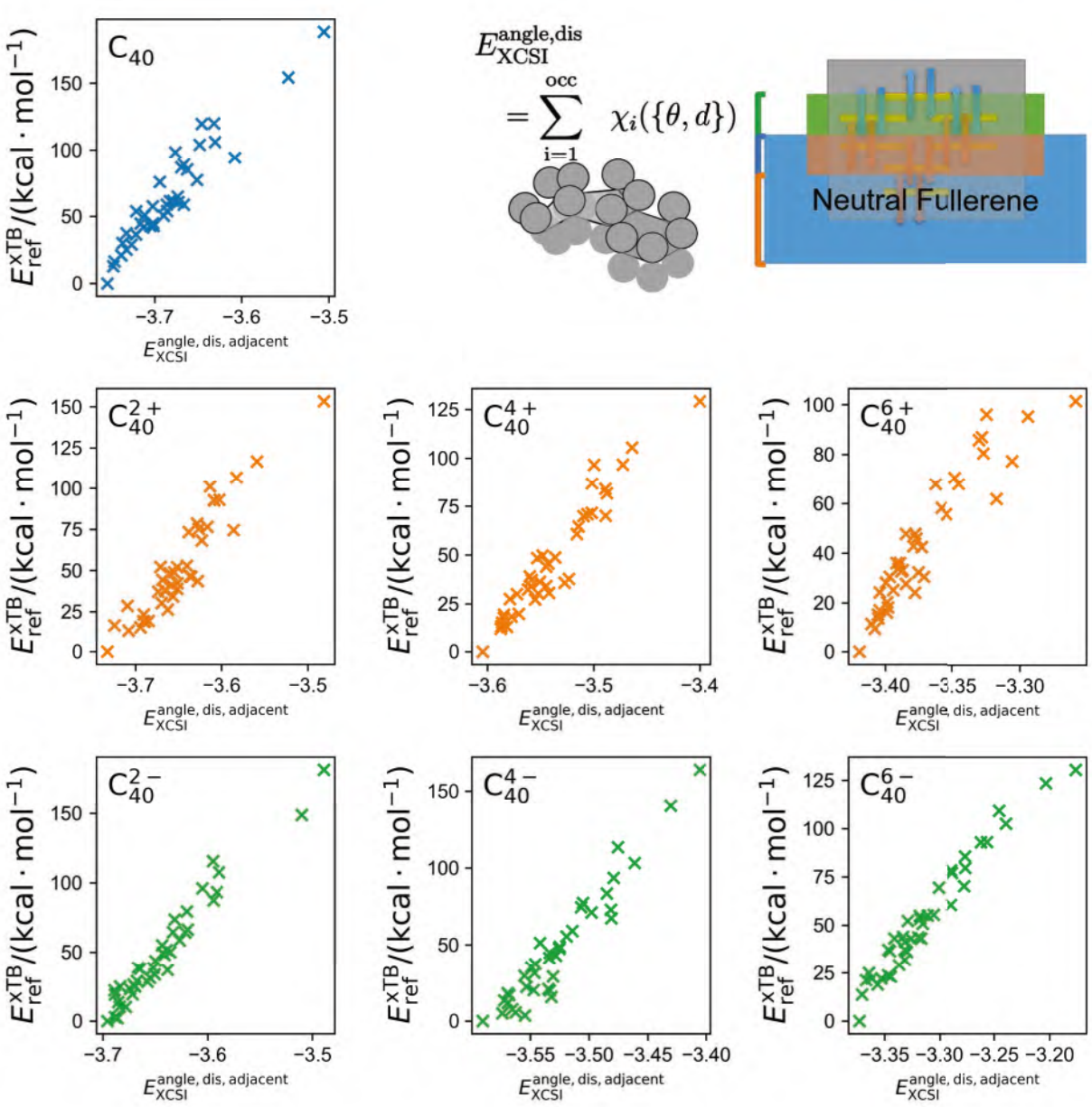


Figure 90: Correlation between xTB energies of $C_{40}$ isomers relative to the most stable one and prediction by XCSI model with angles and distances, without using adjacent matrix mask of $C_{40}$ isomers without and with charge 2+, 4+, 6+, 2-, 4-, 6-, respectively.

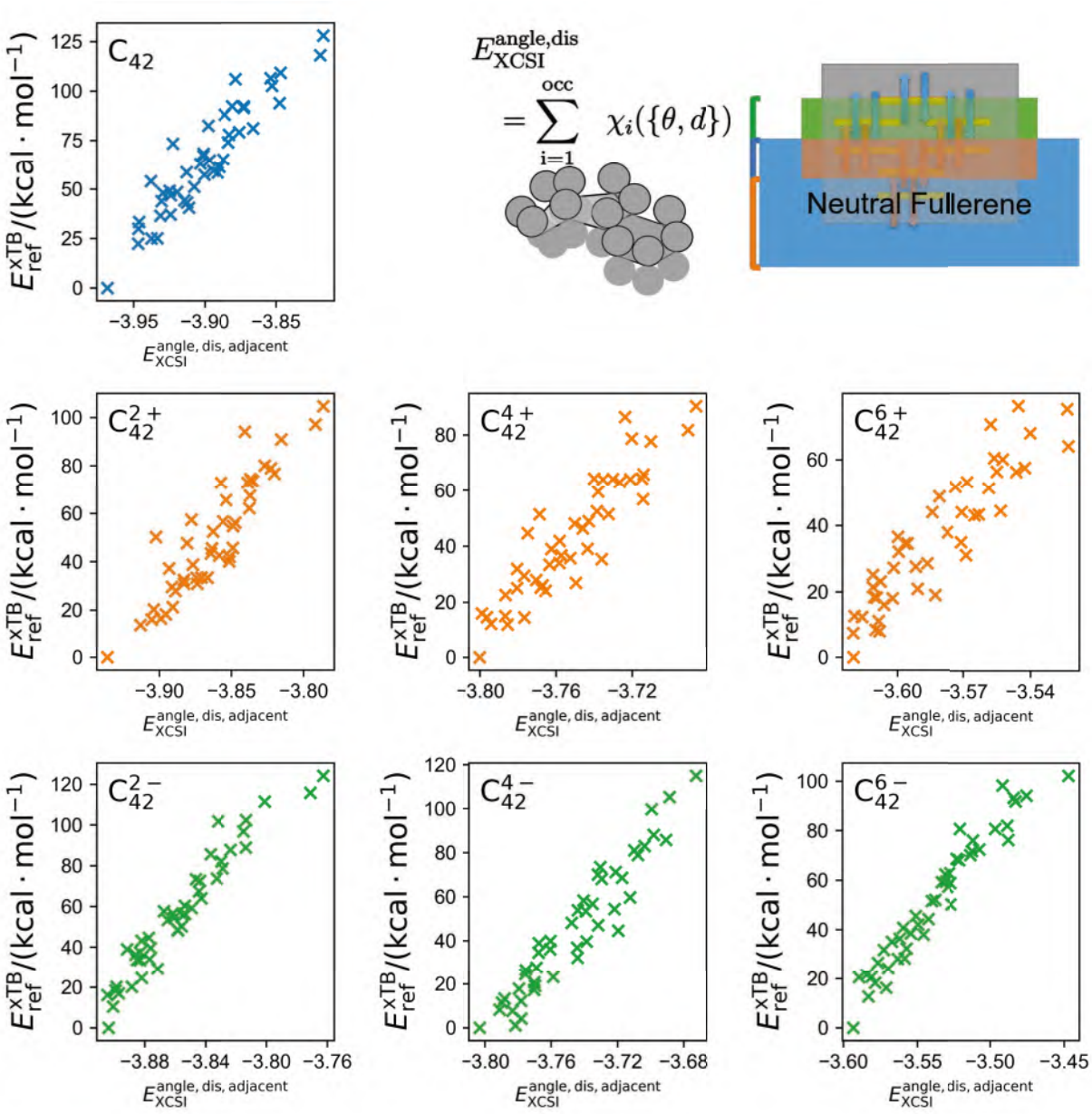


Figure 91: Correlation between xTB energies of $C_{42}$ isomers relative to the most stable one and prediction by XCSI model with angles and distances, without using adjacent matrix mask of $C_{42}$ isomers without and with charge 2+, 4+, 6+, 2-, 4-, 6-, respectively.

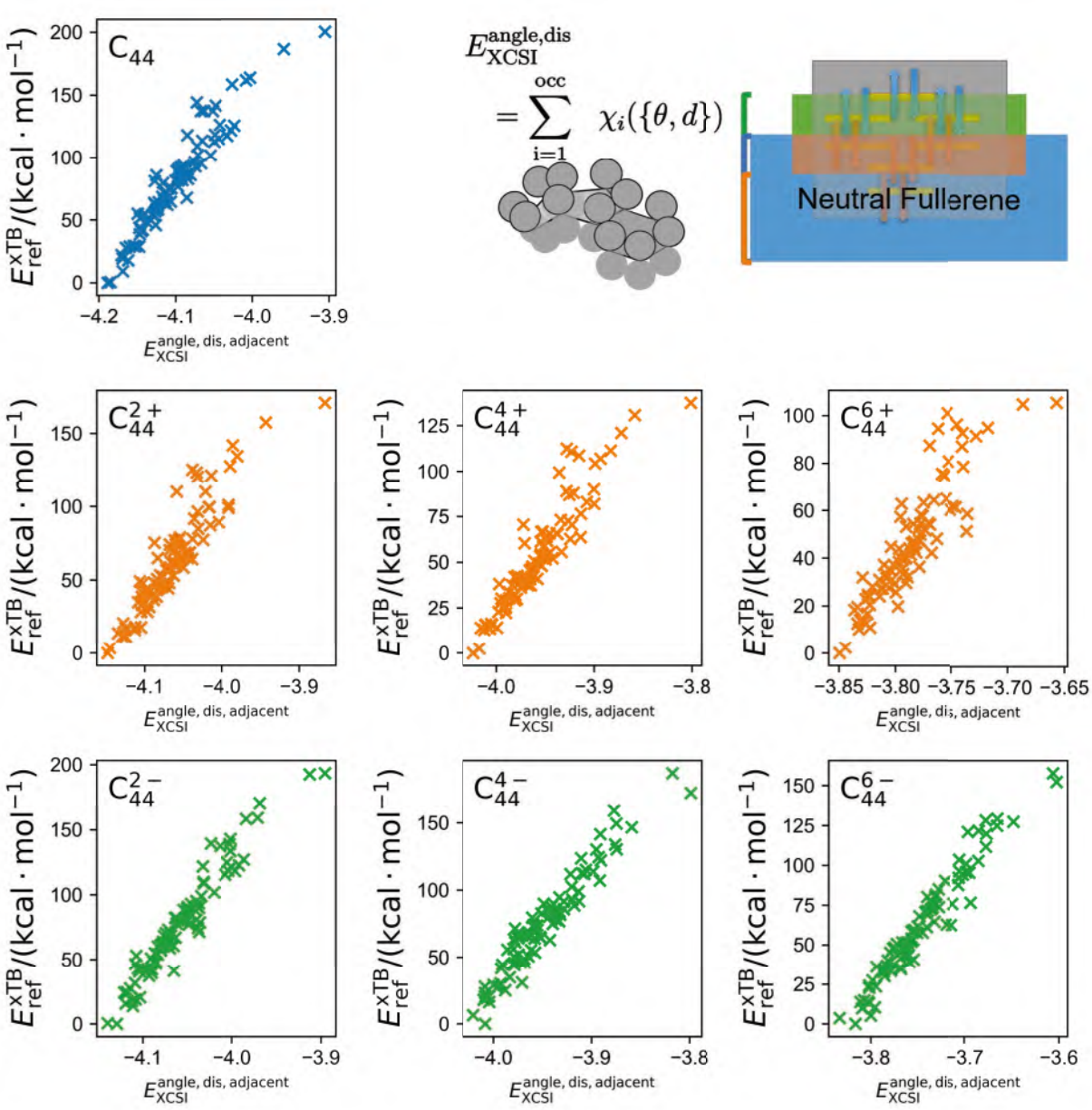


Figure 92: Correlation between xTB energies of $C_{44}$ isomers relative to the most stable one and prediction by XCSI model with angles and distances, without using adjacent matrix mask of $C_{44}$ isomers without and with charge 2+, 4+, 6+, 2-, 4-, 6-, respectively.

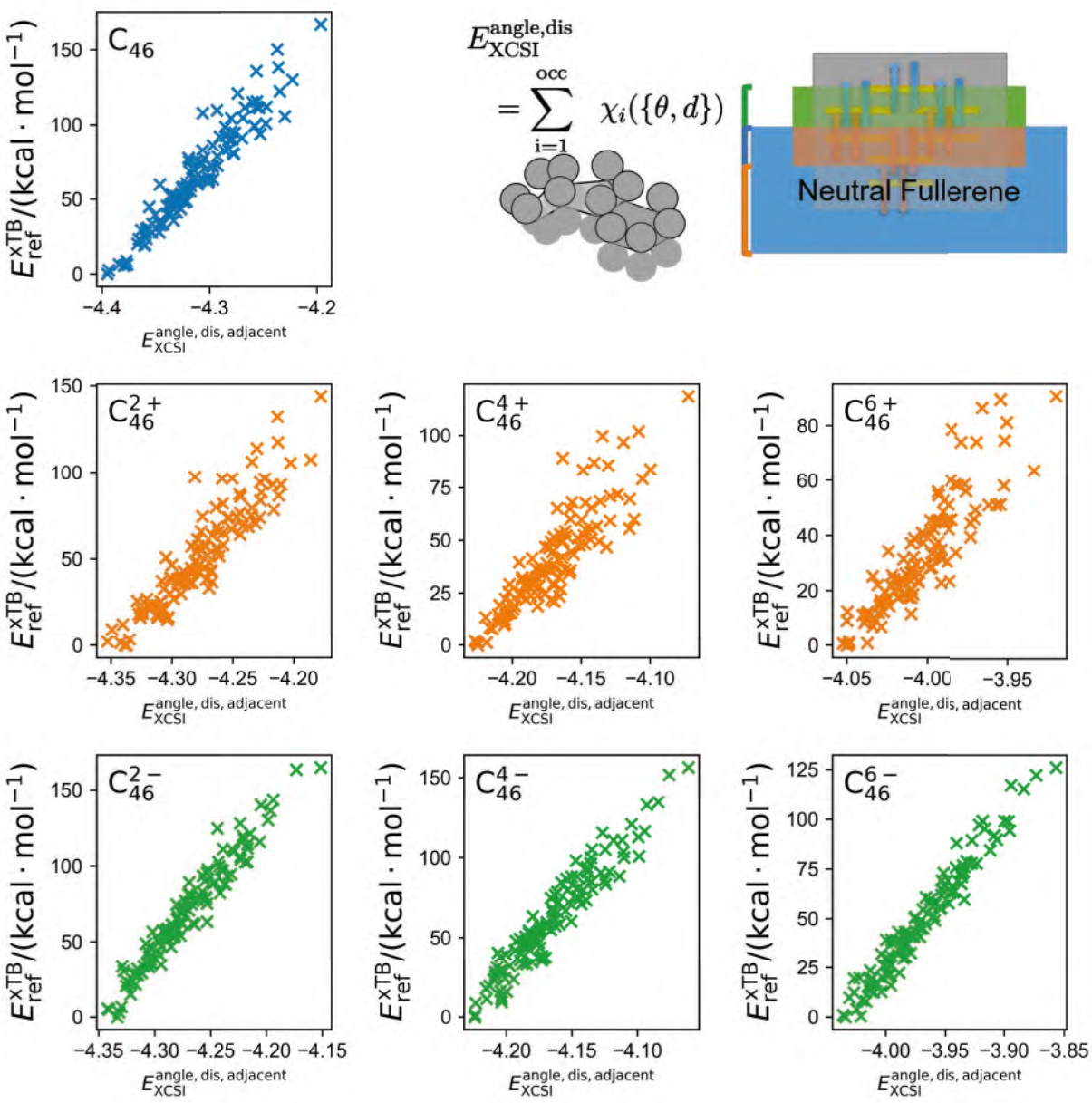


Figure 93: Correlation between xTB energies of $C_{46}$ isomers relative to the most stable one and prediction by XCSI model with angles and distances, without using adjacent matrix mask of $C_{46}$ isomers without and with charge 2+, 4+, 6+, 2-, 4-, 6-, respectively.

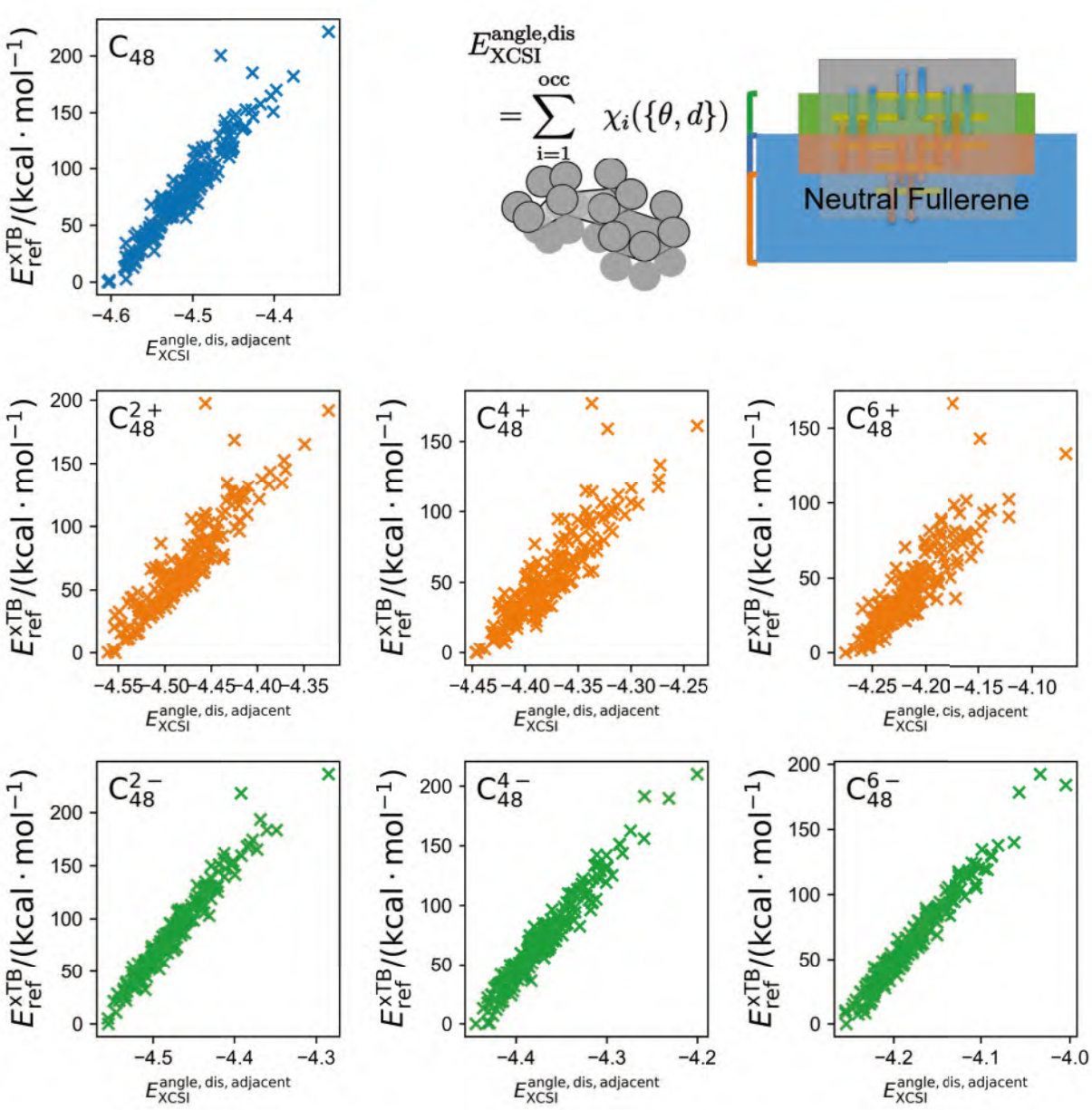


Figure 94: Correlation between xTB energies of $C_{48}$ isomers relative to the most stable one and prediction by XCSI model with angles and distances, without using adjacent matrix mask of $C_{48}$ isomers without and with charge 2+, 4+, 6+, 2-, 4-, 6-, respectively.

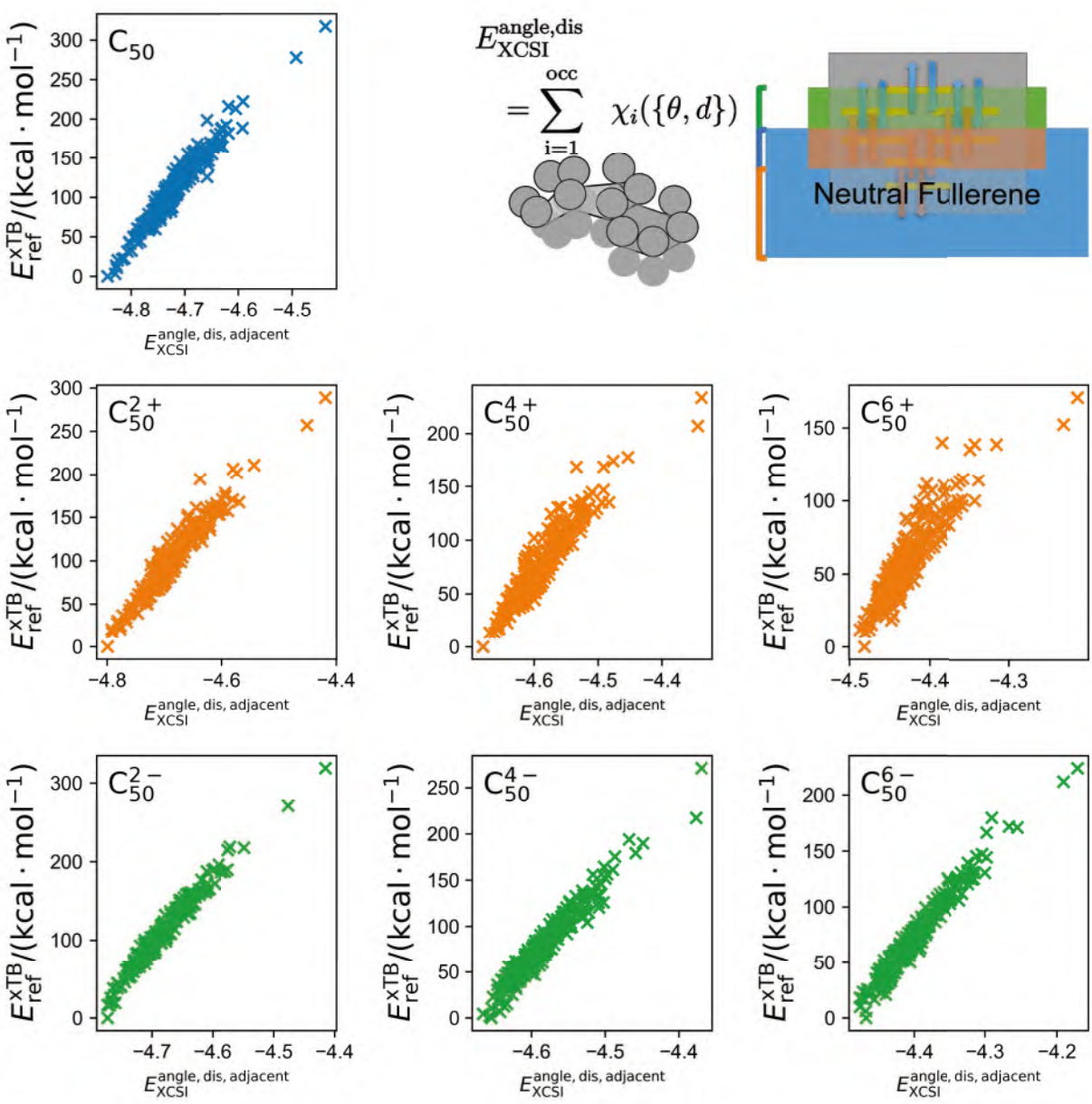


Figure 95: Correlation between xTB energies of $C_{50}$ isomers relative to the most stable one and prediction by XCSI model with angles and distances, without using adjacent matrix mask of $C_{50}$ isomers without and with charge 2+, 4+, 6+, 2-, 4-, 6-, respectively.

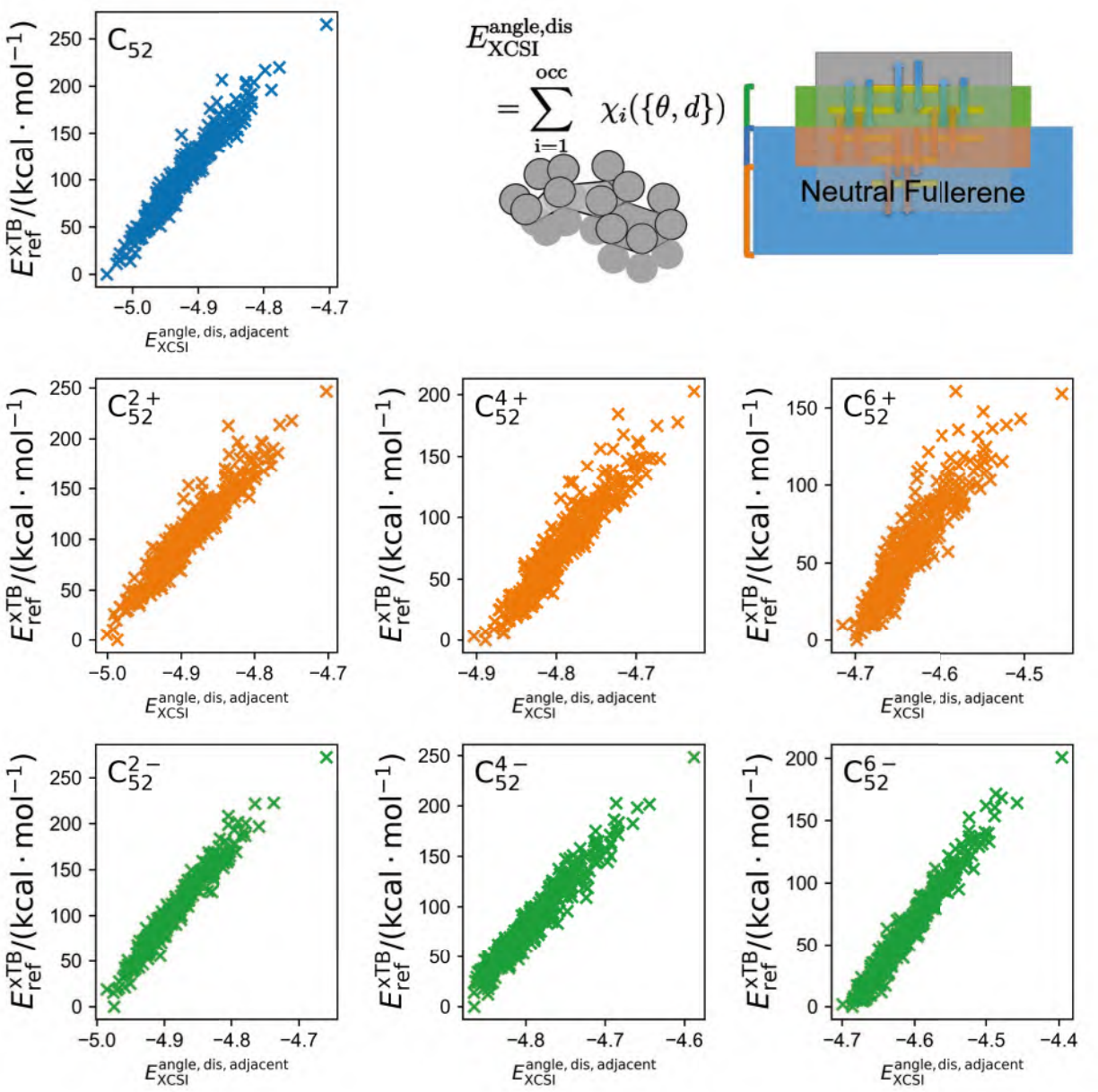


Figure 96: Correlation between xTB energies of $C_{52}$ isomers relative to the most stable one and prediction by XCSI model with angles and distances, without using adjacent matrix mask of $C_{52}$ isomers without and with charge 2+, 4+, 6+, 2-, 4-, 6-, respectively.

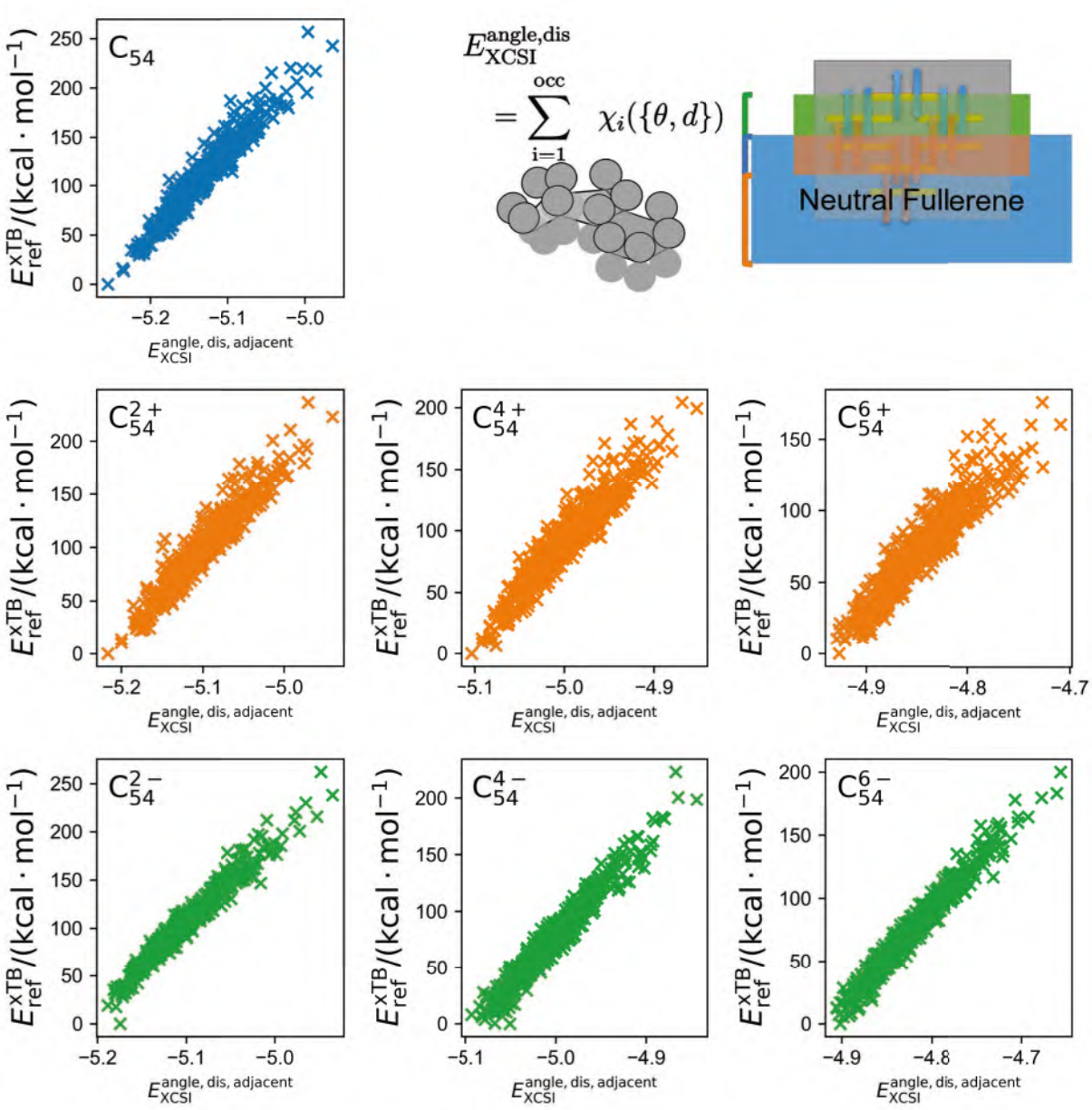


Figure 97: Correlation between xTB energies of $C_{54}$ isomers relative to the most stable one and prediction by XCSI model with angles and distances, without using adjacent matrix mask of $C_{54}$ isomers without and with charge 2+, 4+, 6+, 2-, 4-, 6-, respectively.

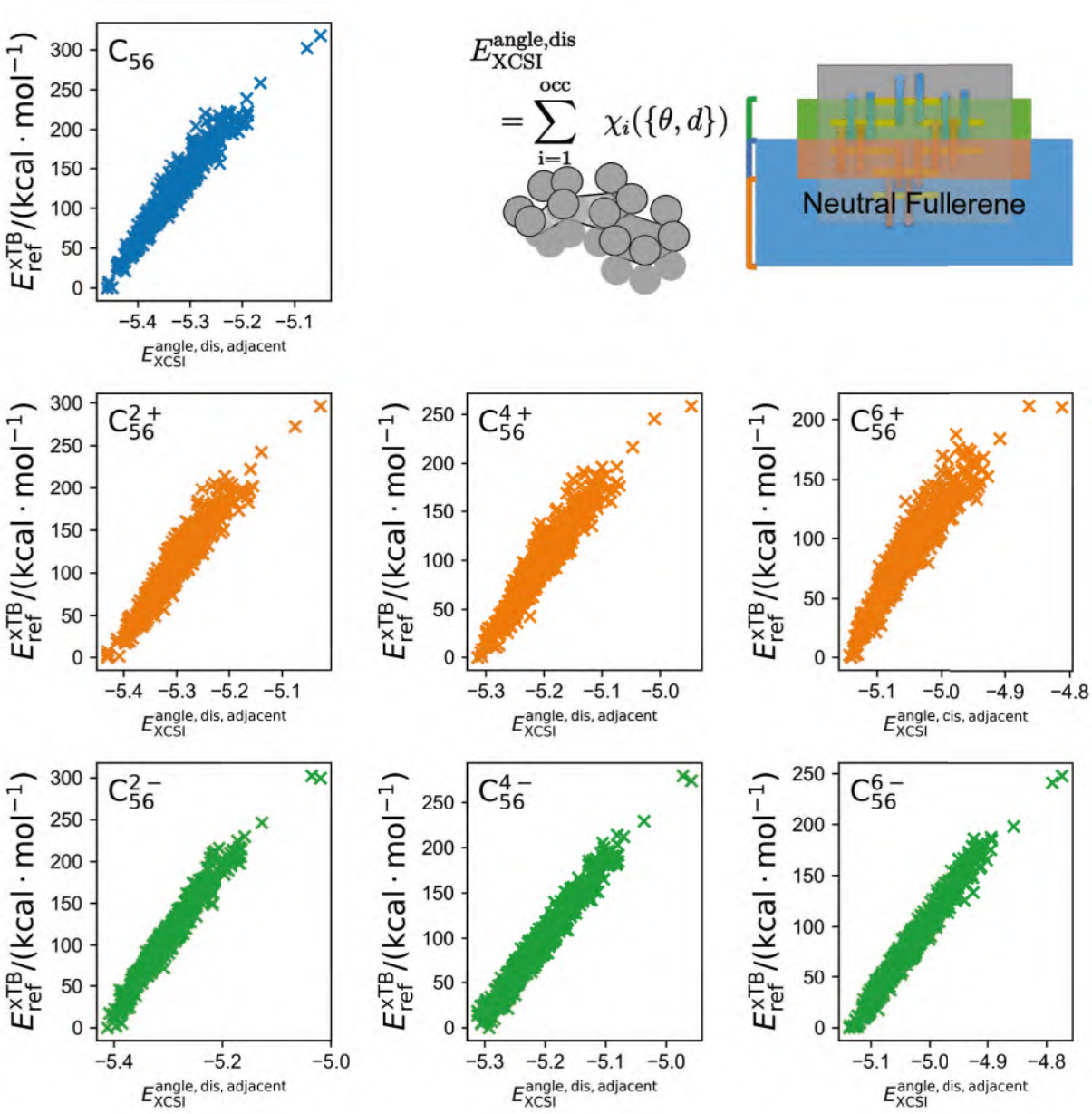


Figure 98: Correlation between xTB energies of $C_{56}$ isomers relative to the most stable one and prediction by XCSI model with angles and distances, without using adjacent matrix mask of $C_{56}$ isomers without and with charge 2+, 4+, 6+, 2-, 4-, 6-, respectively.

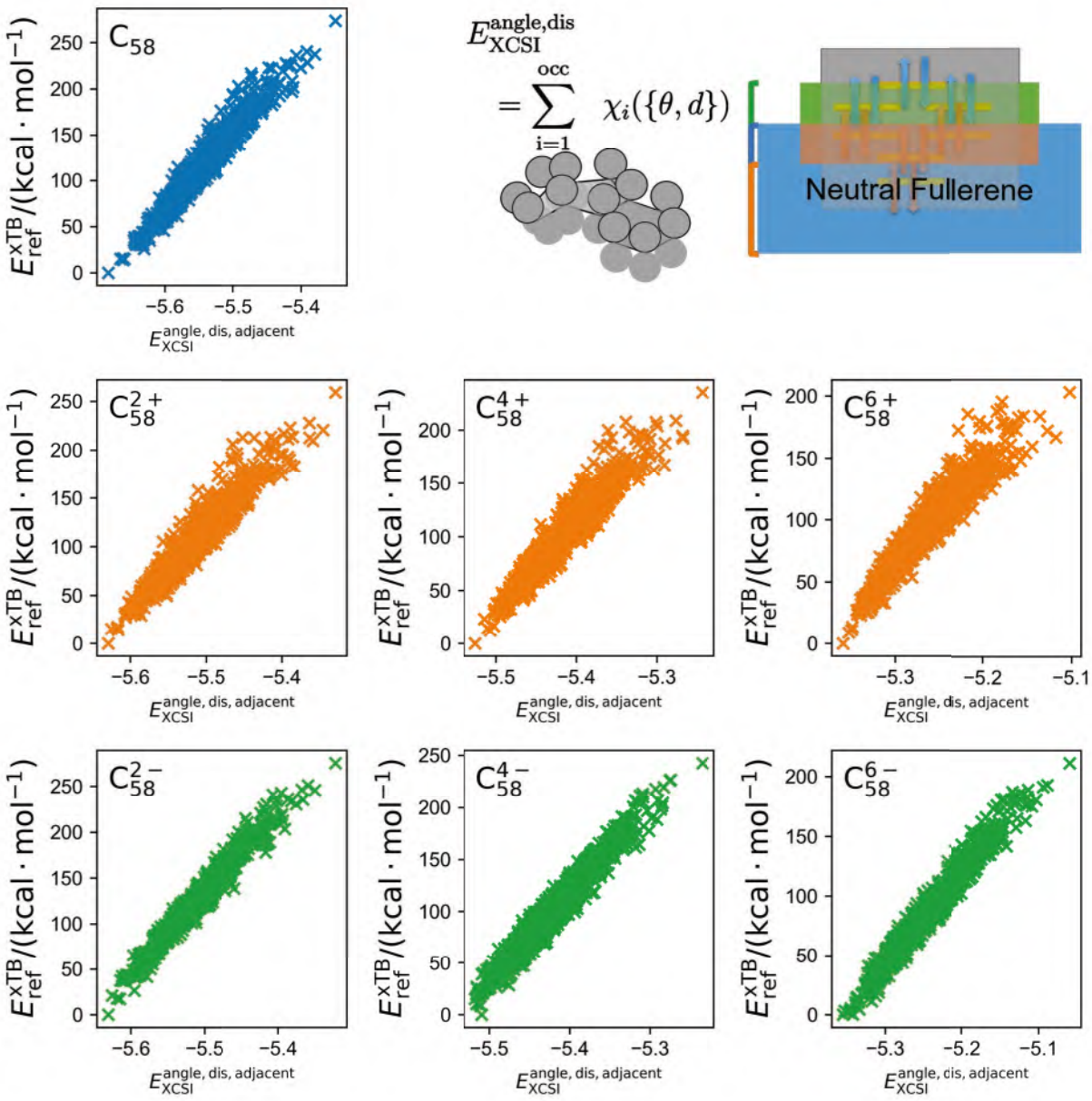


Figure 99: Correlation between xTB energies of $C_{58}$ isomers relative to the most stable one and prediction by XCSI model with angles and distances, without using adjacent matrix mask of $C_{58}$ isomers without and with charge 2+, 4+, 6+, 2-, 4-, 6-, respectively.

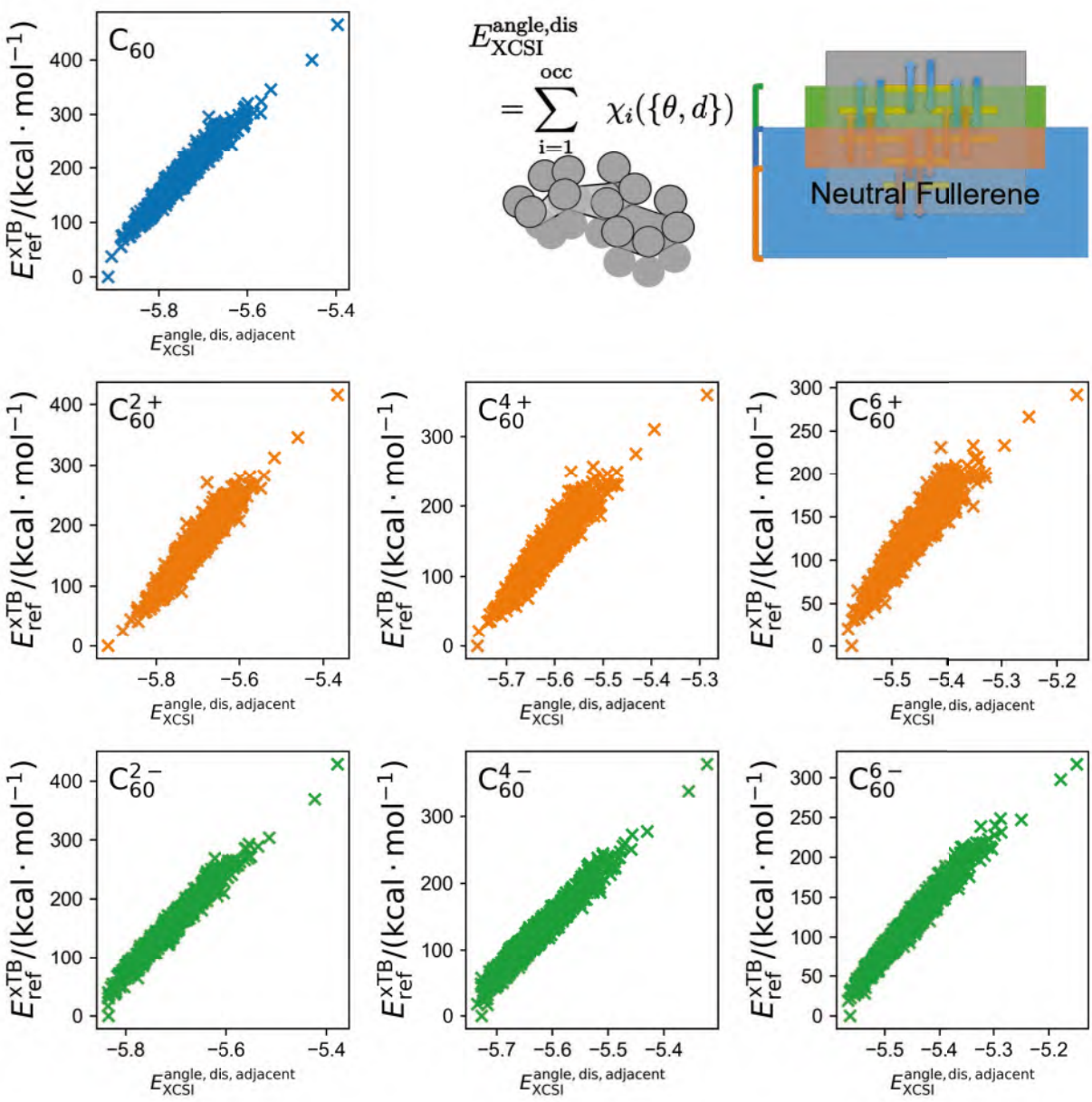


Figure 100: Correlation between xTB energies of $C_{60}$ isomers relative to the most stable one and prediction by XCSI model with angles and distances, without using adjacent matrix mask of $C_{60}$ isomers without and with charge 2+, 4+, 6+, 2-, 4-, 6-, respectively.

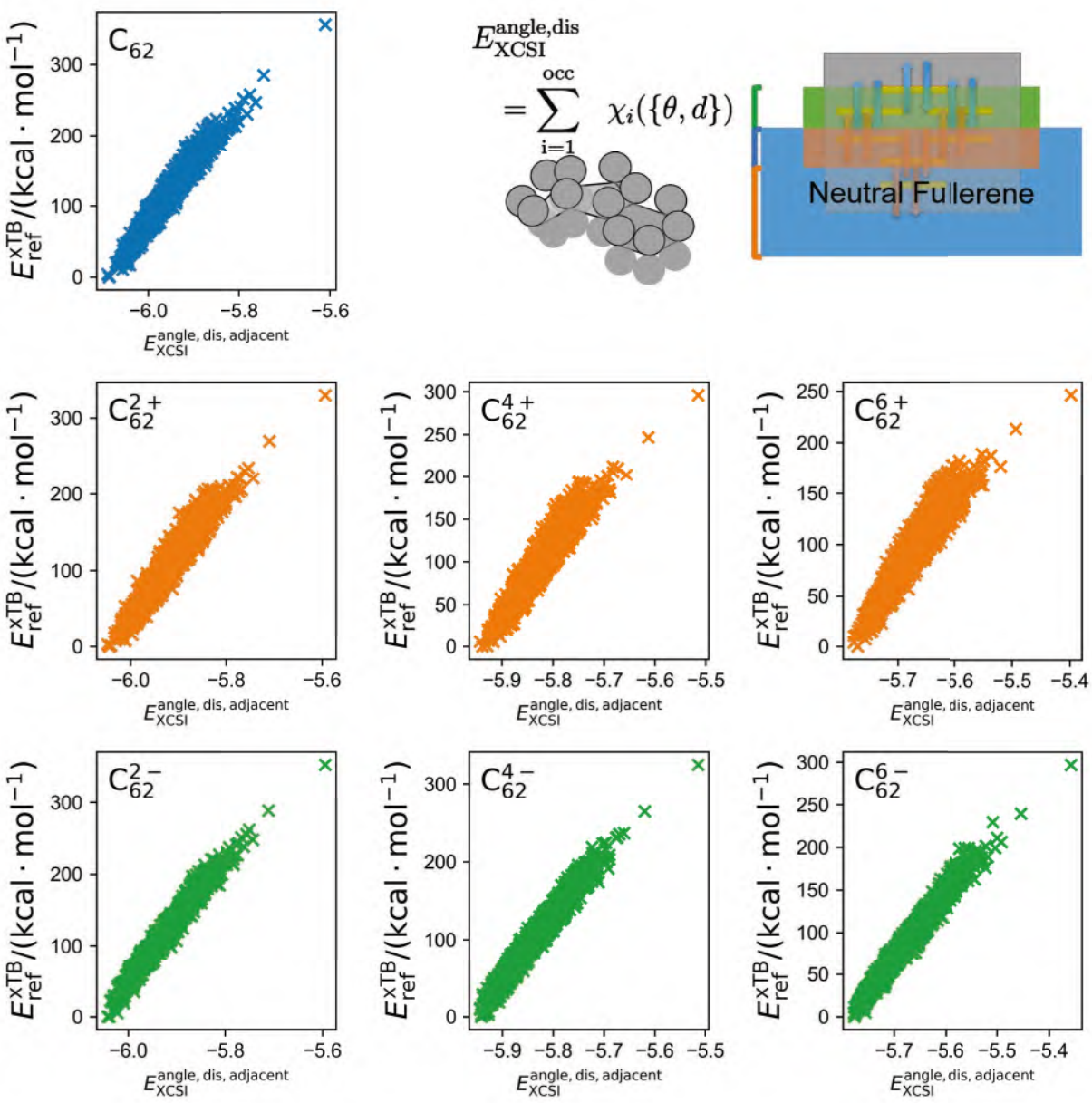


Figure 101: Correlation between xTB energies of $C_{62}$ isomers relative to the most stable one and prediction by XCSI model with angles and distances, without using adjacent matrix mask of $C_{62}$ isomers without and with charge 2+, 4+, 6+, 2-, 4-, 6-, respectively.

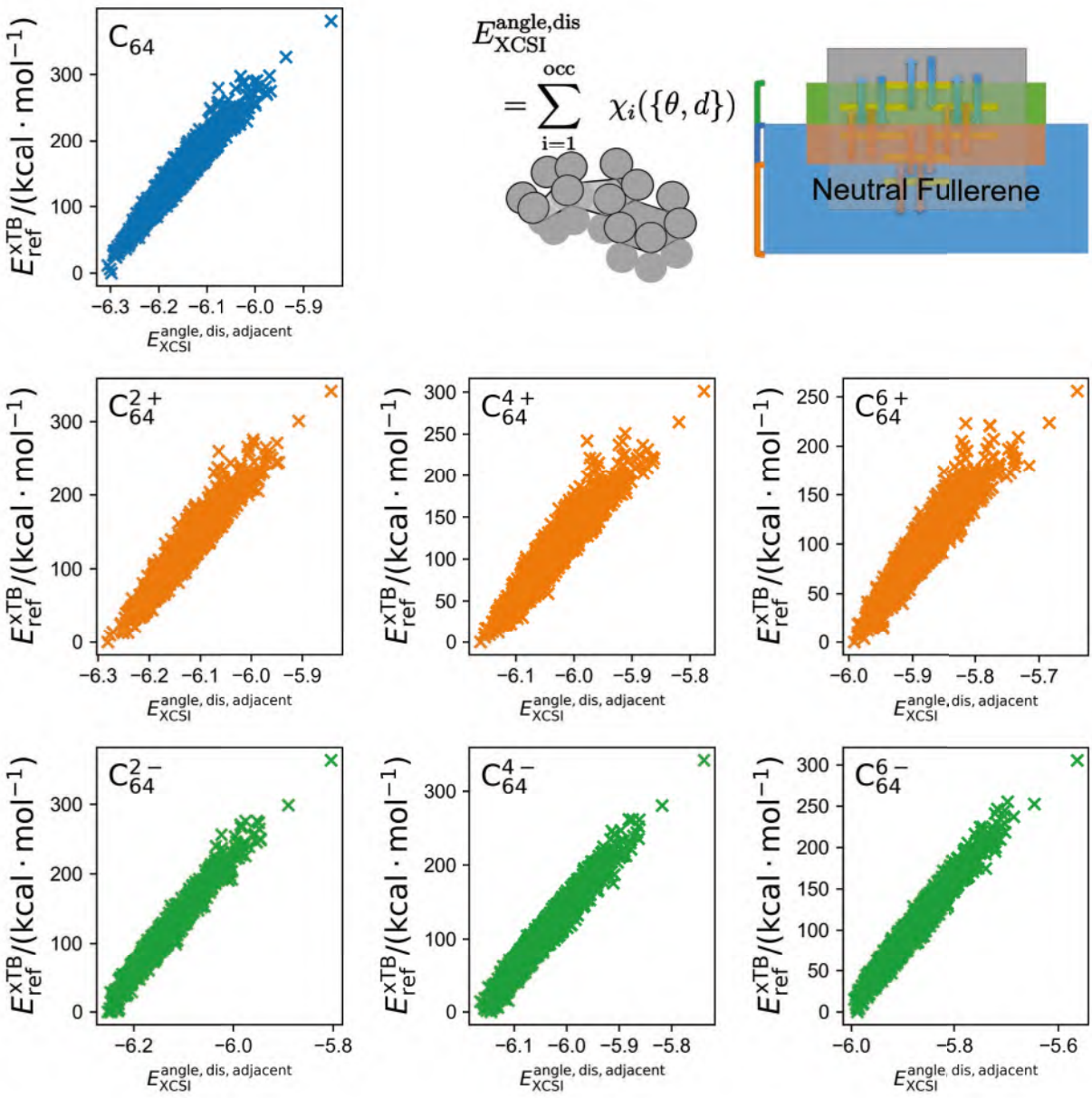


Figure 102: Correlation between xTB energies of $C_{64}$ isomers relative to the most stable one and prediction by XCSI model with angles and distances, without using adjacent matrix mask of $C_{64}$ isomers without and with charge 2+, 4+, 6+, 2-, 4-, 6-, respectively.

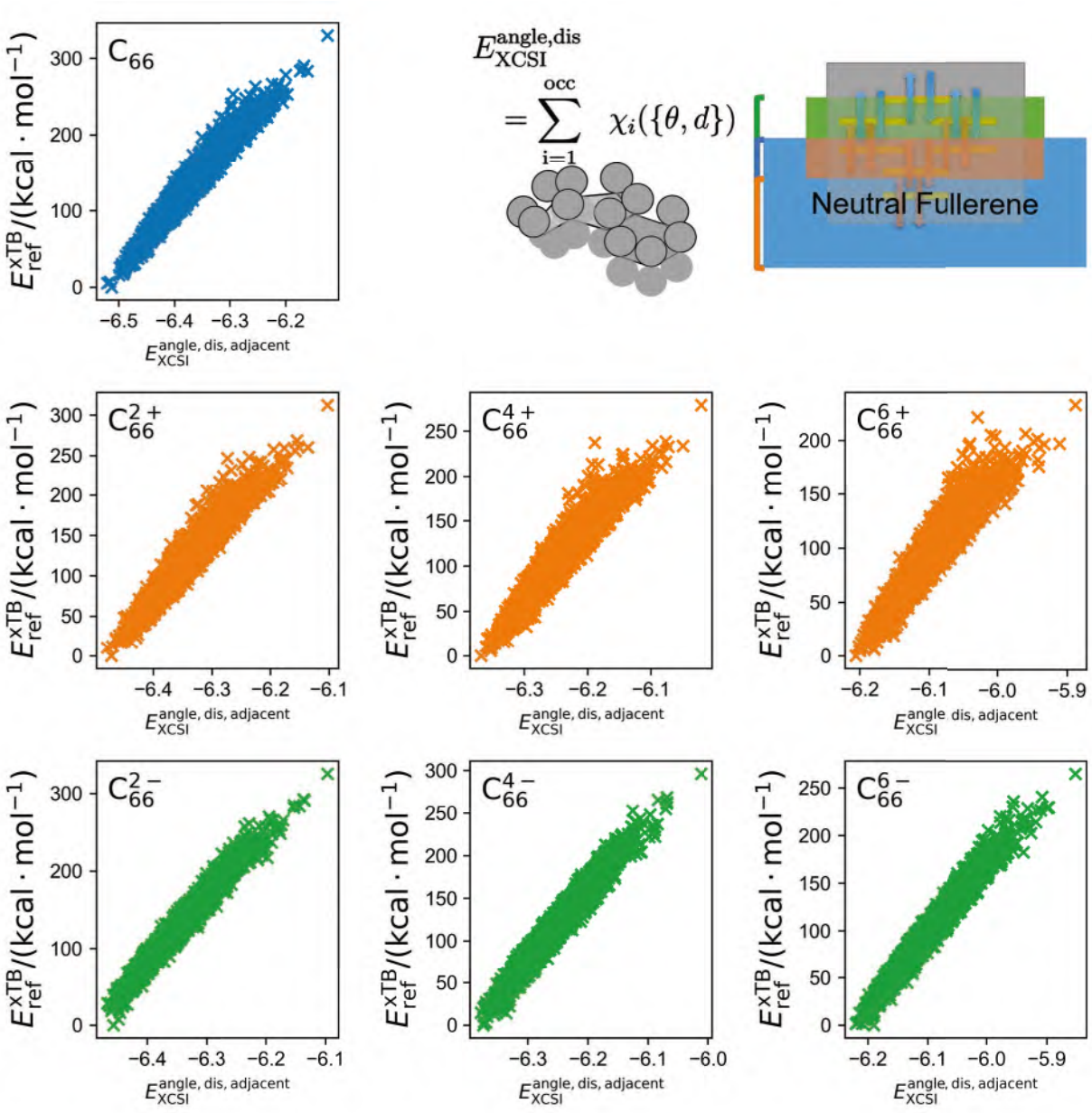


Figure 103: Correlation between xTB energies of $C_{66}$ isomers relative to the most stable one and prediction by XCSI model with angles and distances, without using adjacent matrix mask of $C_{66}$ isomers without and with charge 2+, 4+, 6+, 2-, 4-, 6-, respectively.

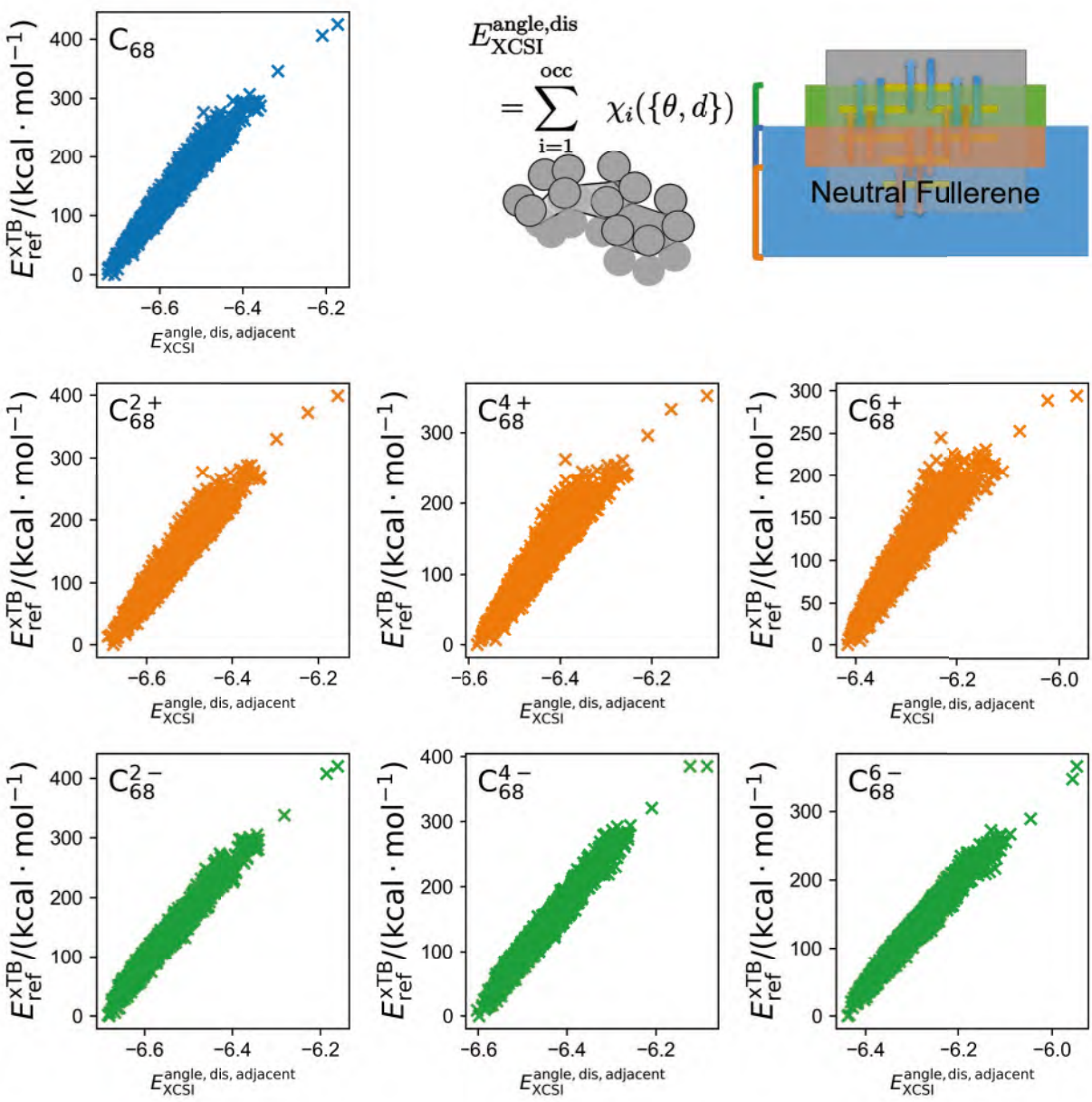


Figure 104: Correlation between xTB energies of $C_{68}$ isomers relative to the most stable one and prediction by XCSI model with angles and distances, without using adjacent matrix mask of $C_{68}$ isomers without and with charge 2+, 4+, 6+, 2-, 4-, 6-, respectively.

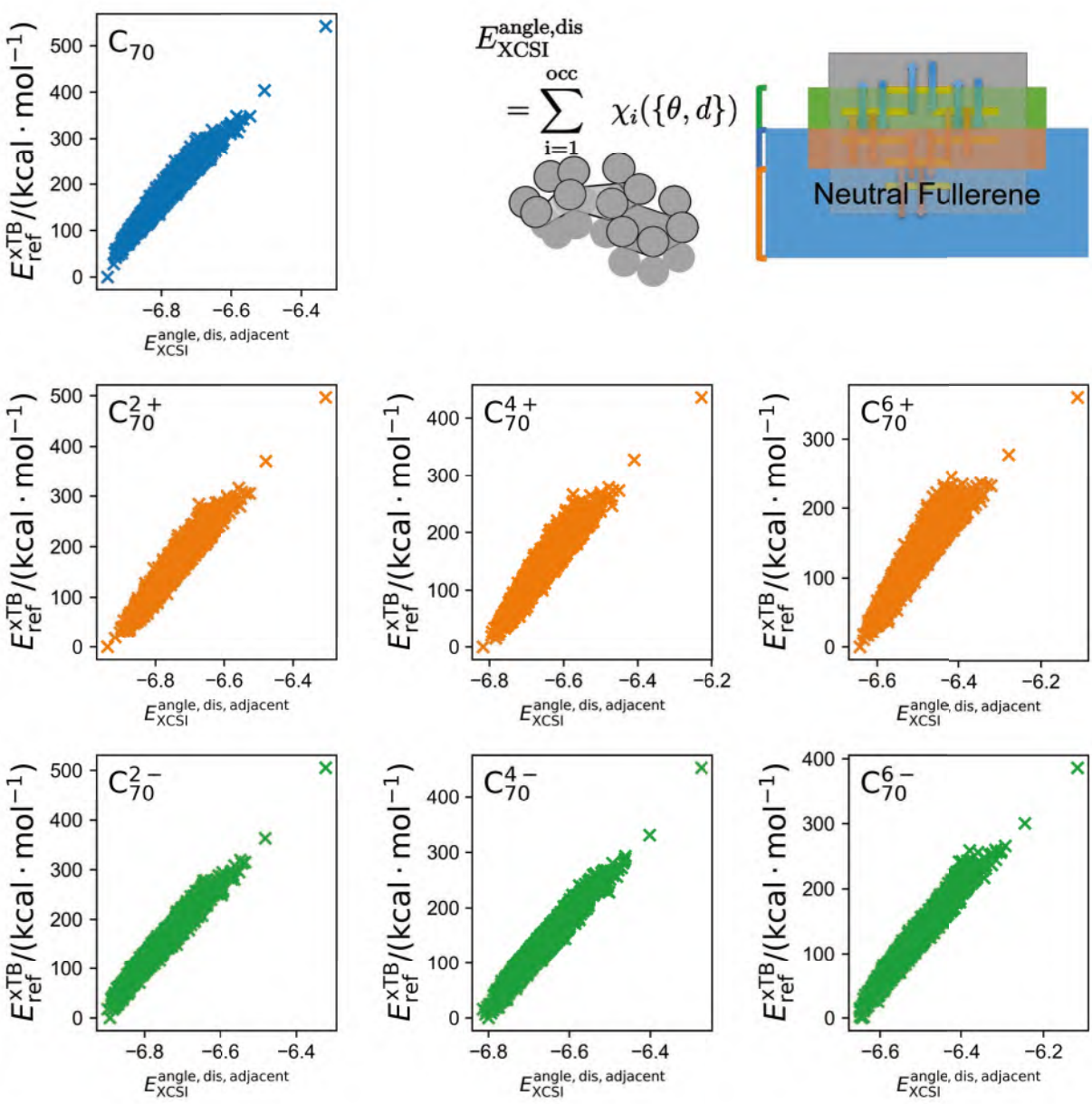


Figure 105: Correlation between xTB energies of $C_{70}$ isomers relative to the most stable one and prediction by XCSI model with angles and distances, without using adjacent matrix mask of $C_{70}$ isomers without and with charge 2+, 4+, 6+, 2-, 4-, 6-, respectively.

# 7 Correlation between xTB energies and prediction by XCSI model with distances but without angles

Predictions by XCSI model with distances, but without angles, are calculated by

$$E_{\mathrm{XCSI}}^{\mathrm{angle,nodis}} \equiv \sum_{k=i}^{n} \chi_{k,i}^{q}(d) \tag{10}$$

where $\chi_{k,i}^{q}$ is eigenvalues of extended adjacency matrix, whose elements are

$$h_{ij}^{k} = \begin{cases} \exp\left(-d_{ij}^{2}\right)\beta' & i,j \text{ are neighbors} \\ 0 & \text{others} \end{cases} \tag{11}$$

.

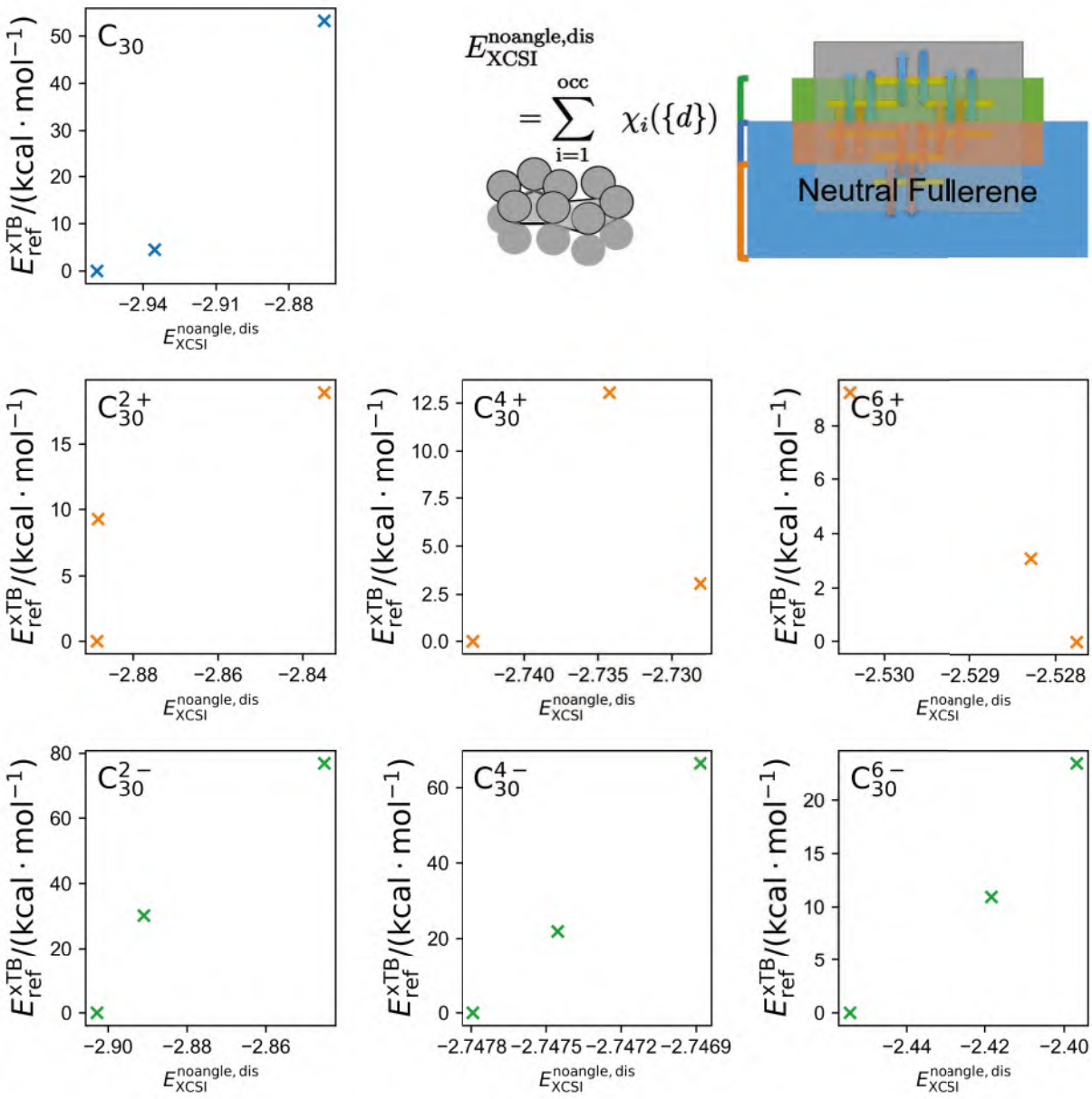


Figure 106: Correlation between xTB energies of $C_{30}$ isomers relative to the most stable one and prediction by XCSI model with distances but without angles of $C_{30}$ isomers without and with charge 2+, 4+, 6+, 2-, 4-, 6-, respectively.

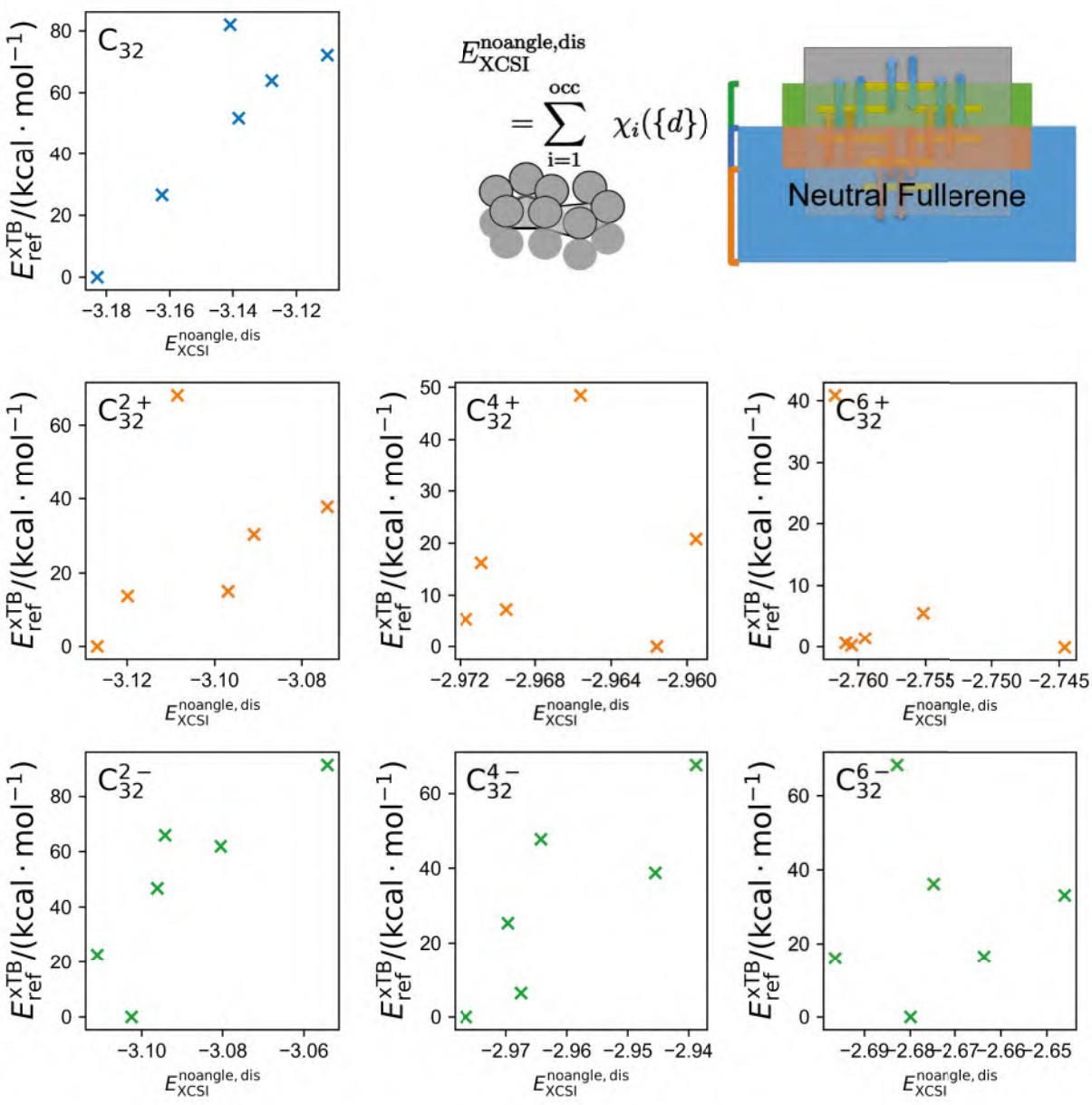


Figure 107: Correlation between xTB energies of $C_{32}$ isomers relative to the most stable one and prediction by XCSI model with distances but without angles of $C_{32}$ isomers without and with charge 2+, 4+, 6+, 2-, 4-, 6-, respectively.

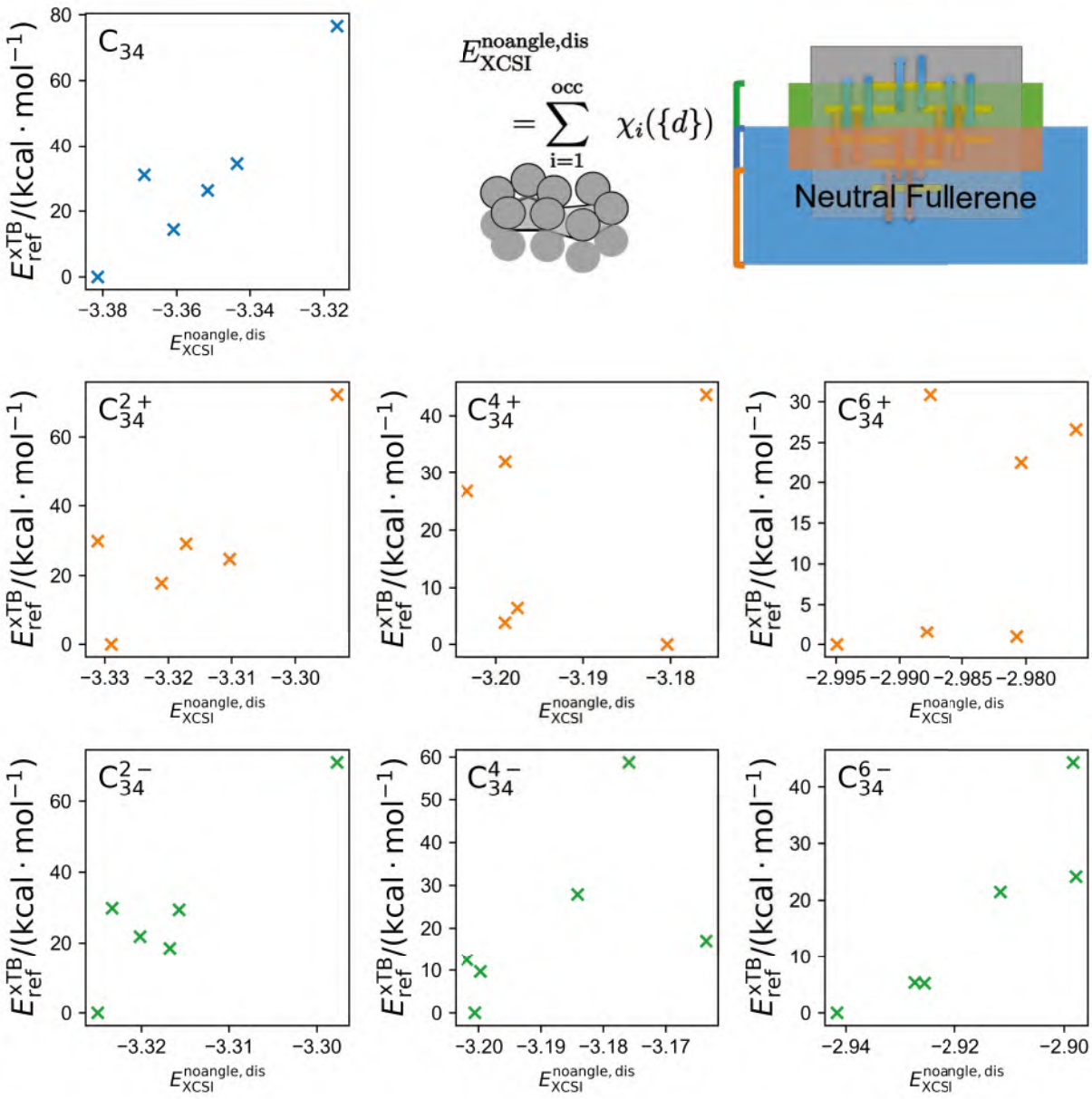


Figure 108: Correlation between xTB energies of $C_{34}$ isomers relative to the most stable one and prediction by XCSI model with distances but without angles of $C_{34}$ isomers without and with charge 2+, 4+, 6+, 2-, 4-, 6-, respectively.

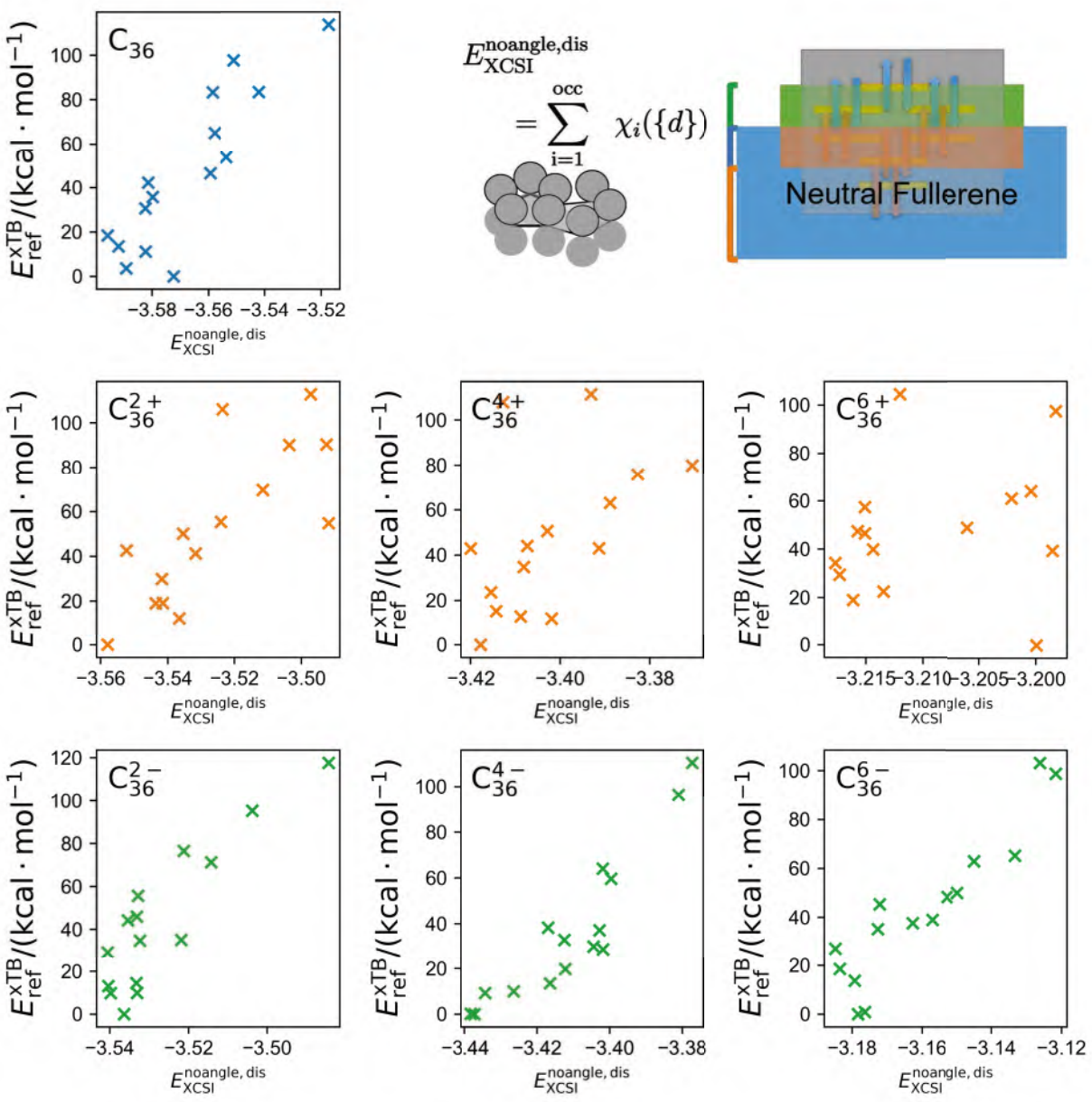


Figure 109: Correlation between xTB energies of $C_{36}$ isomers relative to the most stable one and prediction by XCSI model with distances but without angles of $C_{36}$ isomers without and with charge 2+, 4+, 6+, 2-, 4-, 6-, respectively.

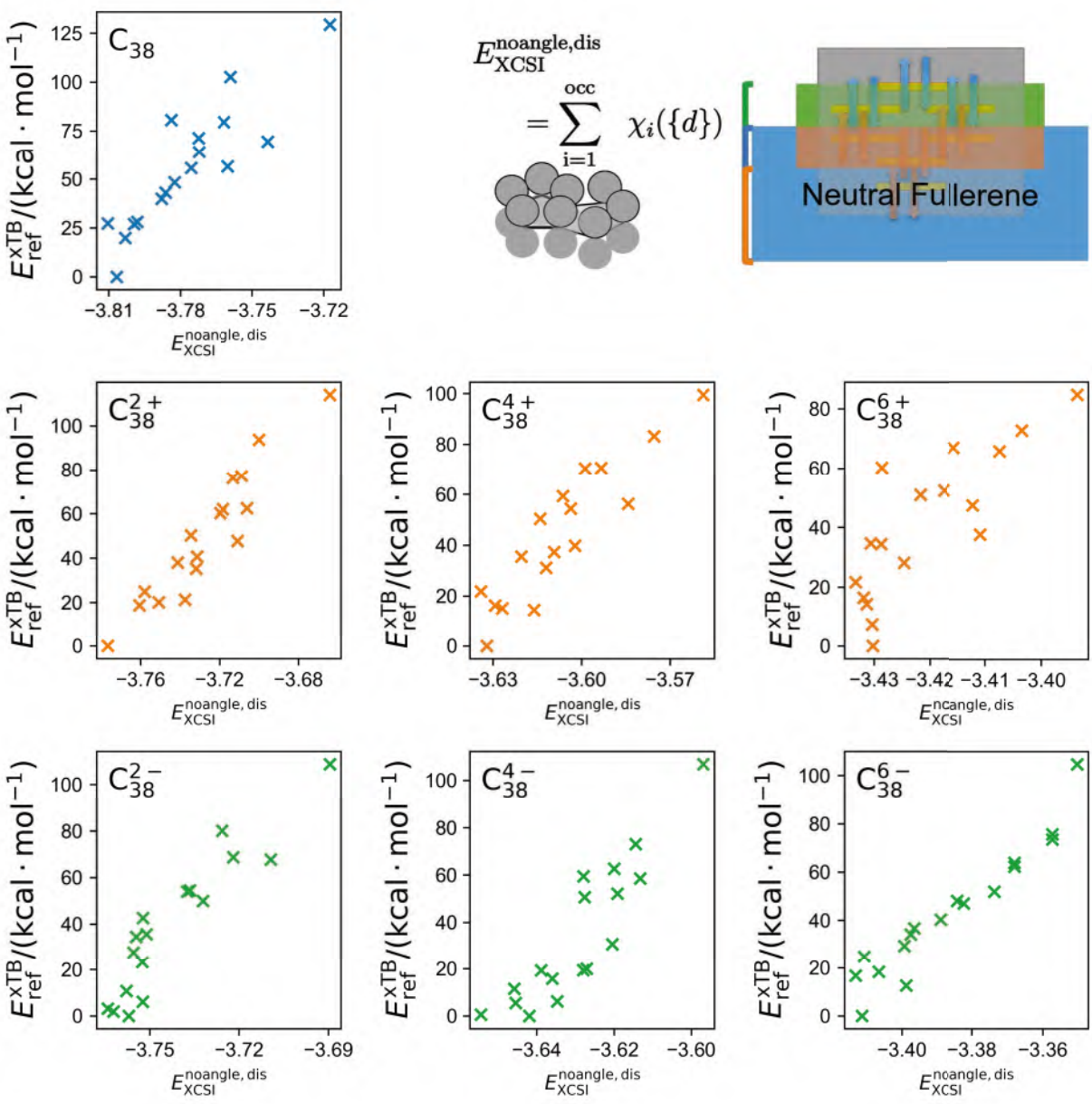


Figure 110: Correlation between xTB energies of $C_{38}$ isomers relative to the most stable one and prediction by XCSI model with distances but without angles of $C_{38}$ isomers without and with charge 2+, 4+, 6+, 2-, 4-, 6-, respectively.

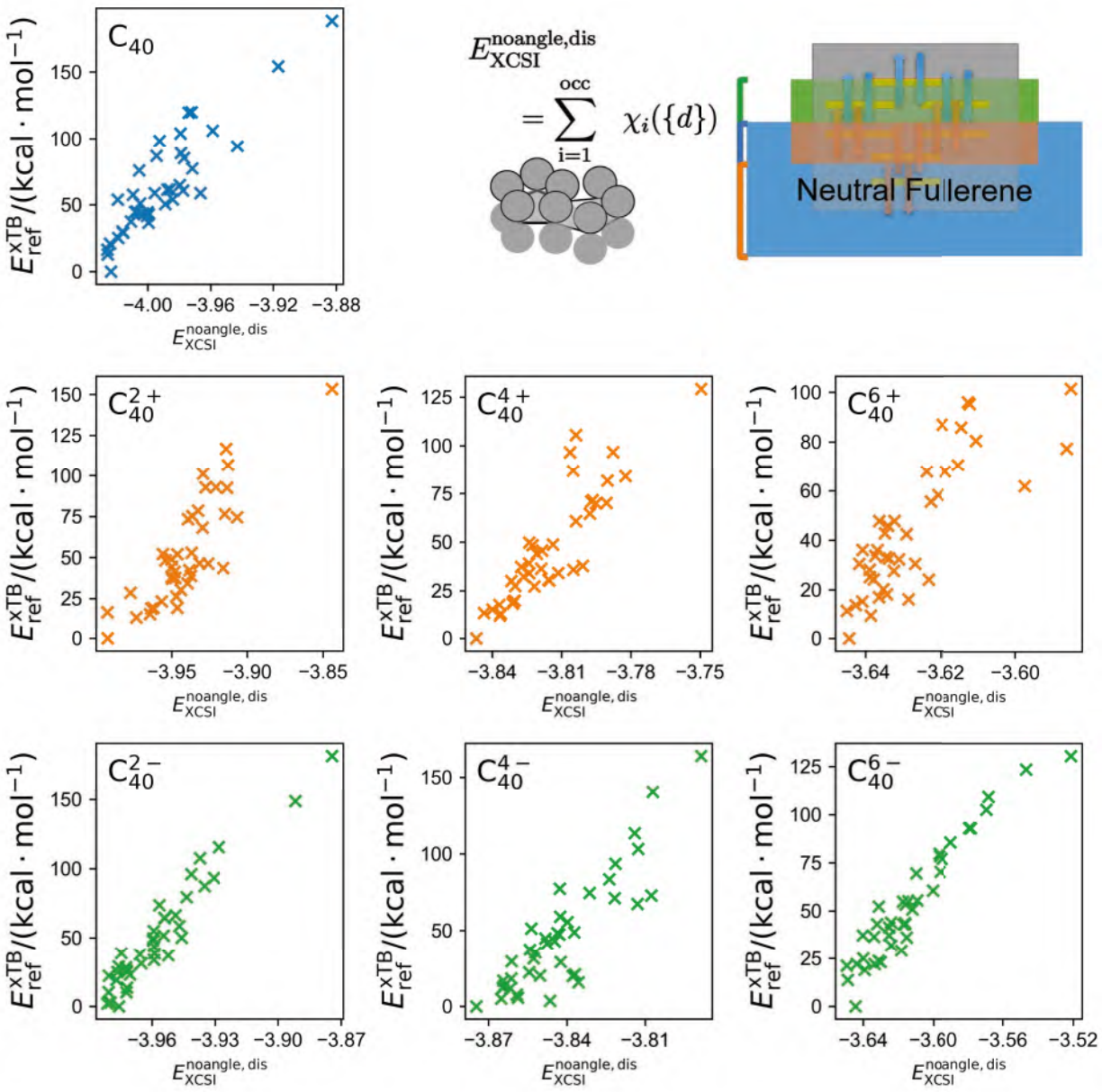


Figure 111: Correlation between xTB energies of $C_{40}$ isomers relative to the most stable one and prediction by XCSI model with distances but without angles of $C_{40}$ isomers without and with charge 2+, 4+, 6+, 2-, 4-, 6-, respectively.

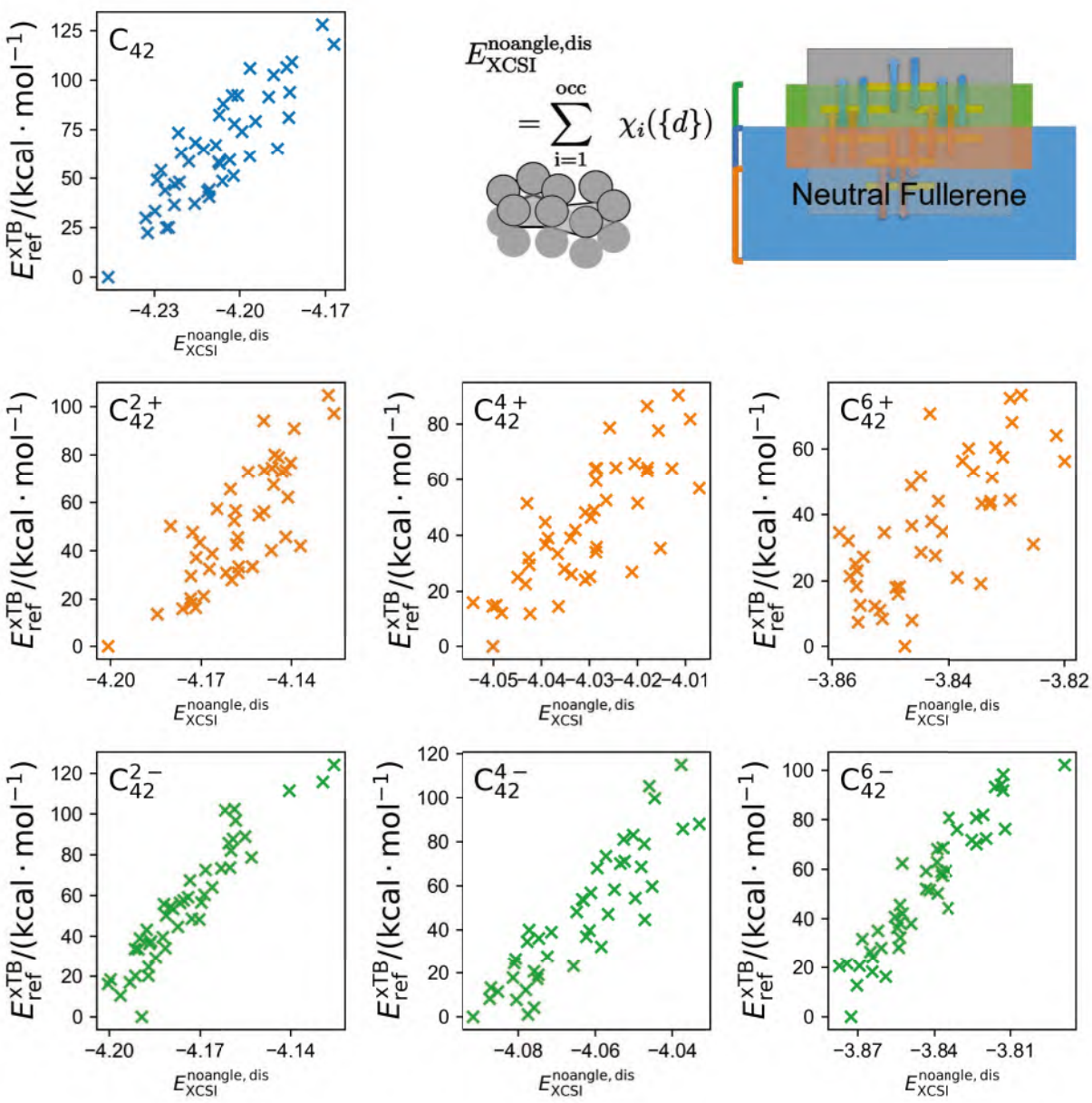


Figure 112: Correlation between xTB energies of $C_{42}$ isomers relative to the most stable one and prediction by XCSI model with distances but without angles of $C_{42}$ isomers without and with charge 2+, 4+, 6+, 2-, 4-, 6-, respectively.

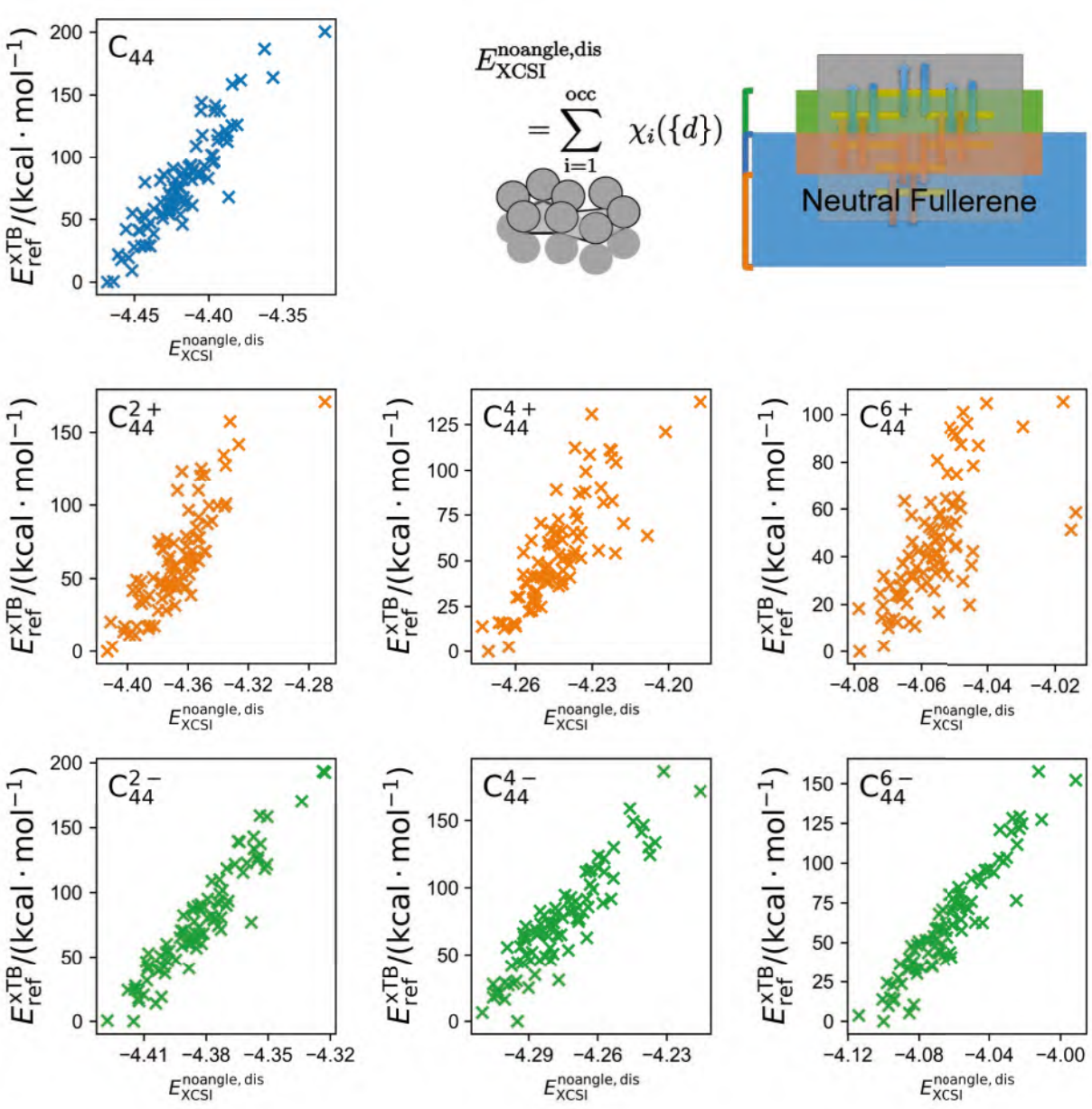


Figure 113: Correlation between xTB energies of $C_{44}$ isomers relative to the most stable one and prediction by XCSI model with distances but without angles of $C_{44}$ isomers without and with charge 2+, 4+, 6+, 2-, 4-, 6-, respectively.

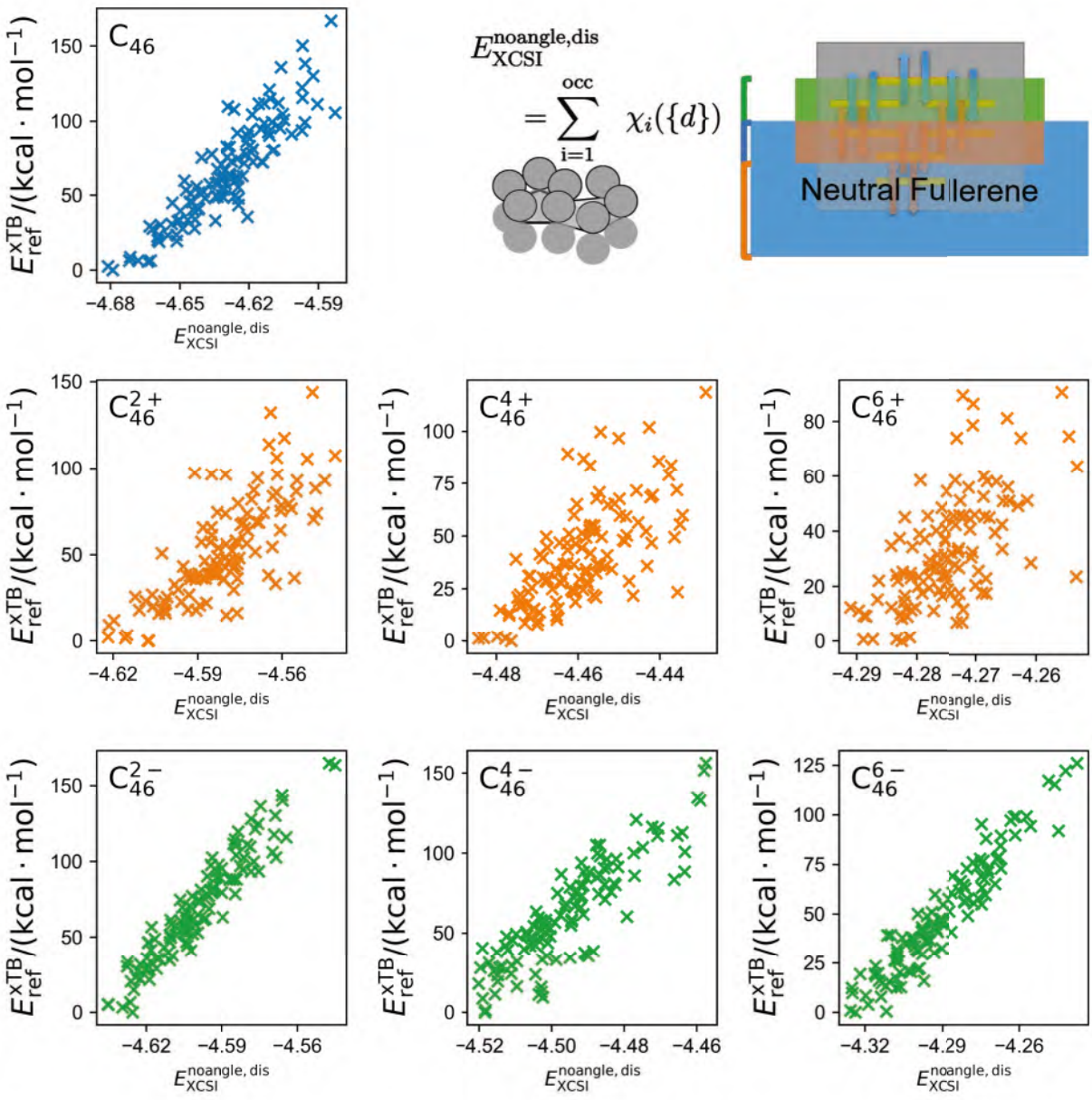


Figure 114: Correlation between xTB energies of $C_{46}$ isomers relative to the most stable one and prediction by XCSI model with distances but without angles of $C_{46}$ isomers without and with charge 2+, 4+, 6+, 2-, 4-, 6-, respectively.

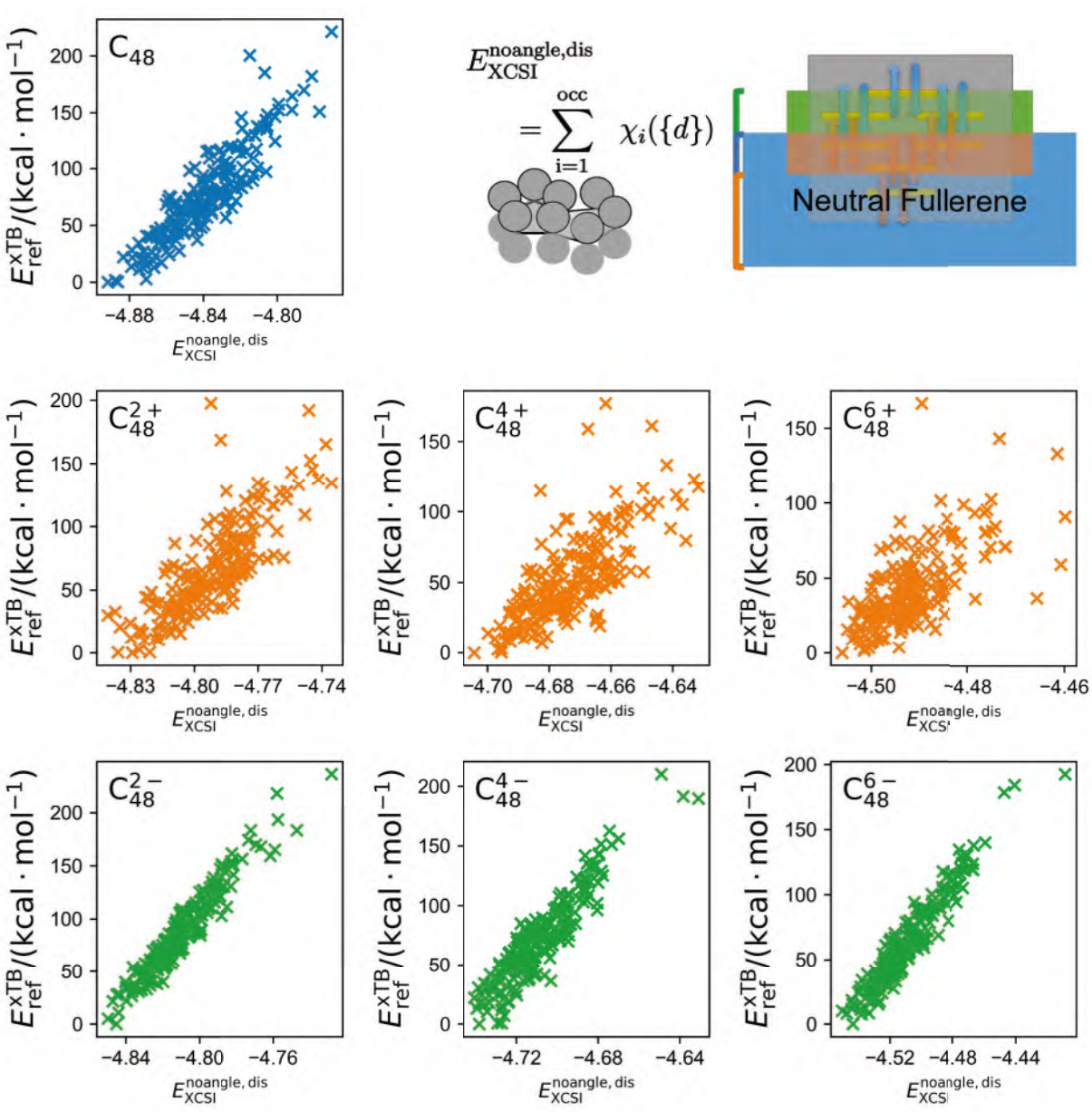


Figure 115: Correlation between xTB energies of $C_{48}$ isomers relative to the most stable one and prediction by XCSI model with distances but without angles of $C_{48}$ isomers without and with charge 2+, 4+, 6+, 2-, 4-, 6-, respectively.

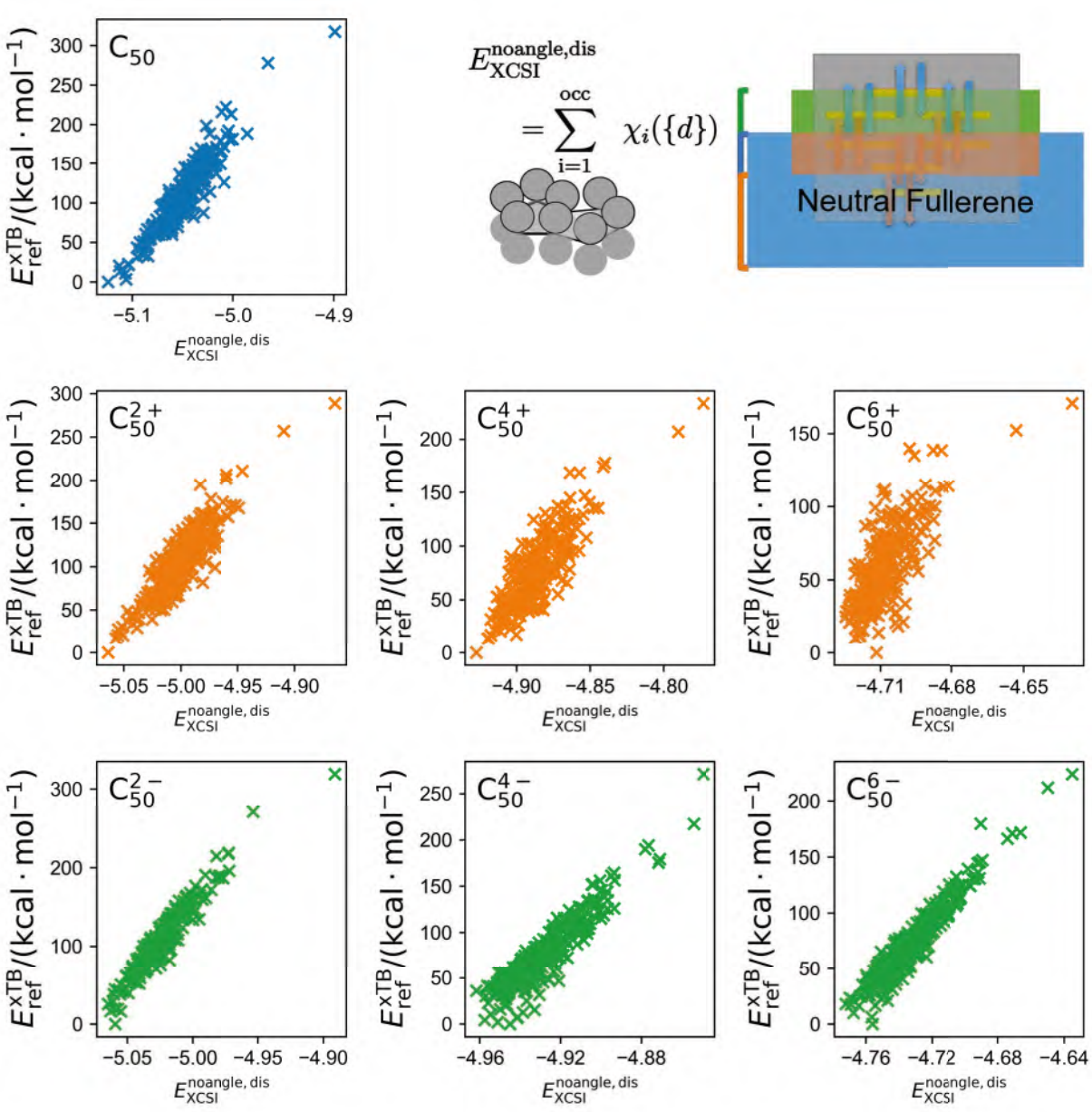


Figure 116: Correlation between xTB energies of $C_{50}$ isomers relative to the most stable one and prediction by XCSI model with distances but without angles of $C_{50}$ isomers without and with charge 2+, 4+, 6+, 2-, 4-, 6-, respectively.

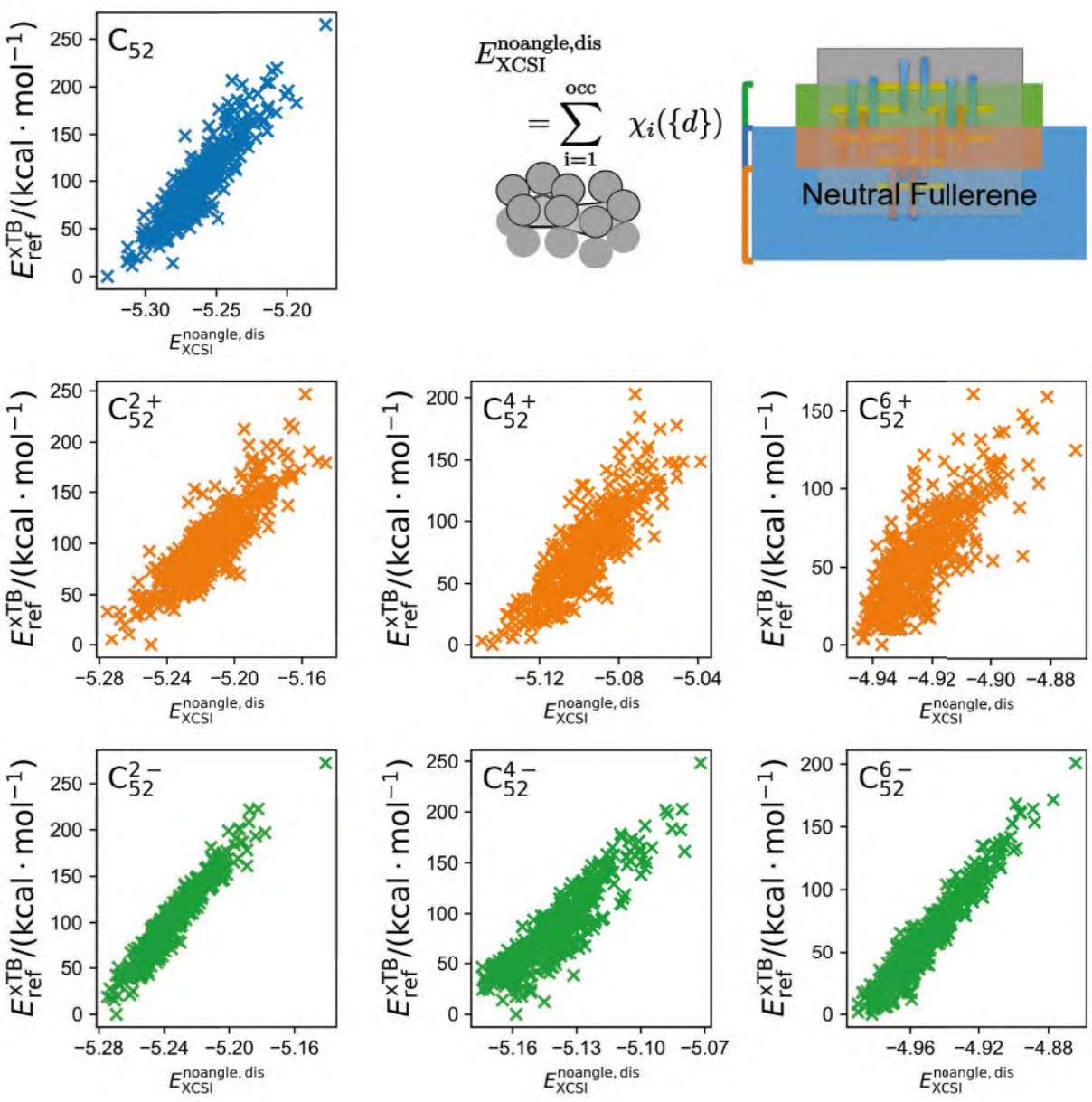


Figure 117: Correlation between xTB energies of $C_{52}$ isomers relative to the most stable one and prediction by XCSI model with distances but without angles of $C_{52}$ isomers without and with charge 2+, 4+, 6+, 2-, 4-, 6-, respectively.

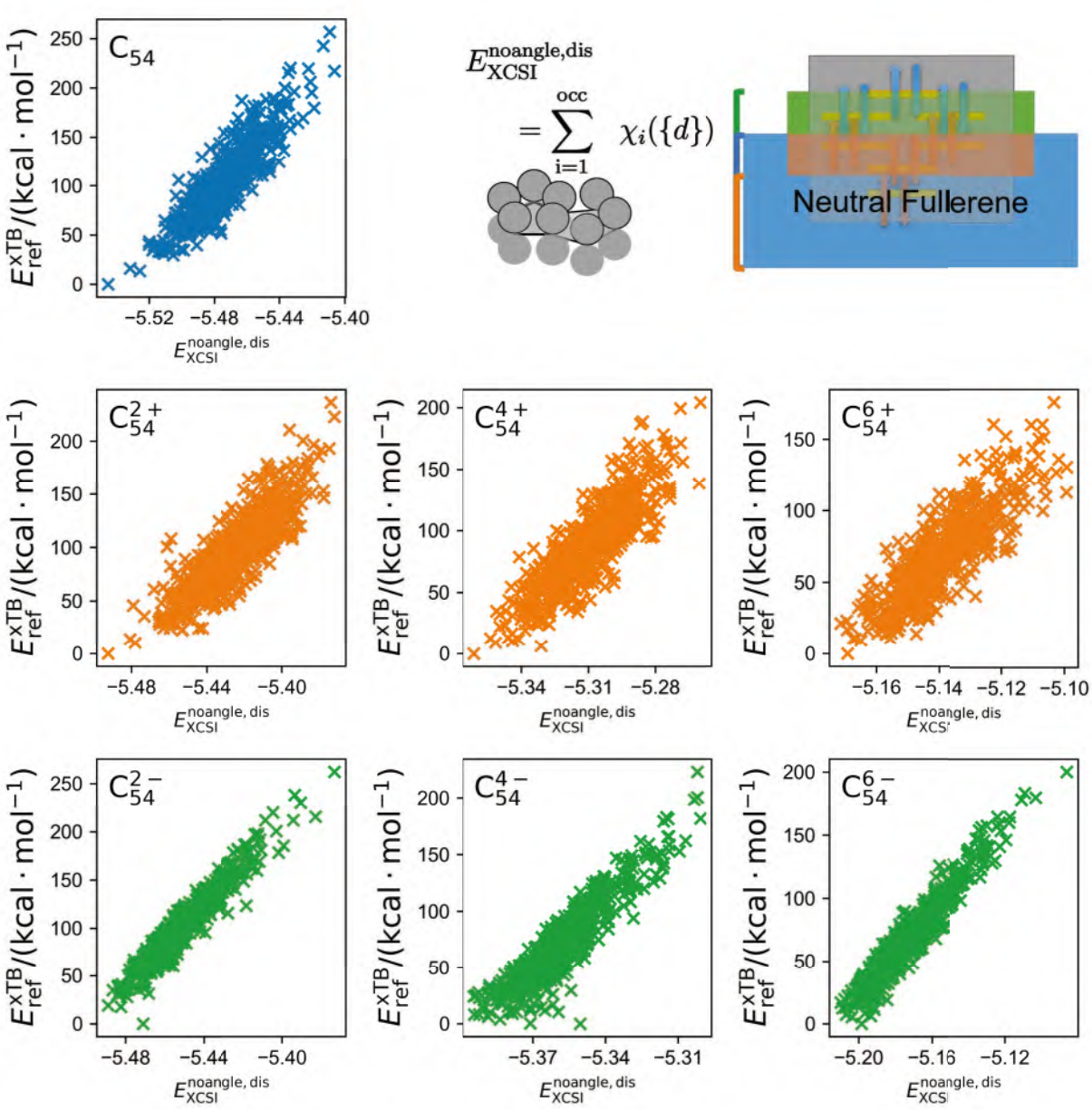


Figure 118: Correlation between xTB energies of $C_{54}$ isomers relative to the most stable one and prediction by XCSI model with distances but without angles of $C_{54}$ isomers without and with charge 2+, 4+, 6+, 2-, 4-, 6-, respectively.

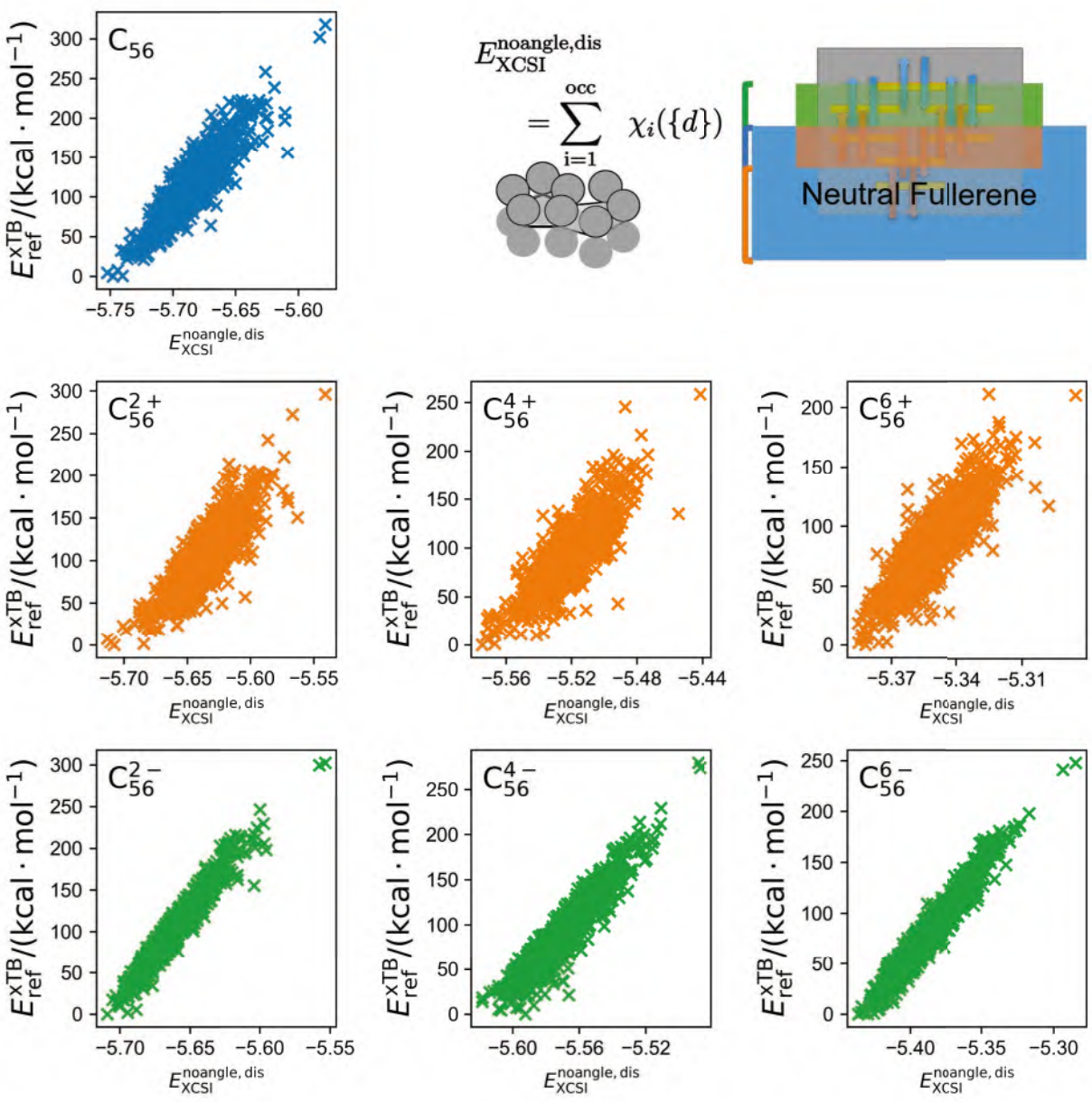


Figure 119: Correlation between xTB energies of $C_{56}$ isomers relative to the most stable one and prediction by XCSI model with distances but without angles of $C_{56}$ isomers without and with charge 2+, 4+, 6+, 2-, 4-, 6-, respectively.

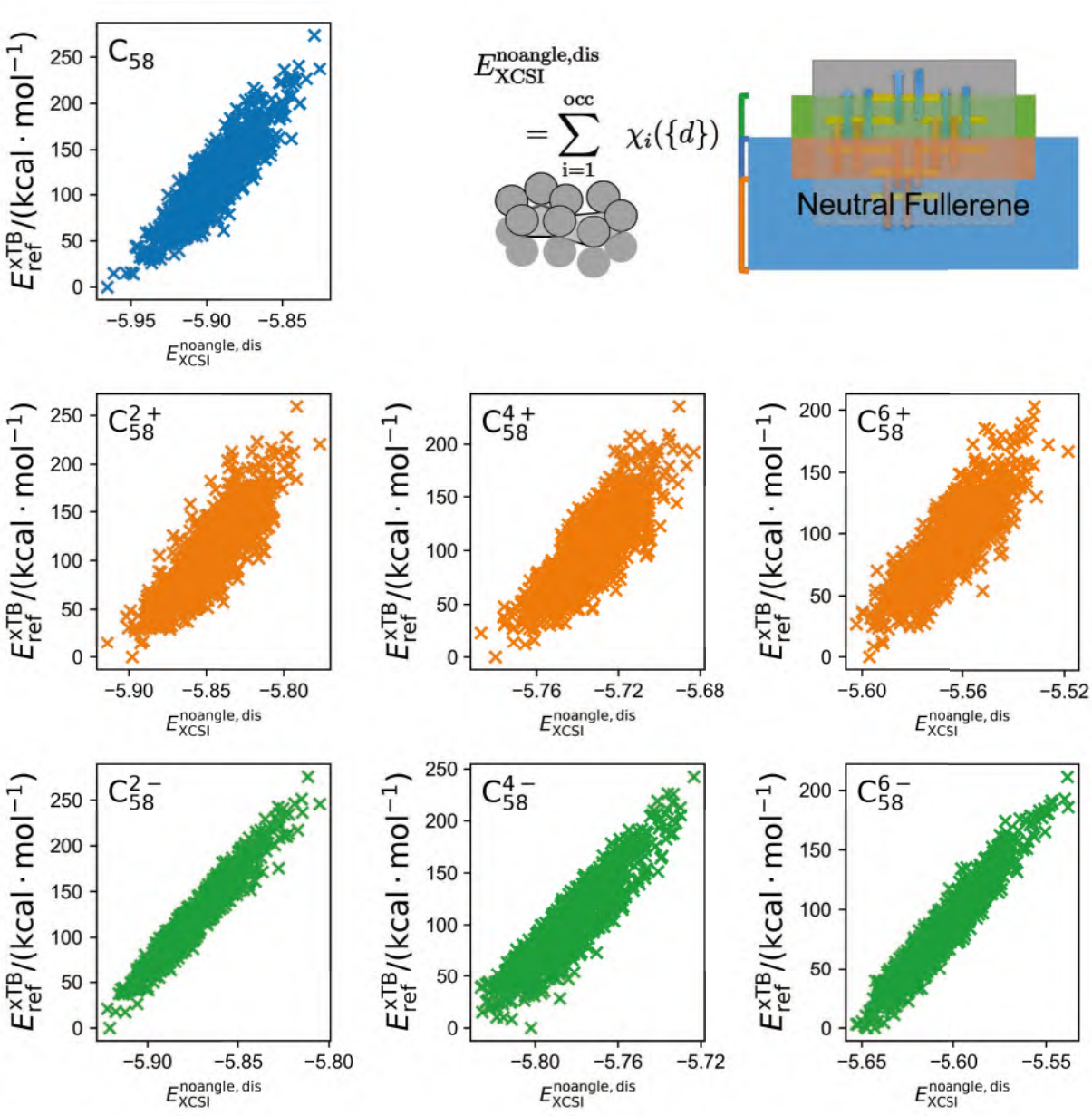


Figure 120: Correlation between xTB energies of $C_{58}$ isomers relative to the most stable one and prediction by XCSI model with distances but without angles of $C_{58}$ isomers without and with charge 2+, 4+, 6+, 2-, 4-, 6-, respectively.

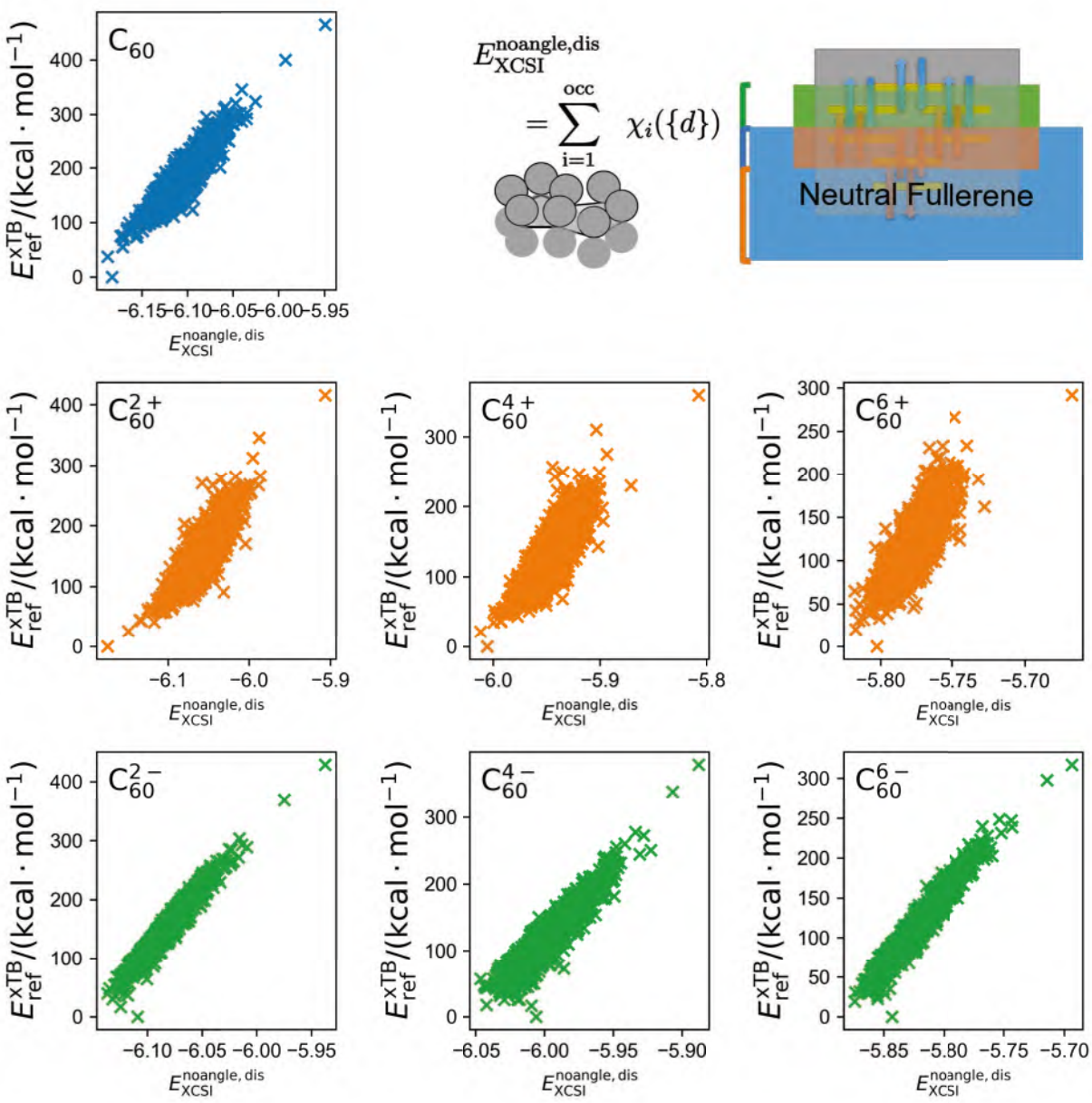


Figure 121: Correlation between xTB energies of $C_{60}$ isomers relative to the most stable one and prediction by XCSI model with distances but without angles of $C_{60}$ isomers without and with charge 2+, 4+, 6+, 2-, 4-, 6-, respectively.

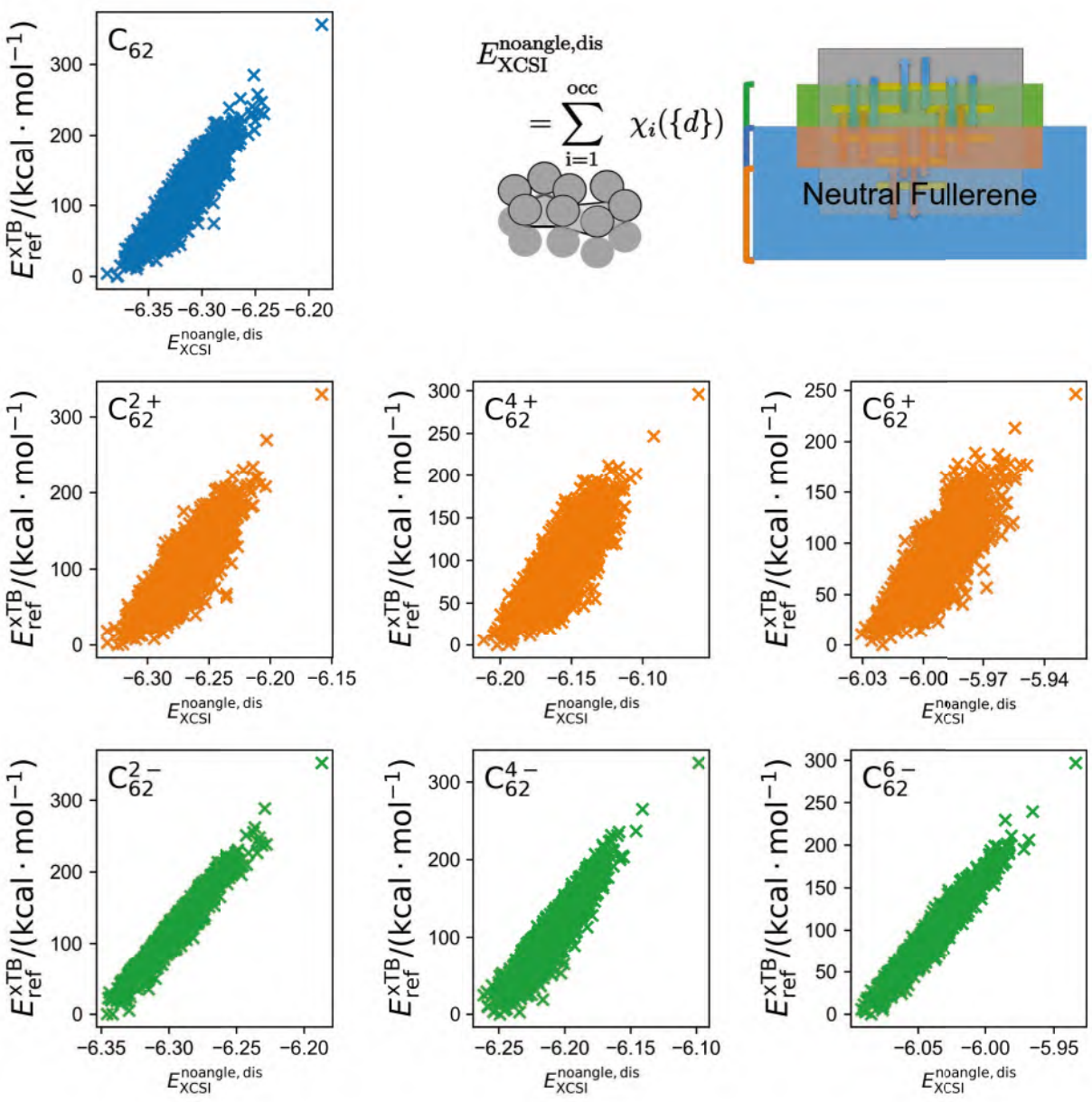


Figure 122: Correlation between xTB energies of $C_{62}$ isomers relative to the most stable one and prediction by XCSI model with distances but without angles of $C_{62}$ isomers without and with charge 2+, 4+, 6+, 2-, 4-, 6-, respectively.

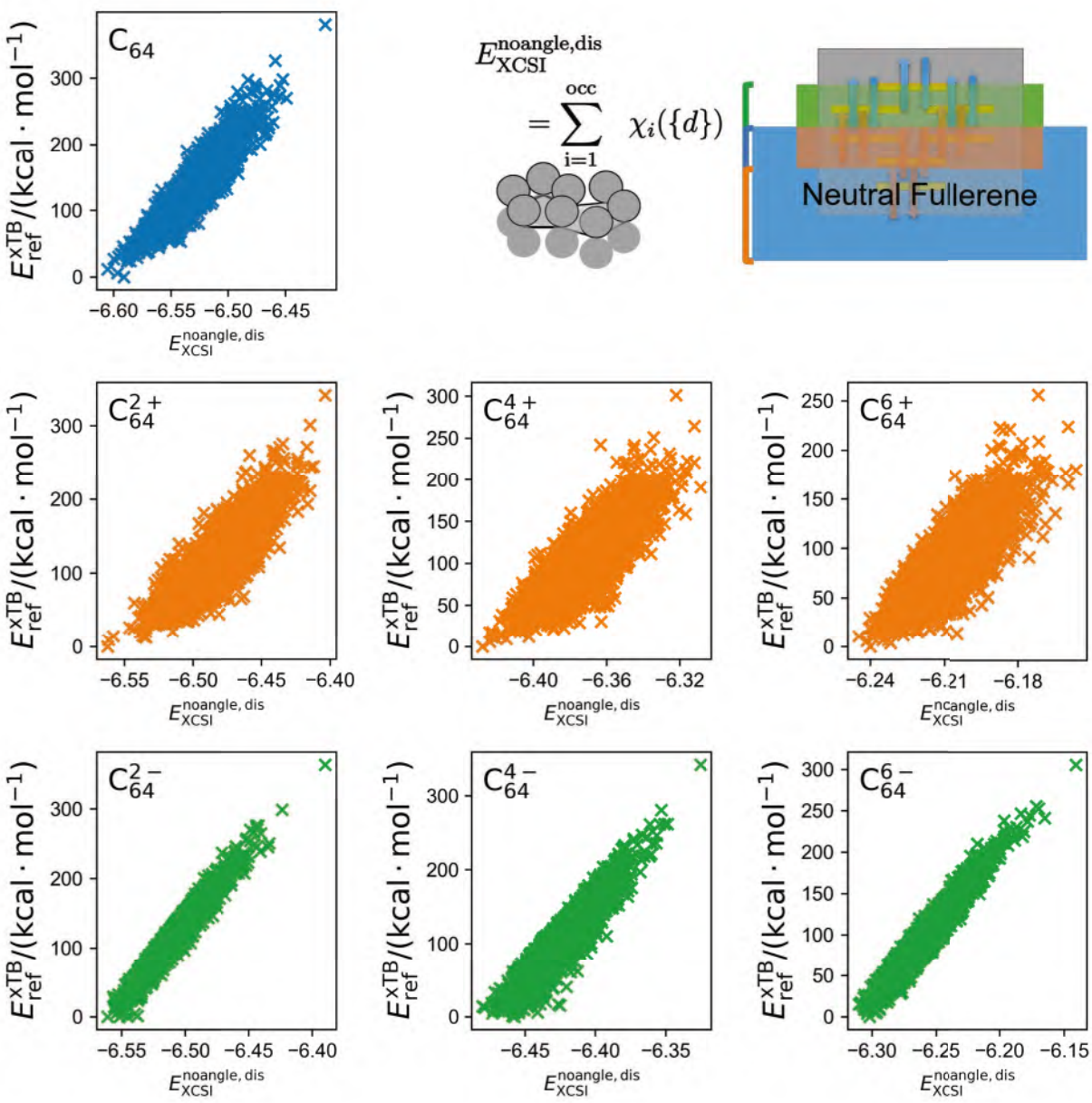


Figure 123: Correlation between xTB energies of $C_{64}$ isomers relative to the most stable one and prediction by XCSI model with distances but without angles of $C_{64}$ isomers without and with charge 2+, 4+, 6+, 2-, 4-, 6-, respectively.

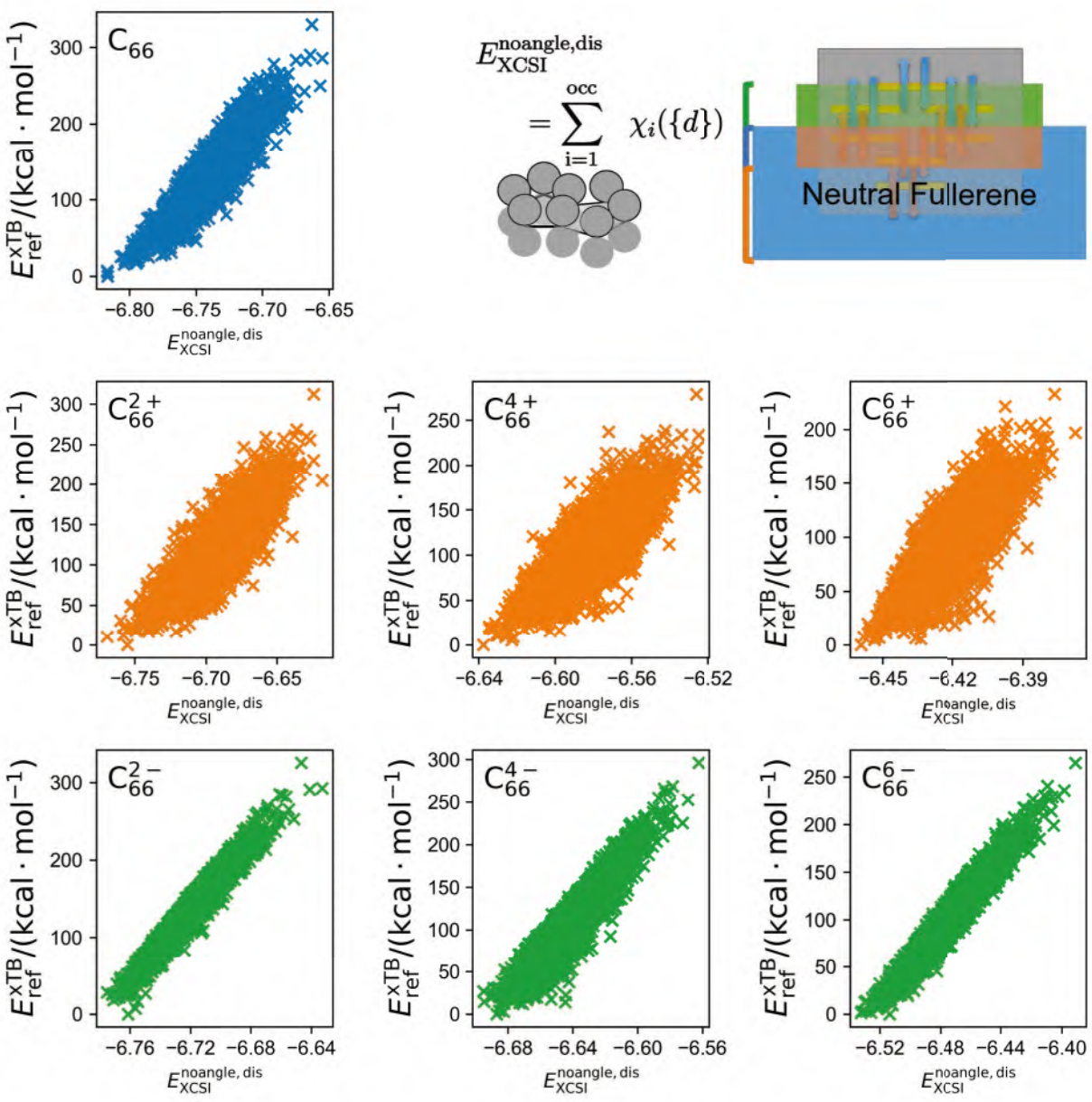


Figure 124: Correlation between xTB energies of $C_{66}$ isomers relative to the most stable one and prediction by XCSI model with distances but without angles of $C_{66}$ isomers without and with charge 2+, 4+, 6+, 2-, 4-, 6-, respectively.

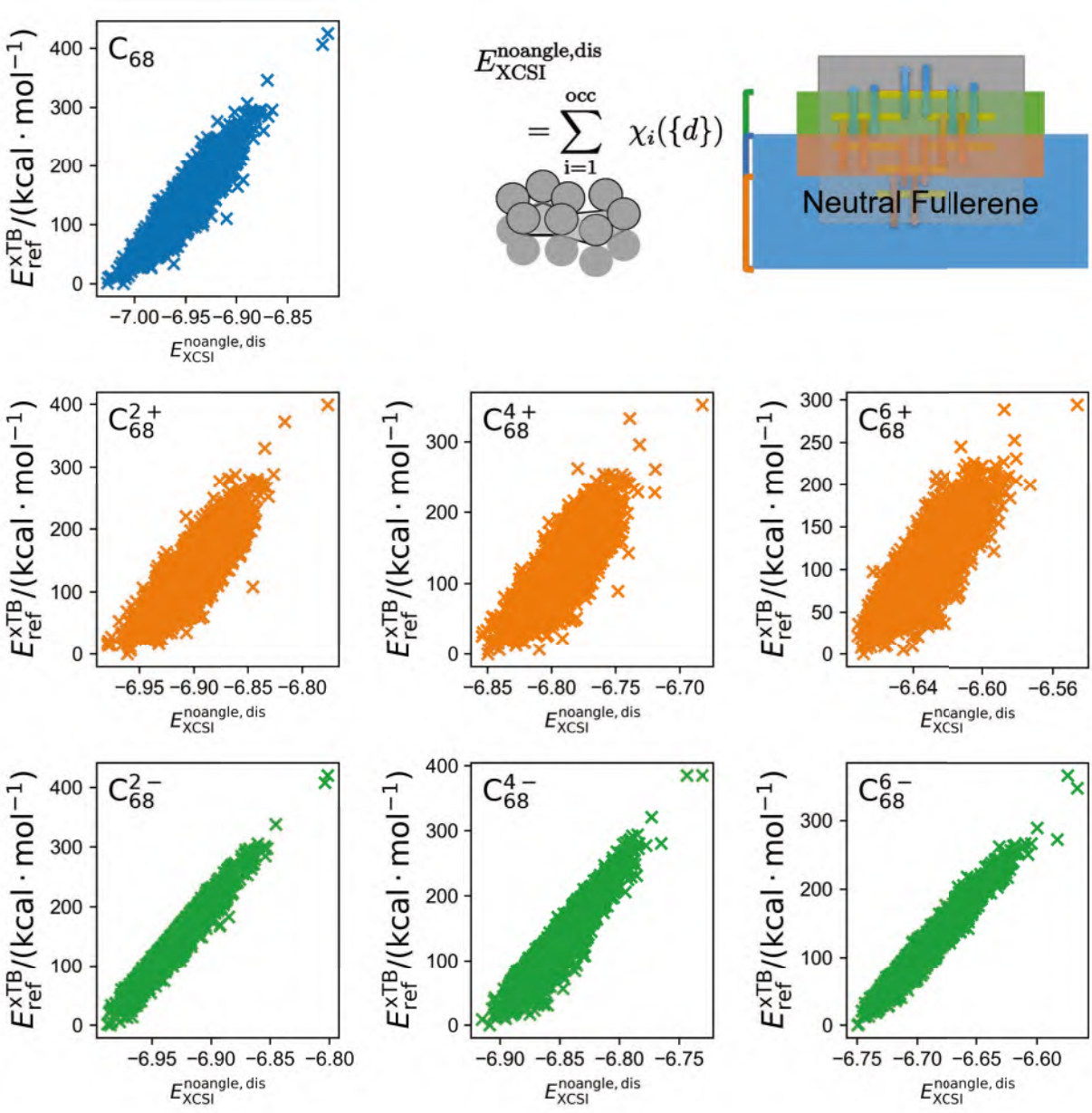


Figure 125: Correlation between xTB energies of $C_{68}$ isomers relative to the most stable one and prediction by XCSI model with distances but without angles of $C_{68}$ isomers without and with charge 2+, 4+, 6+, 2-, 4-, 6-, respectively.

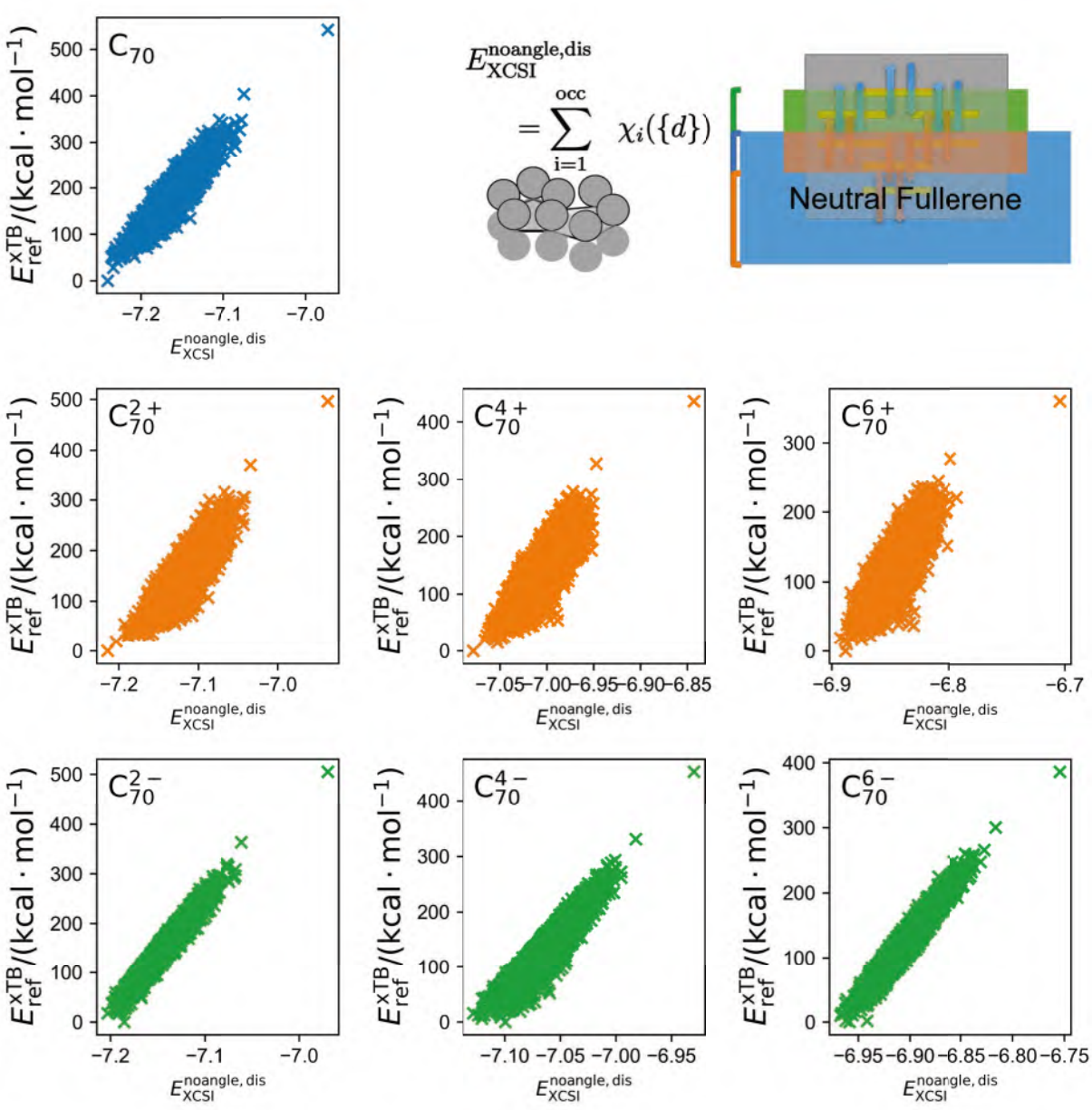


Figure 126: Correlation between xTB energies of $C_{70}$ isomers relative to the most stable one and prediction by XCSI model with distances but without angles of $C_{70}$ isomers without and with charge 2+, 4+, 6+, 2-, 4-, 6-, respectively.

# 8 Correlation between xTB energies and prediction by XCSI model with distances but without angles, without using adjacent matrix mask

Predictions by XCSI model with distances but without angles, and not using adjacent matrix mask, are calculated by

$$E_{\mathrm{XCSI}}^{\mathrm{angle,nodis}} \equiv \sum_{k=i}^{n} \chi_{k,i}^{q}(d) \tag{12}$$

where $\chi_{k,i}^{q}$ is eigenvalues of extended adjacency matrix, whose elements are

$$h_{ij}^{k} = \begin{cases} \exp\left(-d_{ij}^{2}\right)\beta' & i \neq j \\ 0 & i = j \end{cases} \tag{13}$$

.

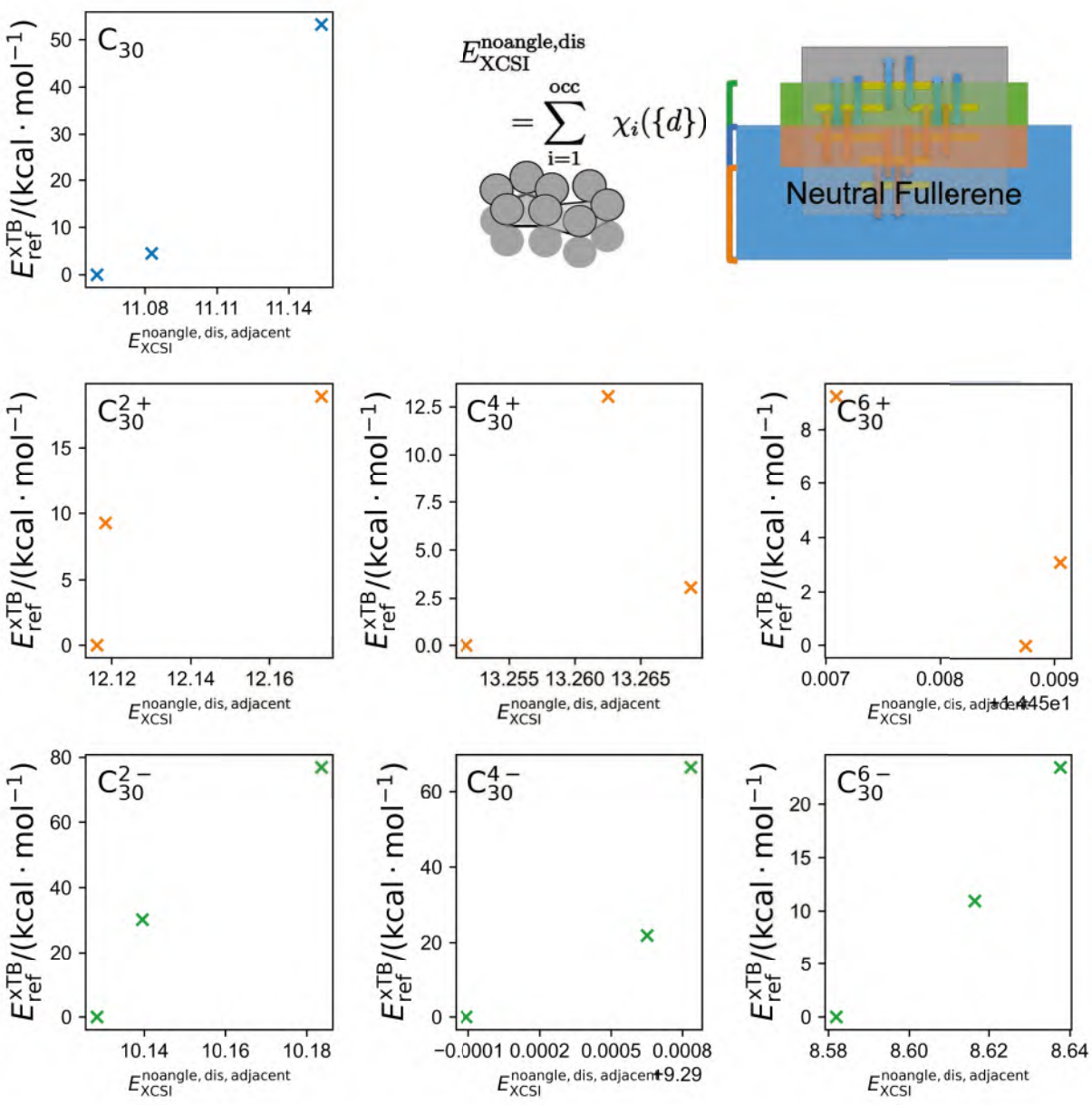


Figure 127: Correlation between xTB energies of $C_{30}$ isomers relative to the most stable one and prediction by XCSI model with distances but without angles, without using adjacent matrix mask of $C_{30}$ isomers without and with charge 2+, 4+, 6+, 2-, 4-, 6-, respectively.

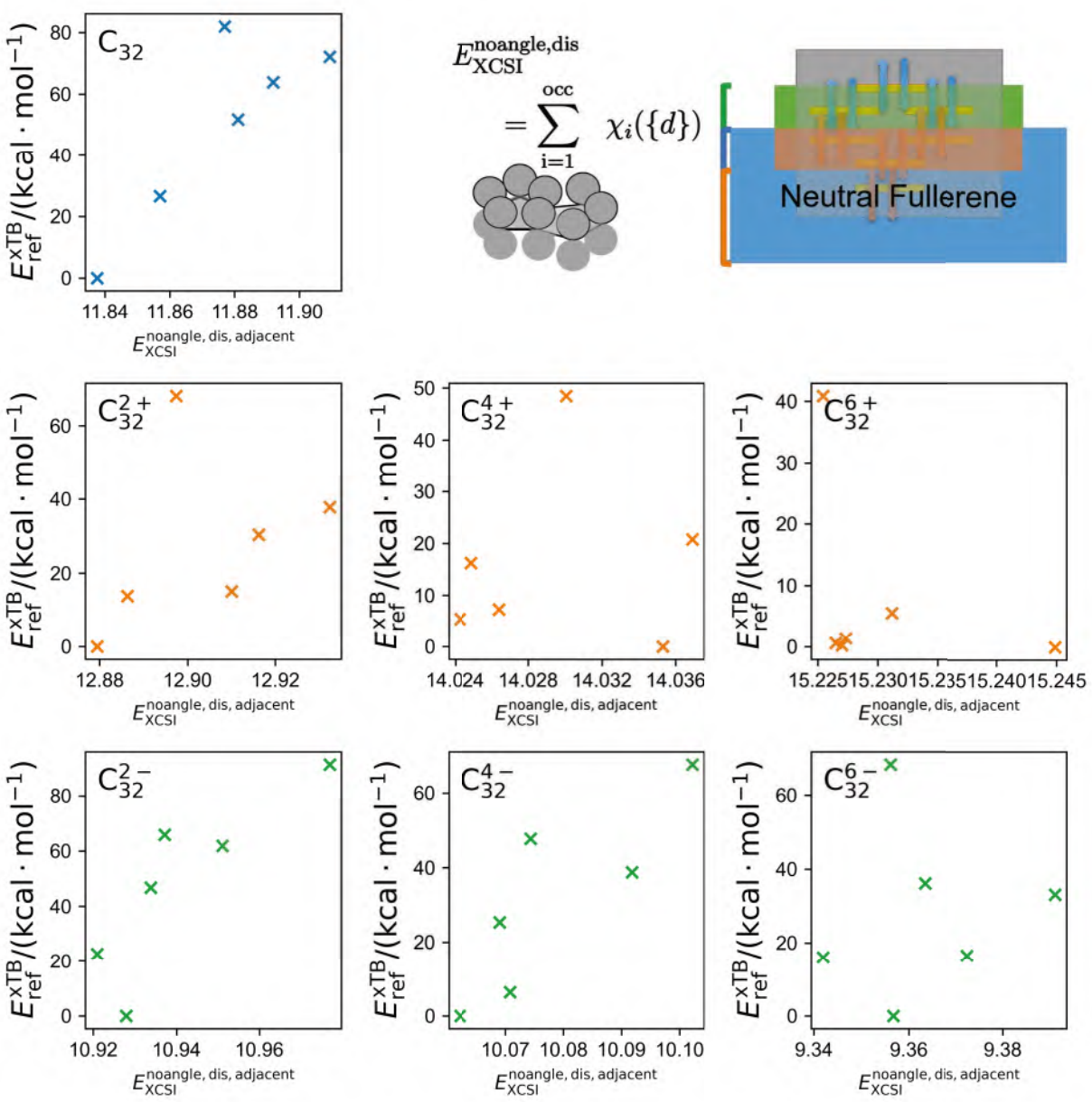


Figure 128: Correlation between xTB energies of $C_{32}$ isomers relative to the most stable one and prediction by XCSI model with distances but without angles, without using adjacent matrix mask of $C_{32}$ isomers without and with charge 2+, 4+, 6+, 2-, 4-, 6-, respectively.

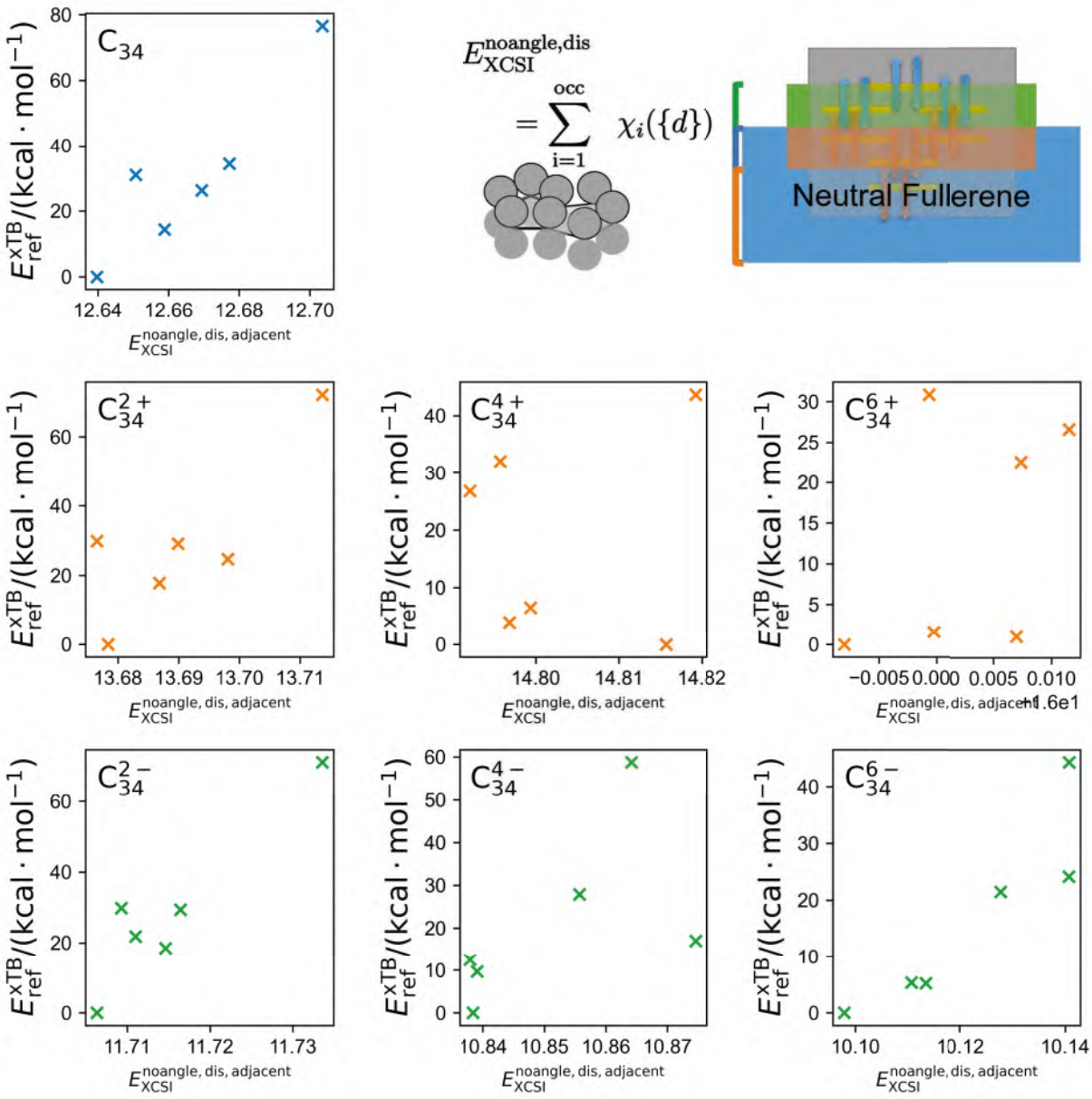


Figure 129: Correlation between xTB energies of $C_{34}$ isomers relative to the most stable one and prediction by XCSI model with distances but without angles, without using adjacent matrix mask of $C_{34}$ isomers without and with charge 2+, 4+, 6+, 2-, 4-, 6-, respectively.

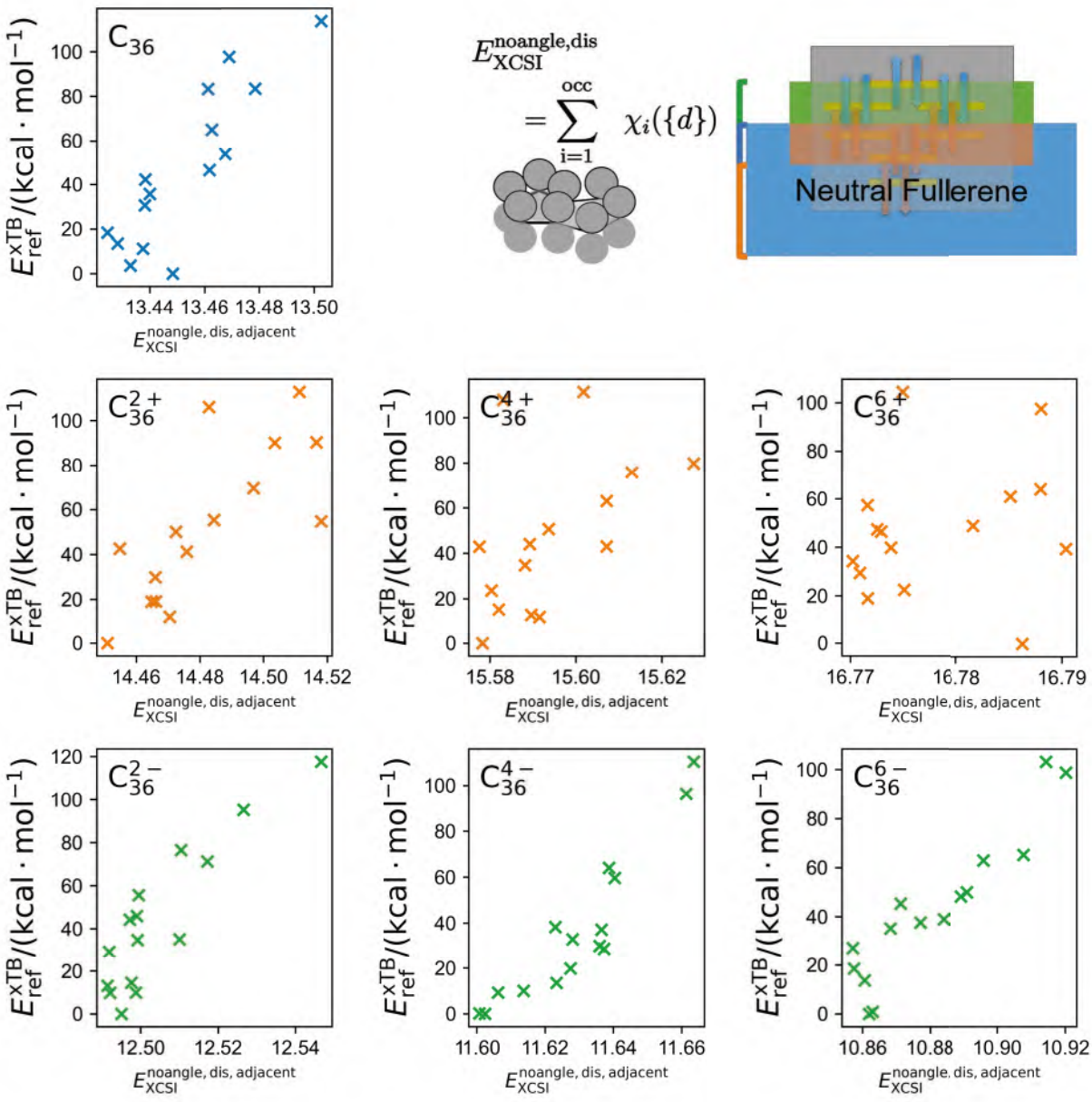


Figure 130: Correlation between xTB energies of $C_{36}$ isomers relative to the most stable one and prediction by XCSI model with distances but without angles, without using adjacent matrix mask of $C_{36}$ isomers without and with charge 2+, 4+, 6+, 2-, 4-, 6-, respectively.

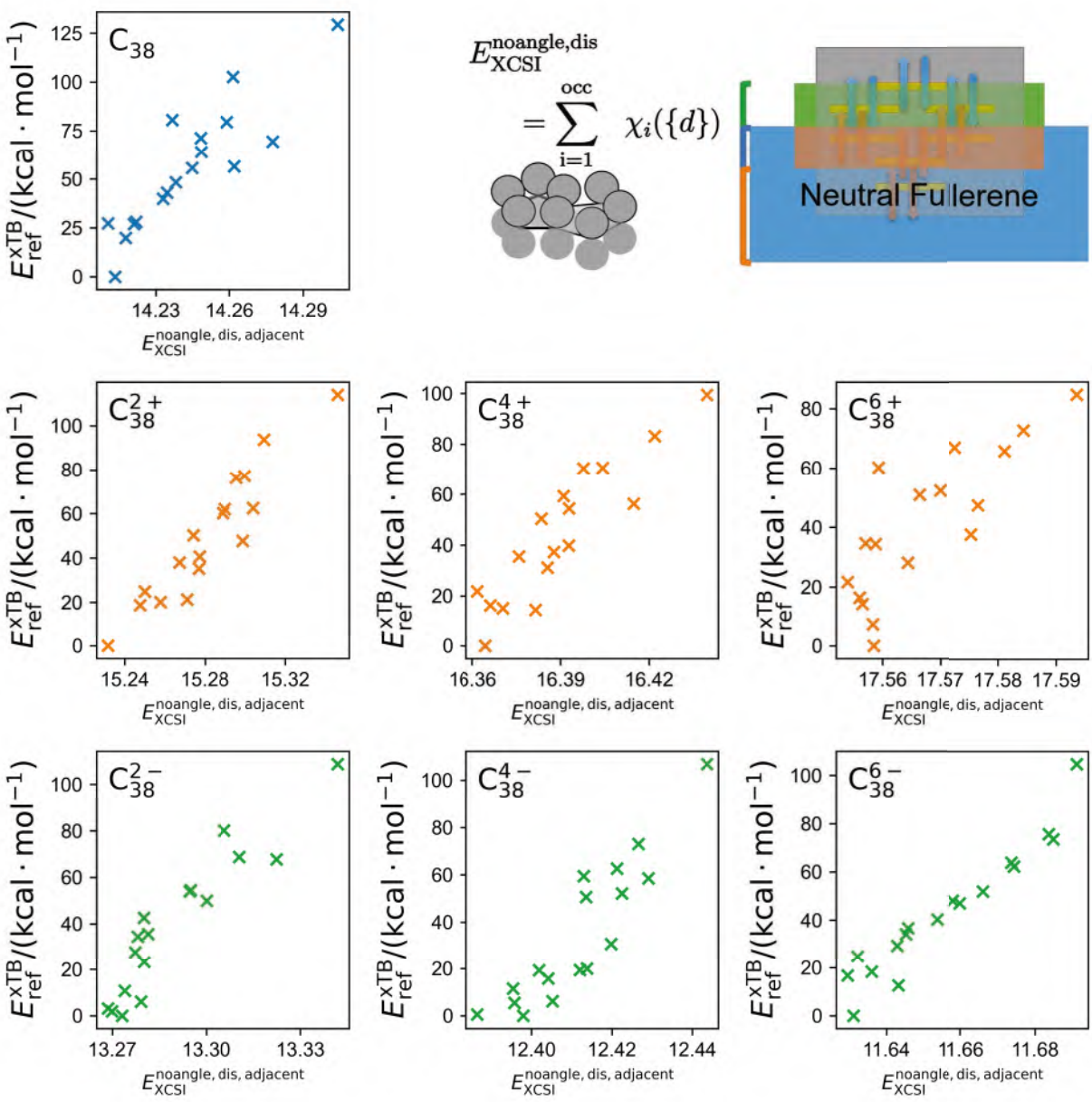


Figure 131: Correlation between xTB energies of $C_{38}$ isomers relative to the most stable one and prediction by XCSI model with distances but without angles, without using adjacent matrix mask of $C_{38}$ isomers without and with charge 2+, 4+, 6+, 2-, 4-, 6-, respectively.

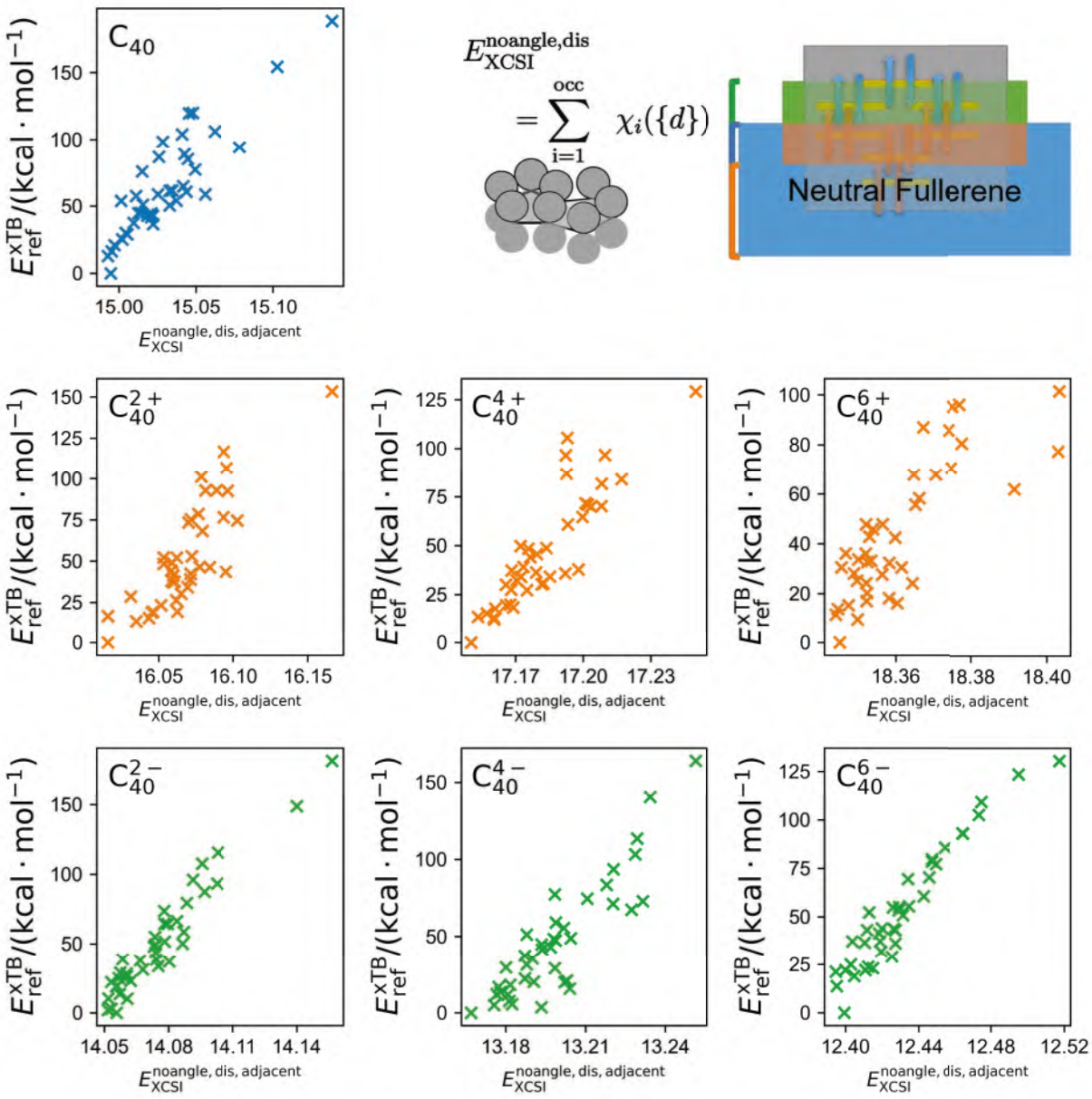


Figure 132: Correlation between xTB energies of $C_{40}$ isomers relative to the most stable one and prediction by XCSI model with distances but without angles, without using adjacent matrix mask of $C_{40}$ isomers without and with charge 2+, 4+, 6+, 2-, 4-, 6-, respectively.

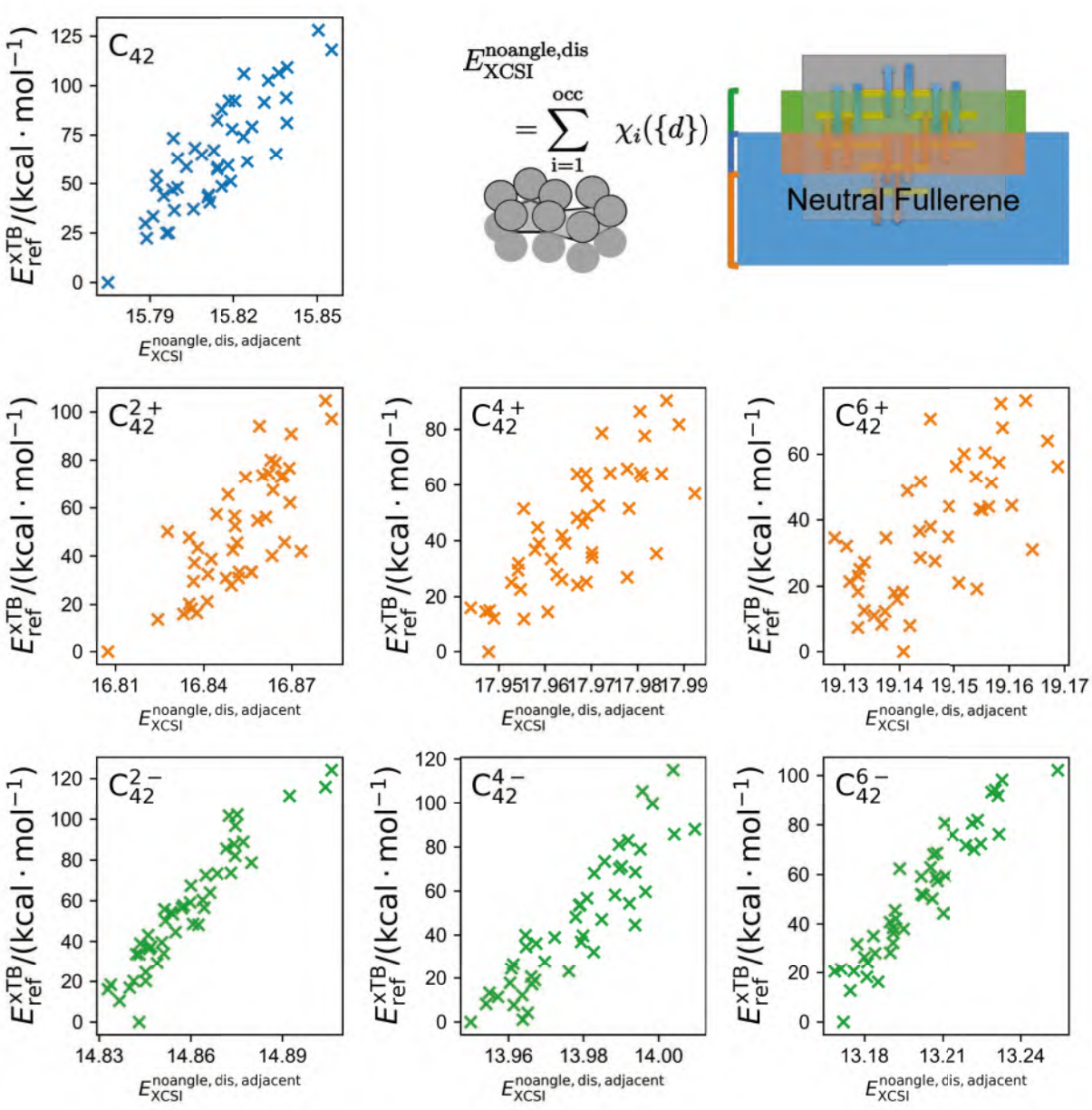


Figure 133: Correlation between xTB energies of $C_{42}$ isomers relative to the most stable one and prediction by XCSI model with distances but without angles, without using adjacent matrix mask of $C_{42}$ isomers without and with charge 2+, 4+, 6+, 2-, 4-, 6-, respectively.

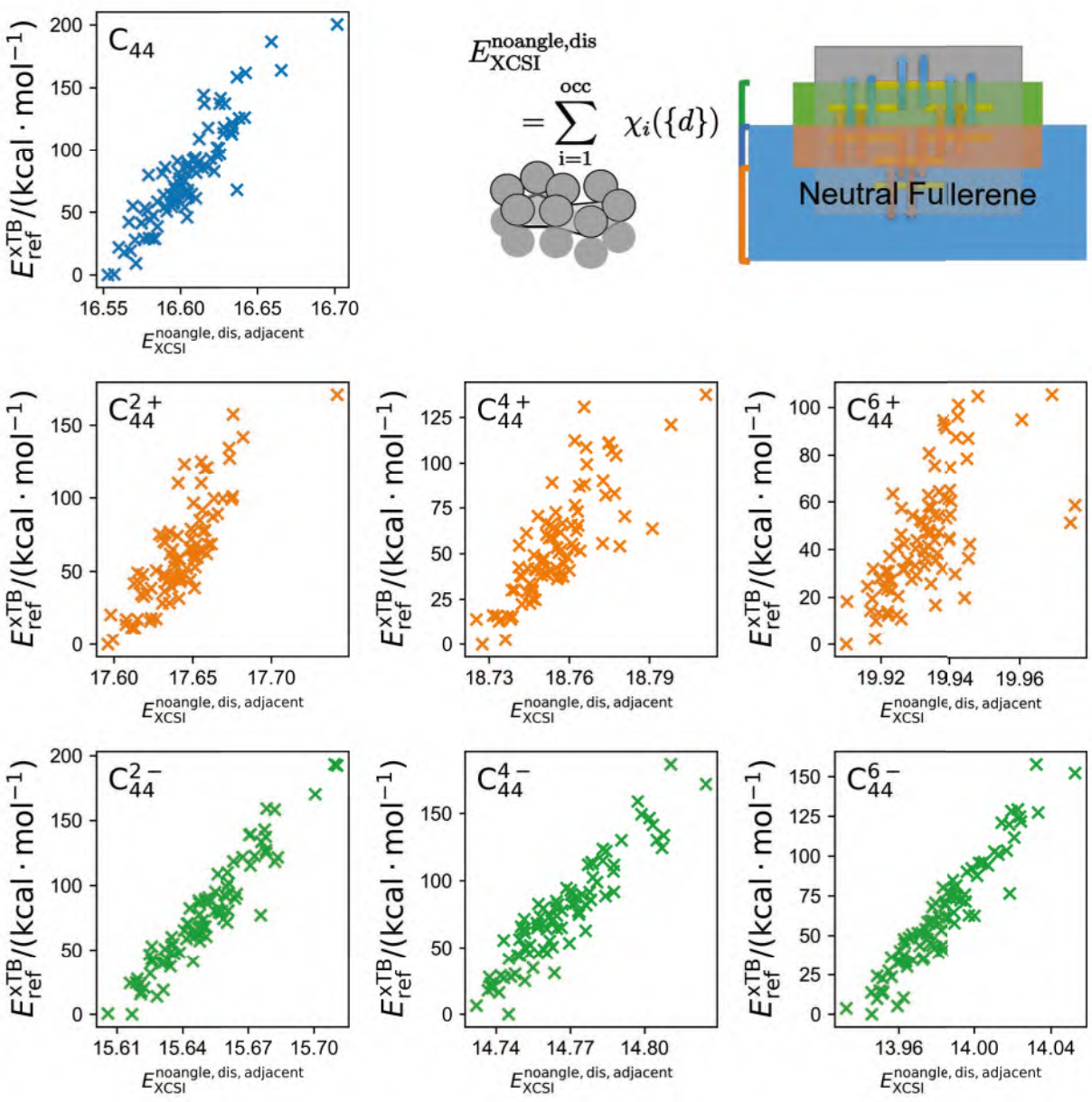


Figure 134: Correlation between xTB energies of $C_{44}$ isomers relative to the most stable one and prediction by XCSI model with distances but without angles, without using adjacent matrix mask of $C_{44}$ isomers without and with charge 2+, 4+, 6+, 2-, 4-, 6-, respectively.

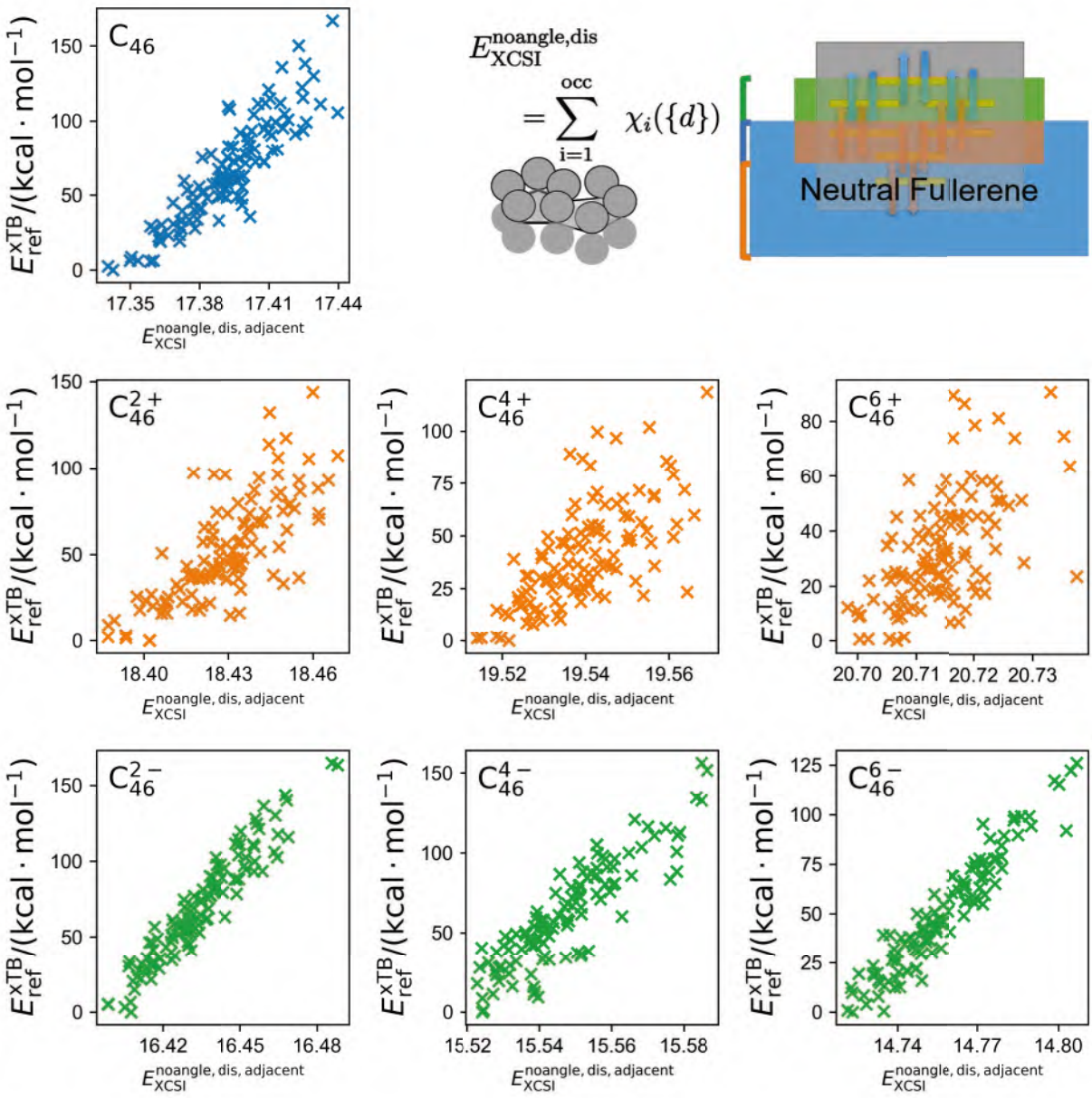


Figure 135: Correlation between xTB energies of $C_{46}$ isomers relative to the most stable one and prediction by XCSI model with distances but without angles, without using adjacent matrix mask of $C_{46}$ isomers without and with charge 2+, 4+, 6+, 2-, 4-, 6-, respectively.

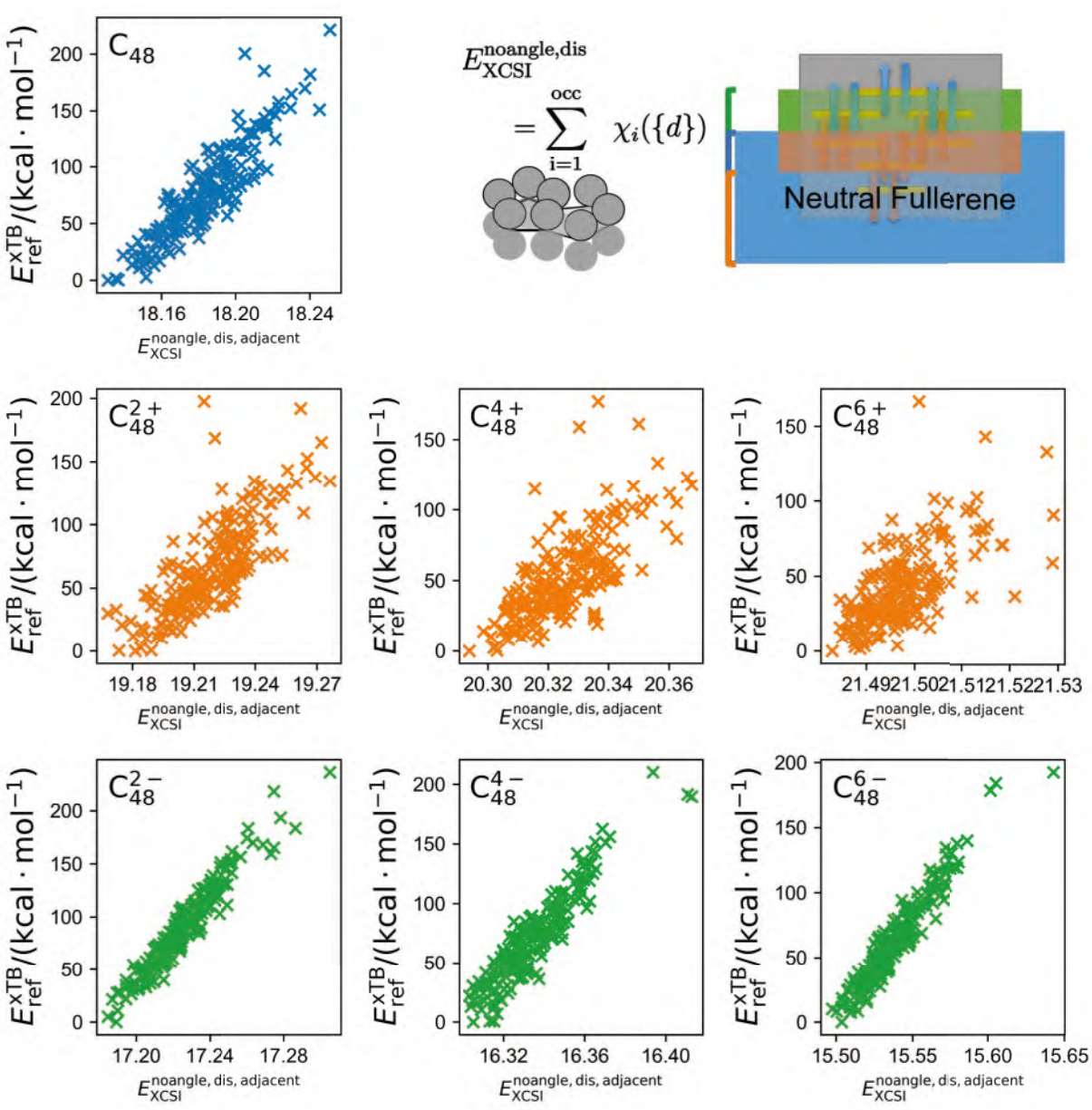


Figure 136: Correlation between xTB energies of $C_{48}$ isomers relative to the most stable one and prediction by XCSI model with distances but without angles, without using adjacent matrix mask of $C_{48}$ isomers without and with charge 2+, 4+, 6+, 2-, 4-, 6-, respectively.

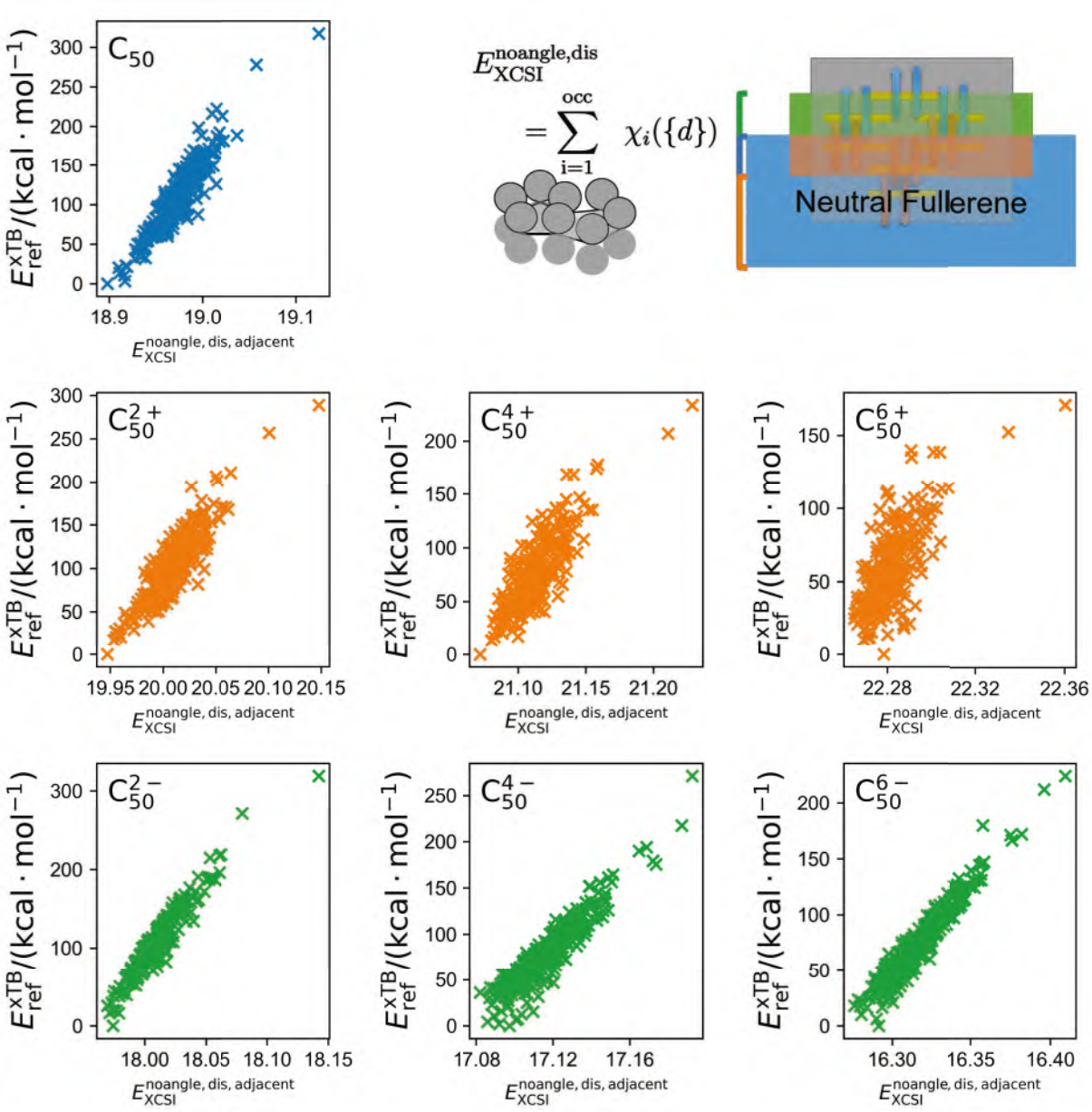


Figure 137: Correlation between xTB energies of $C_{50}$ isomers relative to the most stable one and prediction by XCSI model with distances but without angles, without using adjacent matrix mask of $C_{50}$ isomers without and with charge 2+, 4+, 6+, 2-, 4-, 6-, respectively.

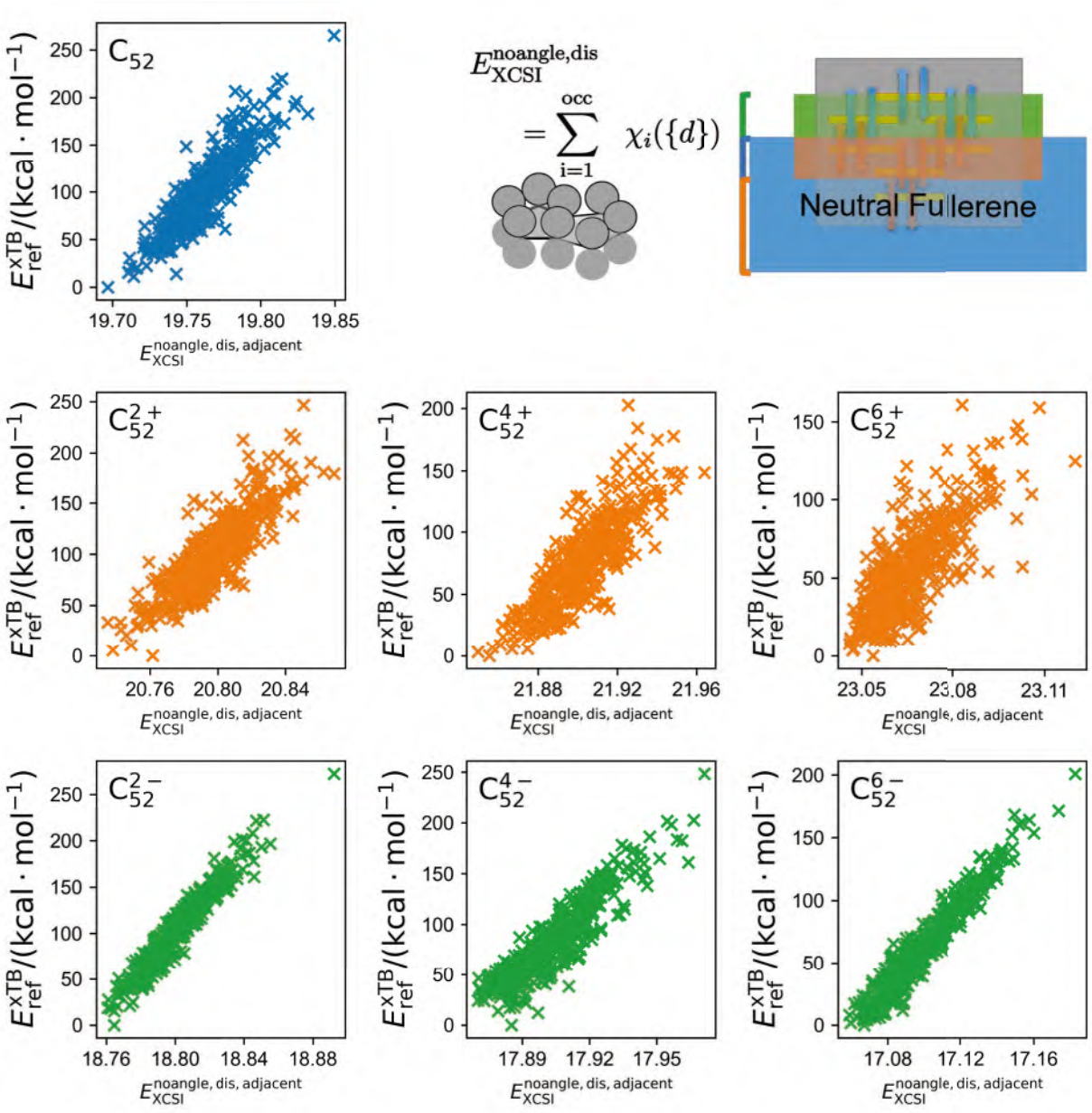


Figure 138: Correlation between xTB energies of $C_{52}$ isomers relative to the most stable one and prediction by XCSI model with distances but without angles, without using adjacent matrix mask of $C_{52}$ isomers without and with charge 2+, 4+, 6+, 2-, 4-, 6-, respectively.

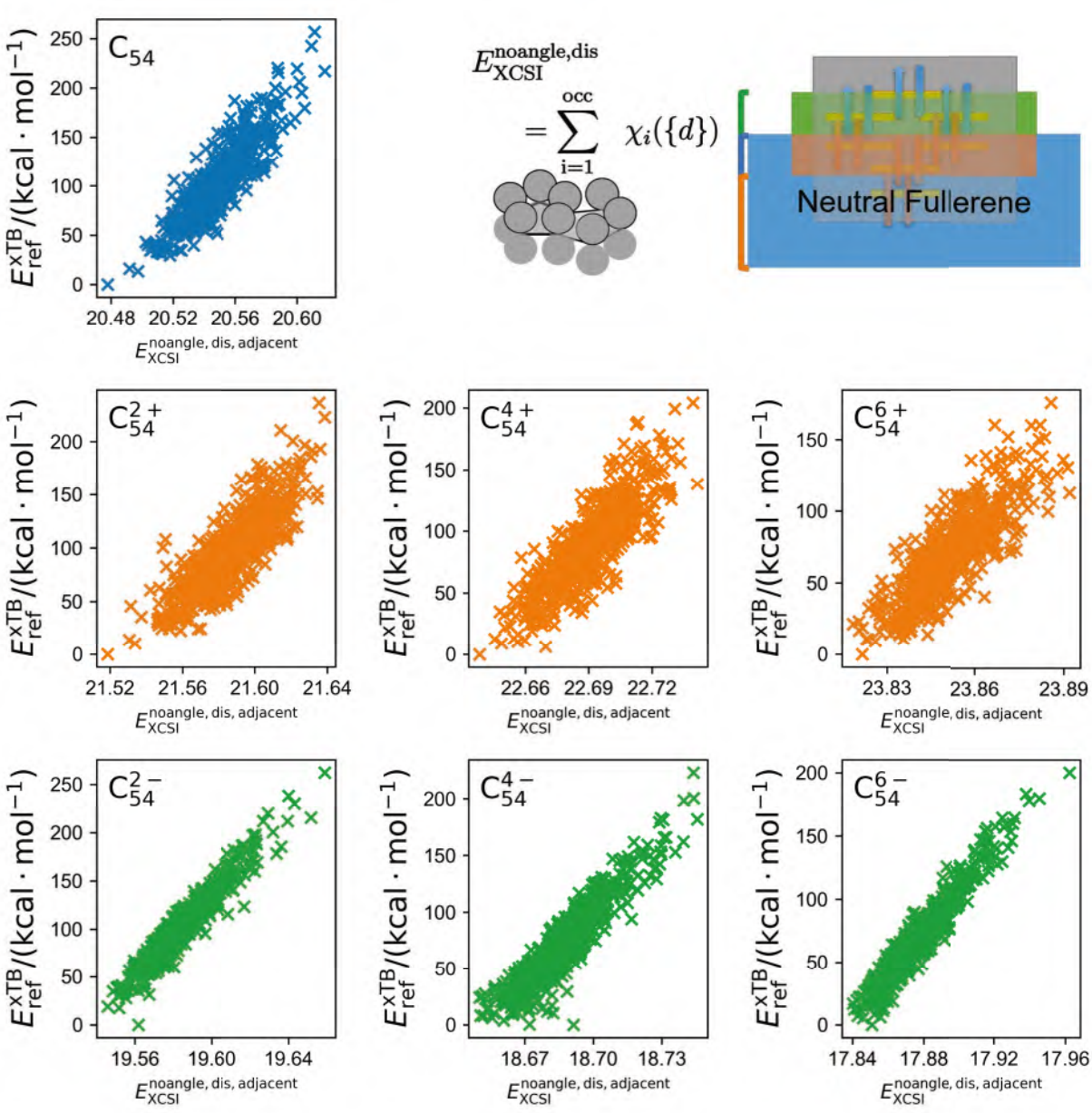


Figure 139: Correlation between xTB energies of $C_{54}$ isomers relative to the most stable one and prediction by XCSI model with distances but without angles, without using adjacent matrix mask of $C_{54}$ isomers without and with charge 2+, 4+, 6+, 2-, 4-, 6-, respectively.

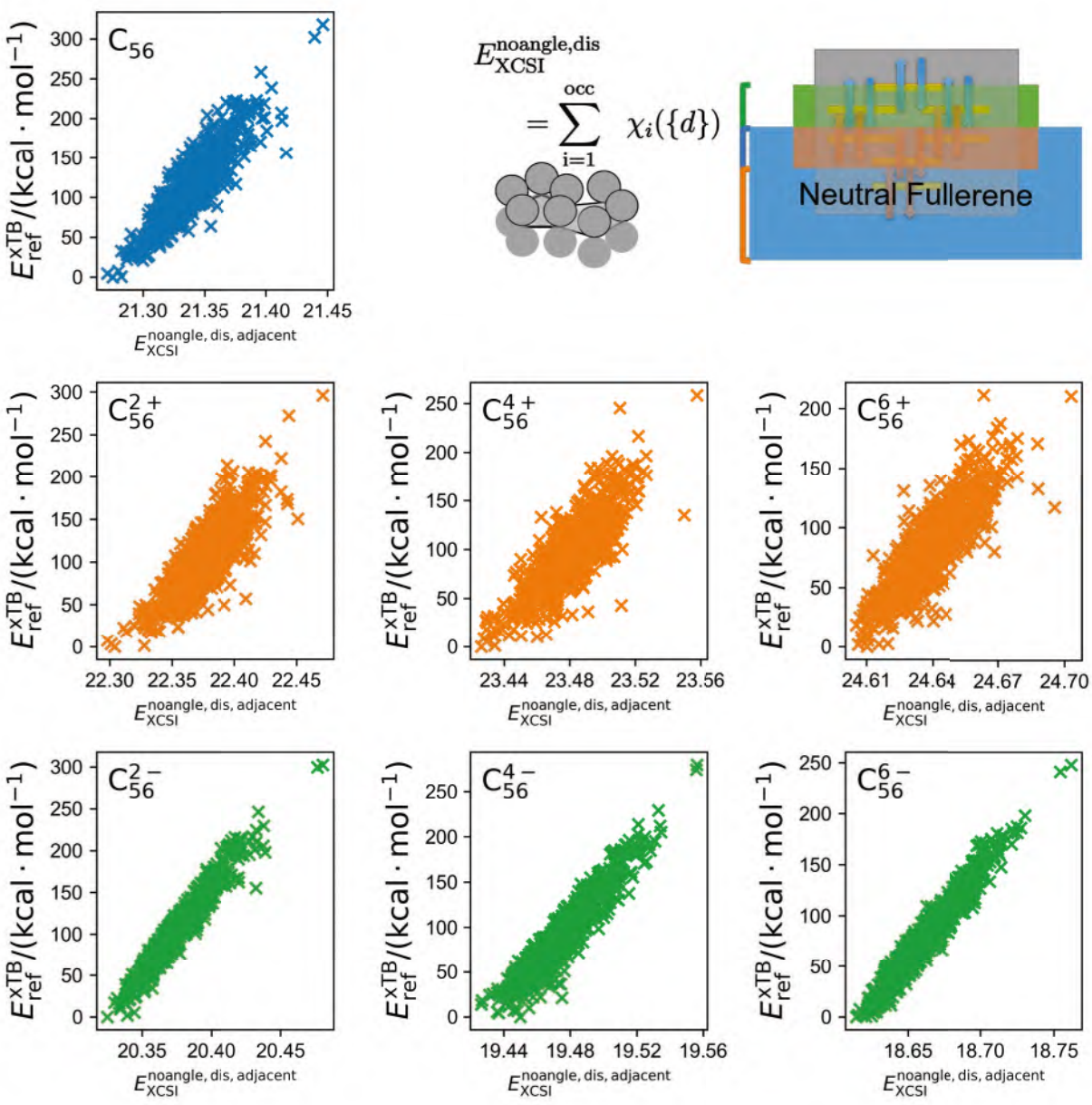


Figure 140: Correlation between xTB energies of $C_{56}$ isomers relative to the most stable one and prediction by XCSI model with distances but without angles, without using adjacent matrix mask of $C_{56}$ isomers without and with charge 2+, 4+, 6+, 2-, 4-, 6-, respectively.

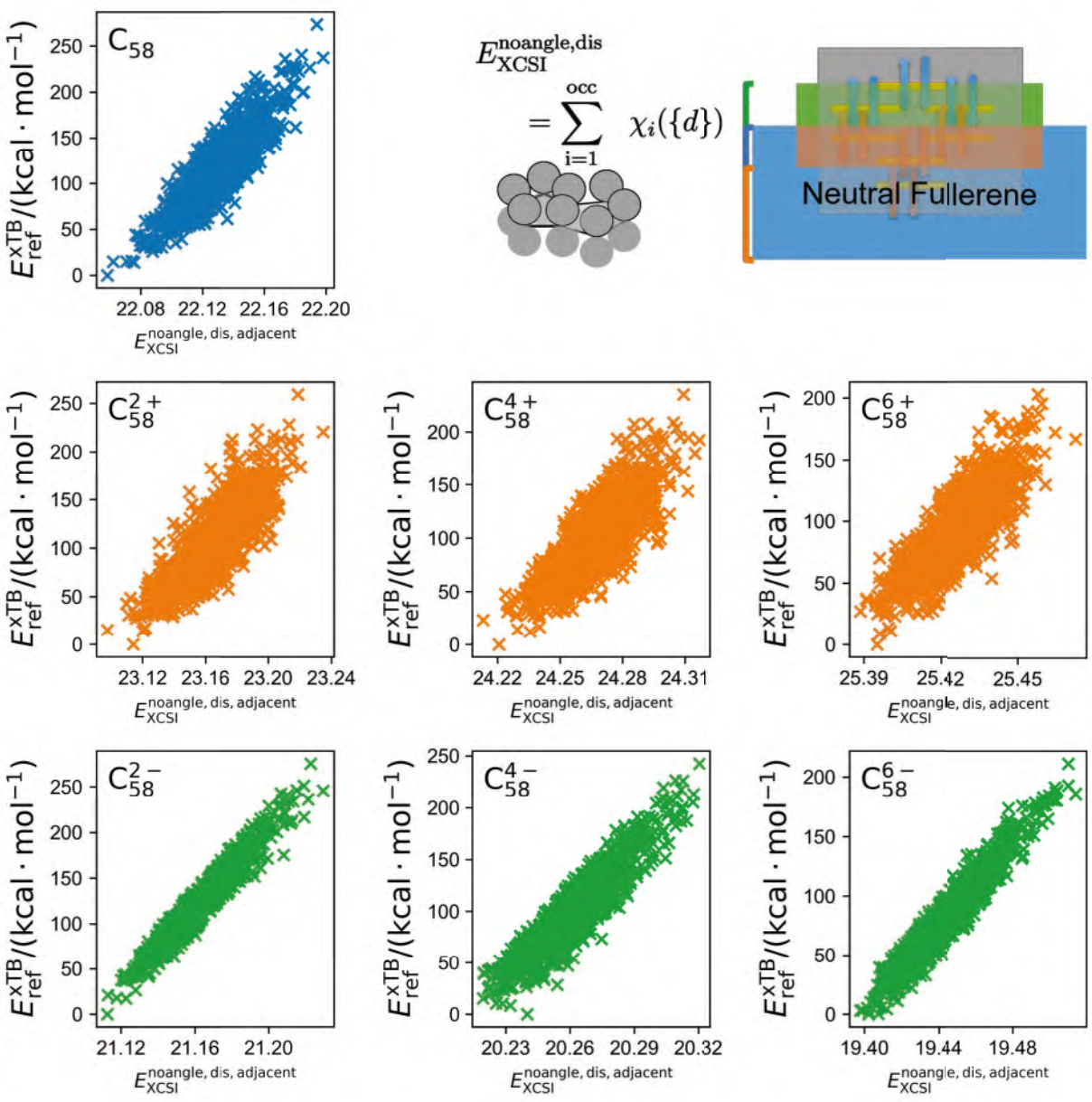


Figure 141: Correlation between xTB energies of $C_{58}$ isomers relative to the most stable one and prediction by XCSI model with distances but without angles, without using adjacent matrix mask of $C_{58}$ isomers without and with charge 2+, 4+, 6+, 2-, 4-, 6-, respectively.

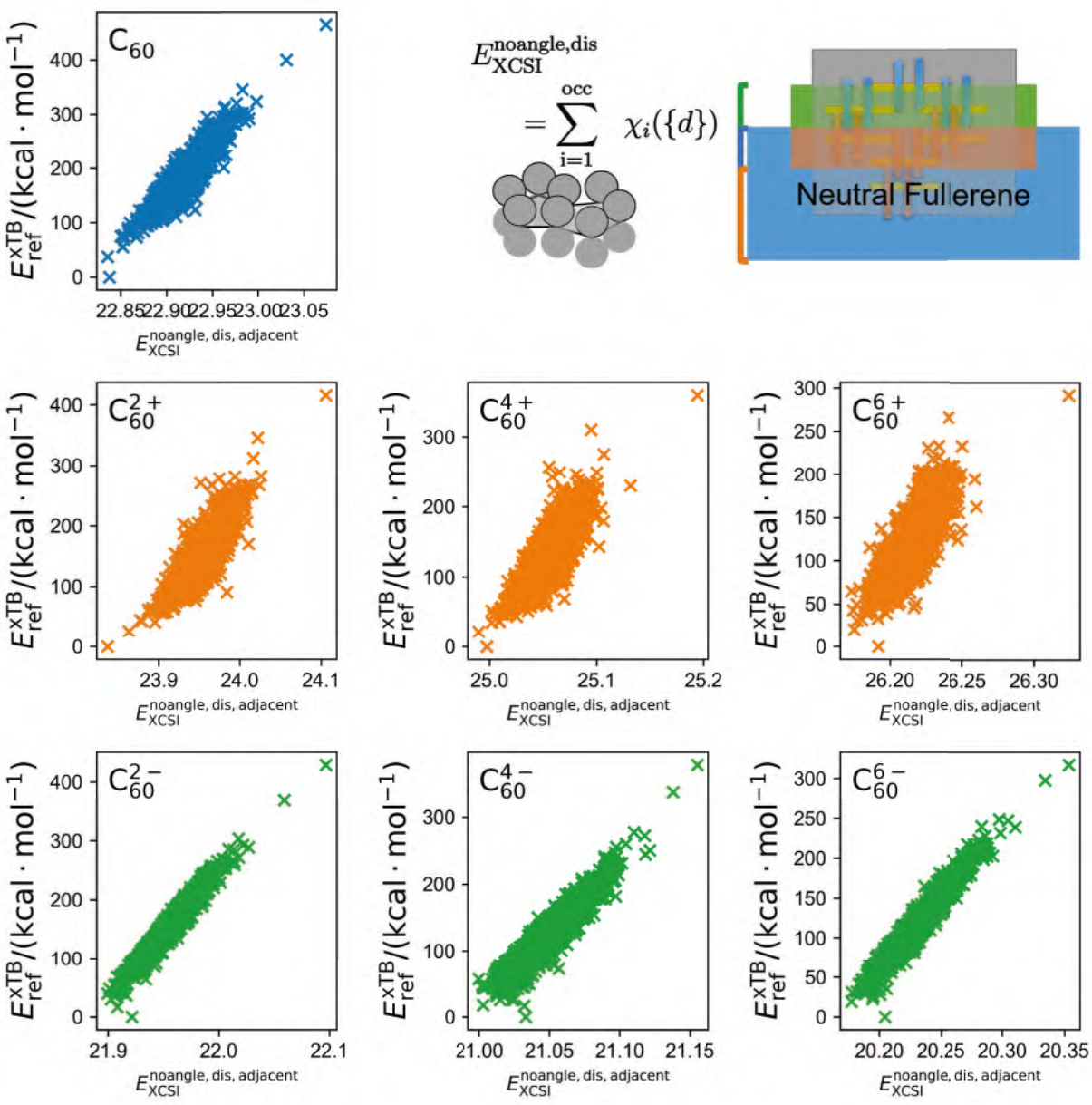


Figure 142: Correlation between xTB energies of $C_{60}$ isomers relative to the most stable one and prediction by XCSI model with distances but without angles, without using adjacent matrix mask of $C_{60}$ isomers without and with charge 2+, 4+, 6+, 2-, 4-, 6-, respectively.

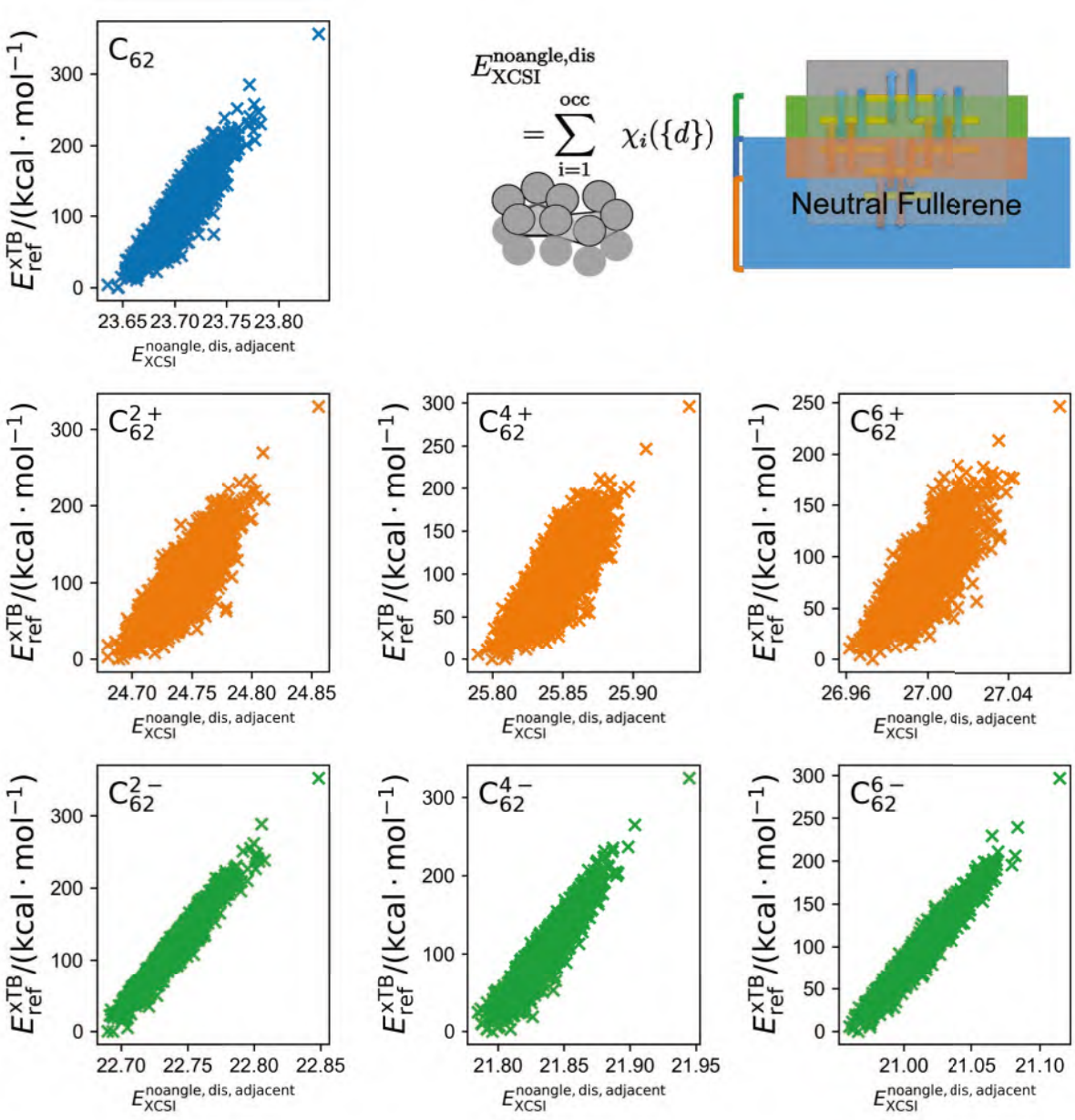


Figure 143: Correlation between xTB energies of $C_{62}$ isomers relative to the most stable one and prediction by XCSI model with distances but without angles, without using adjacent matrix mask of $C_{62}$ isomers without and with charge 2+, 4+, 6+, 2-, 4-, 6-, respectively.

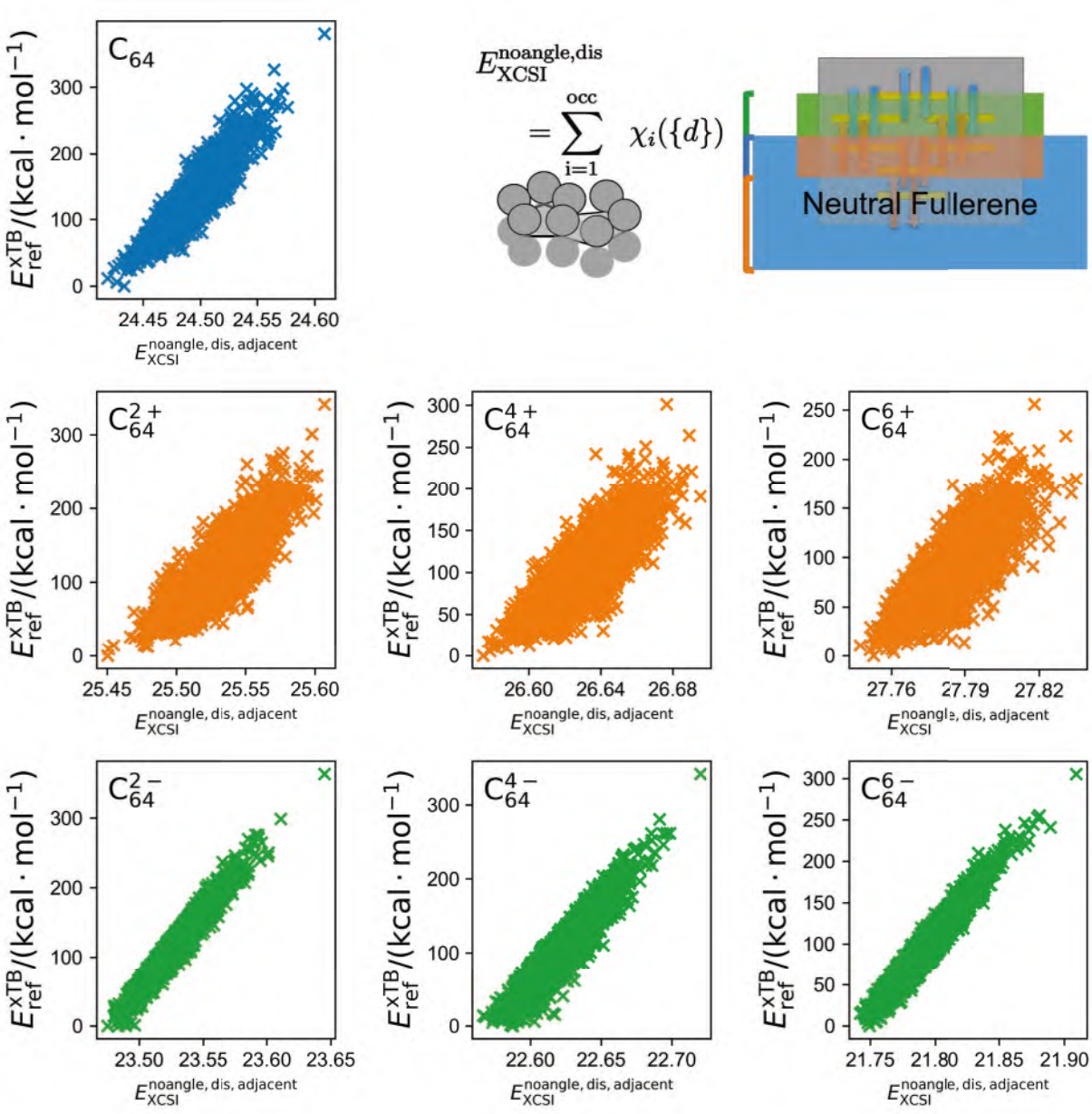


Figure 144: Correlation between xTB energies of $C_{64}$ isomers relative to the most stable one and prediction by XCSI model with distances but without angles, without using adjacent matrix mask of $C_{64}$ isomers without and with charge 2+, 4+, 6+, 2-, 4-, 6-, respectively.

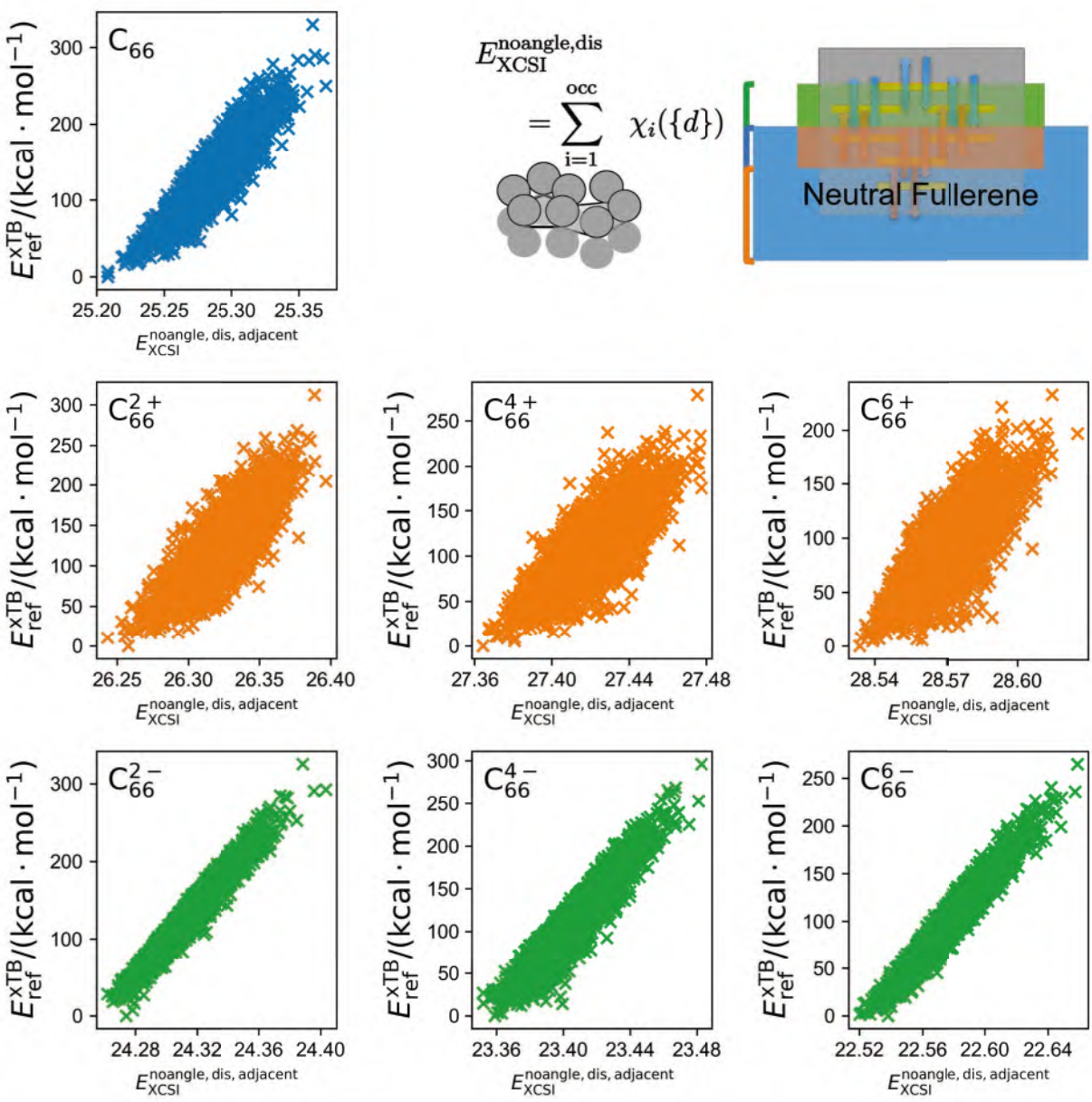


Figure 145: Correlation between xTB energies of $C_{66}$ isomers relative to the most stable one and prediction by XCSI model with distances but without angles, without using adjacent matrix mask of $C_{66}$ isomers without and with charge 2+, 4+, 6+, 2-, 4-, 6-, respectively.

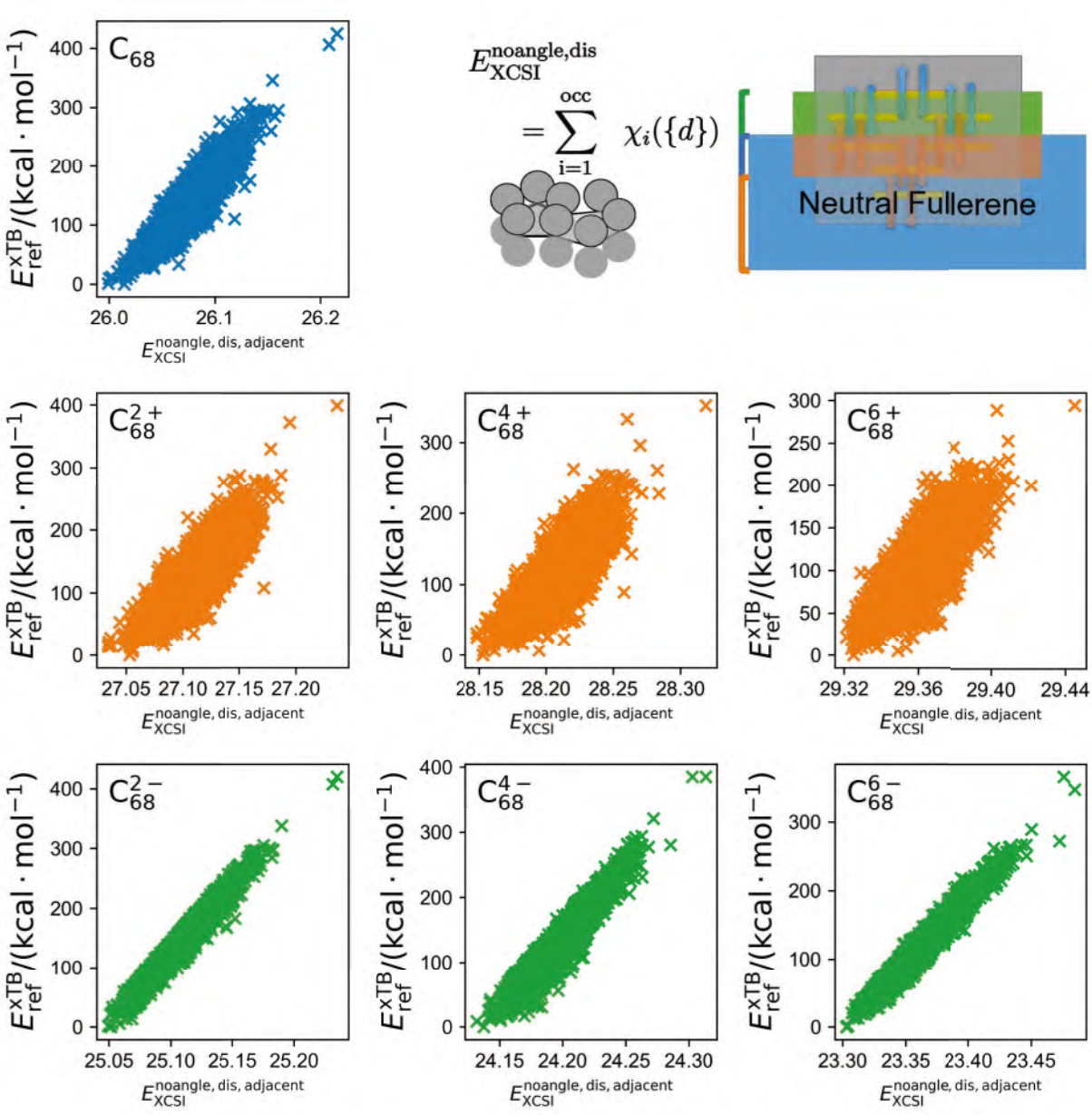


Figure 146: Correlation between xTB energies of $C_{68}$ isomers relative to the most stable one and prediction by XCSI model with distances but without angles, without using adjacent matrix mask of $C_{68}$ isomers without and with charge 2+, 4+, 6+, 2-, 4-, 6-, respectively.

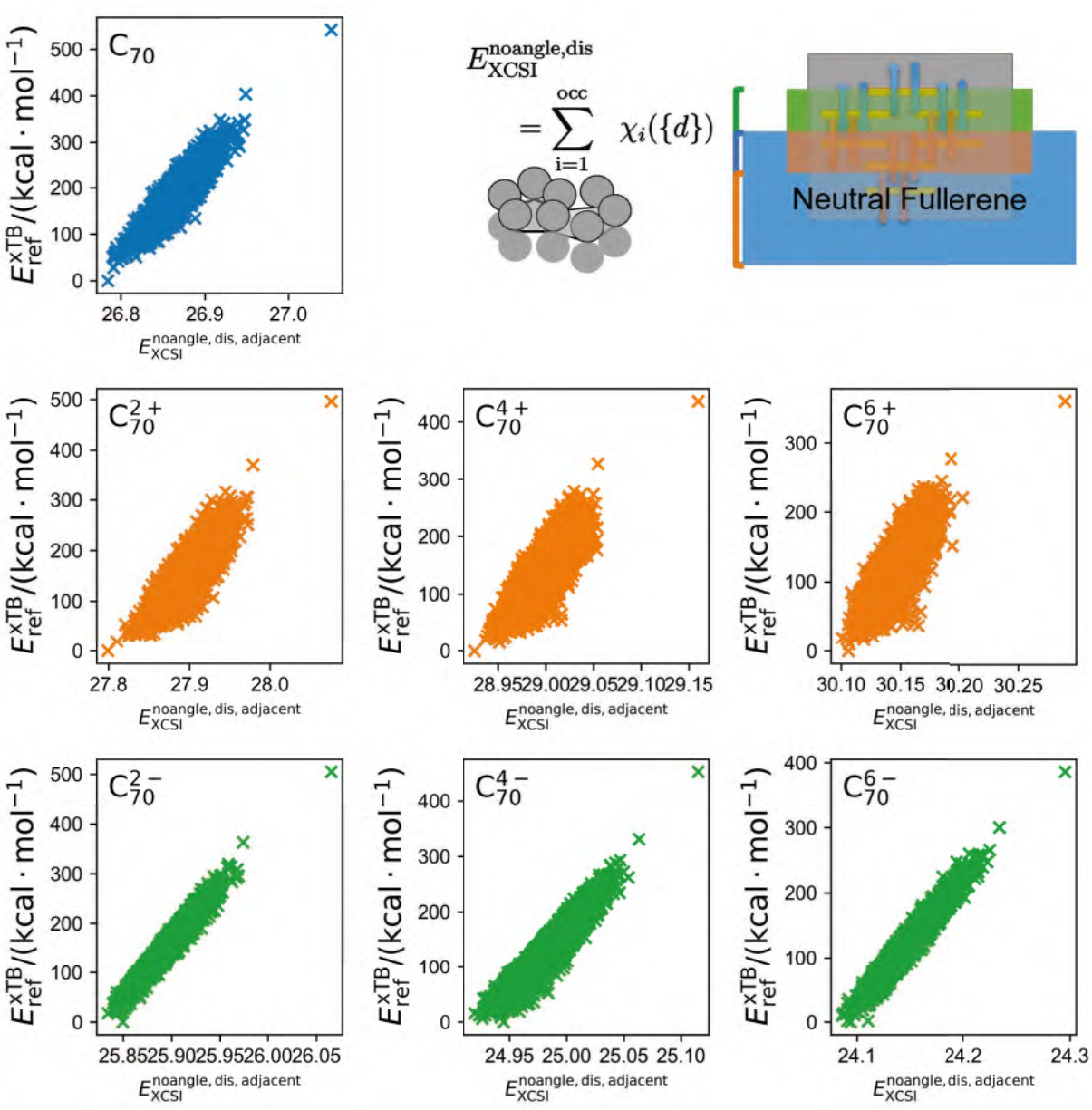


Figure 147: Correlation between xTB energies of $C_{70}$ isomers relative to the most stable one and prediction by XCSI model with distances but without angles, without using adjacent matrix mask of $C_{70}$ isomers without and with charge 2+, 4+, 6+, 2-, 4-, 6-, respectively.

# 9 Correlation between xTB energies and prediction by SpookyNet pretrained model

Predictions by SpookyNet pretrained model are calculated with the help of SpookyNet repository[3] and Atomic Simulation Environment.[6]

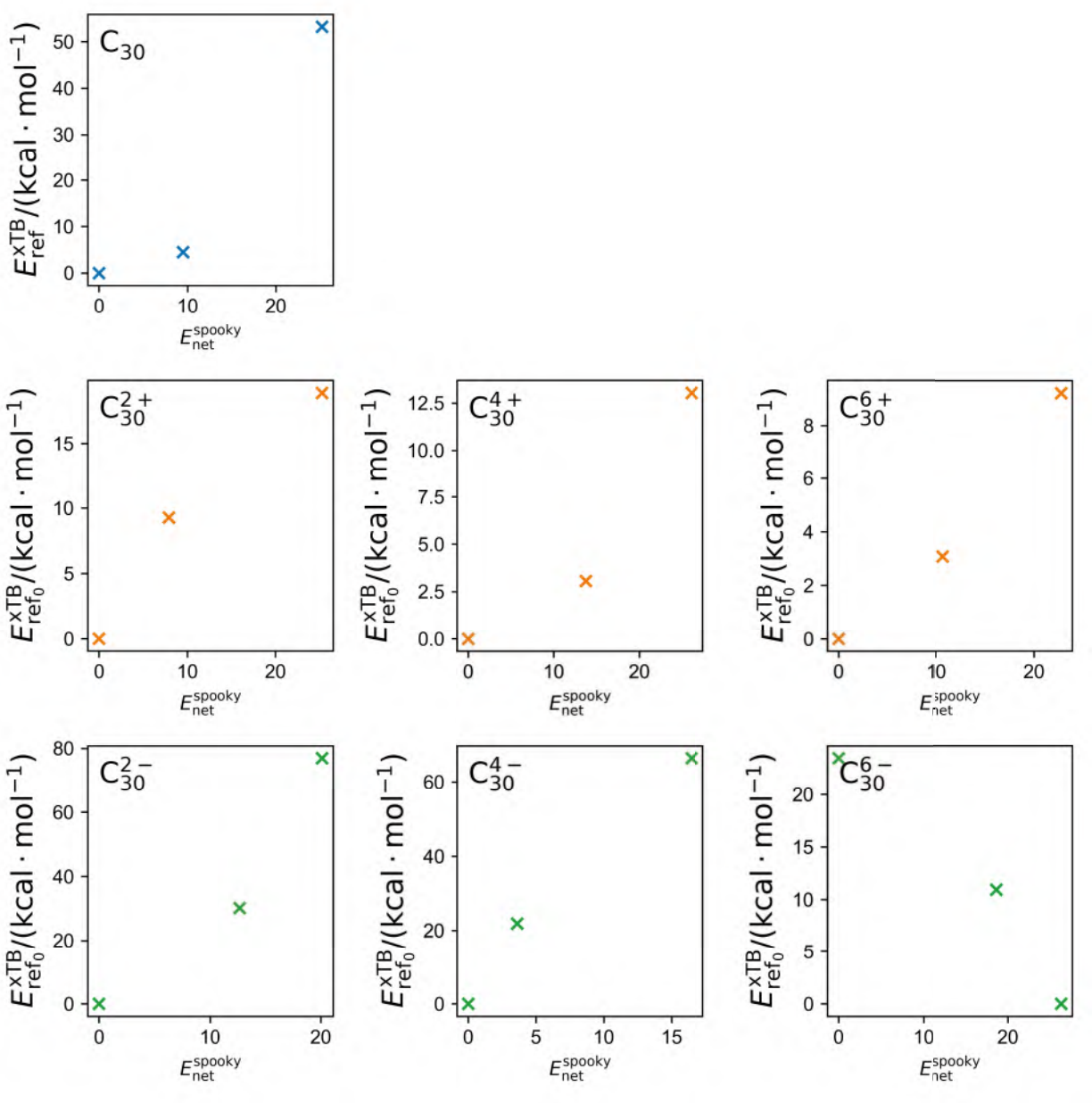


Figure 148: Correlation between xTB energies of $C_{30}$ isomers relative to the most stable one and prediction by SpookyNet pretrained model of $C_{30}$ isomers without and with charge 2+, 4+, 6+, 2-, 4-, 6-, respectively.

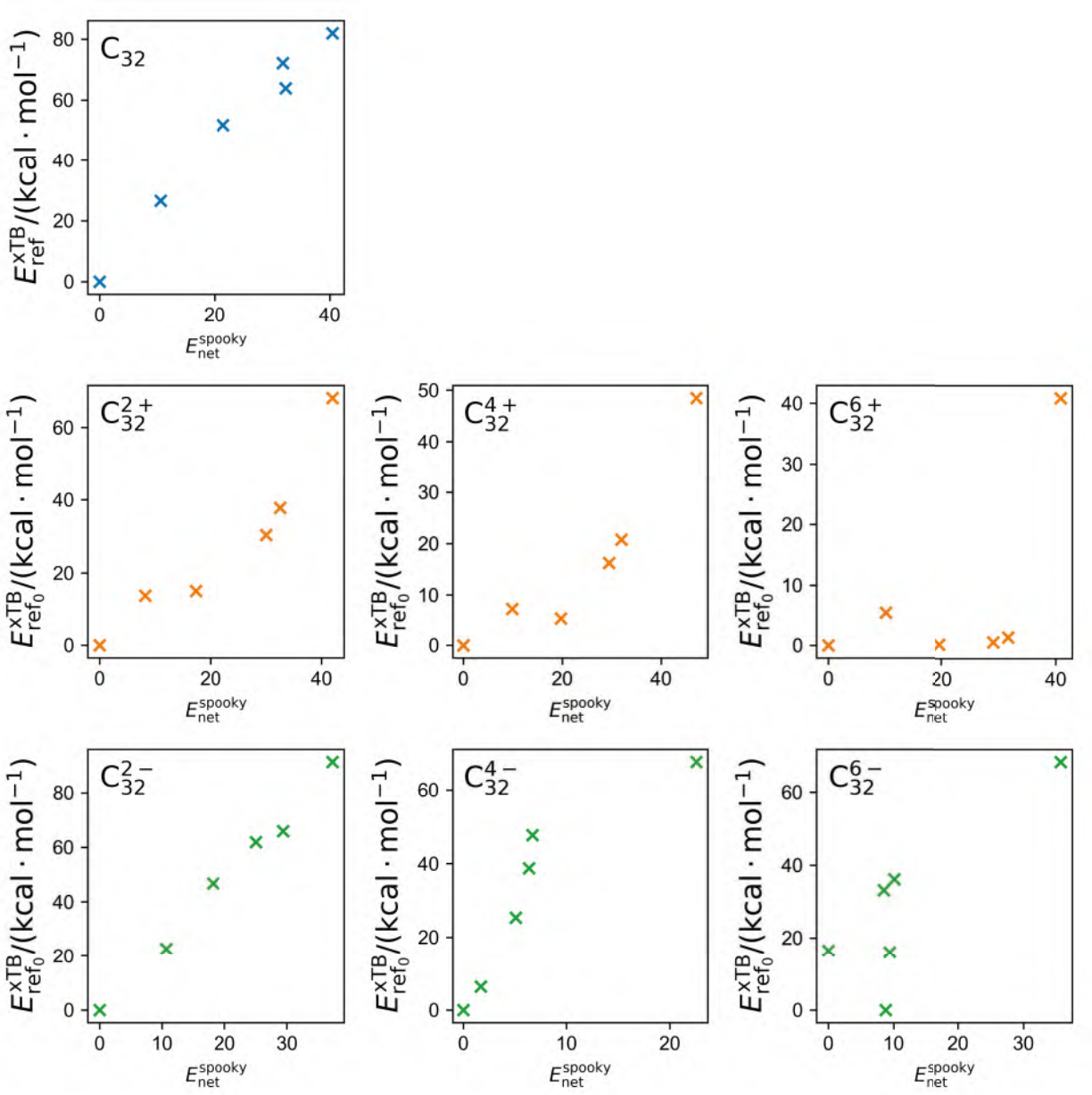


Figure 149: Correlation between xTB energies of $C_{32}$ isomers relative to the most stable one and prediction by SpookyNet pretrained model of $C_{32}$ isomers without and with charge 2+, 4+, 6+, 2-, 4-, 6-, respectively.

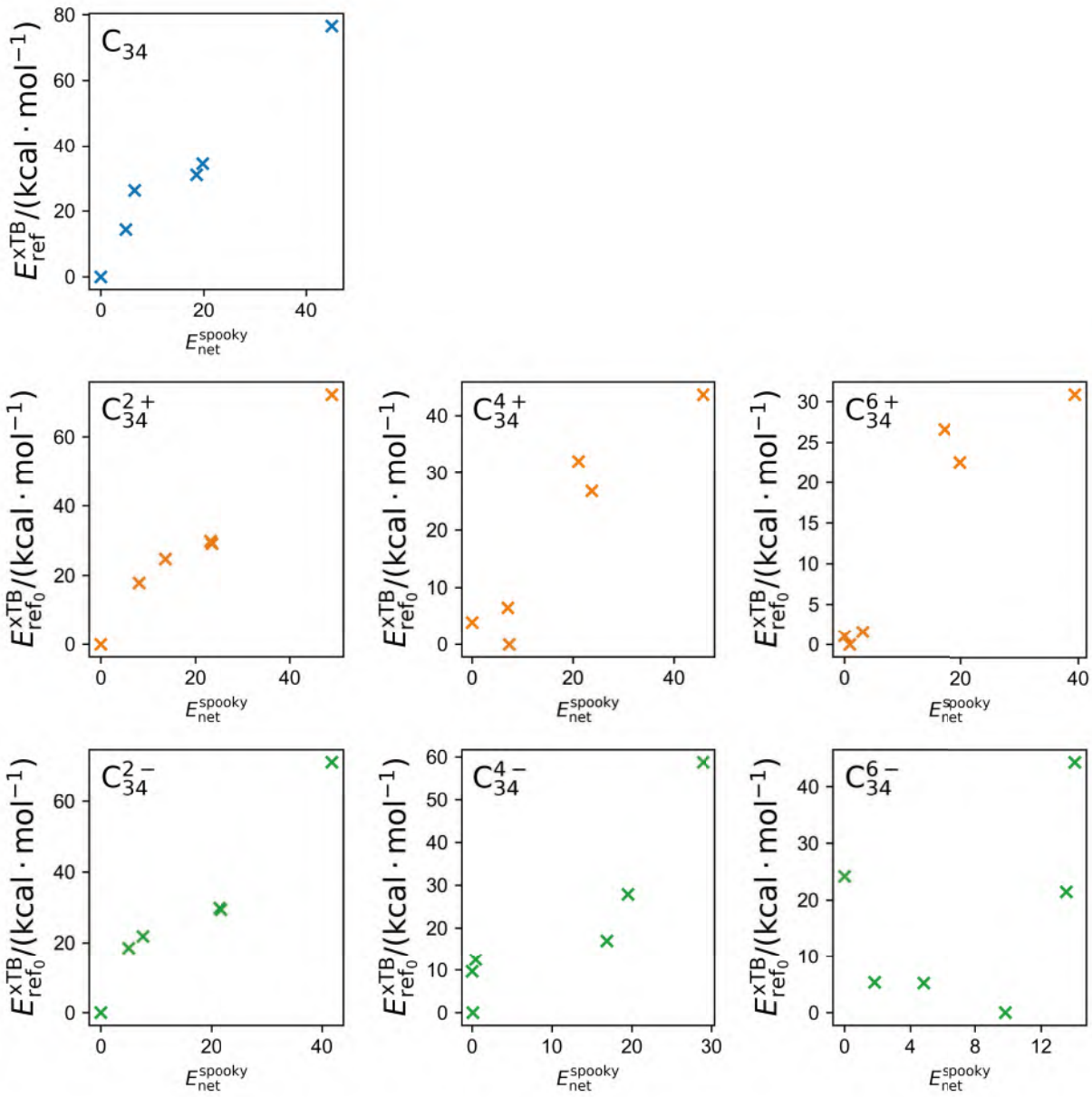


Figure 150: Correlation between xTB energies of $C_{34}$ isomers relative to the most stable one and prediction by SpookyNet pretrained model of $C_{34}$ isomers without and with charge 2+, 4+, 6+, 2-, 4-, 6-, respectively.

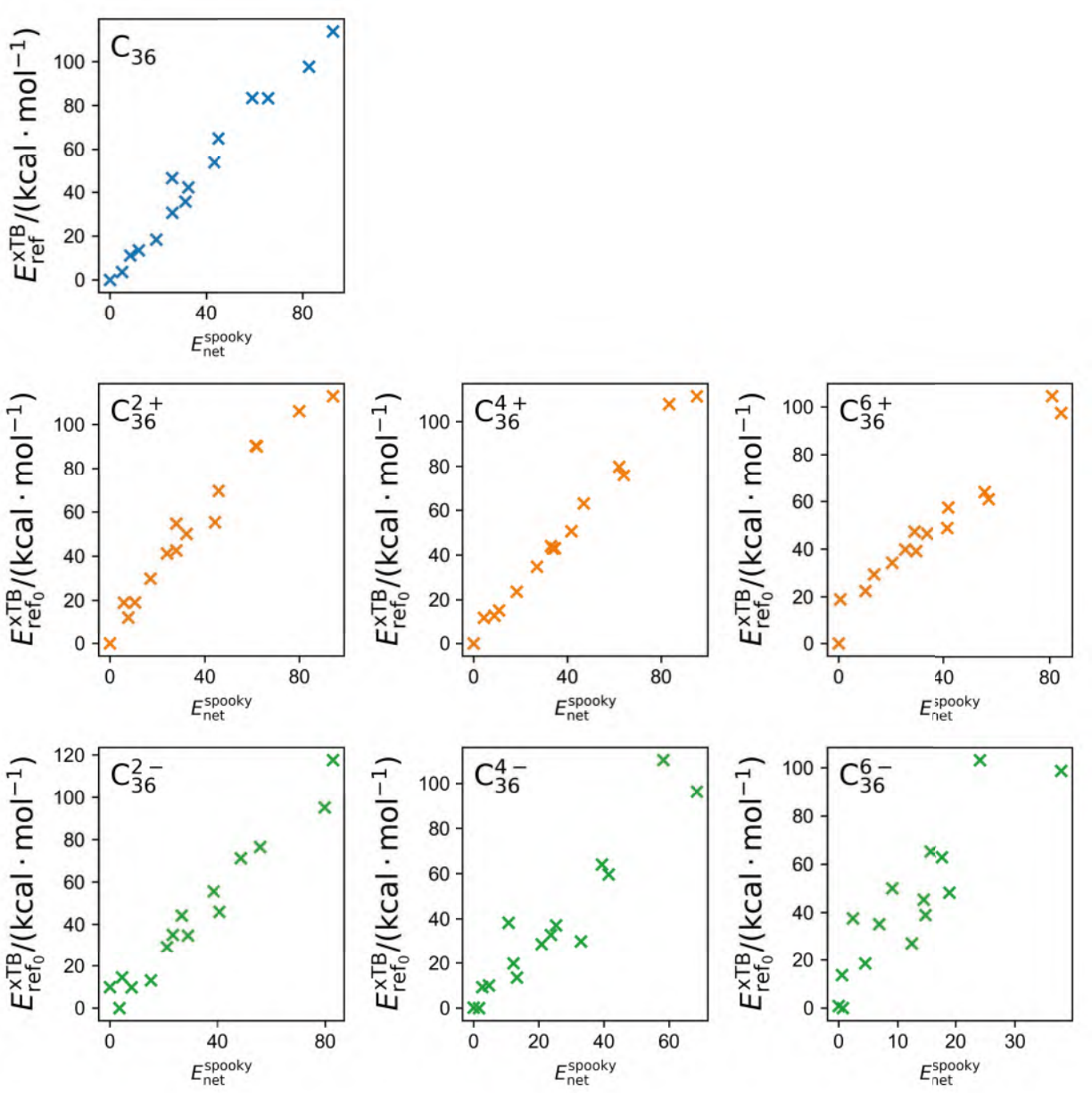


Figure 151: Correlation between xTB energies of $C_{36}$ isomers relative to the most stable one and prediction by SpookyNet pretrained model of $C_{36}$ isomers without and with charge 2+, 4+, 6+, 2-, 4-, 6-, respectively.

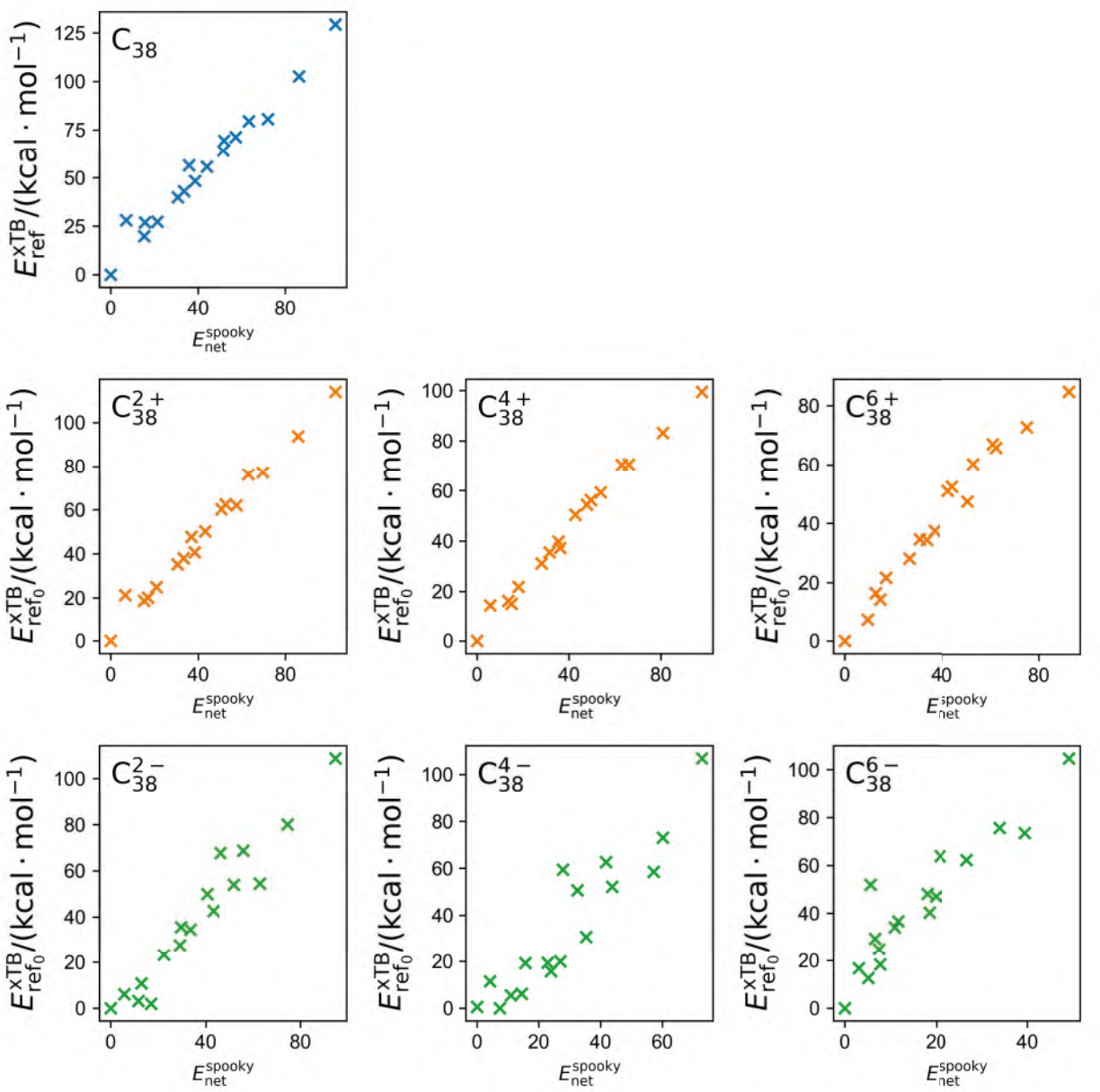


Figure 152: Correlation between xTB energies of $C_{38}$ isomers relative to the most stable one and prediction by SpookyNet pretrained model of $C_{38}$ isomers without and with charge 2+, 4+, 6+, 2-, 4-, 6-, respectively.

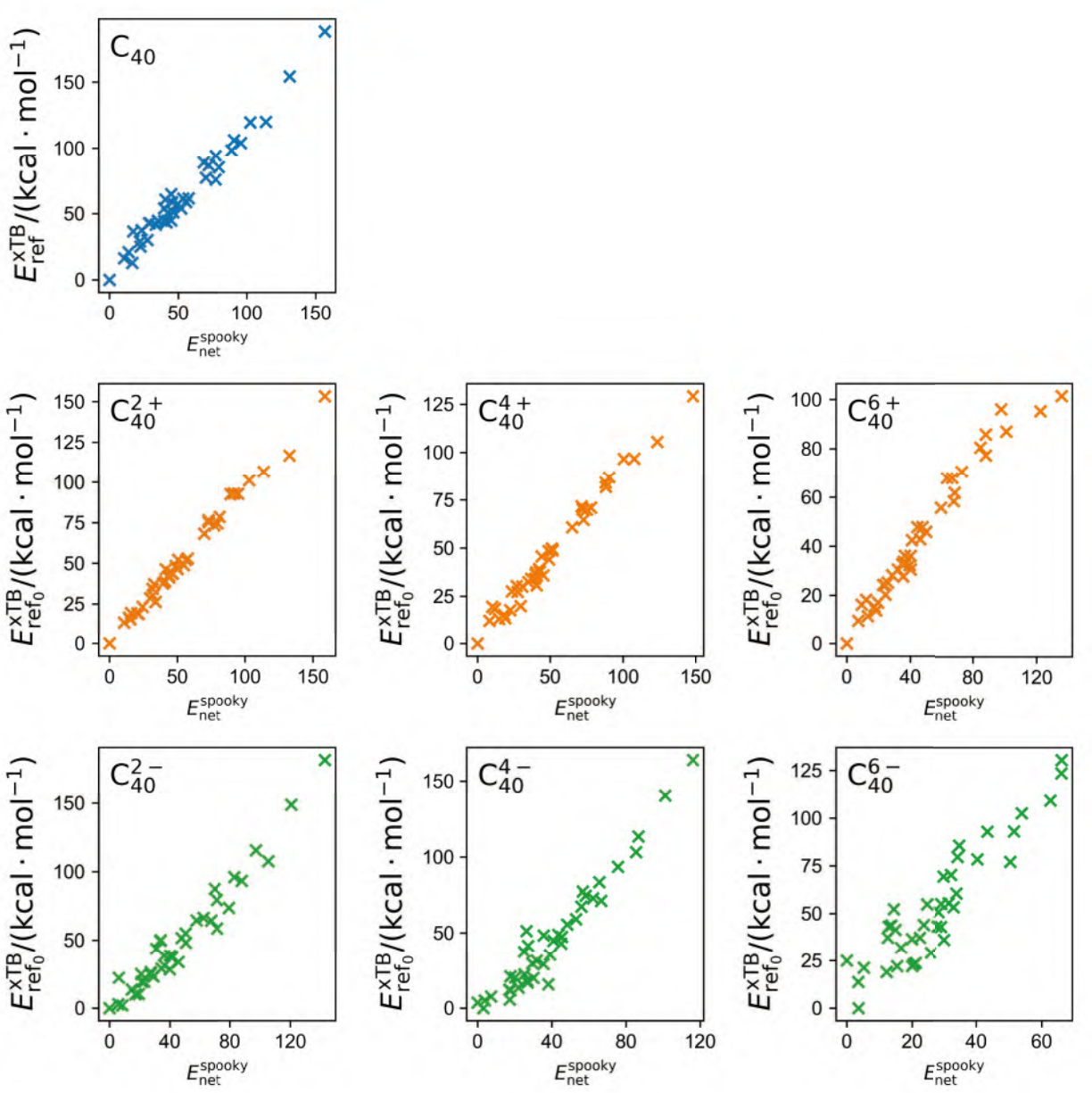


Figure 153: Correlation between xTB energies of $C_{40}$ isomers relative to the most stable one and prediction by SpookyNet pretrained model of $C_{40}$ isomers without and with charge 2+, 4+, 6+, 2-, 4-, 6-, respectively.

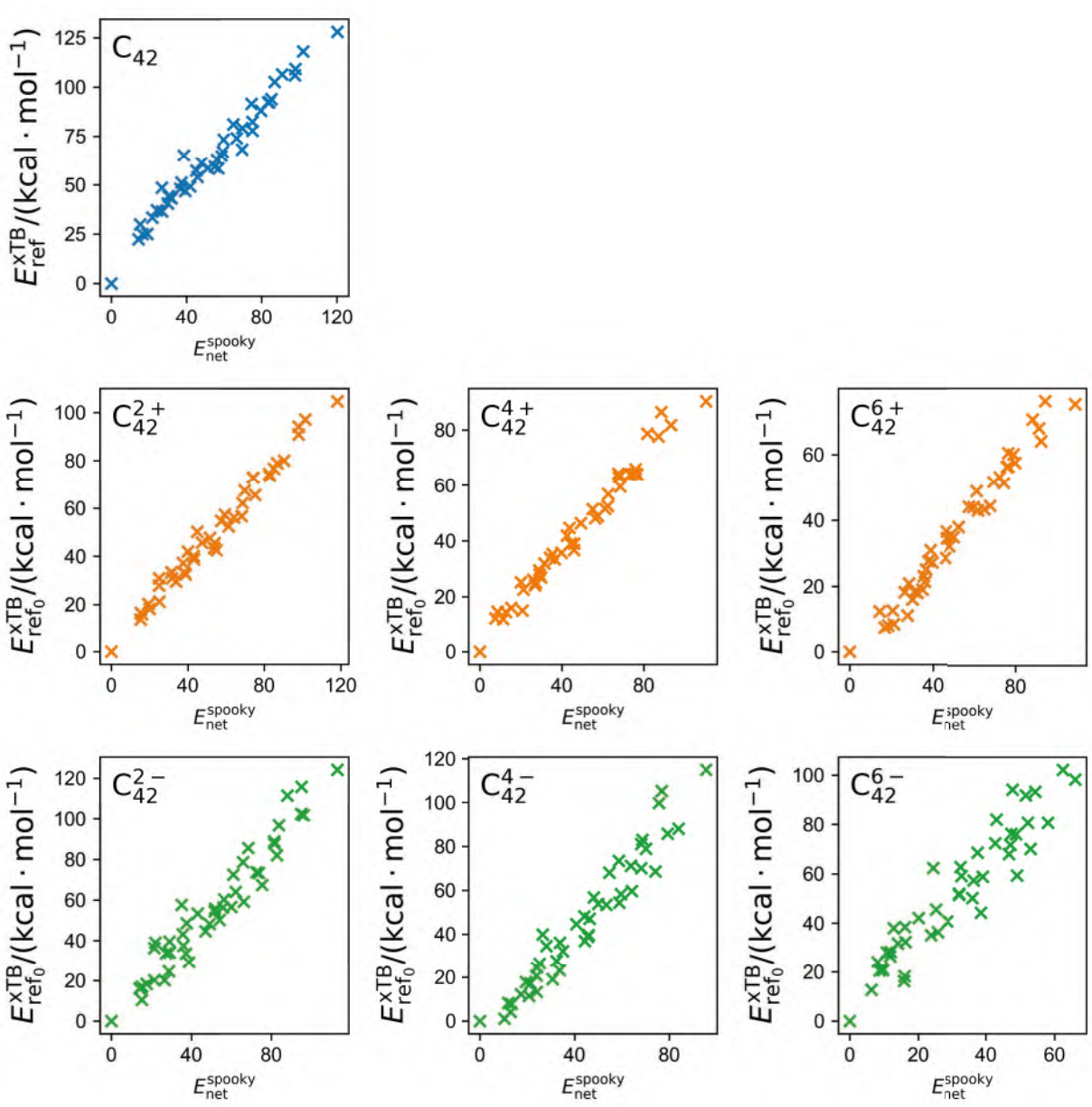


Figure 154: Correlation between xTB energies of $C_{42}$ isomers relative to the most stable one and prediction by SpookyNet pretrained model of $C_{42}$ isomers without and with charge 2+, 4+, 6+, 2-, 4-, 6-, respectively.

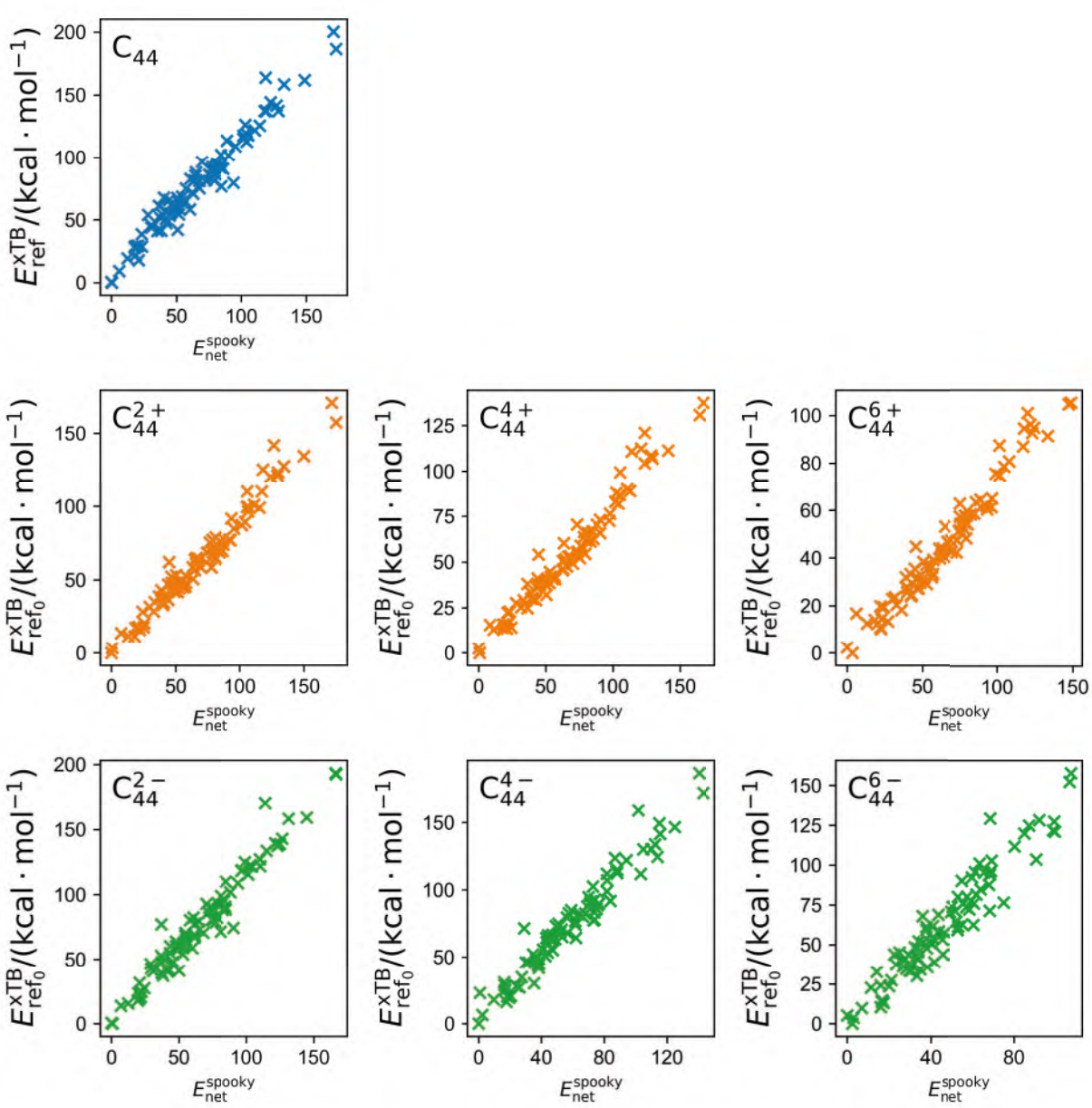


Figure 155: Correlation between xTB energies of $C_{44}$ isomers relative to the most stable one and prediction by SpookyNet pretrained model of $C_{44}$ isomers without and with charge 2+, 4+, 6+, 2-, 4-, 6-, respectively.

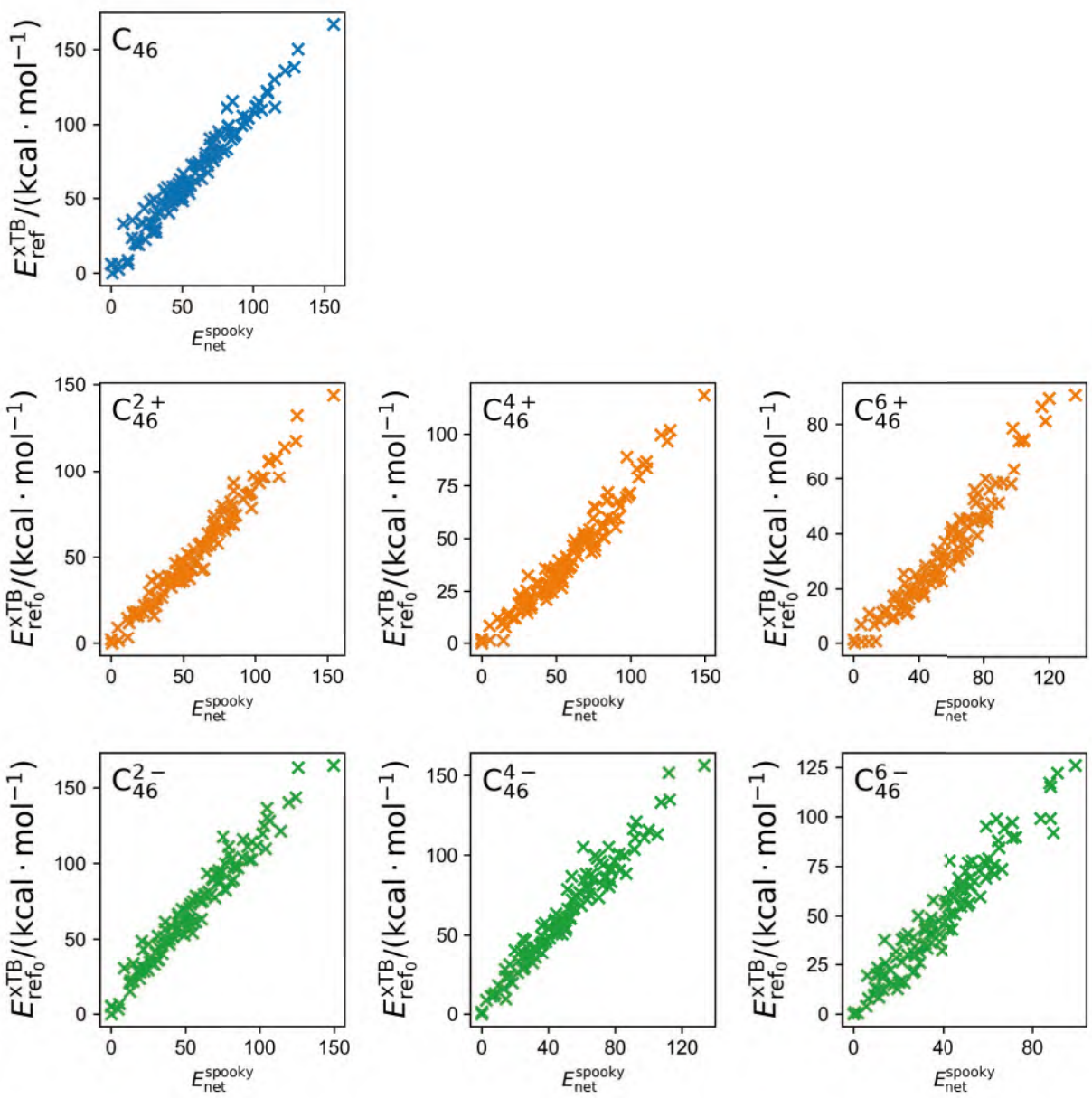


Figure 156: Correlation between xTB energies of $C_{46}$ isomers relative to the most stable one and prediction by SpookyNet pretrained model of $C_{46}$ isomers without and with charge 2+, 4+, 6+, 2-, 4-, 6-, respectively.

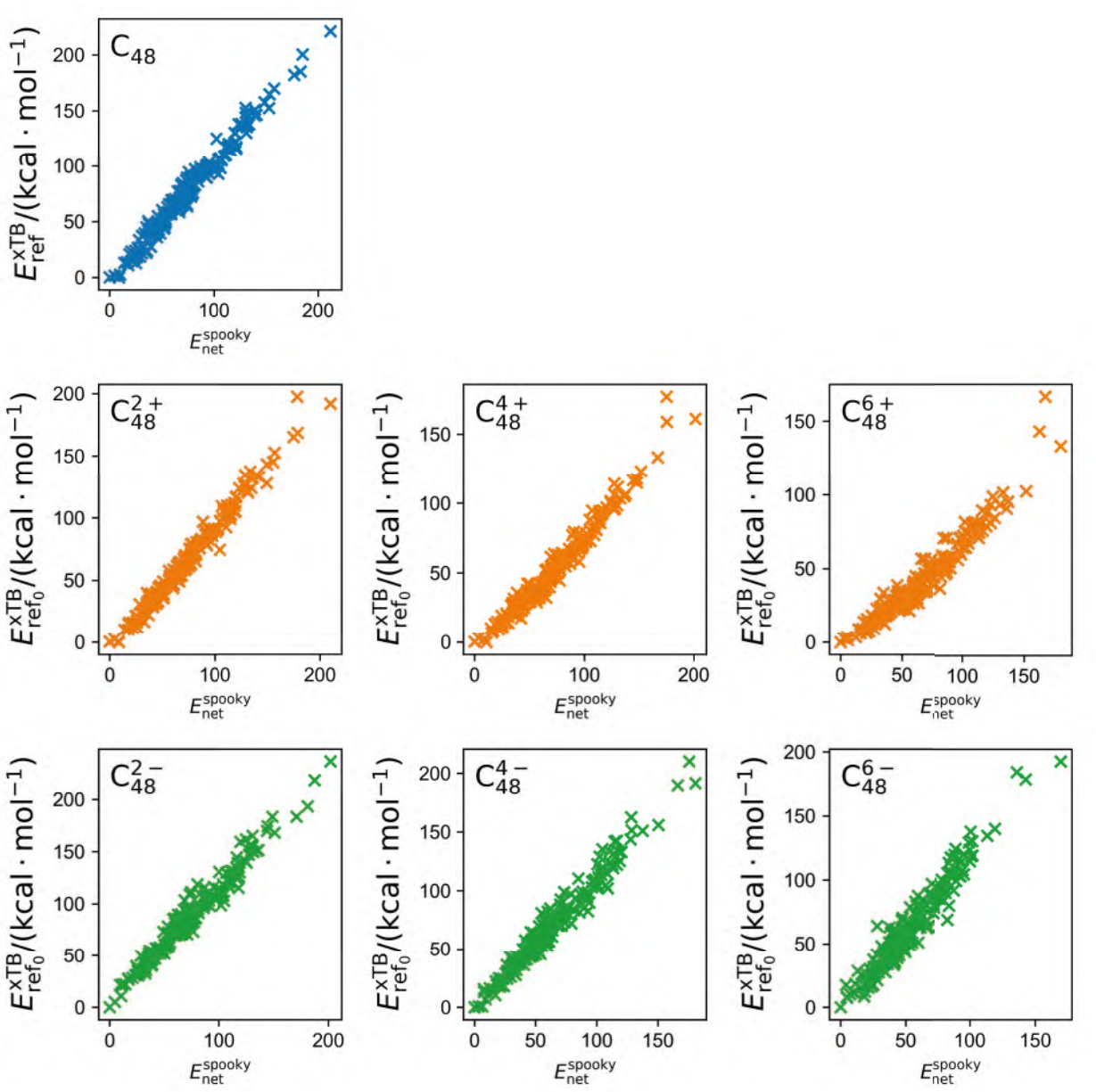


Figure 157: Correlation between xTB energies of $C_{48}$ isomers relative to the most stable one and prediction by SpookyNet pretrained model of $C_{48}$ isomers without and with charge 2+, 4+, 6+, 2-, 4-, 6-, respectively.

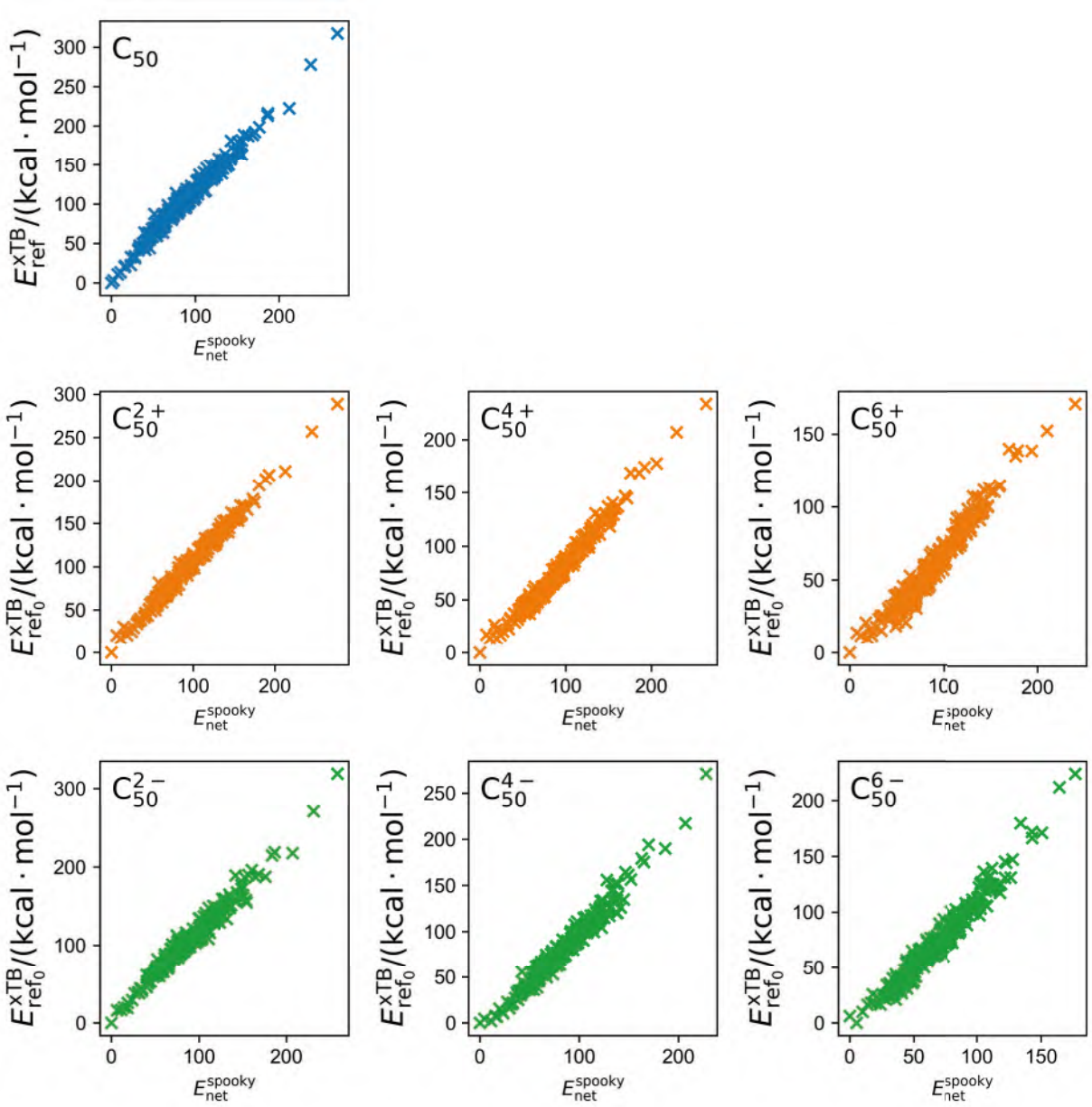


Figure 158: Correlation between xTB energies of $C_{50}$ isomers relative to the most stable one and prediction by SpookyNet pretrained model of $C_{50}$ isomers without and with charge 2+, 4+, 6+, 2-, 4-, 6-, respectively.

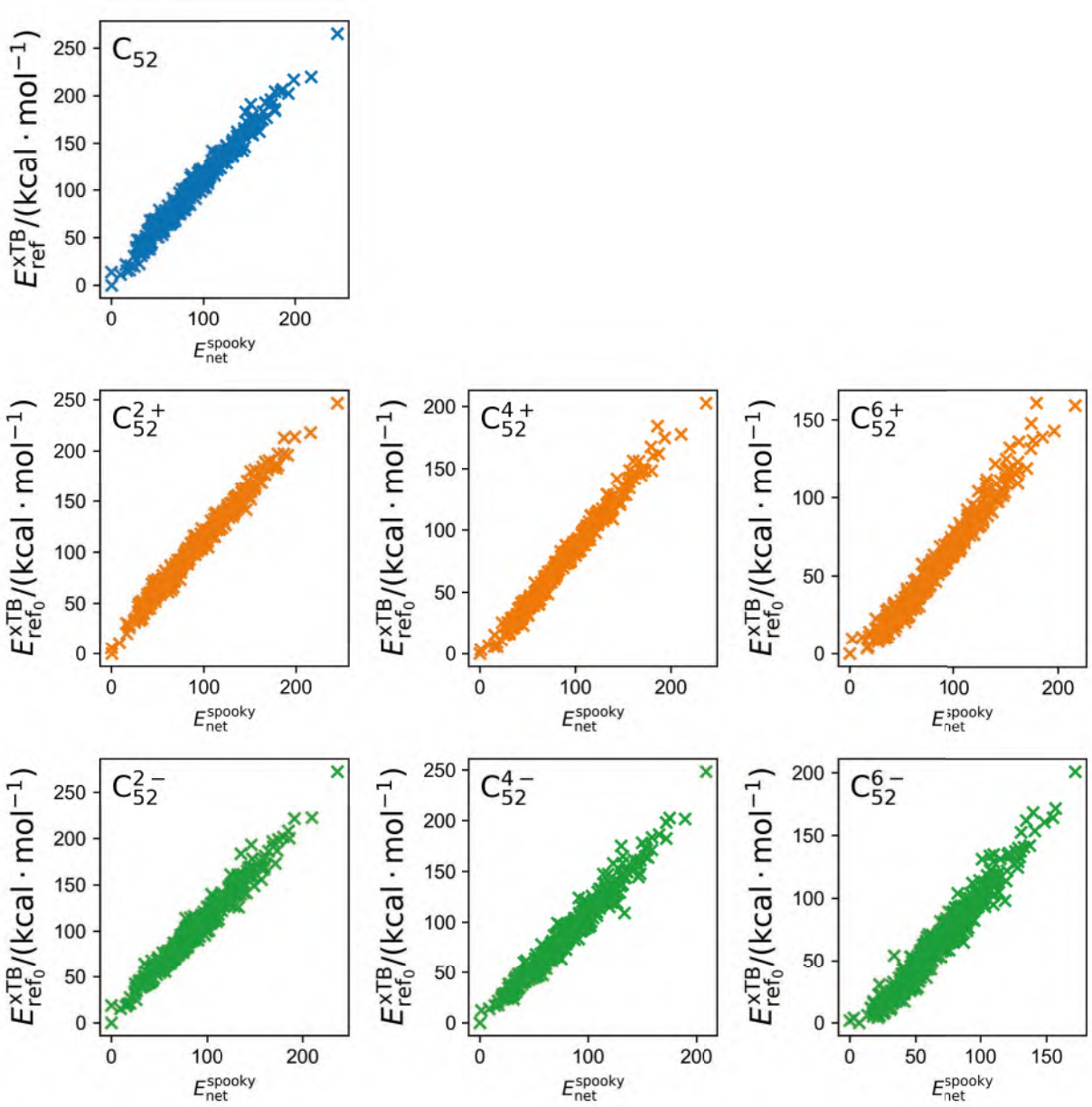


Figure 159: Correlation between xTB energies of $C_{52}$ isomers relative to the most stable one and prediction by SpookyNet pretrained model of $C_{52}$ isomers without and with charge 2+, 4+, 6+, 2-, 4-, 6-, respectively.

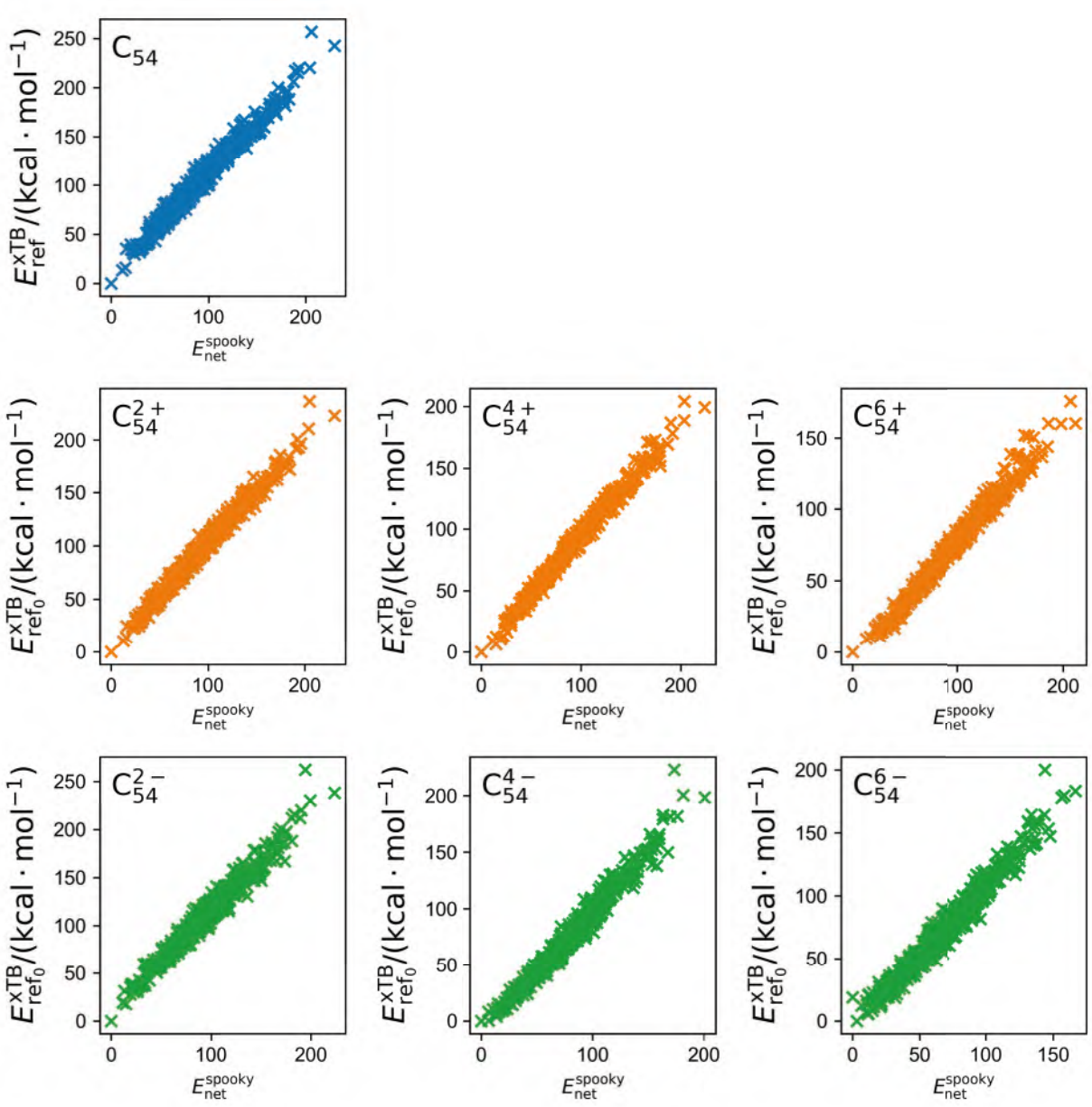


Figure 160: Correlation between xTB energies of $C_{54}$ isomers relative to the most stable one and prediction by SpookyNet pretrained model of $C_{54}$ isomers without and with charge 2+, 4+, 6+, 2-, 4-, 6-, respectively.

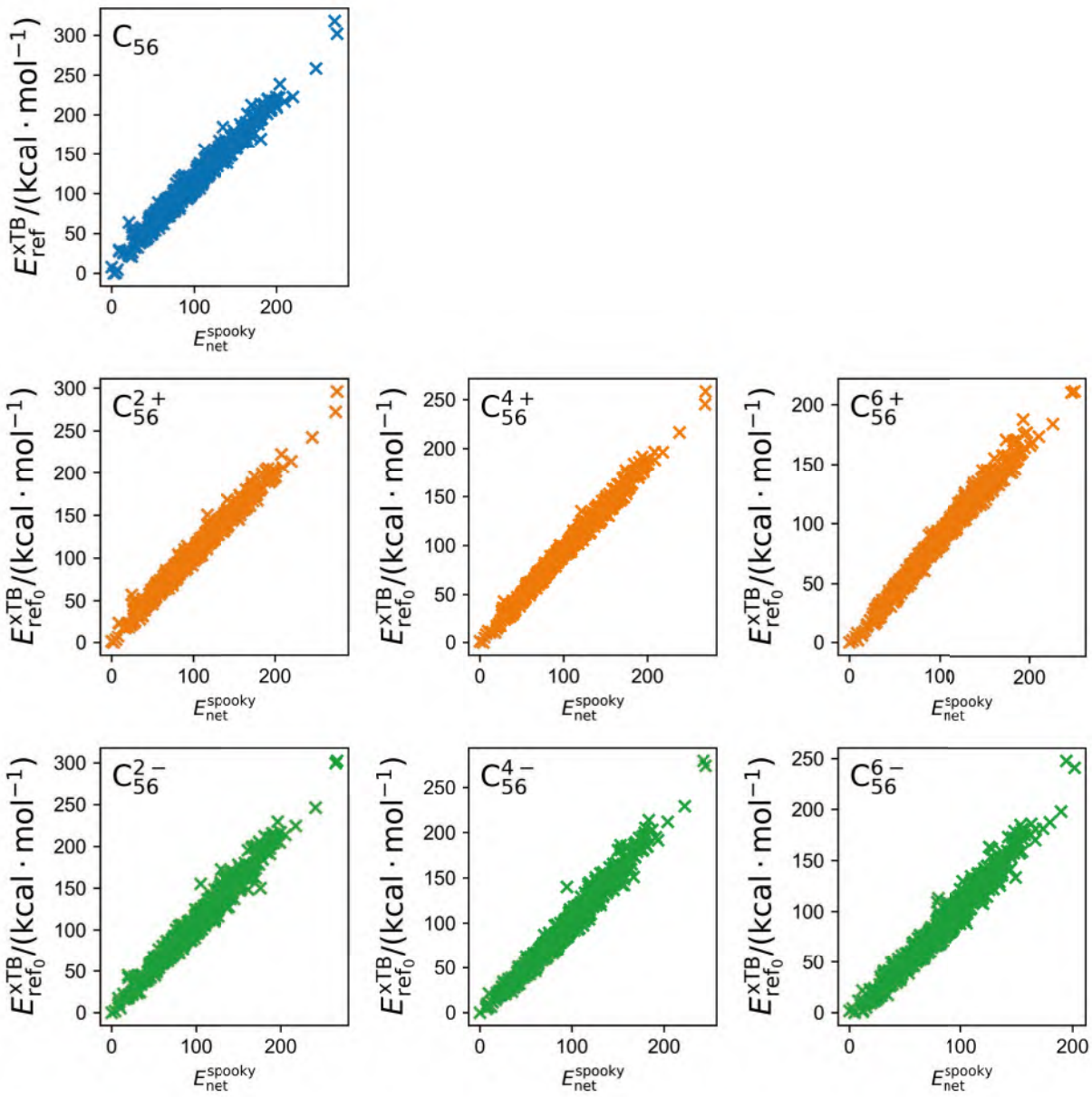


Figure 161: Correlation between xTB energies of $C_{56}$ isomers relative to the most stable one and prediction by SpookyNet pretrained model of $C_{56}$ isomers without and with charge 2+, 4+, 6+, 2-, 4-, 6-, respectively.

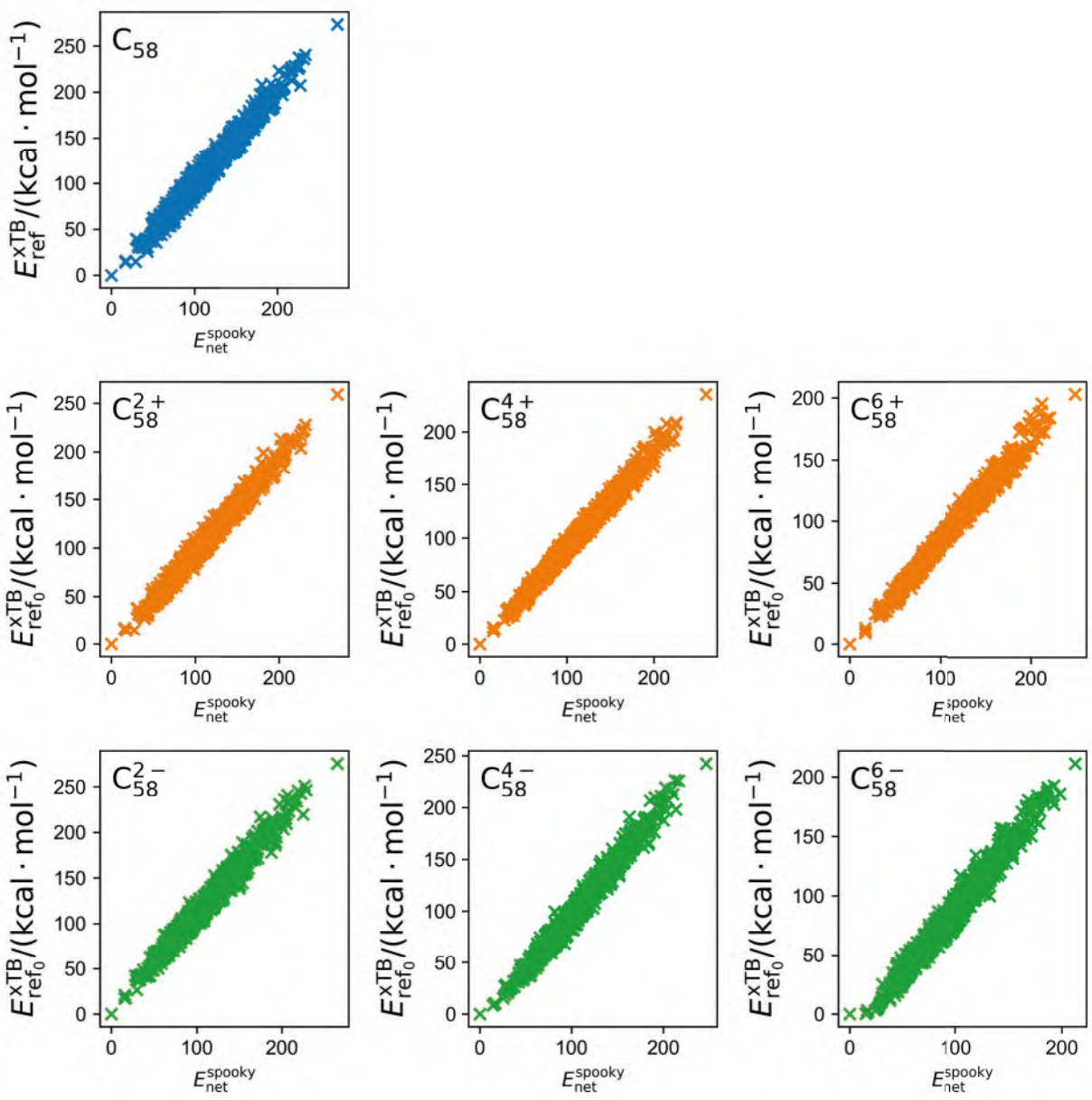


Figure 162: Correlation between xTB energies of $C_{58}$ isomers relative to the most stable one and prediction by SpookyNet pretrained model of $C_{58}$ isomers without and with charge 2+, 4+, 6+, 2-, 4-, 6-, respectively.

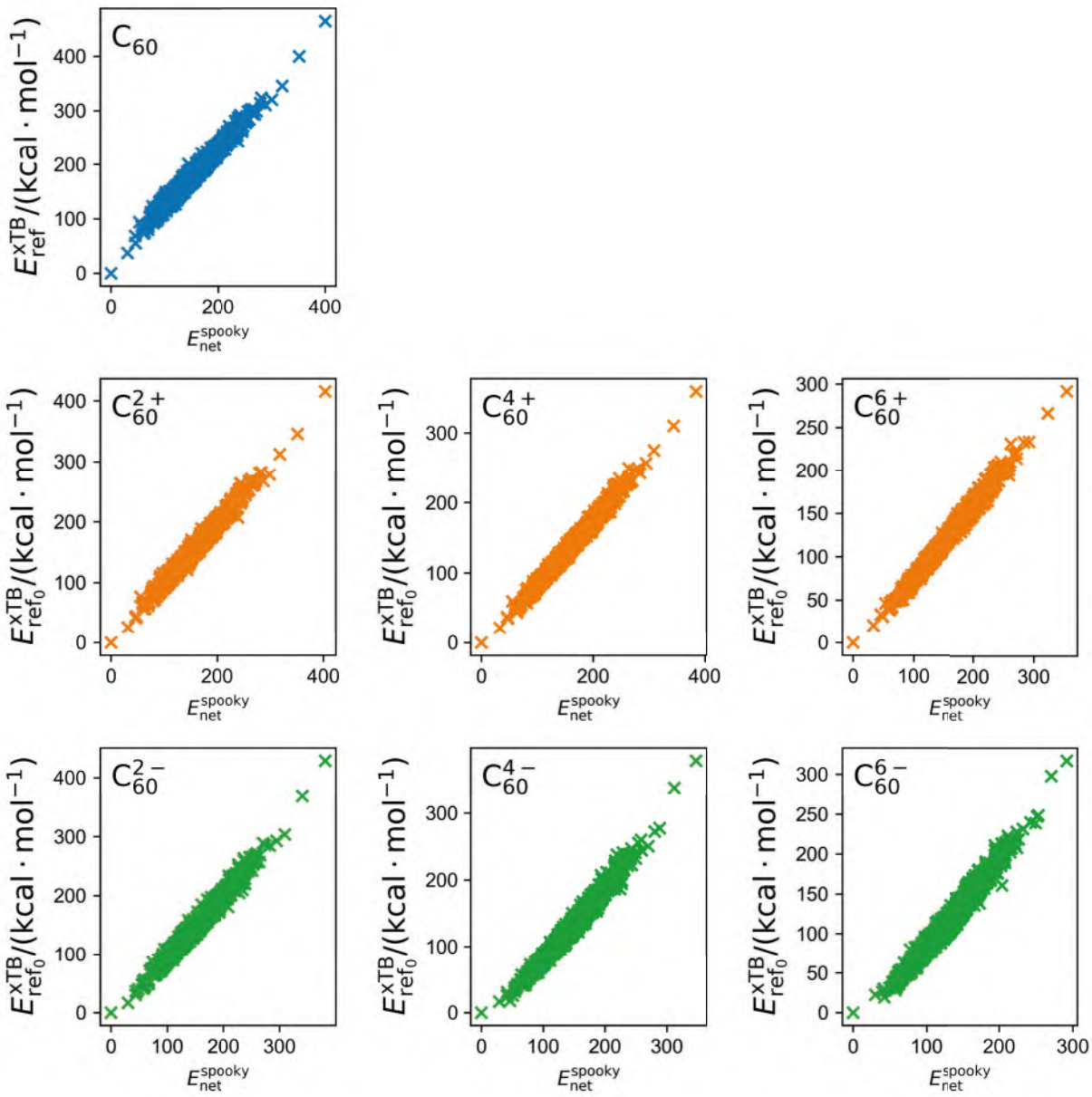


Figure 163: Correlation between xTB energies of $C_{60}$ isomers relative to the most stable one and prediction by SpookyNet pretrained model of $C_{60}$ isomers without and with charge 2+, 4+, 6+, 2-, 4-, 6-, respectively.

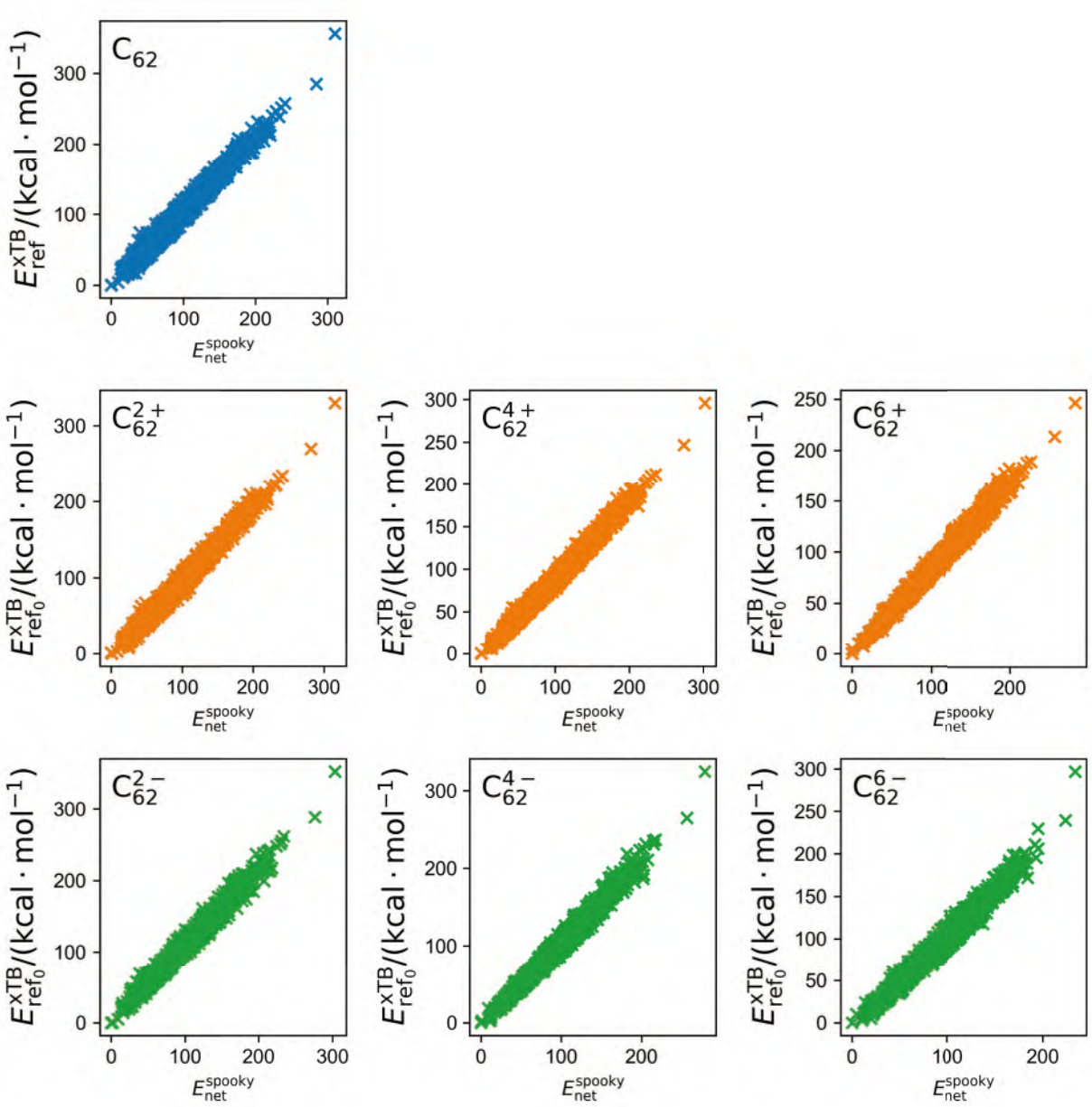


Figure 164: Correlation between xTB energies of $C_{62}$ isomers relative to the most stable one and prediction by SpookyNet pretrained model of $C_{62}$ isomers without and with charge 2+, 4+, 6+, 2-, 4-, 6-, respectively.

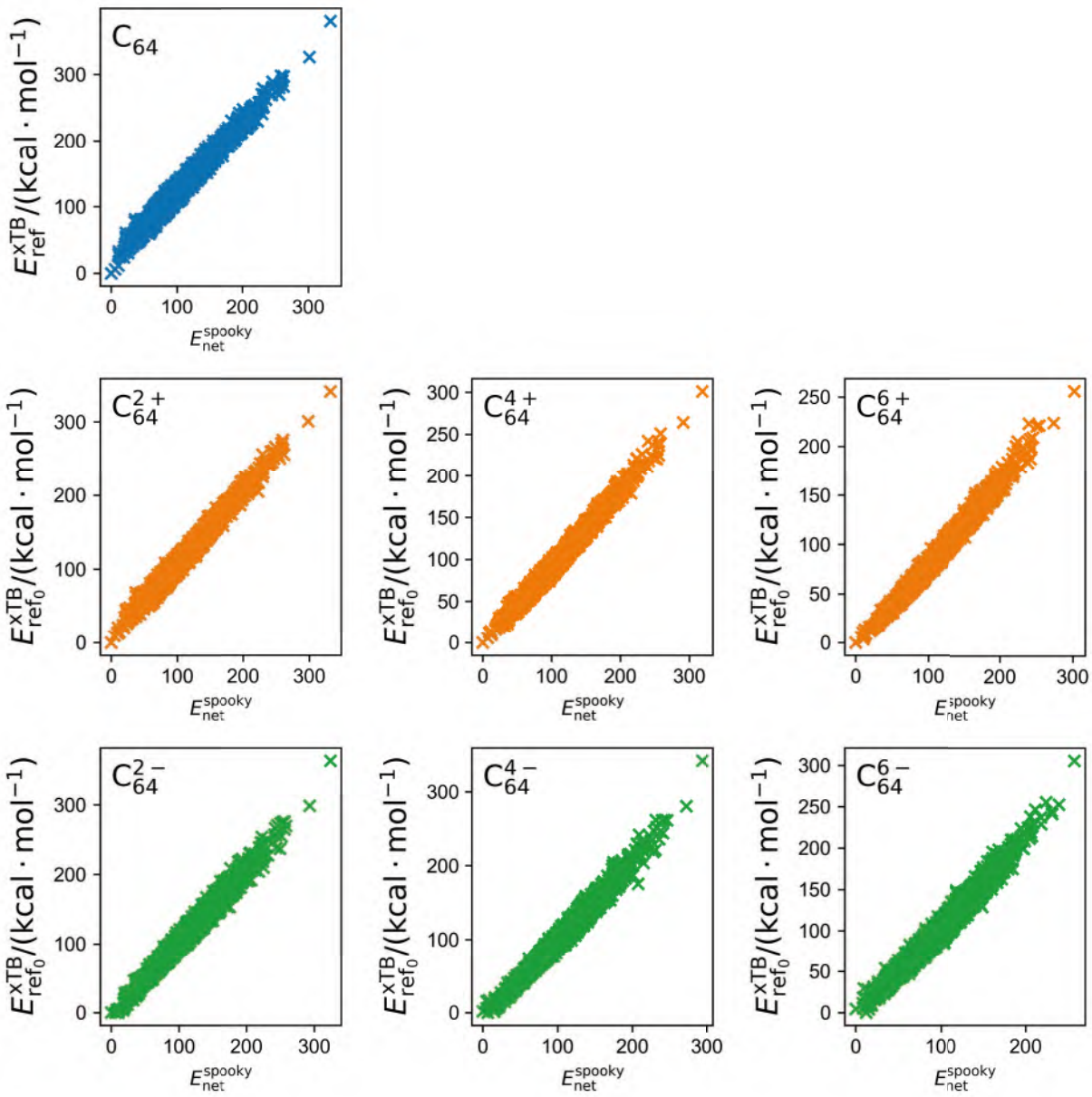


Figure 165: Correlation between xTB energies of $C_{64}$ isomers relative to the most stable one and prediction by SpookyNet pretrained model of $C_{64}$ isomers without and with charge 2+, 4+, 6+, 2-, 4-, 6-, respectively.

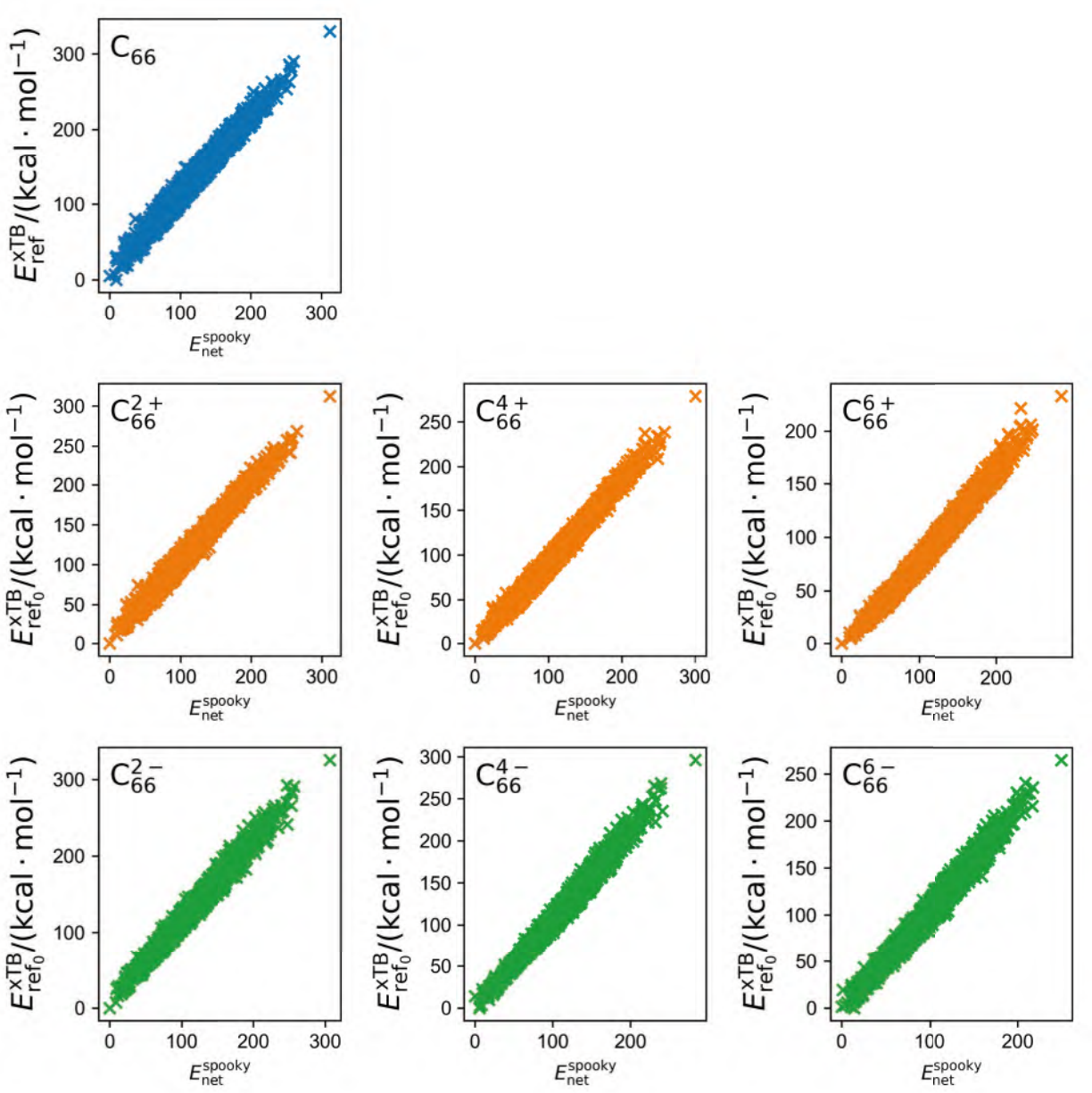


Figure 166: Correlation between xTB energies of $C_{66}$ isomers relative to the most stable one and prediction by SpookyNet pretrained model of $C_{66}$ isomers without and with charge 2+, 4+, 6+, 2-, 4-, 6-, respectively.

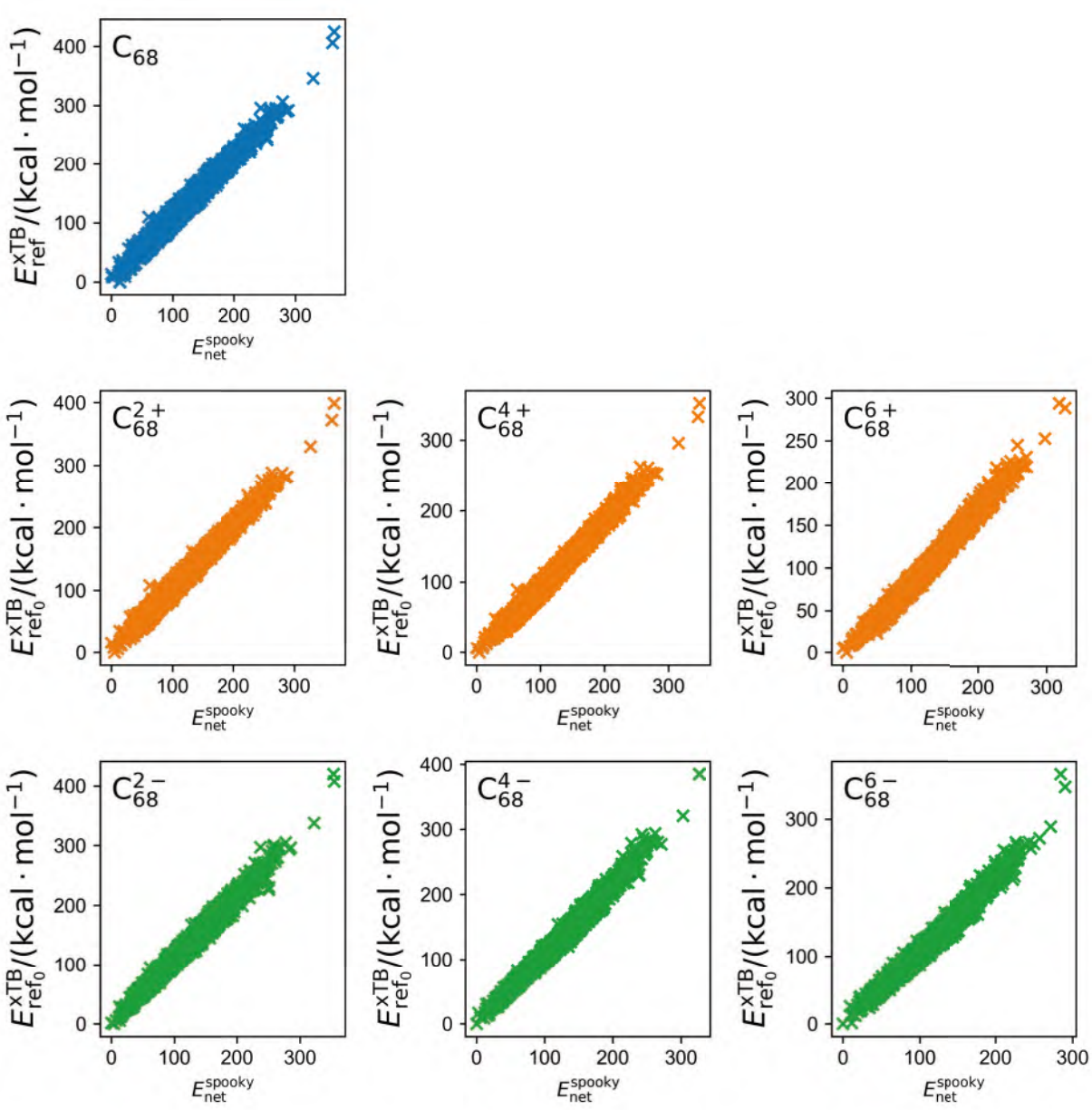


Figure 167: Correlation between xTB energies of $C_{68}$ isomers relative to the most stable one and prediction by SpookyNet pretrained model of $C_{68}$ isomers without and with charge 2+, 4+, 6+, 2-, 4-, 6-, respectively.

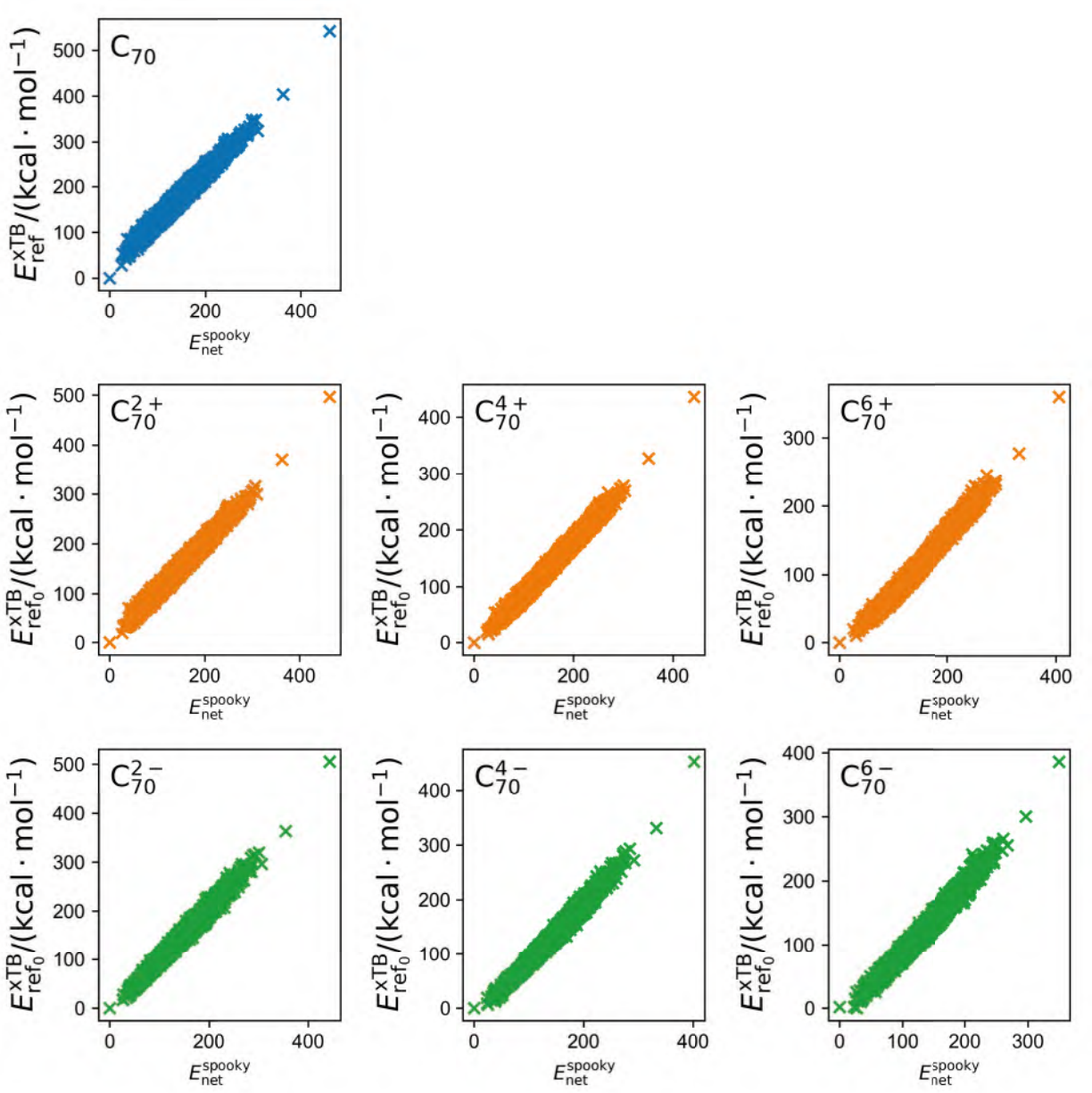


Figure 168: Correlation between xTB energies of $C_{70}$ isomers relative to the most stable one and prediction by SpookyNet pretrained model of $C_{70}$ isomers without and with charge 2+, 4+, 6+, 2-, 4-, 6-, respectively.

# References


(1) Wang, Y.; Diaz-Tendero, S.; Alcami, M.; Martin, F. Topology-based approach to predict relative stabilities of charged and functionalized fullerenes. *Journal of chemical theory and computation* **2018**, *14*, 1791–1810.

(2) Haddon, R. GVB and POAV analysis of rehybridization and $\pi$-orbital misalignment in non-planar conjugated systems. *Chemical physics letters* **1986**, *125*, 231–234.

(3) Unke, O. T.; Chmiela, S.; Gastegger, M.; Schütt, K. T.; Sauceda, H. E.; Müller, K.-R. SpookyNet: Learning force fields with electronic degrees of freedom and nonlocal effects. *Nature communications* **2021**, *12*, 1–14.

(4) Schütt, K. T.; Sauceda, H. E.; Kindermans, P.-J.; Tkatchenko, A.; Müller, K.-R. Schnet–a deep learning architecture for molecules and materials. *The Journal of Chemical Physics* **2018**, *148*, 241722.

(5) Schütt, K.; Kessel, P.; Gastegger, M.; Nicoli, K.; Tkatchenko, A.; Müller, K.-R. SchNetPack: A deep learning toolbox for atomistic systems. *Journal of chemical theory and computation* **2018**, *15*, 448–455.

(6) Larsen, A. H.; Mortensen, J. J.; Blomqvist, J.; Castelli, I. E.; Christensen, R.; Dułak, M.; Friis, J.; Groves, M. N.; Hammer, B.; Hargus, C., et al. The atomic simulation environmenta Python library for working with atoms. *Journal of Physics: Condensed Matter* **2017**, *29*, 273002.